BIOPHYSICAL STUDIES OF SYNTHETIC GENE DELIVERY SYSTEMS

Li Kim Lee

Thesis submitted for the Degree of

Doctor of Philosophy (PhD)

of the University of London

UNIVERSITY COLLEGE LONDON

DEPARTMENT OF BIOCHEMICAL ENGINEERING

March 2002

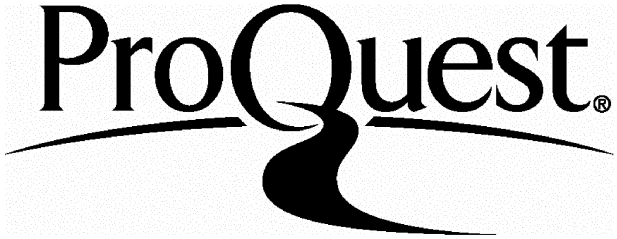

Dedicated to my parents whose understanding, constant support and encouragement during all these years made it possible.

Acknowledgements

I would like to express my gratitude to many people for their help during the work represented by this thesis. I am deeply indebted to my supervisor, Prof. Parviz Ayazi Shamlou for his confidence in my work, for supporting my research with ideas and criticism, and for his enthusiasm, encouragement and guidance. I would also like to thank Prof. Peter Dunnill very much for his support and inspiration.

My appreciation goes to my collaborators at the Molecular Immunology Unit, Institute of Child Health, especially Dr Elena Siapati. The fact that I could spend time at their institute gave me the invaluable opportunity to learn cell transfection techniques. This thesis owes much of its content to the numerous fruitful discussion sessions with them and also with Dr Aima Uduehi. Thanks also to Dr Gisli Jenkins for the *in vivo* studies.

I would like to thank everyone in the Department of Biochemical Engineering for their friendship and for making the department such a pleasant place to work. My gratitude goes especially to Dr Susana Levy and Dr Ronan O'Kennedy for sharing their knowledge of biochemical engineering and for conversations that helped keep things in perspective. Thanks also to Claire Mount for being a joy to work with.

I am especially thankful to Malvern Instruments for allowing me to perform static light scattering studies at their DTS labs. Thanks to Malcolm Connah and Nicola Gummery for PCS instrumentation that made the SLS studies possible, and to Mike Kaszuba, Stephen Ward-Smith, Paul Kear and Richard Mead for their helpful advice during my PhD.

I would also like to thank Prof. John Gregory, Prof. Irina Solomentseva and Dr Samson S. Yim for valuable discussions on the DLVO theory. Thanks also to Tom Warwick and Richard Harris at Digital Instruments, and Prof. Michael Horton, Dr Petri Lehenkari and Guillaume Charras for AFM imaging of plasmid DNA.

Abstract

Driven by the rapid development of therapeutic applications for synthetic gene delivery systems, specifically formulations of plasmid DNA with cationic lipids and/or peptides, the characterisation of DNA complexes has become an important area of research. Current efforts to increase their transfection efficiency has led to the development of analytical techniques for a better understanding of how the structure, stability and biological activity of DNA complexes are affected by their environment.

The effects of ionic strength and pH on the colloidal stability and structure of synthetic gene delivery systems were investigated through salt-induced aggregation of poly-L-lysine/DNA complexes. A two-syringe pump flow system was used to reproducibly prepare the polyplexes. Analysis of the mean hydrodynamic diameter using dynamic light scattering showed that the aggregation rate and polydispersity of the polyplexes increased with ionic strength and pH. Polyplexes with an average diameter of 100-150 nm aggregated to 1500-3000 nm over 1.5 h. Computer simulations using equations based on the DLVO theory were found to adequately describe the stability of the polyplexes. These simulations form the basis for further work on theoretical predictions of the stability of DNA complexes. The concept of DNA complexes as aggregate structures with fractal dimensions was introduced. Static light scattering revealed fractal dimensions of 2.22 and 1.44 for polyplexes at 50-150 and 1000 mM NaCl, respectively. These values correspond to slow and rapid aggregation regimes, respectively.

Biophysical characterisation of a novel receptor-mediated system, Lipofectin/integrin-targeting peptide/DNA, with potential for targeted gene therapy *in vivo*, was conducted. Under physiological ionic strength, lipopolyplexes at 6.8 charge ratio demonstrated instability (average size > 1000 nm) and decreased *in vitro* transfection activity. A PicoGreen assay showed complete binding of the DNA at a charge ratio of 3.0-4.0, corresponding to maximum expression. Lipopolyplexes at high DNA concentrations (150 μg/ml) in distilled water and 5% dextrose possessed small sizes (110 ± 35 nm and 145 ± 35 nm, respectively), but aggregated upon contact with salt or serum albumin.

TABLE OF CONTENTS

List of figures

List of tables

CHAPTER 1

INTRODUCTION

In DNA vaccination and gene therapy, synthetic or non-viral formulations offer potential advantages over viral-based systems, e.g. decreased immunogenicity and easier manufacture. However, low efficiencies of gene transfer *in vivo* have been reported for most DNA formulations, currently limiting their application in clinical trials and eventual widespread use. A range of condensing agents including cationic lipids, liposomes, polypeptides, or a combination of these have been used to form electrostatic complexes with DNA, aimed at improving levels of transfection. Nevertheless many challenges remain before complexes with acceptable transfection efficiency become available. With respect to current formulations for plasmid DNA, the biochemical engineering challenges which form the basis of this thesis include issues related to the physical stability of DNA complexes. Recent research suggests that the integration of vector chemistry and the characterisation of interactions between DNA-containing complexes under physiological conditions is a prerequisite for understanding their mechanisms of binding, internalisation and intracellular trafficking. Research at UCL and elsewhere has shown that packaging of the plasmid containing the therapeutic DNA by cationic lipids or cationic polymers produces charged colloidal particles that are highly susceptible to aggregation. These

studies have also shown that transfection levels are strongly affected by the properties of these particles. In this thesis, an experimental and theoretical study is performed to explain the important factors that influence the stability of colloidal DNA complexes. The results form a basis for the improved design of complexes aimed for minimal aggregation.

The aims of this work are to study the physical stability of polylysine/DNA complexes (polyplexes) with respect to aggregation, to examine the implications of physicochemical properties for the transfection efficiency of a novel integrin-targeted non-viral vector, and to model any effects on the stability of such systems.

Initially, experiments were carried out with a simple model of a synthetic gene delivery system, consisting of poly-L-lysine and DNA, to provide insight into the physicochemical factors affecting the stability of DNA complexes. In such systems, DNA condensation occurs due to mainly the strong electrostatic interaction between the negatively charged DNA and cationic polymer. Charge neutralisation of the DNA phosphates by the lysine residues leads to very rapid collapse of the DNA molecules, typically from diameters of several hundred nanometers into discrete, compact particles of less than 200 nm. This reduction of the size of DNA is generally considered a requirement for successful *in vivo* gene transfer. However, under physiological conditions, a decrease in the repulsive interactions between the primary particles of poly-L-lysine-condensed DNA led to their aggregation. The increase in polyplex size was measured over time as a function of different physicochemical conditions including pH and ionic strength. The data showed that the mean hydrodynamic size of the polyplex aggregates increased from around 100 nm to greater than 2000 nm over a period of 3 hours. The largest particles that could be measured with confidence in this study were about 3000 nm, which was the practical upper limit of the particle analyser. The rate of aggregation was found to depend strongly on the initial size of the polyplexes, and the solution pH and ionic strength. The impact of pH and ionic strength on the stability of the polyplexes was described adequately by the zeta potential, which was measured for each system in this study. The results, obtained

for poly-L-lysine/calf thymus DNA complexes, were confirmed by additional experimental data obtained for poly-L-lysine/plasmid DNA complexes. A two-particle interaction model for the electrical double layer and van der Waals interactions, based on the classical Derjaguin-Landau-Verwey-Overbeek (DLVO) theory, was used to provide a theoretical basis for the susceptibility to aggregation of a given polymer/DNA formulation. The results were used to describe qualitatively the trends observed in aggregation of the polyplexes, and allowed general conclusions about factors that influence the stability of DNA complexes to be drawn. In addition, static light scattering from the polyplex aggregates was measured using photon correlation spectroscopy to obtain information on their internal structure, fractal dimensions and aggregation regimes.

In addition, experiments were carried out with a non-viral integrin-mediated transfection system developed in a parallel study at the Institute of Child Health, University College London Medical School, as part of a gene therapy programme aimed at treating immunodeficiencies, some cancers and cystic fibrosis. In this study, new material properties were obtained for these vectors. These results indicate the conditions in which the complexes are likely to aggregate. It was shown that complexes produced in distilled water have a mean size of less than 150 nm and remain relatively stable following initial complexation up to 1 week. These physicochemical characterisation studies were complemented by *in vitro* transfection of monkey kidney epithelial line COS-7 cells. In parallel experiments performed by collaborators at the Royal Free and University College Medical School, local delivery of the vector to the lungs of mice had demonstrated improved transfection efficiency, i.e. comparable to that observed previously for adenoviral vectors and better than cationic liposomes.

CHAPTER 2

LITERATURE REVIEW

A brief introduction to non-viral or synthetic gene delivery systems is given in Section 2.1. The following two sections highlight some of the important physicochemical and biological properties for successful gene delivery systems (Section 2.2) and the various biological barriers to gene transfer (Section 2.3). An overview of gene delivery systems is given in Section 2.4. In particular, attention is paid to synthetic gene delivery systems incorporating cationic polymers and/or cationic lipids as they are of major interest for the experiments and simulations in this research project. The potential application of such systems for therapeutic use will require approval from regulatory authorities, thus indicating the importance of developing analytical techniques for characterisation of the formulation, reproducibility in preparation procedure, and real-time testing of shelf stability for extended storage before administration (Middaugh *et al.*, 1998). Various analytical techniques used in the characterisation of non-viral formulations are discussed in Section 2.5. The chapter concludes with a brief outline of future prospects for gene therapy and DNA vaccines (Section 2.6).

2.1 Gene delivery

Gene therapy, the transfer of genes to cells for the treatment or prevention of disease, and DNA vaccination, which is based on the direct inoculation of DNA in order to raise immune responses, have enormous potential. The first gene therapy protocols were designed to correct inherited disorders such as cystic fibrosis, hemophilia, Gaucher's disease and Duchenne muscular dystrophy (Anderson, 1998; Nishikawa and Huang, 2001; Zabner *et al.*, 1993). More recently, advances in the genetic basis for disease have led to the development of gene transfer as a tool for curing acquired genetic defects, e.g. cancer and AIDS (Pardoll, 1993; Riddell, 1996; Roth and Yarmush, 1999). This has been reflected by the significant research interest in gene transfer technology over the past decade (Felgner *et al.*, 1999; Mountain, 2000). Important genes connected to diseases, such as Alzheimer's disease and breast and colon cancers, are being identified by genomics and proteomics, hence increasing potential clinical applications and necessitating the development of safe and efficient formulations for gene therapy and DNA vaccines.

The application of nucleic acids as pharmaceutical products is advantageous because DNA and RNA, which represent the genetic code for the manufacture of therapeutic proteins, allows for medicine to focus on the causes of the disease rather than the symptoms. Gene therapy is the process in which corrective genes are introduced into cells to modify the specific genes that result in the disease being treated. The mode of delivery can be viral or non-viral. Both approaches have been used to introduce purified recombinant genes into living cells *in vitro* (cultured cells) and *in vivo* (humans and animals). In the former approach, target cells are removed from the patient for transfection, followed by a selection process, after which the surviving transfected cells are reintroduced into the body. This allows the circumvention of many of the biological barriers encountered within the body, with the advantage of more efficient gene transfer and the prospect of cell propagation to generate higher cell doses. Drawbacks associated with this method include major time and labour demands, and the patient may encounter cell immunogenicity. The *in vivo* procedure involves direct transfer of the vector to the

patient by one of several administration routes, e.g. systemic, intramuscular, oral, topical, ocular or alveolar (Kabanov, 1999). Its advantages include being non-specific to the patient, and reduced cost, logistics and infrastructure requirements (Mountain, 2000). Currently, the major obstacles to successful *in vivo* gene therapy are the uptake and expression of the transgene by the appropriate target cells, as well as interactions of the gene delivery system with macromolecules present in body fluids. These barriers to gene transfer, described later in Section 2.3, may account for the low gene expression levels observed with this mode of gene transfer in comparison to the *in vitro* method.

The development of gene-based vaccines as a unique and effective means of immunisation has progressed rapidly alongside approaches to non-viral gene therapy. DNA vaccination, which is a form of gene therapy, also involves the introduction of recombinant DNA into cells. However, instead of gene replacement or the integration of new genes, as is the aim of gene therapy, cell transfection is followed by expression of antigenic proteins encoded by the DNA vaccine, which in turn induces an immune response to the plasmid-encoded antigen. These proteins can induce humoral (antibody-type) immune responses when they escape from cells, as well as cell-mediated (helper T-cells and killer T cells) immunity when their peptide fragments are carried to the cell surface and displayed in a particular way. DNA vaccines have no risk of infection because they lack the genes responsible for a pathogen replication. Many excellent detailed reviews of gene-based vaccines and their mechanisms in inducing immune responses have been published, which are beyond the scope of this chapter, and the reader is referred to them (Davis, 1999; Donnelly *et al.*, 1997; Lai and Bennett, 1998; Leitner *et al.*, 2000; Mor, 1998; Pardoll, 1993; Wahren, 1996).

The development of molecular biology techniques in the past few decades has led to the design of viral gene delivery systems that involved the packaging of recombinant genes into nonreplicating, recombinant viral vectors while exploiting the ability of viruses to expertly package and deliver nucleic acids to host cells. Viral gene delivery systems, which include retrovirus (Rv) (Valsesia-Wittmann *et al.*, 1996), adenovirus (Ad)

(Wickham *et al.*, 1997), adeno-associated virus (AAV) (Linden and Woo, 1999; Wagner, 1998a), lentivirus (Poeschla *et al.*, 1998) and herpes simplex virus (HSV) (Laquerre *et al.*, 1998; Toda *et al.*, 1999), represent the most widely used approach to date. Approximately 70% of gene therapy clinical protocols in 2001 involved viral-mediated techniques (www.wiley.co.uk/genmed/clinical, 2001).

Although viral systems show high efficiency and specificity in conveying transgenes, non-viral vectors are anticipated to be the preferred choice in the future. Synthetic or non-viral gene delivery systems are regarded as attractive alternatives owing mainly to their safety, decreased immunogenicity, ability to package large-size DNA fragments, and relatively simple manufacturing (Crystal, 1995; Ledley, 1996; Mahato *et al.*, 1999). Synthetic DNA delivery systems, dealt with in this work, typically employ (anionic) liposomes to encapsulate the recombinant plasmid DNA, cationic lipids or polymers to condense and complex the plasmid DNA, or lipid/polymer combinations. However, delivery of the therapeutic genes to the target cells on *in vivo* administration by the non-viral approach is inefficient and often leads to low and/or transient expression levels, thus requiring frequent administration. Efforts to increase their potency hence remains a considerable challenge for the realisation of gene therapy (Lai and Bennett, 1998; Luo and Saltzman, 2000). Other limitations include their *in vivo* sensitivity to serum proteins and formulation instability. The major design hurdles in non-viral gene delivery include the need to increase gene efficiency and target specificity, and regulation of the transgene. Ultimately, the choice of vector type depends on the associated advantages and disadvantages for the intended applications (Crystal, 1995).

2.2 Specific requirements of synthetic gene delivery systems

The design criteria upon which synthetic gene delivery systems (Table 2.1) are based have yet to be met satisfactorily. An important source of data, the National Center for Biotechnology Information's (NCBI; Rockville, MD) MEDLINE database (www4.ncbi.nlm.nih.gov/PubMed/, 2001), indicates an exponential growth in preclinical research and clinical development of non-viral gene delivery. These research efforts encompass an interdisciplinary field with a wide range of topics including synthesis and characterisation of various gene delivery systems, improvement and control of the vector efficacy, applications in clinical trials, understanding of the mode of formation of complexes and the related physical structure, and statistical descriptions of the colloidal interactions of the formulations in the vial and during systemic biodistribution. A gene therapy product is expected to achieve regulatory approval in the twenty-first century, yet advances in the bioprocessing of these vectors are still necessary for development of a stable, single-vial formulation and facilitation of scale-up production (Levy *et al.*, 2000a; Lyddiatt and O'Sullivan, 1998; Marquet *et al.*, 1995).

2.3 Barriers to cellular gene delivery

Successful gene transfer involves the delivery of the transgenes from the site of injection to the surface of the target cells, and subsequent uptake and transport across various intracellular barriers before reaching the cell nucleus. Consequently, the design of a gene delivery system must take into account these various barriers that the recombinant plasmid has to overcome before expression of its encoded therapeutic genes can occur. Like viruses, the synthetic gene delivery system must contain the necessary structural elements required for efficient plasmid condensation, binding to the target cell surface receptor, membrane fusion and nuclear targeting. Fig. 2.1 illustrates the major biological barriers to the gene delivery system in the cell.

Table 2.1 Criteria for the ideal gene delivery system for in vivo gene therapy.

Requirement	*Rationale*
Ease of synthesis, purification and characterisation	Large-scale commercial manufacture and scale-up
Inexpensive/cost-effective	Widespread accessibility
Reproducibility and process control	cGMP guidelines, scale-up potential, quality control criteria
Non-toxic, non-immunogenic, biocompatible/suitable for systemic administration	Safety profile, pharmaceutical drug requirements, minimise likely toxic effects on cells and tissue
Control/regulation of transgene expression for desired period	Therapeutic effect, efficacy
DNA condensation ability (smaller than approximately 150 nm)	Efficient extravasation into target organs and tissues
Protection of plasmid from nuclease degradation/biological stability	Prolonged circulation to increase prospects of reaching target
Extended shelf-life stability	Storage and shipping
Cell-specific targeting and uptake	Efficient gene delivery and expression
pK_a between lysosomal pH (~5.0) and cytoplasmic pH (~7.2)	Efficient release of polyplexes from endocytic vesicles or lysosomal compartments into cytoplasm
Improved vector design for trafficking to the nucleus	Nuclear-associated gene expression

Source: Mumper and Klakamp, 1999

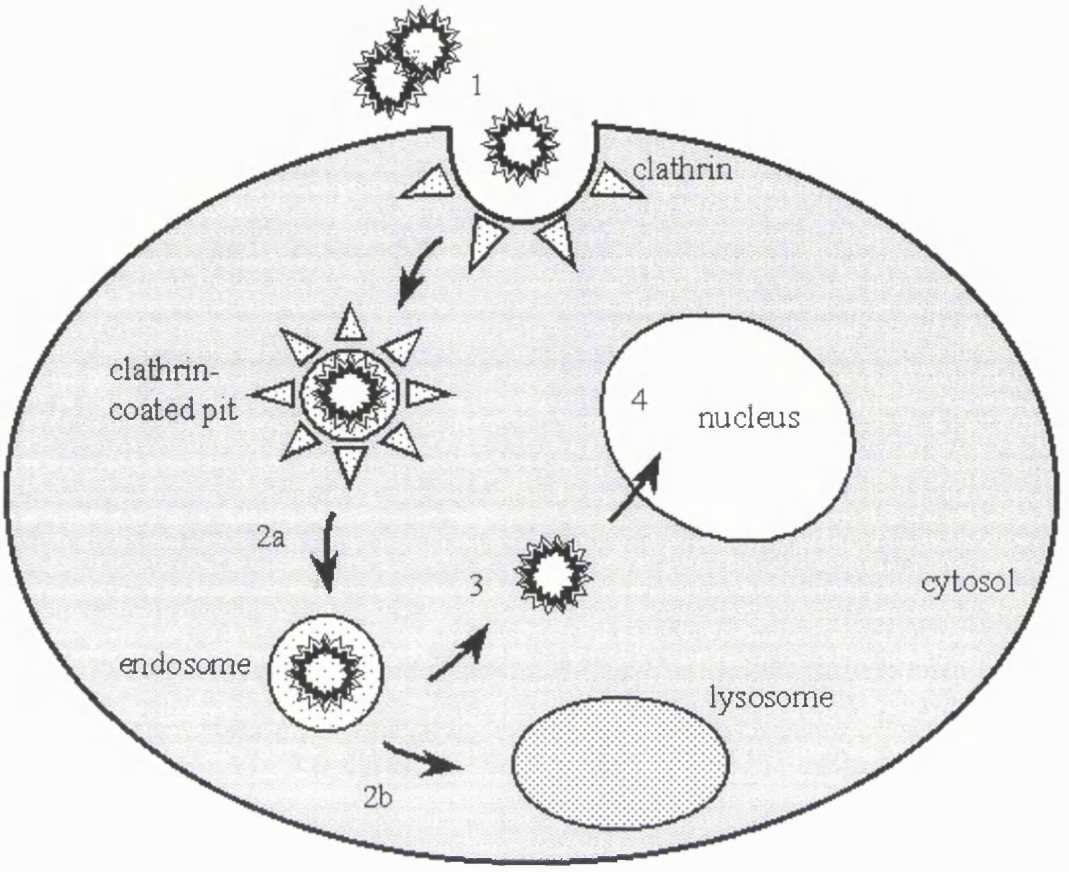

Figure 2.1 Schematic representation of DNA uptake into the cell and intracellular transport: (1) cellular access after transport in blood circulation to targeted cells or tissues, followed by uptake through endocytosis; (2) cytoplasmic trafficking of the transgene: (a) fusion of clathrin-coated vesicles with endosome compartments, (b) accumulation and degradation in lysosomal compartments; (3) release of plasmid from endosome into cytoplasm, dissociation from the synthetic vector, and entry into the nucleus; (4) after entering the nucleus, DNA must escape purging mechanisms and participate in transcription.

In systemic administration, an important requirement is the prolonged circulation of these colloidal vectors in the plasma (Dash *et al.*, 1999). The main biological barriers to the biodistribution of these vectors comprise the blood circulation system that feeds the target tissues and the tissue-specific capillary endothelium through which small

macromolecules must proceed before reaching the target cells. Hence, stabilisation of the vector complexes is essential to minimise their interactions with blood components, for example, digestion by blood nucleases, opsonization following their binding to serum proteins such as lipoproteins and immunoglobulins, and clearance by macrophages in the liver and spleen. However, they must maintain adequate instability so that the transgenes can be released during later interactions in the target cell. In addition, the particles must be sufficiently small (≤ 100 nm) for efficient transport or fenestration through the pores of the capillary endothelia (Perales *et al.*, 1994).

The uptake of most macromolecules, including colloidal gene delivery vectors, into mammalian cells is thought to occur most frequently by clathrin-mediated endocytosis (Parkes and Hart, 2000). This form of uptake involves complementary binding of cell surface receptors to the extracellular synthetic vector complexes, followed by accumulation of the macromolecules in clathrin-coated pits, and then the invagination of the pits into the cytoplasm, and their pinching off to form clathrin-coated vesicles (illustrated in Fig. 2.1). The 100 nm internal diameter of these endocytic vesicles represents a limitation on the size of the internalised particles. However, endocytic internalisation of particles up to 1 μm in size have been reported and are thought to occur by other mechanisms (Pouton, 1999). Other endocytic pathways include non-specific internalisation following adsorptive macropinocytosis where large (0.5–2 μm) heterogeneous "macropinosomes" are formed, non-coated endocytosis, and a form of endocytosis via caveolae, small lipid-enriched plasma membrane domains. However, it has been established that the particles should be less than approximately 150 nm in diameter for endocytosis by various mammalian cells (Guy *et al.*, 1995).

Following endocytosis, the vectors move from early endosomes to late endosomal compartments, as well as lysosomal compartments, in an active cytoplasmic transport process that is regulated by compartment-specific proteins (Kabanov, 1999). For translocation to the nearby nucleus, the vector must be released from the late endosomes. This must take place before the endosomal contents are trafficked to the acidic lysosomal

compartments (pH of 4.5-5.0), where accumulation of the transgenes can result in degradation by hydrolytic enzymes. It is believed that this barrier to endosomal release is the rate-limiting step in gene delivery (Wagner, 1998b). The internal pH of the endosome is kept acidic at pH ~6 by membrane-contained, ATP-driven proton pumps that pump H^+ into the interior from the cytosol which has a pH of about 7.2. Incorporating pH-activated endosomolytic peptides into the gene delivery system may enhance plasmid release into the cytoplasm. This is thought to occur through the "proton-sponge" effect, whereby protonation of amino moieties on the plasmid-condensing polymer buffer the acidic pH of the endosome interior. At the same time, the lytic properties of the peptides are activated, thus causing osmotic swelling and destabilisation of the endosome membranes, followed by lysis and/or fusion (Mahato *et al.*, 1999; Pouton and Seymour, 1998). Two useful polycations that promote this effect are polyethyleneimine (PEI) (Boussif *et al.*, 1995; Pack *et al.*, 2000) and polyamidoamine cascade polymers (dendrimers) (Duncan *et al.*, 1998; Kukowska-Latallo *et al.*, 1996). Similarly, the endosomolytic drug, chloroquine, has been widely used in *in vitro* studies to aid the escape of macromolecules from the endosomes and lysosomes (Murphy *et al.*, 2001; Wagner, 1998b). A weak base with the ability to diffuse into low-pH compartments and inhibit the activity of hydrolytic enzymes, chloroquine can enhance transfection efficiencies. However, the use of chloroquine for systemic application holds little attraction because it is toxic to cells at the more useful high concentrations (> 10 μM), displays side effects in the body, and cannot be co-targeted to gene delivery systems (Pack *et al.*, 2000).

With cationic lipid/DNA delivery systems (lipoplexes) that are not conjugated to targeting ligands, cellular uptake occurs via electrostatic interactions and endocytosis (Chesnoy and Huang, 2000). Following endosomal uptake, the lipoplexes are thought to interact with anionic lipids present in the endosome membrane to promote membrane fusion and subsequent release of the DNA (Xu and Szoka, 1996). This membrane destabilisation process involves flip-flop of the endogenous anionic lipids followed by subsequent formation of charge neutral ion pairs with cationic lipids. The lipid is uncoupled from the DNA which then enters the cytoplasm (Pouton, 1999).

The next major intracellular barrier is the nuclear membrane. The nuclear envelope is perforated by nuclear pores with a size of approximately 25 nm that permit passive diffusion of water-soluble macromolecules no greater than 70 kDa into the nucleus (Pouton, 1999). Larger macromolecules gain access to the nucleus via interactions with the nuclear pore active transport system (Boulikas, 1998). The translocation of the vector complex to the nucleus requires a nuclear localisation signal (NLS). NLSs are amino acid motifs that are present in nuclear proteins and many viruses, e.g. influenza virus and adenovirus. In endeavours to improve plasmid import into the nucleus, scientists have exploited the nuclear transport properties of NLSs by attaching, both noncovalently and covalently, cationic NLS-containing-proteins, peptides or lipids to the purified plasmid (Aronsohn and Hughes, 1998; Branden *et al.*, 1999; Morris *et al.*, 1999). Following successful nuclear uptake of the plasmid, most of the exogenous DNA remains extrachromosomal whilst a small proportion may be incorporated into the host cell genome, leading to persistent expression of the transgene.

In receptor-mediated endocytosis or ligand-mediated uptake, the gene delivery system may utilise ligands, which are conjugated to the DNA-condensing polycation for targeting to the appropriate cellular receptor. Such ligands include transferrin (Liang *et al.*, 2000), the folate receptor (Sudimack and Lee, 2000; Wagner *et al.*, 1990) the asialoglycoprotein receptor (Planck *et al.*, 1992), and Arg-Gly-Asp (RGD)-containing peptides (Hart *et al.*, 1998). This method offers opportunities for cell-specific targeting.

There are several reports describing the biodistribution and intracellular trafficking of cationic polymer/DNA complexes but it is not easy to compare data between them due to the variety of techniques and formulations used (Godbey and Mikos, 2001). Generally, with several different formulations and cell types, several mechanisms of gene delivery have been proposed and experimentally demonstrated. For example, following endocytosis and endosomal escape, polylysine/DNA (PLL/DNA) complexes (without chloroquine) were degraded in lysosomal compartments, whereas poly(ethylenimine)/DNA (PEI/DNA) complexes remained as intact structures even

during entry into the nucleus (Godbey *et al.*, 1999; Godbey *et al.*, 2000). Results from these studies are shown in Figs. 2.2 (PEI/DNA) and 2.3 (PLL/DNA). Results similar to that of PEI/DNA complexes were observed for the delivery of short oligonucleotides by starburst polyamidoamine (PAMAM) dendrimers, in which the dendrimer/oligonucleotide complexes remained associated throughout the delivery process, including nuclear uptake (Yoo and Juliano, 2000). Intracellular tracking of plasmid DNA complexed with an integrin-targeting peptide and a cationic liposome has also been studied (Colin *et al.*, 2000). Additionally, chemical modification of the surface of these complexes, typically through fluorescent labelling in order to track their intracellular paths, may also affect other biophysical properties, including the transfection efficiency. Further research is required to allow a deeper understanding and satisfactory explanations of these mechanisms, especially that of active uptake into the nucleus, as well as to help enhance gene transfer efficiencies.

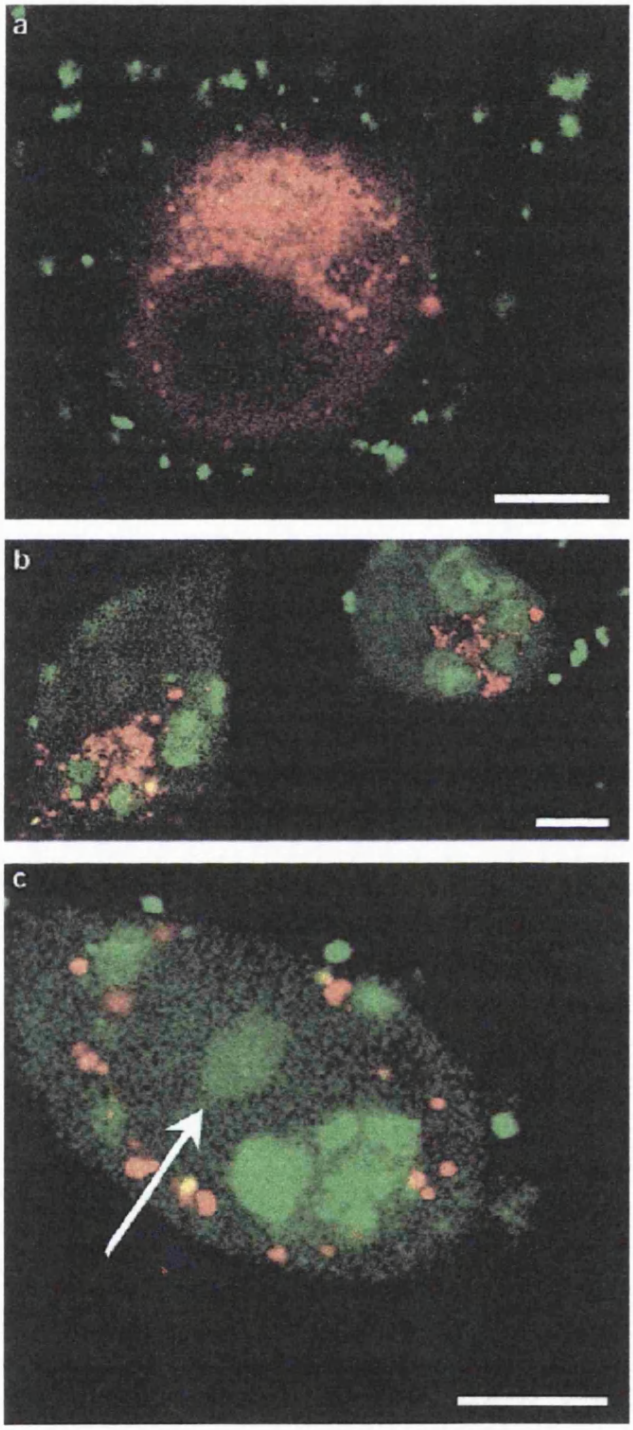

Figure 2.2 Confocal images showing cellular trafficking of labelled poly(ethylenimine)/DNA (PEI/DNA) complexes (green) in cells with labelled lysosomes (red) at various time points following transfection: (a) 2 h — clumps of PEI/DNA complexes are present on the cell surface and lysosomes are scattered throughout the cytoplasm; (b) 3 h — PEI/DNA complexes are located in endocytotic vesicles and are somewhat surrounded by lysosomes. There is no overlap of PEI and lysosomal probes; (c) 5 h — PEI/DNA complexes have entered the nucleus (arrow) while cytoplasmic vesicles containing PEI/DNA complexes still have not fused with lysosomes. (Bar = 10 μm.) Source: Godbey et al., 2000.

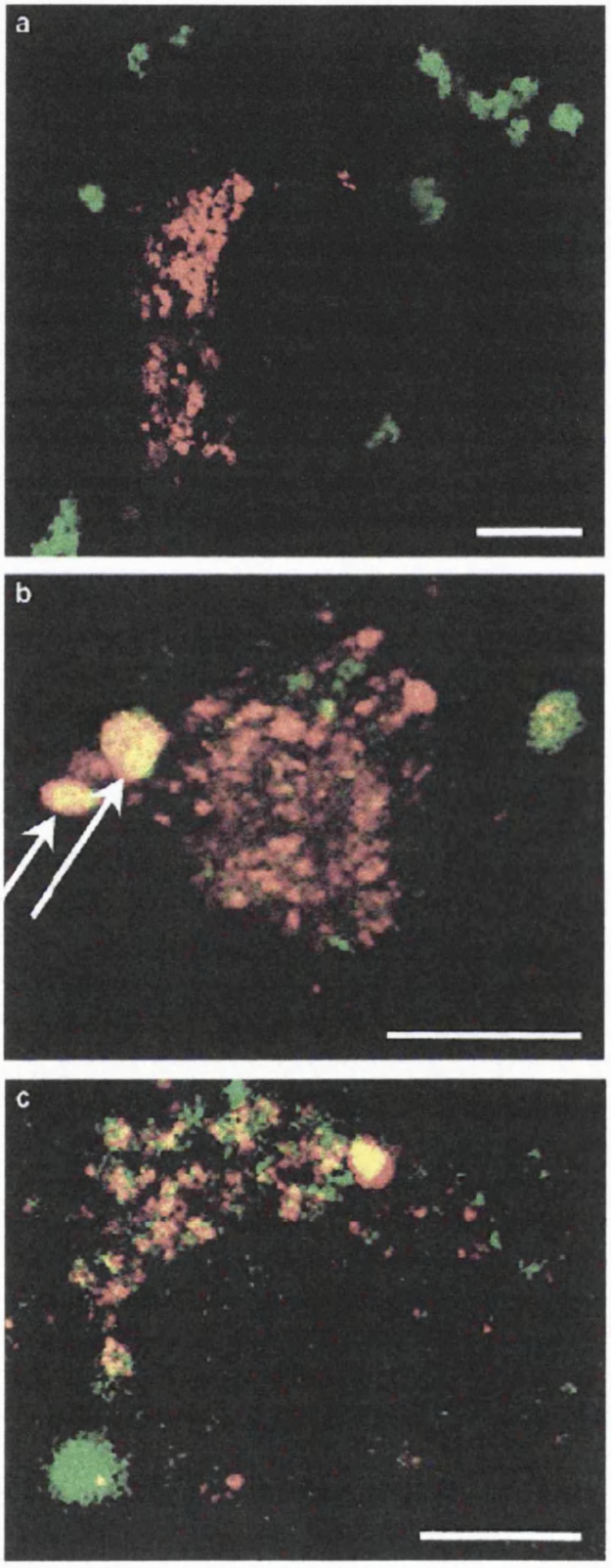

Figure 2.3. Confocal images showing cellular trafficking of labelled polylysine/DNA (PLL/DNA) complexes (green) in cells with labelled lysosomes (red). Times post-transfection are as follows: (a) 2 h — as with PEI, PLL/DNA complexes aggregate in clumps on plasma membrane; (b) 4 h — after the PLL/DNA complexes enter the cytoplasm, they meet up with lysosomes. These complex/lysosomes (endolysosomes) are indicated by yellow colour and denoted by arrows; (c) 5 h — the large endolysosomes are quickly dissipated as the PLL/DNA complexes are degraded. (Bar = 10 μm.) Source: Godbey et al., 2000.

2.4 Gene delivery methods

Currently, therapeutic genes are delivered to a target cell population by two main types of vectors, i.e. viral and non-viral. Non-viral vectors can be further divided into two categories: delivery of purified DNA complexed with a carrier and delivery of naked DNA by physical methods. The various vehicles for gene delivery systems have resulted in a diversity of clinical protocols, as shown in Fig. 2.4. The following table (Table 2.2) provides a list of the commonly employed vectors in preclinical and clinical gene therapy research, alongside their major advantages and disadvantages.

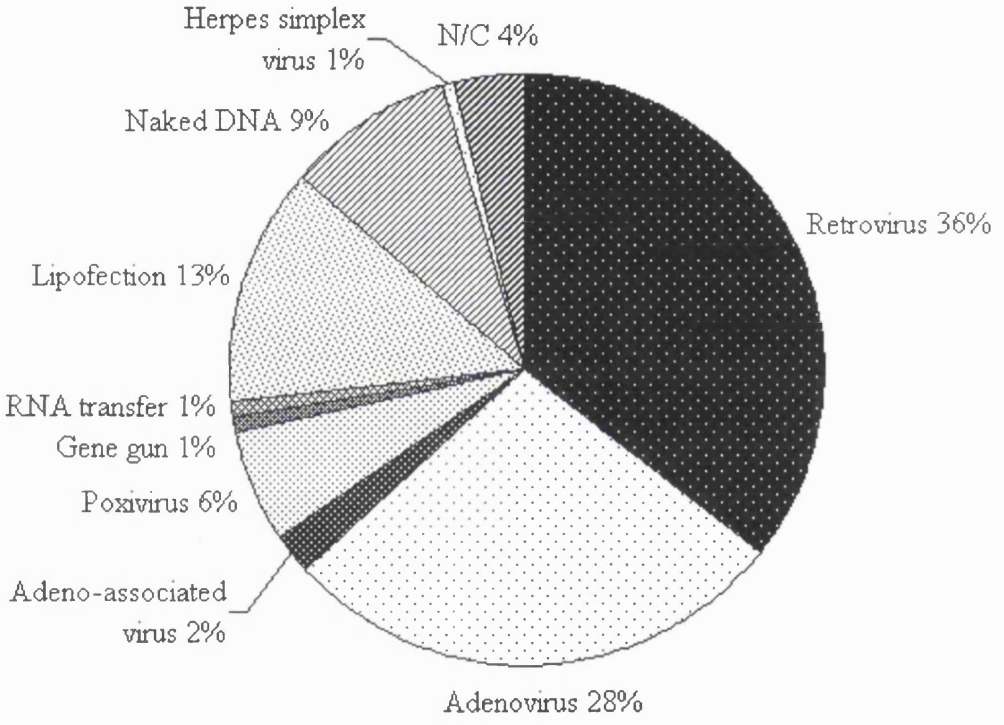

Figure 2.4 Distribution of protocols by vector. The pie chart shows the distribution of gene transfer clinical protocols approved by or submitted to regulatory authorities in Europe and the U.S. by type of vector, and also reflects the distribution of patients treated. Note that the number of protocols that employ lipofection, the most common non-viral approach, and the patients receiving treatment by these protocols, are less than half those occurring by retroviral gene transfer. Source: (www.wiley.co.uk/genmed/clinical, 2001).

Table 2.2 Comparison of commonly used methods for gene transfer.

Vector	*Advantages*	*Disadvantages*
Retrovirus (Rv)	• Widespread use in *ex vivo* gene transfer trials • Prolonged expression *ex vivo* • High transfection efficiencies *ex vivo* • Low immunogenicity	• Chronic over-expression and insertional mutagenesis risks • Maximum insert size 10 kb • Sensitivity to inactivation • Target cells must proliferate for integration of proviral DNA • Difficult recombination, rearrangements, and low titres
Adenovirus (Ad)	• Substantial clinical experience • Suitable for *in vivo* transfer • High titre (> 10^{11}-10^{12} per ml) • Efficient transfer to replicating and nonreplicating cells • Low risks of permanent genotype alteration and mutagenesis	• Maximum insert size 7.5 kb • Limited expression duration • Non-specific inflammation and antivector cellular immunity • Difficulties in manufacture, storage, and quality control
Adeno-associated virus (AAV)	• Low immunogenicity • Broad infectivity range • Very prolonged expression *in vivo*	• Maximum insert size 4.5 kb • Requires helper virus, possible formulation contamination • Risk of insertional mutagenesis • Manufacture and quality control very difficult • Very low titres

Table 2.2 (Continued)

Vector	*Advantages*	*Disadvantages*
Naked DNA	• Very low immunogenicity • Easy and simple manufacturing, quality control and storage • Very good safety profile	• Transient expression in majority of cells • Transfection efficiency *in vivo* and *ex vivo* very low • Very limited targeting capability
Artificial lipids	• Potentially unlimited insert size • Low immunogenicity • Low insertional mutagenesis risks • Relatively simple manufacturing, quality control and storage • Good safety profile	• Inefficient gene transfer *in vivo* • Transient gene product expression • Repetitive administration required • Unsubstantial clinical experience
Peptides	• Potentially unlimited insert size • Low immunogenicity • Low insertional mutagenesis risks • Relatively simple manufacturing, quality control and storage • Good safety profile • Targeting capabilities	• Inefficient gene transfer *in vivo* • Transient gene product expression • Unsubstantial clinical experience

2.4.1 Viral vectors

The majority of research, taking into account vector types and clinical trials, to date has focused on viral-based gene transfer methods (Anderson, 1998). Replication-deficient, recombinant viral vectors have been traditionally and widely used because of their inherent ability to condense DNA efficiently, enter target cells, avoid degradation, replicate using host cellular machinery, and provide long-term expression of the transduced gene. To construct a viral vector, the required healthy human gene is first isolated and spliced into a genetically altered virus. Along with the exogenous gene(s), the infectious non-replicating virus also contains promoters, enhancers, and genes for transcription and translation. The viruses are then produced in a packaging cell line that contains the necessary gene products to make the viruses. Although all viral vectors achieve gene delivery by infecting the target cells, different vectors employ distinct strategies, derived from their model virus counterparts, to mediate gene transfer.

As shown in Fig. 2.4, retroviral vectors are currently the most widespread viral gene therapy approach in clinical trials (www.wiley.co.uk/genmed/clinical, 2001). Retroviral vectors, which are usually approximately 80 to 130 nm in diameter, are capable of integrating permanently into the genome of the target cell for stable, long-term expression of the gene product (Andreadis *et al.*, 1997; Andreadis *et al.*, 1999; Braas *et al.*, 1996; Fry and Wood, 1999). However, in the future, adenoviral vectors are predicted to be the most likely choice for *in vivo* applications that require short-term transgene expression, whilst adeno-associated viral vectors will find increased use in the long term replacement of defective proteins (Mountain, 2000). Recombinant adenoviral vectors have so far shown the highest gene transfer efficiency *in vivo* in a wide range of host cells (Lu *et al.*, 1999; O'Malley, Jr. and Couch, 1999; Watkins *et al.*, 1997). Adeno-associated virus vectors are relatively new to the field. They consist of small, single-stranded DNA virus genomes with virtually no viral genes, and require a wild-type helper virus, usually adenovirus or herpes simplex virus, for replication (Samulski *et al.*, 1989; Verma and Somia, 1997).

Other viral vectors undergoing development for gene transfer include herpes simplex virus (HSV), vaccinia virus, human papilloma virus, poliovirus, RNA virus, baculovirus, and avipox (pox) virus. HSV is a large (152 kb) double-stranded DNA virus that can accommodate 40-50 kb of foreign DNA. Its ability to express many residual, cytopathic viral proteins limits its clinical applications. Nevertheless, HSV presents an attractive option for the targeting of neuronal tissue in brain cancer gene therapy. Vaccinia virus has transient expression and is also suitable for cancer gene therapy. For reviews of viral vectors, (Peng and Russell, 1999; Verma and Somia, 1997) serve as excellent references.

2.4.2 Synthetic vectors

Non-viral approaches to gene transfer, utilising synthetic gene delivery systems, have been the focus of intensive study over the past several years. Ongoing research and development of various non-viral vectors for commercial products testify to the significant potential of these systems. The advantages of non-viral systems (Table 2.2), such as excellent targeting, low immunogenicity, and reliable large-scale manufacture at relatively reduced costs, make them very attractive alternatives to the viral approach. However, prolonging expression of the therapeutic genes considerably beyond the current typical period of only a few days remains a major challenge (Mountain, 2000).

In 1997, a committee of leading scientists in the research area of synthetic gene delivery met to resolve the increasingly troublesome problem of terminology for these systems as more publications emerged in this field. A common nomenclature was determined (Felgner *et al.*, 1997). Complexes produced upon the mixing of nucleic acids (DNA, RNA, or synthetic oligonucleotides) with a cationic polymer, cationic lipid, or combination thereof were termed "polyplex" (cationic polymer/nucleic acid complex), "lipoplex" (cationic lipid/nucleic acid complex), and "lipopolyplex" (cationic polymer/cationic lipid/nucleic acid), respectively. Likewise, the transfection by cationic polymers and cationic lipids were termed "polyfection" and "lipofection", respectively. In this work, DNA complexes shall be referred to by these terms.

2.4.2.1 Physical methods

"Naked" plasmid DNA without any viral or non-viral association is the simplest form of gene delivery, and gives virtually insignificant expression in cell culture transfection experiments. Nevertheless, naked DNA injected *in vivo* demonstrates activity, especially in muscle, as first shown by researchers at Vical, Inc. and the University of Wisconsin (Wolff *et al.*, 1990; Wolff *et al.*, 1992). Furthermore, transfection efficiencies can be as high, if not higher, as those observed with equivalent non-viral gene delivery systems (Yang and Huang, 1996). Physical methods of gene delivery, usually mechanical and electrical procedures, tend to have limited applicability compared to other gene transfer approaches. However, several of the available techniques such as needle-free injectors and electroporation are promising (Mountain, 2000; Wells *et al.*, 2000). Despite being laborious and time-consuming, microinjection of DNA directly into the tumour cell nucleus has long been employed in *in vitro* studies where individual cell manipulation is necessary. Electroporation, which employs strong electrical pulses to transiently create pores in the target cell, hence allowing the DNA to enter the target cells, is a more efficient approach for *in vitro* applications (Lockie *et al.*, 1999). The more recent "gene gun" approach, or biolistic particle delivery, entails the use of electrical currents and magnetic properties to accelerate DNA-coated microparticles of gold or tungsten into cells (Luo and Saltzman, 2000; Mahvi *et al.*, 1997).

Since free DNA as a gene delivery system is unsuitable for targeting to many cells and tissues, its applications are limited to superficial layers of the body that are available for direct injection such as the skin, or cancer gene therapy where the expression vector DNA can be injected directly into the tumour. The most encouraging applications of naked DNA at present are the injection or gene gun delivery in preventative vaccination against infectious diseases, and the delivery of naked DNA containing genes promoting angiogenesis for cardiovascular disorders (Donnelly *et al.*, 1997; Mountain, 2000). The mechanism by which *in vivo* delivery of naked plasmid DNA to the cells occurs is still unknown (Lockie *et al.*, 1999) and further studies are needed to better exploit this method of gene delivery (Nishikawa and Huang, 2001).

2.4.2.2 Cationic lipid-based gene delivery systems

In vivo use of cationic lipids as synthetic gene delivery systems is being actively pursued today. Cationic lipid/nucleic acid complexes, or lipoplexes, provide efficient transfection for many cell types and are currently being evaluated in phase I and phase II clinical trials, for example, in the treatment of cystic fibrosis (Caplen *et al.*, 1995), or the direct or immunological killing of tumour cells (Stopeck *et al.*, 1997). Another promising application for cationic liposomes is DNA vaccines (Gregoriadis *et al.*, 1997). The interested reader is referred to recent reviews that discuss various formulations and their applications (Chesnoy and Huang, 2000; Chonn and Cullis, 1998; Hope *et al.*, 1998; Lasic and Templeton, 2000; Podgornik *et al.*, 2000; Scherman *et al.*, 1998; Thierry and Mahan, 1999).

Liposomes are phospholipid bilayer vesicles that entrap a fraction of aqueous fluid. They possess structures resembling that of biological membranes. Their hydrodynamic diameter is similar to that of supercoiled DNA in an aqueous environment, i.e. more than 100 nm. Cationic liposomes are prepared from synthetic amphiphilic molecules with a hydrophilic head group that carries the single or multiple positive charges, and a hydrophobic portion of, for example, fatty acyl, alkyl or alkoxy chains. They interact hydrophobically and electrostatically with DNA to spontaneously form complexes. These liposomes will also interact with the cell membrane. The inclusion of dioleoyl phosphatidylethanolamine (DOPE), an inverted cone-shaped neutral ("helper") lipid, in lipoplexes promotes cytosolic release of the vector by fusion to and/or disruption of the plasma and endosomal membranes. One example is the well-known transfection reagent, Lipofectin, a cationic liposome composed of 1:1 (w/w) ratio of the cationic lipid *N*-[1-(2,3-dioleyloxy)propyl]-*N*,*N*,*N*-trimethylammonium chloride (DOTMA) and DOPE. Lipofectin was used in the present study (Chapter 5). Other commonly used cationic lipids include 2,3 dioleyloxy-*N*-[2(spermine carboxaminino)ethyl]-*N*,*N*-dimethyl-1-propanaminium trifluoroacetate (DOSPA), 1,2-dioleoyl-3-trimethylammonium propane (DOTAP), and 1,2-dimyristyloxypropyl-3-dimethyl-hydroxyammonium bromide (DMRIE). Fig. 2.5 shows the structures of some of these lipids. The behaviour of cationic

lipids, their interactions with DNA, and the structure of the resulting complexes are complicated and not fully understood, although numerous research groups have published varying studies on various lipoplex formulations (Hafez *et al.*, 2000; Harries *et al.*, 198; Huebner *et al.*, 1999; Kennedy *et al.*, 2000; Koltover *et al.*, 1999; Lewis and McElhaney, 2000; MacDonald *et al.*, 1999; May *et al.*, 2000; Oberle *et al.*, 2000; Tang and Hughes, 1998; Xu *et al.*, 1999). Several modes of formation, e.g. phase transitions and lipid restructuring, were proposed, to gain a better understanding of the resulting lipoplex structures and how the structures affect efficacy in transfection.

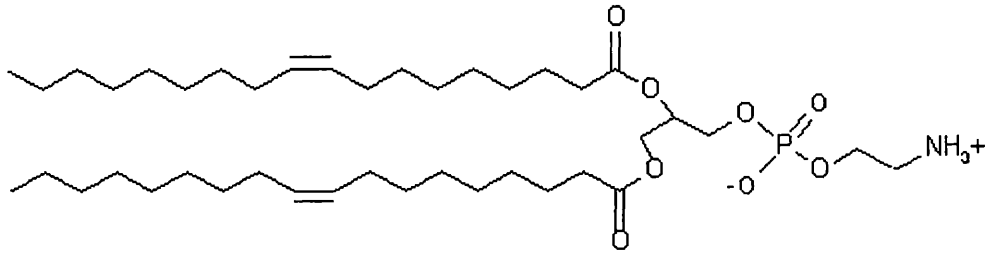

dioleoyl phosphatidylethanolamine (DOPE)

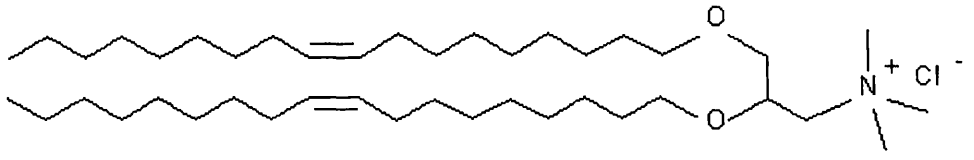

N-[1-(2,3-dioleoyloxy)propyl]-*N*,*N*,*N*-trimethylammonium chloride (DOTMA)

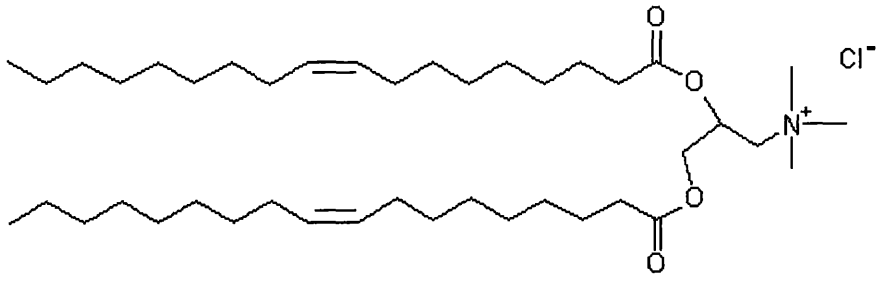

1,2-dioleoyl-3-trimethylammonium propane (DOTAP)

Figure 2.5 Three common types of lipid used in lipid-based gene delivery systems.

Cationic lipid/nucleic acid complexes, or lipoplexes, that possess a net positive charge mediate, by virtue of their charge, gene transfer. To enhance DNA delivery to the target cells and cellular internalisation of the transferred therapeutic gene, receptor ligands can be covalently attached to the vector. These ligands, such as transferrin (Simões *et al.*, 1999), monoclonal antibodies (Wang and Huang, 1987), or folate receptors (Lee and Huang, 1996), allow specific interactions with the target cells.

Liposomes with a net neutral or negative charge entrap DNA rather than complex with it. The latter are also known as pH-sensitive liposomes owing to their destabilisation at low pH conditions in the acidic endosomal environment. These liposomes have been shown to encapsulate plasmid DNA in their aqueous interiors, albeit inefficiently, by reverse-phase evaporation, repeated freezing and thawing, and detergent dialysis (Lee and Huang, 1997; Schoen *et al.*, 1998).

2.4.2.3 Cationic polymer-based gene delivery systems

Although the predominantly used synthetic vector in recent years is lipoplexes, increasingly, many workers are using cationic polymers for both *in vitro* and *in vivo* DNA delivery owing to their versatility. The most common cationic polymers are polylysines (Dash *et al.*, 1999; Ramsay *et al.*, 2000; Wu and Wu, 1987; Zauner *et al.*, 1997), polyarginines, polyethyleneimine (PEI) (Gautam *et al.*, 2000; Godbey *et al.*, 1999; Goula *et al.*, 1998), spermine (Blagbrough *et al.*, 2000), spermidine (Gosule and Schellman, 1976), dendrimers (Bielinska *et al.*, 1999; Kukowska-Latallo *et al.*, 1996), and chitosans (Koping-Hoggard *et al.*, 2001; Lee *et al.*, 1998). The cationic peptide poly-L-lysine (PLL), which efficiently condenses DNA, has been used in many studies, including the present one (see Chapter 4). However, disadvantages of PLL include polymer heterogeneity, toxicity and potential immunogenicity (Han *et al.*, 2000; Mumper and Klakamp, 1999).

Like lipid-based systems, cationic polymers can be conjugated to targeting ligands, such as antibodies or antibody fragments, vitamins, glycoproteins and peptides, for delivery of DNA to specific tissues. For example, poly-L-lysine conjugated with the asialoorosomucoid (AsOR) ligand, which allows attachment to a liver-specific asialoglycoprotein receptor, has been used in *in vivo* studies of gene delivery to the liver (Kwoh *et al.*, 1999; Perales *et al.*, 1997). Other targeted systems include transferrin-conjugated PEI (Kircheis *et al.*, 1999; Ogris *et al.*, 1998) and polylysine linked to epidermal growth factor (Schaffer and Lauffenburger, 1998; Schaffer *et al.*, 2000; Xu *et al.*, 1998). Arg-Gly-Asp (RGD)-containing peptides are another commonly used targeting ligand. The RGD sequence is found in many extracellular matrix proteins including integrin, vitronectin, laminin, fibrinogen and fibronectin. A bifunctional peptide comprising a DNA-binding moiety of 16 lysine residues and a cyclic integrin-targeting domain was used in the present study (see Chapter 5). Previously, it has been used in *in vitro* transfection of human tracheal cells (Colin *et al.*, 1998), keratinocytes (Compton *et al.*, 2000), fibroblasts from patients with lysosomal storage diseases (Estruch *et al.*, 2001), and corneal endothelial cells (Hart *et al.*, 1998), as well as *in vivo* transfection of lungs of rats (Jenkins *et al.*, 2000).

One limitation to the use of cationic polymer/DNA complexes, or polyplexes, for *in vivo* gene delivery is their tendency to bind with blood proteins, lipids, carbohydrates and other molecules. Polyplexes may interact with and become coated by specific plasma proteins in a process known as opsonization, resulting in their clearance. They may also be destabilised by salt-induced aggregation or enzymatic degradation. The overall surface charge of the polyplexes may also affect their binding to cell surfaces, which have many areas of high negative charge density, contributing to non-specific binding rather than active targeting of the polyplexes to a specific site.

The importance of DNA release from complexes was demonstrated in a recent study using imidazole-containing endosomolytic polymers to transfect mammalian cells *in vitro* (Schaffer *et al.*, 2000). Other studies have focused on steric stabilisation of the vector

complexes by using cationic polymers conjugated with linear polyethylene glycol (PEG) (Choi *et al.*, 1999; Ogris *et al.*, 1999). To improve the effectiveness of synthetic formulations, the use of both peptide-based polycations and liposomes in designing an optimised synthetic vector represents the most viable option. Such a vector would be likely to have a chemistry of multiple components for DNA condensing, cell-targeting, endosome-disrupting and nuclear-translocating elements (Mahato, 1999). Hence the ideal vector should comprise the following components: 1) a gene core of condensed plasmid DNA, nuclear localisation signal, and integration signal, 2) a fusogenic layer of pH-sensitive, membrane-destabilising polymer-lipid surrounding the DNA centre for cytoplasmic release, 3) an external steric coat of cleavable hydrophilic block copolymer to prolong circulation and promote stability, and 4) exposed binding ligands conjugated to the outermost layer, for cell-specific targeting (Dyer and Herrling, 2000). For a comprehensive description of polymeric gene delivery systems the reader is referred to excellent reviews on the topic (De Smedt *et al.*, Hart, 2000; Lasic and Templeton, 2000; Mahato, 1999; Mahato *et al.*, 1999; Mumper and Klakamp, 1999; 2000).

2.5 Characterisation of synthetic gene delivery vectors

Gene delivery and expression are dependent on various physicochemical factors relating to the formulated DNA complexes. Hence, in order to improve the effectiveness of gene transfer, it is important to understand the properties of DNA complexes as well as determine which properties are crucial. The methods to characterise DNA complexes are critical in assessing whether the complexes have reproducible physical properties and in the prediction of transfection efficiency. Additionally, to proceed into advanced clinical trials, regulatory agencies including the World Health Organization (WHO) and the US Food and Drug Administration (FDA) have specified that it is necessary for gene therapy products to be assessed in the same pharmaceutically rigorous fashion as other pharmaceutical products, e.g. recombinant proteins (Marquet *et al.*, 1997a). The accurate characterisation of DNA formulations as a drug substance for therapeutic use involves establishing, among others, formulation purity, particle size, charge, morphology,

stability in physiological salt and serum, transfection efficiency and cytotoxicity (Mahato, 1999).

Bloomfield *et al.* have characterised extensively the DNA condensation process and related properties including morphology, topology, radius of gyration, and persistence length. The reader is referred to these excellent publications (Arscott *et al.*, 1990; Baumann and Bloomfield, 1995; Bloomfield, 1991; Bloomfield, 1996; Bloomfield and Rau, 1980; Deng and Bloomfield, 1999; Ma and Bloomfield, 1994; Plum *et al.*, 1990; Rouzina and Bloomfield, 1996; Rouzina and Bloomfield, 1997; Wilson and Bloomfield, 1979). This section deals with some of the available methods for the characterisation of DNA complexes in aqueous suspension. These tests can be broadly categorised according to the properties of the complexes, as given in Table 2.3. The stability of DNA complexes are governed by several factors, including the rate of mixing of the components, order of addition of the components, ionic strength of the solutions, and DNA concentration. Hence it is also crucial that these formulations are characterised under the appropriate conditions.

Table 2.3 Characterisation of DNA complexes according to their properties.

Property	*Technique*
Appearance	Electron microscopy (EM), atomic force microscopy (AFM)
Hydrodynamic behaviour	Dynamic light scattering (DLS), electrophoretic light scattering, centrifugation
Optical behaviour	Static light scattering (SLS), circular dichroism (CD)
Binding to cations	Fluorescence quenching, nuclease protection assay
Biological activity	*In vitro* or *in vivo* bioassay for gene expression or function

2.5.1 Direct visualisation

DNA complexes, typically of the order of up to 100 nm in size, have been observed and measured by conventional electron microscopy (EM). It was found that the favoured morphologies generated by DNA compacted using different condensing agents, such as polylysine, histones, spermine, spermidine and cobalt (III) hexaamine, were mainly toroids, and sometimes rods (Gosule and Schellman, 1976; Kwoh *et al.*, 1999; Laemmli, 1975; Plum *et al.*, 1990; Tang and Szoka, Jr., 1998). EM is susceptible to artefacts, like the reduction in apparent size of the complexes, owing to the drying and selective sampling of complexes during preparation of the grid for visualisation.

Atomic force microscopy (AFM) is an extremely valuable method for direct observation of DNA complexes on a single molecule level (Dunlap *et al.*, 1997; Golan *et al.*, 1999; Hansma *et al.*, 1998; Wolfert and Seymour, 1996; Ziady *et al.*, 1999). The method allows subnanometer resolution of the complexes, as well as measurement of the molecular width and height. Although uncondensed DNA molecules in buffers have been observed *in situ* under the microscope (Hansma *et al.*, 1993; Lyubchenko and Shlyakhtenko, 1997), references in which AFM imaging was applied to DNA complexes in a fluid cell were unable to be found for this literature review. Fig. 2.6 shows AFM images of asialoorosomucoid-polylysine/DNA complexes that were prepared in saline, immobilised onto mica surfaces, dried, and imaged in air (Hansma *et al.*, 1998). AFM has become increasingly utilised not only as an imaging tool, but also as a probe of interaction forces and mechanical properties for biological samples. The development of this technique is important as it will allow biomolecular interactions and structural details of DNA complexes to be measured (Colton *et al.*, 1997; Heinz and Hoh, 1999).

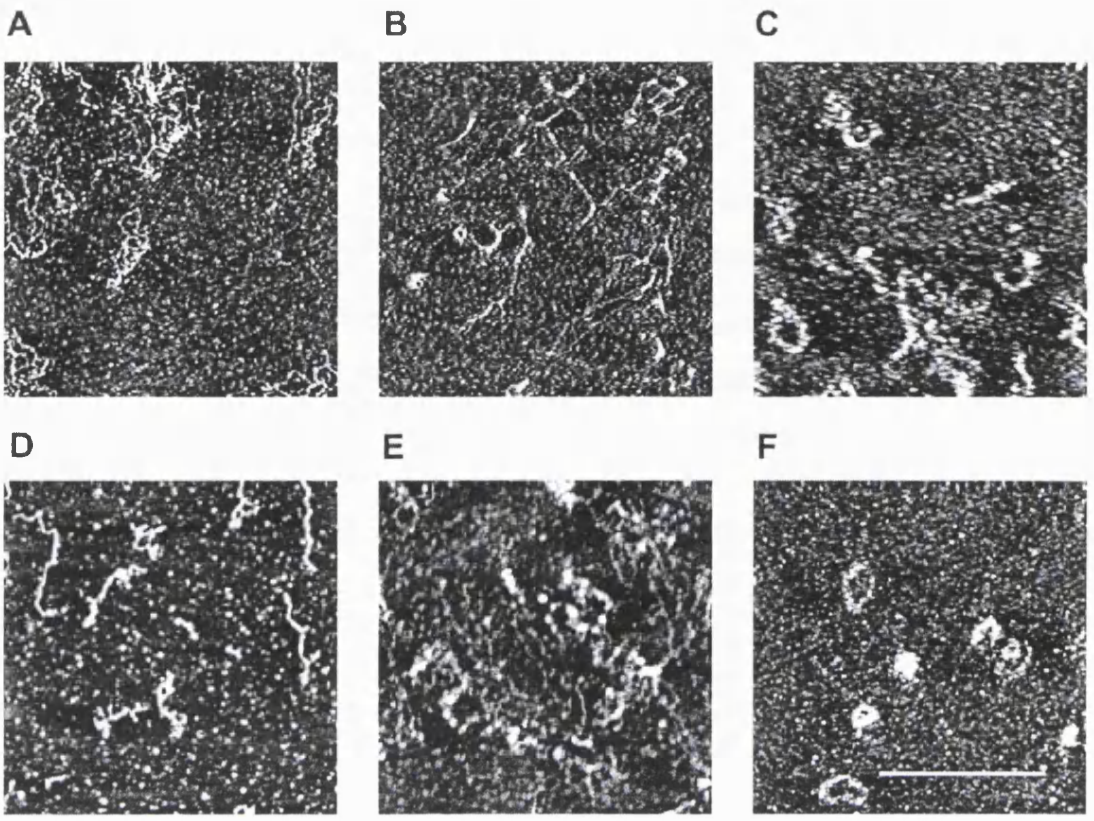

Figure 2.6 Atomic force micrographs of 2.9 kb plasmids complexed with asialoorosomucoid-polylysine. The DNA concentration was 10 ng/μl and the polylysine size was 10 kDa for all complexes. Complexes were prepared in: neutral saline (150 mM NaCl, pH ~7) (A – C), or alkaline saline (150 mM NaCl, 2 mM NaOH, pH ~11) (D – F), then dried and imaged by AFM in air. Charge ratios are: 0.5 (A and D), 0.6 (B and E), and 2 (C and F). Images are 2 × 2 μm. Scale bar 1 μm. Source: Hansma et al., 1998.

2.5.2 Light scattering techniques

Classical static light scattering (SLS) is used to obtain the molecular weight of dispersed particles. By measuring the absolute intensity of light scattered by particles at various concentrations in solutions as a function of scattering angle, it is possible to obtain the absolute value of the weight-averaged molecular weight, the radius of gyration and the second virial coefficient (Bloomfield, 2000). The scattered light intensity is also

dependent on the change in the solution refractive index as the particle concentration varies. This technique, usually carried out using a goniometer (computer controlled moveable detector) or multiple detectors mounted at fixed angles, is particularly stringent and complex, and requires an intense light source, sensitive detectors and information on the optical properties of the system (Mike Kaszuba, personal communication). Angle-dependent light scattering for molecular weight determination is rarely applied to systems of DNA complexes. However, a recent study on the aggregation of poly-L-lysine/DNA complexes utilised time-resolved multi-angle laser light scattering and showed that the final mass of the polyplexes were dependent on the poly-L-lysine/DNA mass concentration ratio, and to a lesser extent on the poly-L-lysine molecular weight (Lai and van Zanten, 2001). It also showed that the highest DNA loading, or greatest number of DNA molecules per complex volume, which was expected to be related to optimum transfection efficiency, occurred at a charge ratio of about one.

The size and charge of DNA complexes in fluids are two important properties to assess, since the former determines whether the complexes are small enough to escape from blood vessels and then diffuse through tissue, and the latter plays a key role in controlling aggregation processes, especially in serum. With the availability of affordable, user-friendly instruments, dynamic light scattering (DLS) has been increasingly used as a straightforward and sensitive technique of characterising the particle size of a large population of DNA complexes in solution (Tang and Szoka, 1997; Zelphati *et al.*, 1998a). In DLS, which is the principle of photon correlation spectroscopy (PCS), fluctuations in intensity due to the Brownian motion of the particles are detected and then analysed through an autocorrelation analysis. This yields the particle diffusion coefficient and consequently the particle hydrodynamic size. Although the accuracy of the results are determined by the shape and behaviour of the particle size distribution, data from DLS assays can be analysed by Gaussian methods (the method of cumulants) to yield a mean or z-average diameter and polydispersity index. The practical lower and upper limits of accurate particle size detection are of the order of about 20 nm and 3 μm, respectively. A detailed description of PCS is given in Appendix A.

The surface charge and hydrodynamic properties of particles in solution determine their interactions and dispersion characteristics. A measure of surface charge, the zeta potential is the electrical potential between the shear plane surrounding the particle and the bulk solution (see Section 4.2.1.1). It can be calculated from the electrophoretic mobility of particles in buffer, and is increasingly being used to investigate aqueous formulations of DNA complexes (Dash *et al.*, 1999; Pouton *et al.*, 1998; Ramsay *et al.*, 2000; Xu *et al.*, 1998). It is often possible to directly use the zeta potential to assess the stability of suspensions of DNA complexes. The zeta potential can be measured by electrokinetic methods, like electrophoresis, electroosmosis, streaming and sedimentation potential. A common technique is laser Doppler velocimetry (LDV), also known as Doppler electrophoretic light scattering. LDV is an electrophoresis method where the migration rate of the dispersed particles is measured under the influence of an electric field. While DNA has a high negative zeta potential, typically ranging from –30 to –50 mV in an aqueous colloidal suspension (Ledley, 1996), DNA complexed to cationic lipids and polymers tend to have a positive surface charge, depending on the environmental conditions. Positively charged complexes, although desirable for charge-mediated transfection, may lead to non-specific charge interactions with plasma proteins.

2.5.3 Circular dichroism

Circular dichroism (CD) spectroscopy monitors the difference in absorption of left- and right-handed circularly polarised light by the sample medium. Different DNA conformations (A, B, C, D or Z forms) give very sharply altered CD spectra. Hence, CD can be used for characterising conformational changes of DNA in the complex. Since most of the protein CD signal occurs at wavelengths below 250 nm, it is possible to independently monitor the CD spectra of supercoiled plasmid DNA, which is characterised by a 275 nm DNA band (Middaugh *et al.*, 1998). The CD spectra of plasmid DNA in the presence and absence of various condensing agents are unique and can be used to point to a given formulation. Several groups have shown a structural alteration of plasmid DNA in the complex (Cherng *et al.*, 1999; Choi *et al.*, 1999; Kim *et*

al., 1998). This is usually exhibited by nonconservative negative ellipticity at wavelengths between 250 and 290 nm.

2.5.4 DNA quantitation

Various dyes or probes have been used to quantify the degree of interaction between DNA and cationic liposomes and/or polycations. This method is frequently used to measure the protection conferred by cationic lipids or peptides upon DNA in the presence of nucleases, shear stress, salts and/or detergent. It can also be used to quantify the extent of DNA binding by different amounts of condensing agents, for example, across a range of charge ratios.

Ethidium bromide is a widely used DNA-intercalating dye that fluoresces when it is bound to double-stranded or single-stranded nucleic acids. Accessible or free DNA can be separated from complexed DNA using agarose or polyacrylamide gel electrophoresis. Following staining of the gel with ethidium bromide, the DNA bands, which are separated by size, can be viewed under ultraviolet light. Ethidium bromide has been used with a fluorescein-labelled peptide as a competitor for DNA binding (Plank *et al.*, 1999), as a probe to assess the binding affinity of DNA complexes (Geall and Blagbrough, 2000), and in other assays (Niidome *et al.*, 1999; Turek *et al.*, 2000).

Fluorescence-based assays such as PicoGreen are also often used to measure the amount of exposed or unbound DNA in the sample because they are very sensitive, requiring only minimal amounts of sample, typically of the order of nanograms, and are quick to perform, with only a 5-minute incubation (Levy *et al.*, 2000b; Noites *et al.*, 1999; Singer *et al.*, 1997). The PicoGreen fluorophore binds specifically to double-stranded DNA and is minimally inhibited by single-stranded DNA, RNA, proteins, ethanol, chloroform, salts, and detergents. During a PicoGreen displacement experiment, which can be performed using a standard fluorometer, binding of the plasmid DNA with increasing amounts of a condensing agent will cause a decrease in the fluorescence signal. Ferrari *et*

al. showed that PicoGreen could be used to determine the concentration of DNA recovered in lipoplex formulations that were treated with detergent (Ferrari *et al.*, 1998). PicoGreen assays have also been used alongside agarose gel electrophoresis in studies of lipoplexes (Capan *et al.*, 1999; Ferrari *et al.*, 2001).

2.5.5 Centrifugation

Analytical ultracentrifugation techniques are generally utilised for the determination of the sedimentation coefficient and molecular weight of DNA complexes. Sedimentation velocity experiments can be used to separate multiple species in a sample, for example, the more dense and compact DNA complexes from the uncomplexed components. In sedimentation equilibrium experiments, a time-invariant concentration gradient is generated during centrifugation of a secondary solute, sucrose for example. This allows separation of the complexes by density (Eastman *et al.*, 1997; Li *et al.*, 1999; Trubetskoy *et al.*, 1999). Usually, equilibrium density gradient centrifugation of DNA complexes is followed by assessment of the fractions for the extent of DNA complexation using another technique.

2.5.6 Biological assays

Like other conventional pharmaceutical formulations, DNA complexes for gene therapy and DNA vaccines should be tested for biological potency and cytotoxicity, both *in vitro* and *in vivo* (Mahato, 1999). A directly injected DNA therapeutic should transfect the target cells, ultimately resulting in the correctly folded active protein being biologically available. Hence, development of potency assays, with calibrated national or international units of biological activity, for the testing of DNA-based gene therapeutics is necessary (Marquet *et al.*, 1997b). Although *in vitro* observations are poor predictors of performance *in vivo*, they provide important models for developing and understanding gene uptake and expression. It is important that the development of potency testing be co-ordinated with physicochemical characterisation of the product. Sufficient correlation

demonstrated between biological and physicochemical test results may simplify the potency testing protocols (Marquet *et al.*, 1997b).

Excellent reviews on the characterisation of plasmid DNA and formulations for gene delivery have been published and the reader is referred to those that already exist (Anchordoquy, 1999; Hutchins, 2000; Marquet *et al.*, 1997a; Marquet *et al.*, 1997b; Middaugh *et al.*, 1998; Tang and Szoka, Jr., 1998). Further information on the above analytical techniques, as well as other methods, can be found in these publications.

2.5.7 Application of the DLVO theory

Colloidal aggregation processes have long been studied but the interest has been focused mainly in the fields of water treatment, food processing, production of new materials, and particle deposition (Kyriakidis *et al.*, 1997). Although the application of colloidal stability is also of interest to the pharmaceutical industries, there have been only a few relevant studies, which involved proteins or liposomes, e.g. protein-covered polystyrene latex particles (Molina-Bolívar *et al.*, 1998; Molina-Bolívar *et al.*, 1999), dipalmitoyl phosphatidylcholine vesicles (Gamon *et al.*, 1989). The author believes that, until recently, there were no studies in the literature on the application of the Derjaguin-Landau-Verwey-Overbeek (DLVO) theory of colloidal stability to DNA complexes. Since the DLVO theory is a central topic in colloid science, and the stabilisation of colloidal suspensions of DNA complexes is an important aim, it is useful to employ computer simulations in conjunction with experimental data for the characterisation of DNA complexes in solution. Accordingly, the control of the stability of suspensions of poly-L-lysine/DNA complexes were explained by experimental data and theoretical model predictions in a recent publication (Lee *et al.*, 2001). Similar results will also be shown in Section 4.2.

2.5.8 Application of fractal theory

It is well established that the structures of colloidal aggregates can be described by their fractal properties. The fractal dimension provides information concerning the packing in such systems and can help to control or predict the behaviour of their aggregation processes. This concept has been applied to biomolecules, including β-lactoglobulin (Le Bon *et al.*, 1999), *Escherichia coli* flocs (Tang *et al.*, 2001), wastewater solids (Guan *et al.*, 1998), alpha-crytallin (the major protein of the eye lens) (Bassi *et al.*, 1995) and human transferrin receptor (Schüler *et al.*, 1999). The author believes that the fractal approach for the characterisation of DNA complexes has not been mentioned anywhere in the literature, even though DNA complexes represent an important class of colloids for clinical applications. Two commonly used techniques for determining the fractal dimension of colloidal suspensions are static light scattering (SLS), in which the time-averaged intensity of scattered light is measured over a range of angles, one angle at a time, and small angle laser light scattering (SALLS), also known as multiangle laser light scattering (MALLS), in which the scattered light intensities at a range of scattering angles are simultaneously measured. In Section 4.3, static light scattering studies are applied to poly-L-lysine/DNA complexes to generate their fractal dimensions and subsequently describe their aggregation.

2.6 Future prospects

A critical outline of human gene therapy prospects published nearly three decades ago (Friedmann and Roblin, 1972) detailed the therapeutic potential of both viral gene therapy vectors and synthetic gene delivery systems. The following years saw considerable research interest and progress in gene delivery techniques. The earliest authorised human gene therapy trial was conducted at the National Institutes of Health (NIH), Bethesda, USA, in September 1990, involving a four-year old girl with an inherited immunodeficiency syndrome. A few years later, groups at Vical (San Diego), Merck (West Point, Philadelphia), the University of Texas Southwestern Medical Center (Dallas), University of Massachusetts and University of Pennsylvania demonstrated that gene delivery could be exploited as a vaccine strategy to provide potent immune

responses or protective immunity against viruses, bacteria and parasites. This led to increased research in DNA vaccines for inducing protective immunity against malaria, hepatitis B, human immunodeficiency virus and other pathogens. The first DNA vaccination trial, in 1995, involved the delivery of plasmid DNA containing HIV genes to individuals already infected with HIV. During the past 10 years, more than 590 other clinical trials involving ~3500 patients have been conducted for therapies designed to treat genetic and acquired diseases (www.wiley.co.uk/genmed/clinical, 2001; Hart, 2000; Levy *et al.*, 2000a; Mountain, 2000). Nevertheless, the rate of progress of gene therapy and DNA vaccination has been disappointingly slow, as evidenced by the remarkably few clinical trials that show an unequivocal benefit.

The majority of human clinical trials for gene therapy are involved in the treatment of cancer. In Europe over 80% of trials are concerned with cancer therapy, while in the United States the figure is 72% (Verma and Somia, 1997). Protocols for the treatment of genetic diseases, mainly cystic fibrosis, account for around 20% of clinical trials, while in the US there are a small number of trials for the use of DNA vaccination in the treatment of AIDS. As the increase in scientific progress sets the stage for gene therapy products to follow, the number of clinical trials will correspondingly grow, with more products entering late stage clinical trials. Production and processing of vectors for gene transfer will receive increasingly more attention and necessitate considerable biotechnological advances. The manufacturing process must also incorporate good manufacturing practice (GMP) and quality assurance/quality control (QA/QC) procedures dictated by the FDA (Anderson, 1998). Crucial to the development of human gene therapy and DNA vaccines, then, is the reproducible large-scale production of vectors with an improved biosafety profile (Palu *et al.*, 1999).

Viral-based approaches have shown the most promise so far, with the use of AAV for the treatment of haemophilia B, an inherited single-gene disorder where the patients are dependent on injections of blood clotting factor IX (Kay *et al.*, 2000). However, in September 1999, an eighteen-year-old in a University of Pennsylvania clinical trial died

from a severe immune reaction as a result of the received adenoviral gene therapy for an inherited deficiency in ornithine transcarbamylase (an enzyme involved in the urea cycle and ammonia metabolism) (Dyer and Herrling, 2000). The first confirmed casualty in a gene therapy clinical trial that did not result from an underlying illness, the fatality promptly launched investigations by the press and regulatory agencies. Later, in April 2000, Prof. Fischer's group in Paris announced a significant breakthrough involving the viral-based gene therapy treatment of babies affected by SCID X1, an immune deficiency disease that strips their bodies of protection against infections such as cold sores or chickenpox (Cavazzana-Calvo *et al.*, 2000; Highfield, 2000). This accomplishment may have, to some extent, restored confidence in the public and investor audience. Nevertheless, the clinical introduction and evaluation of many anticipated new gene delivery systems are likely to come under increased stringent approval from the Recombinant DNA Advisory Committee (RAC) of the US National Institutes of Health (NIH) and the FDA (Carter, 2000; Grisham, 2000; Morris *et al.*, 1999). Already, an RAC meeting in June 2000 led to the revaluation of the drug development of gene therapy, in particular the conduct of clinical trials (Grisham, 2000).

On the non-viral front, the development of a vector capable of efficient gene delivery *in vivo* has yet to reach pharmaceutical reality. Phase I and phase II clinical trials involving cationic lipid-based delivery systems are currently being conducted in Europe, the majority of which are focused on the treatment of cystic fibrosis (Alton *et al.*, 1999; Caplen *et al.*, 1995; Gill *et al.*, 1997; Porteous *et al.*, 1997) and cancer (Stopeck *et al.*, 1997). Lipid-based gene delivery systems are also being developed for clinical trials by Vical (San Diego, CA, USA), Genzyme (Cambridge, MA, USA), Targeted Genetics (Seattle, WA, USA), and Megabios (Burlingame, CA, USA) in collaboration with Glaxo Wellcome plc (Research Triangle, NC and UK) (Thierry and Mahan, 1999). Additionally, a promising AIDS vaccine that combines a naked DNA vaccine with an adenovirus vector boost has been developed by Merck (Whitehouse Station, New Jersey) and is currently in small human studies (Cohen, 2001).

Other non-viral approaches, such as the use of synthetic peptides, multi-component PEGylated agents and lipid/polycation combinations, are relatively new, but the ever-increasing research in various related scientific areas presents great potential for the development and application of efficient synthetic gene delivery systems. With clinical trials for DNA vaccines showing great promise, there are high expectations for its future applications and research is being carried out to improve gene delivery systems that can target tissue-specific sites (Lai and Bennett, 1998; Mor, 1998). To attain such progress, control over the manifold determinants of the activity and practical applicability of these systems is crucial. The current technological advances in combinatorial chemistry, microelectronics and nanotechnology, alongside immunology and human genomics, should contribute to the development of biomolecules capable of achieving site-specific gene delivery (Langer, 1998). Additionally, the understanding of transport phenomena and interactions of these systems in the body and on the shelf, as well as the use of mathematical models to describe these processes will provide insight into gene delivery strategies and formulation stability.

CHAPTER 3

MATERIALS AND METHODS

The charge ratio is presented as the N/P ratio, that is, the molar ratio of nitrogen (N) of the polycation to DNA phosphate (P). The molar concentration of DNA phosphate was calculated by dividing the plasmid DNA concentration by 330, the average nucleotide molecular mass. Calculation of the charge ratio was done according to a standard method as described in Appendix C.

3.1 Materials

All solutions were prepared from deionised Milli-Q water (resistivity ≈ 18.2 MΩcm) (Millipore Ltd, Bedford, MA, USA) and cleaned with 0.2 μm pore size Millipore filters to remove particulates. HEPES (*N*-[2-hydroxyethyl] piperazine-*N*'-[2-ethanesulfonic acid]) (Sigma-Aldrich, Poole, Dorset, UK) was dissolved in deionised water and titrated with NaOH to pH 7.2, 7.7 and 8.0. For select experiments, concentrated NaCl was added to the solutions to give final salt concentrations of 10, 50, 100 or 150 mM NaCl. Phosphate-buffered saline (PBS, contains no calcium or magnesium) and Opti-MEM were obtained from Life Technologies, Inc. (Paisley, UK). TrisCl, EDTA, NaCl, NaOH, trypsin, bovine serum albumin and dextrose were obtained from Sigma-Aldrich. Particle

free water (Sterile water for irrigation, Fresenius Kabi Ltd, Warrington, UK) was kindly provided by Malcolm Connah (Malvern Instruments Ltd, Malvern, Worcester, UK).

3.2 Calf thymus and plasmid DNA

Initially, experiments were carried out using commercially available calf thymus DNA, in order to obtain knowledge about process issues. Thereafter, four different types of plasmid were used in further experiments. These are described below.

Linear calf thymus DNA (10-15 $\times$ 10^6 average MW or 15-23 kb, a mixture of single- and double-stranded DNA) was purchased as the sodium salt (Sigma-Aldrich) and dissolved in sterile TE buffer (10 mM TrisCl pH 8.0, 1 mM EDTA) at a concentration of 1 mg/ml.

The 6.9 kb plasmid, pSVβ (Promega Corp., Madison, WI, USA), containing the bacterial β-galactosidase gene, is a common plasmid which is routinely used at UCL Biochemical Engineering. The plasmid was transformed and propagated in *Escherichia coli* DH5α (Life Technologies, Inc., Gaithersburg, MD, USA). Further details are given in Levy *et al.* (Levy *et al.*, 2000c). The plasmid DNA was purified by the alkaline lysis procedure whereby bacterial cells are lysed and the plasmid DNA adsorbed onto an ion-exchange column, according to the supplier's protocol (Qiagen plasmid Mega-prep kit, Qiagen Ltd, West Sussex, UK). The eluted plasmid DNA was isopropanol-precipitated, washed with 70% (v/v) ethanol, air-dried and resuspended as described in Sambrook *et al.* (Sambrook *et al.*, 1989). Concentrations and quality were assessed by spectrophotometric analysis at 260 and 280 nm as well as by electrophoresis in 0.6% agarose gel. DNA concentration was determined using a value of 50 μg DNA per one absorbance unit at 260 nm. The plasmid had 260 nm/280 nm absorbance ratios greater than 1.8 and was predominantly supercoiled. The final purified plasmid DNA was resuspended in either sterile TE buffer (10 mM TrisCl pH 8.0, 1 mM EDTA) at a concentration of 3.83 mg/ml or sterile 20 mM HEPES buffer (pH 7.2) at a concentration of 1.96 mg/ml and frozen (-20°C) in aliquots.

The 29 kb plasmid DNA (pMT103) used for the shear studies was provided by Dr Myriom Susana Levy (Department of Biochemical Engineering, University College London). More details on this plasmid are given in Levy *et al.* (Levy *et al.*, 1999a).

The pEGFP plasmid (4.7 kb, coding for green fluorescent protein, resuspended in water) and pCI-luc plasmid (5.7 kb, coding for luciferase, resuspended in water) were provided by Dr Elena Siapati (Molecular Immunology Unit, Institute of Child Health). These plasmids were routinely used at ICH in *in vivo* and *in vitro* studies (K. Elena Siapati, personal communication).

Calf thymus DNA, pSVβ and pMT103 were used in physicochemical characterisation studies of PLL/DNA complexes. pEGFP and pCI-luc were used in Lipofectin/integrin-targeting peptide/DNA (LID) physicochemical characterisation studies and *in vitro* transfection experiments.

3.3 Peptides

Poly-L-lysine of average molecular mass 2,900, 25,250, 25,900, 34,300 and 99,500 was purchased as the HBr-salt from Sigma-Aldrich and used without further purification or modification. Stock solutions for each poly-L-lysine molecular weight were prepared by dissolving the lyophilised white powder in 20 mM HEPES (pH 7.2) at a concentration of 5 mg/ml.

The integrin-targeting peptide, or peptide 6, $[K]_{16}$GACRRETAWACG (3331.5 MW), was provided by Dr Elena Siapati (Molecular Immunology Unit, Institute of Child Health). The peptide, from Zinsser Analytic (Maidenhead, UK), was dissolved in deionised water to 2 mg/ ml and incubated overnight at 4°C exposed to air to allow oxidation of cysteine residues to cyclise the RGD domains. Further details are given in Section 2.4.2.3 and elsewhere (Hart *et al.*, 1998). The solution was then stored at -20°C

in 1 ml aliquots prior to use. Peptide K or FIB10, a 36-lysine peptide with an integrin-binding domain, was kindly provided by Dr A. Uduehi (Molecular Immunology Unit, Institute of Child Health).

3.4 Liposomes

The transfection reagent Lipofectin, a 1:1 (w/w) mixture of the cationic lipid *N*-[1-(2,3,-dioleyloxy)propyl]-*N,N,N*-trimethylammonium chloride (DOTMA) and the neutral lipid dioleoyl phosphatidylethanolamine (DOPE), from Life Technologies, Inc., was stored at 4°C. These lipids are described in Section 2.4.2.2.

3.5 Preparation of poly-L-lysine/DNA (PLL/DNA) complexes

Polyplexes were prepared by mixing an equal volume of DNA (25 μg/ml) with PLL in 20 mM HEPES at predetermined solution pHs (7.2, 7.7 or 8.0) and salt concentrations (0, 10, 50, 100, 150 or 1000 mM NaCl). Both components were mixed either by pipette mixing or by a two-syringe mixing method as described below (see Section 3.7) and elsewhere (Lee *et al.*, 2001; Zelphati *et al.*, 1998a). In pipette mixing, a solution (of DNA, for example) is rapidly added to another solution (of PLL, for example) in an appropriate container using a pipette tip, followed by about five seconds of mixing using the same pipette tip. Unless stated otherwise, proportions of PLL and DNA are specified as the N/P ratios. For example, a working solution of PLL at a concentration of 31.67 μg/ml was used for a polyplex charge ratio of 2.0 (12.67 μg/ml for a N/P of 0.5, 15.83 μg/ml for a N/P of 1.0 and 23.75 μg/ml for a N/P of 1.5). Polyplexes were formed at a final DNA concentration of 12.5 μg/ml solution.

For static light scattering studies, sample preparation was performed in a laminar flow cabinet (Bigneat Clean Air CLF 360, Bigneat Ltd, Waterlooville, Hants) to avoid dust contamination. The volume of the sample was 4 ml. The polyplex dispersions were prepared and analysed in a Burchard sample cell (Malvern Instruments Ltd). The sample

cell was thoroughly rinsed with particle free water (Sterile water for irrigation, Fresenius Kabi Ltd) before use.

3.6 Preparation of Lipofectin/integrin-targeting peptide/DNA (LID) complexes

Unless otherwise indicated, lipopolyplexes were prepared by mixing the Lipofectin/integrin-targeting peptide (LI) and plasmid DNA (D) components in the optimal weight ratio 0.75:4:1 (L:I:D), to give a charge ratio of ~6.8. The LID vector was used at this charge ratio in all experiments except in cases where the aim was to assess the impact of lipopolyplex charge ratio on biophysical properties (see Table 3.1). The integrin-binding peptide has a charge of +17, whereas DOTMA contributes a charge of +1. The two cationic components, L and I, were first mixed together. Lipopolyplexes containing a peptide with a 36-lysine tail (K) were made in the ratio 0.75:1.56:1 (L:K:D) to maintain an approximate charge ratio of 3.

Table 3.1 Equivalent charge and weight ratios of Lipofectin, integrin-targeting peptide and DNA.

Charge ratio	*L:I:D: weight ratio*
0.5	0.75 : 0.3 : 1
1.0	0.75 : 0.6 : 1
2.0	0.75 : 1.3 : 1
3.0	0.75 : 1.9 : 1
4.0	0.75 : 2.5 : 1
5.0	0.75 : 3.1 : 1
6.8	0.75 : 4.0 : 1
7.0	0.75 : 4.4 : 1
8.0	0.75 : 5.0 : 1
10.0	0.75 : 6.3 : 1

Lipopolyplexes were made in various buffers at DNA concentrations of 5 and 160 μg/ml (see Table 3.2). For the preparation of lipopolyplexes at a DNA concentration of 5 μg/ml, DNA solution (10 μg/ml) was mixed with an equal volume, typically 1.5 to 3.0 ml, of

Lipofectin/integrin-targeting peptide solution. The lipopolyplexes were prepared either by pipette mixing or by the two-syringe mixing method (2 ml/min).

For the preparation of lipopolyplexes at a DNA concentration of 160 μg/ml, the DNA stock solution was first diluted into the appropriate buffer in an Eppendorf tube, after which it was added to the lipid/peptide solution in a sample cell to give a final DNA concentration of 160 μg/ml in a total volume of 500 μl. The DNA and lipid/peptide solutions were mixed briefly by pipetting the mixture up and down for approximately 5 s.

Table 3.2 Solutions used in the preparation of LID complexes.

Buffer / DNA concentration	*5 μg/ml*	*160 μg/ml*
Deionised water	✓	✓
Opti-MEM	✓	×
Phosphate-buffered saline (PBS)	✓	✓
20 mM HEPES, 150 mM NaCl (HBS)	✓	×
150 mM NaCl	×	✓
5% (252.3 mM) dextrose	×	✓
Addition of PBS	×	✓
Addition of bovine serum albumin (BSA)	×	✓

No effect of formulation volume on particle size of the lipopolyplexes in the volume range used was observed under these experimental conditions. All complexes were prepared at 25°C as described below unless otherwise specified.

3.7 Two-syringe mixing method

PLL/DNA and LID complexes were prepared with the aid of a two-syringe pump flow system previously described (Lee *et al.*, 2001; Zelphati *et al.*, 1998a) (see Fig. 3.1). The DNA solution and cationic polymer preparation were mixed using a vertically mounted two-syringe pump (PHD 2000 Infuse/Withdraw; Harvard Apparatus, Holliston, MA, USA). The pump had the capacity to deliver flow rates between 0.2 and 100 ml/min. Two standard Becton-Dickinson plastic syringes (Becton-Dickinson Labware, Lincoln Park, NJ, USA) were each fitted with a three-way luer-lock adapter and 0.8 mm internal diameter silicone tubing (Bio-Rad, Hercules, CA, USA).

For complexes prepared by the two-syringe mixing method, the cationic polymer and DNA were initially prepared at twice the final formulation concentration. Equal volumes of DNA and PLL or LI solutions were loaded into separate syringes and driven by the pump through a T-connector. The mixture was collected either in a 10 mm round quartz cell (PCS8400; Malvern Instruments Ltd) or disposable polystyrene cuvette (DTS0012 or DTS0112; Malvern Instruments Ltd) for particle size analysis, or in a polystyrene Universal container (201152; Greiner Labortechnik Ltd, Stonehouse, UK) for determination of zeta potentials. Mixing rates of the solutions were between 0.2 and 17 ml/min.

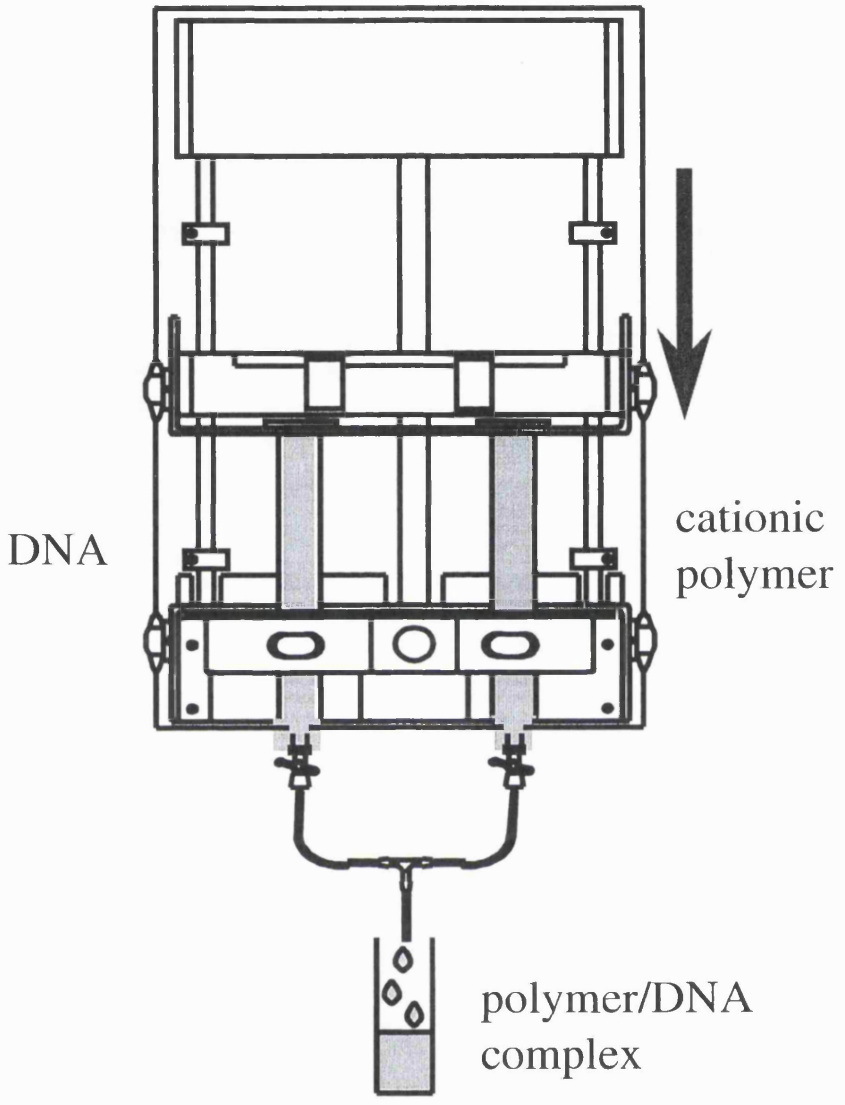

Figure 3.1 Schematic representation of the two-syringe mixing method. The two syringes were loaded separately with the DNA solution and cationic polymer (polylysine or Lipofectin/integrin-targeting peptide) and placed on the pump. Then the plungers of the syringes were pushed simultaneously at a controlled speed by the syringe pump, and the mixing of the solutions occurred in the T-connector.

3.8 Zeta potential measurements

As described previously (Section 2.5.2), the zeta potential is automatically calculated based on the movement of the complexes in an electric field, that is, the electrophoretic mobility. It is a measure of the repulsion between the complexes and is measured in mV at the outer edge of the ionic cloud, or the slipping plane boundary. The zeta potential of complexes was measured by laser Doppler velocimetry (LDV) on a Malvern Zetasizer 3000 (Malvern Instruments Ltd). Zeta potential measurements were done after particle size measurements, typically within 5 hours of mixing, at 25°C. Although the complexes were often aggregated (> 3 μm), it is worth remembering that the quoted size range for zeta potential measurements of particles in aqueous dispersions is 5 nm to 30 μm. The instrument was calibrated with a –50 ± 5 mV standard (DTS5050; Malvern Instruments Ltd) between measurements. The zeta potential was averaged from 5 measurements.

3.9 Dynamic light scattering (DLS)

The particle size of the complexes were performed using dynamic light scattering, described in Section 2.5.2 and Appendix A. Unless otherwise stated, the particle size of all complexes were measured on a Malvern Zetasizer 3000 (Malvern Instruments Ltd) equipped with a 10 mW He-Ne laser operating at 633 nm wavelength and 90° scattering angle. The lower and upper limits of photon correlation spectroscopy is dependent on the laser power and sensitivity of the detection system, as well as the properties of the sample such as density, concentration and refractive index. The practical lower and upper size limits for particle size analysis of macromolecules in clear mobile liquids on the Zetasizer are typically 20 nm and 3 μm, respectively.

In cases when concentrated NaCl was added following polyplex formation in salt-free buffer, that is, where the salt concentration of the sample was adjusted rapidly to the desired level by manually injecting the required volume of concentrated NaCl solution into the sample, particle size measurements were carried out with the use of a Malvern Autosizer 4700 system at a scattering angle of 90°C. The laser used was a diode-pumped,

frequency-doubled, single-frequency laser (Series 142, Lightwave Electronics, Elliot Scientific Ltd, Hertfordshire, UK) with an output power of 100 mW and wavelength of 532 nm. Given the power of the laser and the sensitivity of the instrument, the practical lower limit of accurate particle size detection is approximately of the order of 10 nm and the upper limit, which is determined by the onset of aggregation, is about 1500-3000 nm.

The size distributions were obtained from light-scattering profiles reported as the intensity of light scattered by polyplex particles in each size class. Particle size measurements were made with counting times of more than 101 s per measurement to ensure the application of automatic dust rejection and hence reduce the sensitivity of the results to any contaminants present. All measurements were made at a set temperature of 25°C. At least two duplicates were performed for each sample. The particle sizer was calibrated with polystyrene spheres between 60 nm and 3000 nm (Duke Scientific Corp., Palo Alto, CA, USA) in 10 mM NaCl. In a typical experiment, 0.5 to 3 ml of polyplex or lipopolyplex dispersion was put into the spectrometer cell and the size distribution measured.

The intensity of light scattered at a given angle from a visible laser beam is related to the Brownian motion of the scattering particles in suspension and is measured by a photon detector. This temporal fluctuation is analysed by a correlator that computes, in real time, the autocorrelation function to yield the effective translational diffusion coefficient, D. Thus the Brownian motion of the particles is related to their hydrodynamic diameter, D_H, by the Stokes-Einstein relation:

$$D = \frac{kT}{3\pi\mu D_H} \tag{3.1}$$

where k is Boltzmann's constant, T is the absolute temperature of the sample, and μ is the viscosity of the solution. A more detailed description of photon correlation spectroscopy can be found in Appendix A.

Sample size was analysed by the unimodal cumulants method (monomodal analysis) using the software supplied by the manufacturer. The autocorrelation function analysis software calculates the *z*-average mean diffusion coefficient, and gives the average effective hydrodynamic diameter or *z*-average mean size (from the application of the Stoke-Einstein relationship), and the polydispersity based on a lognormal population distribution of the data. The mean particle size was also calculated from the result of a distribution analysis algorithm such the CONTIN "constrained regularisation" algorithm (Provencher, 1979; Provencher, 1982a; Provencher, 1982b) but the results were not always as reproducible as those obtained by the monomodal analysis method. The polydispersity index is a measure of the width of the particle size distribution. It is scaled such that a monodisperse distribution will have a polydispersity index less than 0.2 and a heterogeneous system will have values greater than 0.7, the maximum value being 1.0.

3.10 Static light scattering (SLS)

Static light scattering (SLS), performed on a Malvern Autosizer 4800 computer controlled spectrometer (Malvern Instruments Ltd), was used to obtain quantitative structural information for the calculation of the fractal dimension of the PLL/DNA (polyplex) aggregates. The light source used was a 75 mW 488 nm air-cooled Argon ion laser operating at an output power of 14.7 mW. The scattered light was collected by an avalanche photodiode detector positioned at angle θ relative to the forward direction of the incident beam. All experiments were performed at the constant temperature of 25°C. The spectrometer was calibrated by performing angular measurements of intensity on toluene. Before each experiment, the sample cell and buffer used was checked for cleanliness by measuring the scattering at low angles (θ = 12° to 30°). If the background noise was unacceptable, the sample cell would be cleaned and the buffer polished with 0.2 μm pore size filters (Sterile Acrodisc®, Gelman Sciences Inc., Portsmouth, Hampshire, UK) again. In our experiment, angular scans were performed from θ = 12° to 100°, with a measurement made every 4° (23 steps) for an acquisition time of 10 s (sample acquisition time ≥ 230 s). The intensity measurements were repeated at different times following sample preparation. SLS experiments were performed once only (n = 1).

3.11 Shear experiments

The plasmid pMT103 (29 kb) and PLL/pMT103 complexes were subjected to controlled shear in a small purpose-built high-speed rotating disk shear device, first described by Levy *et al.* (Levy *et al.*, 1999a; Levy *et al.*, 1999b). Brief details of the experiment have been published in Levy *et al.* (Levy *et al.*, 2000a). The rotating disk shear device was designed and constructed with the capacity to shear-treat millilitre quantities of process material at speeds that mimic the local flow conditions during the processing of plasmid DNA. The instrument consisted of a PTFE rotating disk (3 cm diameter, 1 cm thickness), around which the test solution flows, mounted centrally in an airtight Perspex cylindrical chamber. The disk could be rotated at speeds between 5,000 and 27,700 rpm (corresponding approximately to shear rates between 1.0×10^5 s^{-1} and 1.3×10^6 s^{-1}; see Appendix B) by a battery or electrical mains driven motor. Ports located at the top and base of the chamber allowed the test solution to be filled into and siphoned from the chamber.

Before the shear experiments, formulations of plasmid DNA and polyplexes in TE buffer (pH 8) were prepared. In some cases 3M NaCl was added to TE buffer to give a final salt concentration of 150 mM NaCl. One volume (13.5 ml) of polylysine (average molecular weight 2,900, 25,900 or 99,500) was mixed with an equal volume of DNA using the two-syringe mixing method with a mixing rate of 1 ml/min. Polyplexes were prepared at a charge ratio of 1.5; all formulations were prepared at a final DNA concentration of 2 μg/ml.

A typical experimental run consisted of completely filling the chamber of the shear device and its tubing with approximately 20 ml of test solution. For the air-liquid interface experiment the chamber was filled using approximately 7 ml of test solution. The solution was then stirred at a fixed speed of 27,700 rpm (corresponding to a shear rate of $\sim 1 \times 10^6$ s^{-1}) for 5 s. The chamber was emptied and washed with distilled water

followed by TE buffer before the start of each run. All experiments were performed at room temperature (~25°C).

To dissociate the plasmid DNA from the polylysine, the control (unsheared) samples of each solution and the sheared samples (700 µl each) were digested with 70 µg of trypsin for 15 min at 37°C, followed by extraction with phenol/chloroform. The samples were then precipitated with 0.1 volumes of 3 M NaCl and 0.7 volumes of isopropanol, washed with 70% ethanol and resuspended in TE buffer. Control (0.5 µg DNA) and sheared samples were applied to a 0.6% (w/v) agarose gel containing ethidium bromide and electrophoresed at 80 V for 2 h 30 min. Gels were scanned using UVP 5000 Gel Documentation System software (Ultra Violet Products Ltd, Cambridge, UK).

3.12 DNA accessibility assays

The accessibility of DNA in complexes was monitored by either the PicoGreen assay or agarose gel electrophoresis (AGE). AGE was used to directly observe the level of protection conferred by PLL on DNA subjected to controlled shear, as described in the previous section (Section 3.11).

The PicoGreen assay was used to measure accessible plasmid DNA in LID complex formulations. Formulations were prepared at a DNA concentration of 5 µg/ml in Opti-MEM and incubated for 3 h at room temperature, then diluted 1:5 with TE buffer pH 8.0 and used for the PicoGreen assay. All dilutions were made in polystyrene Universal containers (Greiner Labortechnik Ltd) to avoid PicoGreen absorption to container surfaces. The PicoGreen reagent (Molecular Probes, Leiden, The Netherlands) was diluted (1:200) into TE buffer (pH 8) according to the manufacturer's instructions (Singer *et al.*, 1997). Diluted PicoGreen reagent (500 µl) was added to 800 µl of formulation or DNA control. Samples were prepared in polymethacrylate fluorimeter cuvettes (C-0793, Sigma-Aldrich) and incubated at room temperature for 2 min in the dark. Fluorescence was measured in a TD-700 Laboratory Fluorometer (Turner Designs, Sunnyvale, CA, USA) at excitation and emission wavelengths of 489 and 520 nm, respectively. All

measurements were carried out at 84% sensitivity. Measurements were corrected for background fluorescence from a solution containing buffer (200 µl Opti-MEM + 800 µl TE) and diluted PicoGreen reagent. The results were averaged from 3 readings.

3.13 *In vitro* gene expression

All *in vitro* transfection experiments were performed with Dr Elena Siapati (Molecular Immunology Unit, Institute of Child Health). The experiments were carried out with the SV-40 virus transformed monkey kidney epithelial cell line, COS-7, obtained from the European Collection of Animal Cell Cultures (ECACC, Salisbury, UK). COS-7 cells were cultured in Dulbecco's modified Eagle's medium (DMEM, Life Technologies, Inc.) supplemented with 10% fetal calf serum (FCS), 2 mM L-glutamine, penicillin and streptomycin. The cells were grown in Falcon 75-cm^2 cell culture flasks (Becton Dickinson Labware) in a humidified, 5% CO_2, 37°C incubator. For transfections, cells were harvested by trypsinisation, pelleted by centrifugation and resuspended in the culture medium in Falcon 48-well tissue culture plastic plates (Becton-Dickinson Labware). The cells were incubated overnight at 37°C to reach cell confluency of more than 50% (approximately 2.5×10^4 cells). Following incubation, the cells were washed with PBS to remove serum, and 200 µl of Opti-MEM buffer was added to the cells in each well. The LID complexes containing the reporter gene pEGFP were prepared as described previously and 200 µl (1 µg DNA) immediately pipetted to triplicate wells. Cells were exposed to the complexes for 3 h at 37°C, followed by aspiration of the transfection media and addition of regular growth medium. After 48 h, cells were washed twice with PBS and detached from the tissue culture plastic by incubation in 1 × Trypsin-EDTA (Life Technologies, Inc.) for 5 to 10 min at 37°C. The harvested cells were centrifuged, washed and resuspended in PBS containing 0.01% sodium azide. A fluorescence-activated cell sorter, FACSCalibur (Becton-Dickinson, Oxford, UK), was used to automatically analyse the GFP expression of individual cells. Each measured number of GFP positive cells was determined on the basis of one sample of pooled triplicates.

CHAPTER 4

RESULTS AND DISCUSSION:

POLY-L-LYSINE/DNA (PLL/DNA) COMPLEXES

The aggregation of cationic polymer/DNA complexes (polyplexes) under physiological conditions is thought to be a major cause of poor transfection and remains a major obstacle to successful non-viral gene delivery. To gain a better understanding of the causes of this aggregation, the work in this chapter focuses on the stability of poly-L-lysine/DNA (PLL/DNA) complexes. This chapter is divided into three main parts. The first one (Section 4.1) deals with the influence of parameters such as preparation method, ionic strength and pH on the biophysical properties of the polyplexes, with special emphasis on the particle growth behaviour and surface charge. The effect of shear on the polyplexes is also examined. The second part (Section 4.2) is concerned with the connection between the particle interaction potential and colloidal stability of the polyplex systems. In order to achieve this, an overview of the interactions that govern the stability of the colloidal systems is given in Section 4.2.1. It includes a description of simulations that aim to establish a link between the change in the interparticle potential with various critical parameters, e.g. salt concentration, zeta potential. The simulation

results are then presented for the polyplex system (Section 4.2.2). The third part of this chapter (Section 4.3), which is concerned with the fractal nature of aggregating polyplexes, begins with a description of the background and techniques used to obtain the fractal dimensions (Section 4.3.1). This is followed by presentation of the static light scattering results (Section 4.3.2), measurement of the fractal dimensions (Section 4.3.3) and analysis of the relevant aggregation regimes (Section 4.3.4).

4.1.1 Particle size measurements by the Malvern Zetasizer

Initial particle size measurements were carried out with commercially available calf thymus DNA and poly-L-lysine (average MW = 25,900). Calf thymus DNA is a short, double-stranded DNA molecule that has been used (Deng and Bloomfield, 1999; Geall *et al.*, 1999; Geall and Blagbrough, 2000; Shapiro *et al.*, 1969) to serve as a reference for studying the behaviour of plasmid DNA in terms of stability during formulation. The calf thymus DNA used in this project had an average molecular weight of $10\text{-}15 \times 10^6$ (15-23 kb) and was a mixture of double- and single-stranded DNA, as claimed by the supplier. Poly-L-lysine has been used by many groups in the past for DNA condensation in studies involving *in vitro* and in *vivo* transfection although there is a degree of uncertainty over whether or not poly-L-lysine is immunogenic (Deshmukh and Huang, 1997; Pouton *et al.*, 1998).

The particle size is taken as the light scattering mean or z-average hydrodynamic diameter, which is calculated by the PCS software using the monomodal cumulants method. The cumulants method, described previously in Section 3.9, assumes nothing about the distribution form. However, it gives a good idea of the mean size (z-average) and spread (polydispersity), and is the best method for studying complex biological systems such as those reported here. Hence, the particle size reported for all results in this work refer to the mean hydrodynamic size.

Typical size distributions obtained by PCS as a function of time following the mixing of a calf thymus DNA solution with poly-L-lysine in HEPES buffer (pH 7.2) are shown in Fig. 4.1. Measurements of particle size were made continually and the results are displayed at fixed intervals shown in the plot. The data in Fig. 4.1 show that the PLL/DNA complexes in buffer containing no added salt are stable, over at least 25 min, and have an average hydrodynamic diameter of 84.4 nm. It should be noted that the distributions are shown as semi-logarithmic plots (Fig. 4.1) so that any small changes occurring at the larger particle sizes can be easily seen (Richard Mead, personal communication). In each case, the smooth curves drawn through the data points were mathematically fitted using analysis methods provided by the particle sizing instrument. A typical display of the analysis for a particle size measurement of the above polyplexes is shown in Fig. 4.2A. Also shown is a typical overplot of five measurement results by PCS on the same PLL/DNA sample (Fig. 4.2B). The tabulated data indicate a repeatability of 84.4 ± 3.4 nm, i.e. measurement reproducibility of particle size for one sample, with a mean hydrodynamic diameter of 84.4 nm and 3.4 nm standard deviation).

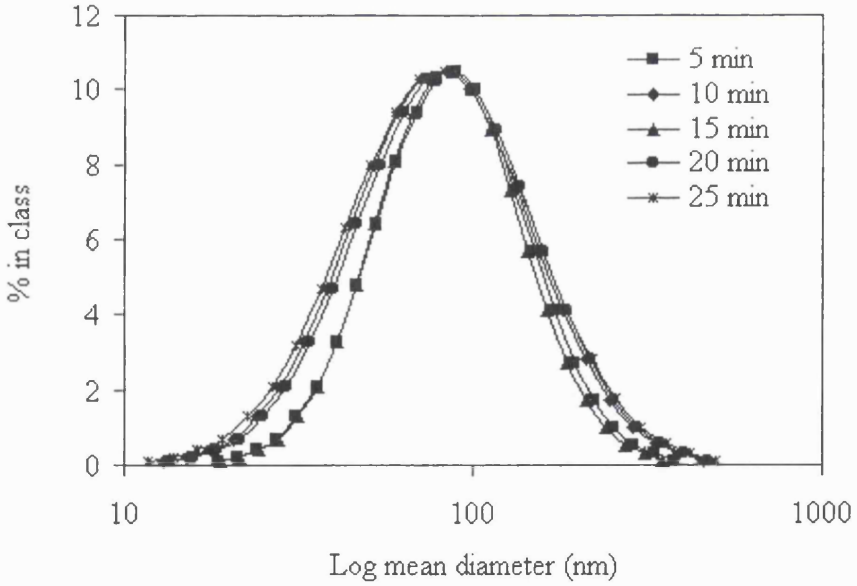

Figure 4.1 Particle size distributions of poly-L-lysine/calf thymus DNA complexes formed at a charge ratio of 2.0 in 20 mM HEPES pH 7.2 as a function of time after preparation. Size distributions were determined as mean of diameter on the

basis of intensity of scattered light at 90°. The data shown were obtained from a single representative sample.

The hydrodynamic diameter of uncomplexed DNA (pSVβ) could not be determined by photon correlation spectroscopy (PCS) because of the worm-like random coil shape of the molecule (Bloomfield, 1996; Kwoh *et al.*, 1999). However, other PCS studies have demonstrated that plasmid molecules smaller than 5 kb had hydrodynamic diameters of ~100 nm (Ledley, 1996; Rolland *et al.*, 1994) and ~170 nm (Lai and van Zanten, 2001). The size of poly-L-lysine alone could not be measured by PCS either (Kwoh *et al.*, 1999; Lai and van Zanten, 2001).

The size analysis and zeta potential measurements reported in this chapter were performed with PLL of three slightly different molecular weights, i.e. 25,250, 25,900 or 34,400. They were purchased from Sigma-Aldrich (Poole, Dorset, UK) as qualitatively similar batches of PLL within a defined molecular weight range of 15,000–30,000. These molecular weights were based on viscosity and provided by the manufacturer. No differences were noted in the physicochemical characteristics of polyplexes formed with any of these three PLL molecular weights. This has been shown for a wider range of PLL molecular weights in another study (Tsai *et al.*, 1999).

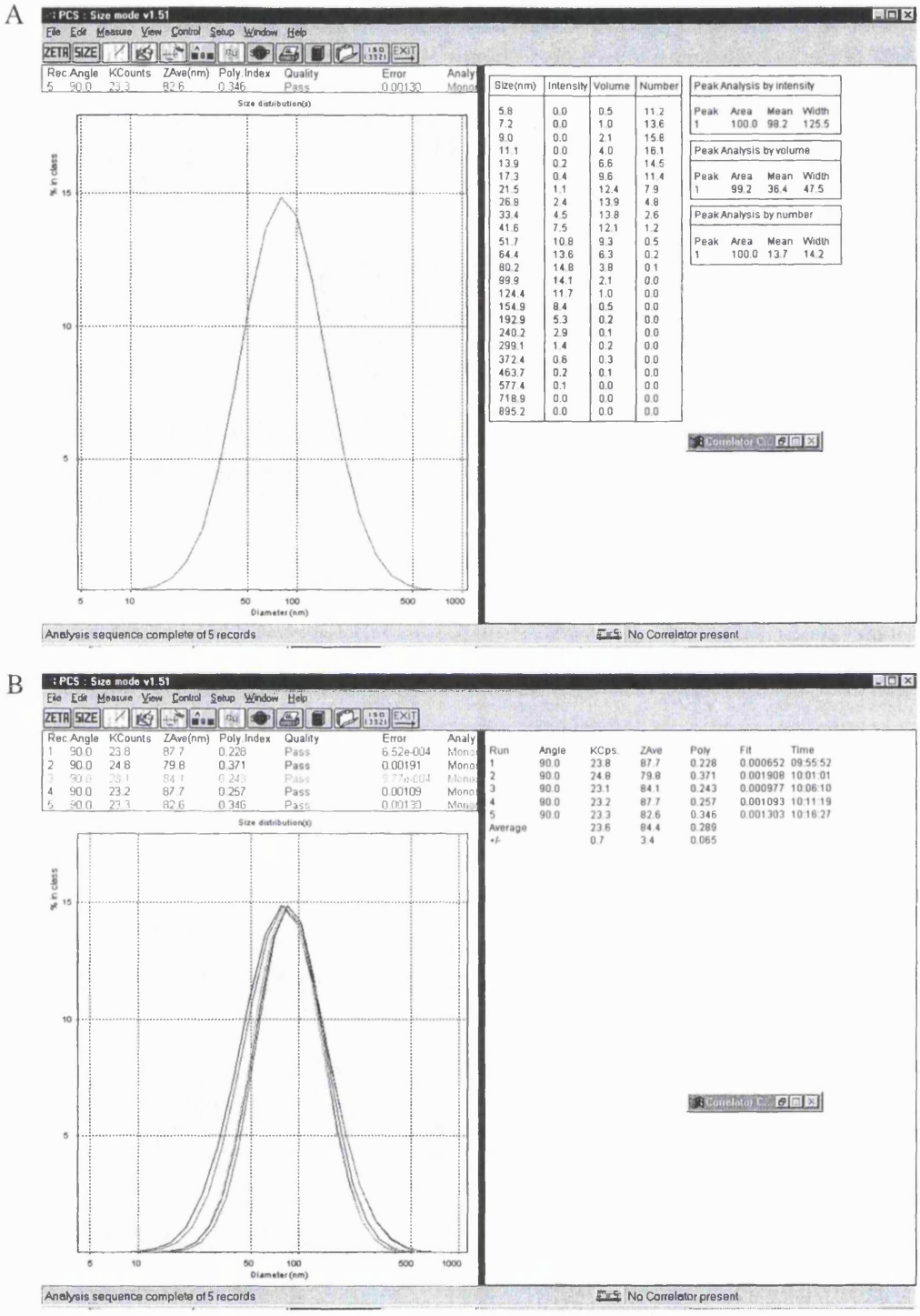

Figure 4.2 Typical particle size measurement data generated by Malvern Zetasizer 3000 software, using monomodal analysis, for poly-L-lysine/calf thymus DNA complexes prepared using the two-syringe mixing method (6 ml/min mixing rate), at a charge ratio of 2.0 in 20 mM HEPES pH 7.2: (A) a typical analysis

table, where the particle size distribution is presented as the intensity of light scattered and (B) tabulated data showing the measurement repeatability of the mean size and standard deviation over 5 minute runs on the same sample.

4.1.2 Optimisation of polyplex preparation methods

4.1.2.1 Reproducibility of polyplexes and size measurements

It was important to standardise the preparation of complexes and hence reduce handling inconsistencies between different workers. The commonly used methods of pipette mixing (see Section 3.5) or vortex mixing the constituents of a formulation were considered unsatisfactory because mixing conditions such as mixing speed and duration were difficult to control. The method utilised here was a scaleable, semi-automated, continuous mixing method, using a two-syringe pump flow system (see Section 3.7), first described by Zelphati *et al.* (Zelphati *et al.*, 1998a). Their studies demonstrated the reproducibility of a two-syringe mixing method, where physically stable, monodisperse cationic lipid/DNA complexes (lipoplexes) were prepared from 400 and 100 nm liposomes at the optimal mixing rates of 3.24-8.10 ml/min and 15.7 ml/min, respectively.

Experiments were conducted to investigate the reproducibility of the particle size of poly-L-lysine/calf thymus DNA (PLL/DNA) complexes prepared using the two-syringe mixing method, and to optimise the mixing rate of the PLL and DNA solutions (Fig. 4.3). Both components were loaded into separate vertically mounted syringes on the syringe pump (Fig. 3.1) and then mixed simultaneously at predetermined speeds ranging from 0.2 to 17 ml/min. The polyplexes were prepared at charge ratios of 1.0 and 2.0. Fig. 4.4 shows the *z*-average size of the polyplexes calculated from the size distributions for ten samples prepared independently. The *z*-average or mean particle size was calculated using the cumulants analysis (detailed in Section 3.9). The results demonstrate the reproducibility in particle size of polyplexes formed in salt-free HEPES buffer at charge ratios 1.0 and 2.0. The polyplexes were prepared by the two-syringe mixing method at a

mixing rate of 6 ml/min. The diameters of polyplexes at a charge ratio of 1.0 were approximately 140 nm, with a standard deviation between samples of about 20 nm (n = 8), whereas complexes formed at a charge ratio of 2.0 were smaller, with a uniform size of approximately 90 ± 20 nm (n = 8). The sample variance of the particle size of polyplexes at charge ratios 1.0 and 2.0 was about 400 and 200 nm, respectively.

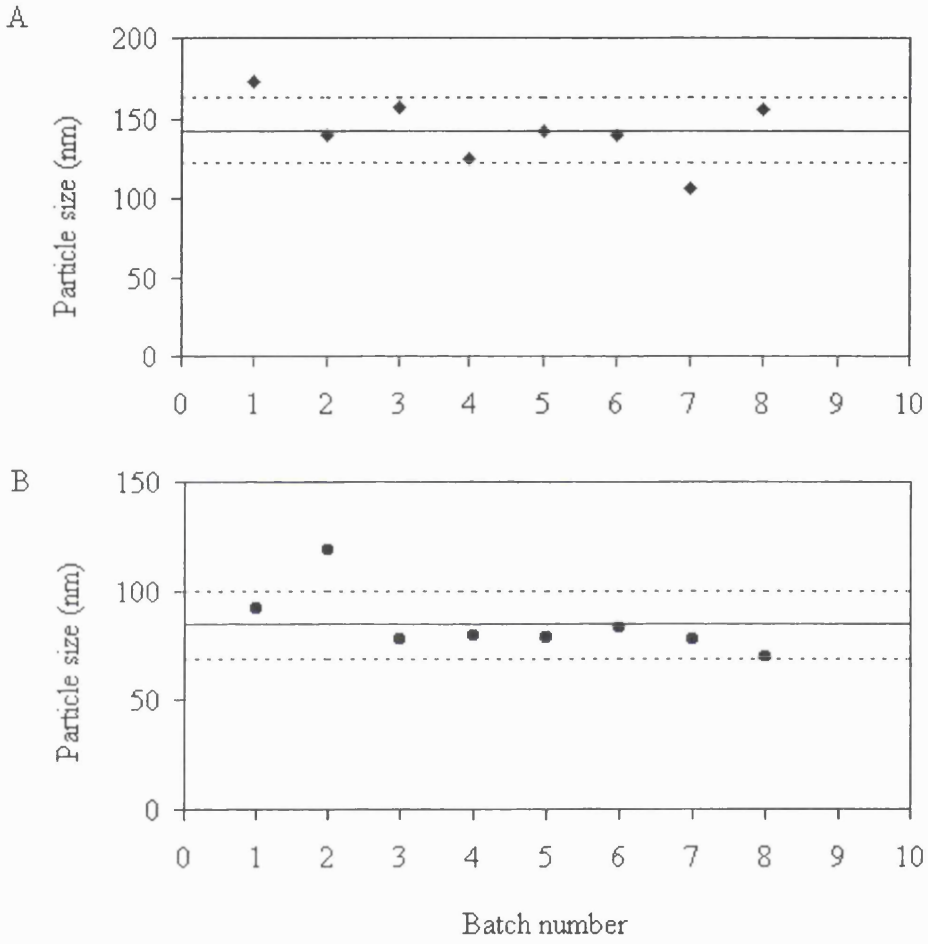

Figure 4.3 Sample-to-sample reproducibility of mean particle size for poly-L-lysine/calf thymus DNA complexes. The data were based on separate samples of polyplexes prepared using the two-syringe mixing method (6 ml/min mixing rate) and charge ratios of: (A) 1.0 and (B) 2.0, in 1 mM HEPES, pH 7.7. The mean hydrodynamic diameter (solid line) and standard deviation (dotted lines) were calculated using the Excel standard deviation worksheet function.

4.1.2.2 Optimisation of mixing rates

Fig. 4.4 shows the variation in the *z*-average size of polyplexes of PLL (average MW = 25,900) and calf thymus DNA prepared at different mixing rates and charge ratios. Considering the data in Fig. 4.4, mixing rates greater than about 6 ml/min gave reasonably consistent polyplex sizes from batch to batch, practically independent of charge ratio, except for polyplexes at 0.8 charge ratio, which had large errors (average coefficient of variation = 0.8). Given the possible significant sources of error (related to the use of different batch solutions) in the experiments, the variation of about ± 50 nm for each particle size in these studies was assumed to be acceptable. Mixing rates in the region of 17 ml/min (data not shown) resulted in significantly aggregated polyplexes with sizes above the range of detection of the instrument, i.e. greater than 3000 nm. Unless otherwise stated, all subsequent preparation of PLL/DNA complexes were performed using the two-syringe mixing method at a mixing rate of 6 ml/min.

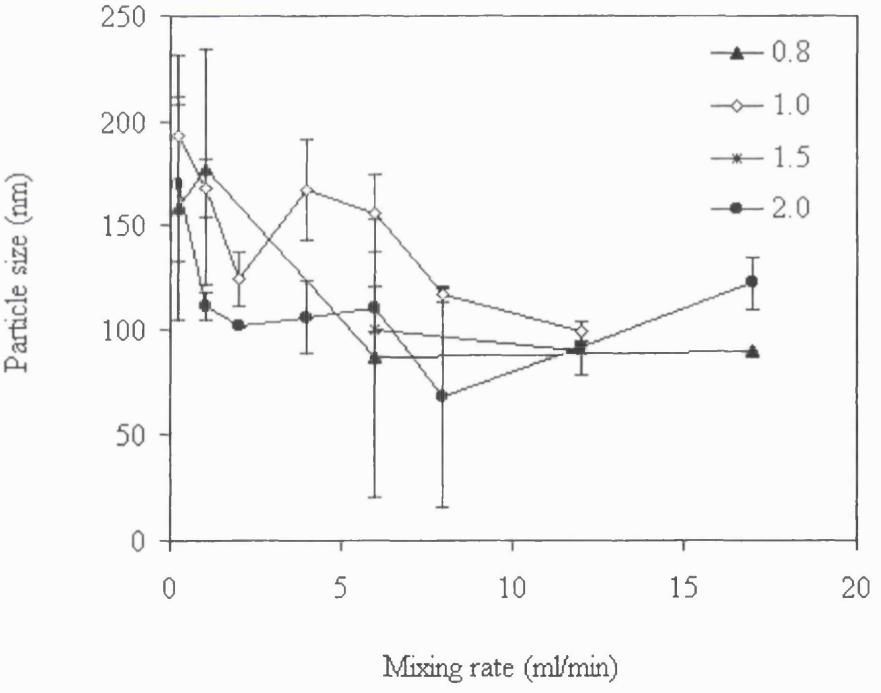

Figure 4.4 Influence of the mixing rate on the mean particle size of polyplexes formed between PLL and calf thymus DNA at various charge ratios in 1 mM HEPES, pH 7.7. The results shown are averages of at least two experiments. Note

the large error bars at the mixing rates of 6 and 8 ml/min for polyplexes at 0.8 charge ratio.

4.1.2.3 Influence of preparation method and charge ratio on storage stability

Currently, the instability of formulations of DNA complexes requires that in clinical trials the complexes be prepared at the bedside, in a relatively uncontrolled manner, immediately prior to injection (Caplen *et al.*, 1995). Hence, the stability of DNA complexes must be investigated, characterised and improved. An experiment was conducted to determine the storage stability of PLL/DNA complexes in salt-free buffer. Polyplexes were prepared both by the two-syringe mixing method (described in Section 3.7) and also by pipette mixing (Section 3.5). Briefly, pipette mixing entails the rapid addition of all of one component to the other component using a pipette tip, followed by about five seconds of mixing using the same pipette tip. It appears to be a standard practice to assume that polyplex formation occurs immediately after mixing, as observed in studies on DNA condensation or complexation processes (Lai and van Zanten, 2001; Tang and Szoka, Jr., 1998).

Following initial particle size measurements at room temperature, where the polyplexes were observed to be physically stable (Fig. 4.5), subsequent particle size measurements after 24 and 72 hours of refrigeration (4°C) were also performed. No significant change in the particle size of the polyplexes was observed. The results in Fig. 4.5 illustrate the physical stability of polyplexes prepared by the two-syringe mixing method at charge ratios of 0.8, 1.0 and 2.0. The freshly mixed polyplexes had mean diameters no greater than 200 nm, even after storage at 4°C for three days. Although the polyplexes were shown to be stable over 72 h, it may be possible that the polyplexes could have aggregated over a much longer period. This was not pursued here. However, it has been shown by dynamic light scattering that PLL/DNA complexes of charge ratio 5.0 aggregate significantly, from ~220 nm to > 450 nm, after a 14 day storage (Jones *et al.*, 2000).

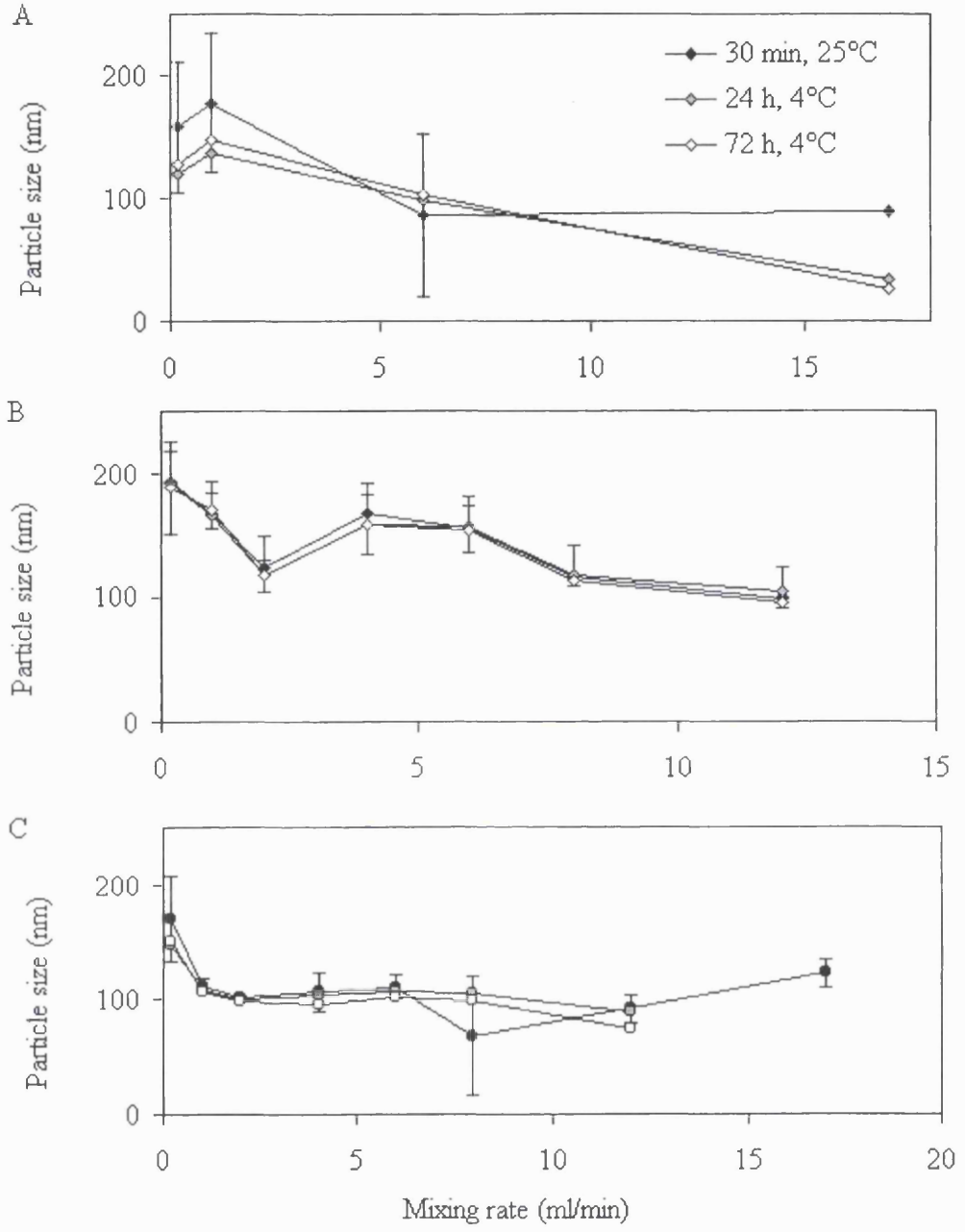

Figure 4.5 Mean particle size of poly-L-lysine/calf thymus DNA complexes prepared using the two-syringe mixing method, at charge ratios of: (A) 0.8, (B) 1.0 and (C) 2.0, as a function of the mixing rate and time of measurements. n = 2, bars indicate the value of standard deviation.

Fig. 4.6 shows the influence of the sample preparation method (two-syringe mixing method as shown in Fig. 4.5, addition of PLL to DNA by pipette mixing, or addition of DNA to PLL by pipette mixing) on the mean particle size of polyplexes after storage for 24 h. In pipette mixing, a solution (of DNA or PLL) is rapidly added to another solution (of PLL or DNA, respectively) using a pipette tip, followed by ~5 s of mixing.

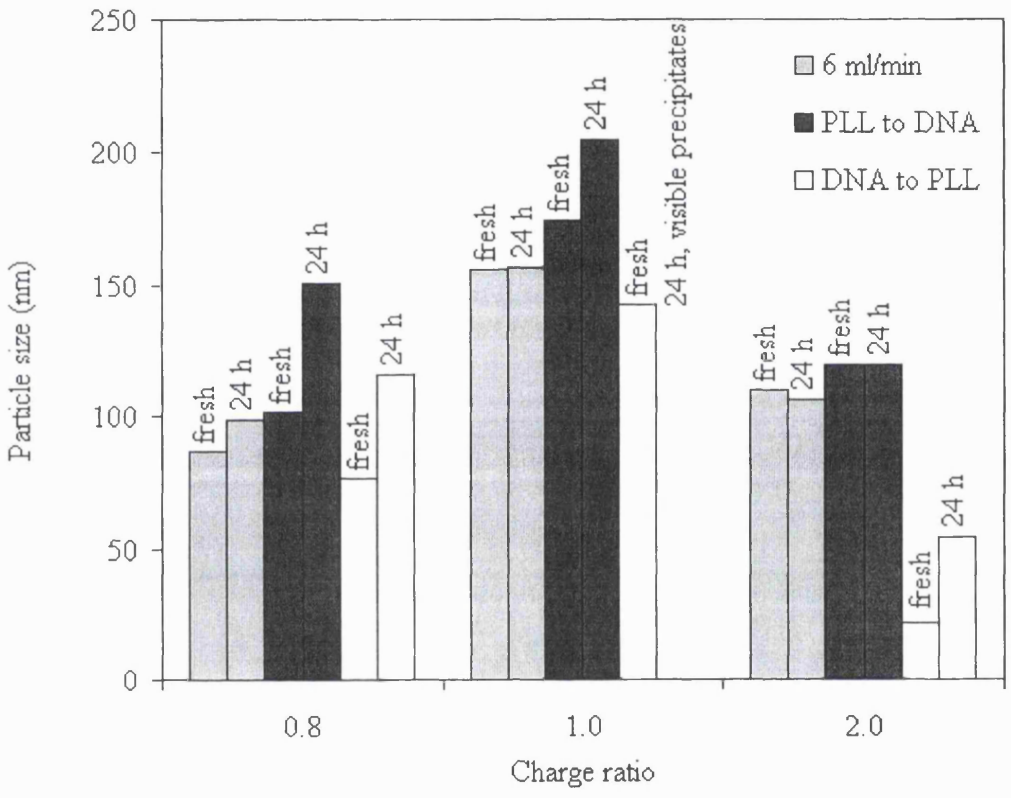

Figure 4.6 Mean particle size of polyplexes formulated using the two-syringe mixing method (6 ml/min mixing rate) and pipette mixing (addition of PLL to DNA, and DNA to PLL). Polyplexes were prepared at charge ratios 0.8, 1.0 and 2.0. Particle size measurements were performed immediately after mixing ("fresh") and following storage at 4°C for 24 h ("24 h").

There was a problem of physical stability for polyplexes prepared by the pipette mixing method at charge ratios of 0.8 and 1.0, where the net charge on the polyplex is theoretically negative or neutral, respectively. Polyplexes at these charge ratios prepared by pipette mixing showed a distinct increase in size after storage at 4°C overnight. For polyplexes at a charge ratio of 1.0, prepared by DNA-into-PLL mixing, precipitates were observed in the sample after overnight storage at 4°C (Fig 4.6). The size of these aggregates could not be measured because they were beyond the detection range of the light scattering equipment, which is about 20–3000 nm. This significant aggregation at charge ratio 1.0 could be due to the approximately neutral charge on the external surface of those particles. Other authors have also found that polyplexes formed by the rapid addition of DNA into PLL (Kwoh *et al.*, 1999) and of PLL into DNA (Tsai *et al.*, 1999) at neutral charge ratio aggregate under salt-free conditions.

In comparison with polyplexes at charge ratios 0.8 and 1.0 prepared by pipette mixing, polyplexes at these charge ratios prepared by two-syringe mixing demonstrated better storage stability. This suggests that pipette mixing could lead to the presence of free DNA in the solution. The free DNA, which is not detected by the light scattering equipment, contributes to the polydispersity of the system and encourages aggregation. The instability of the system is undesirable because aggregated DNA complexes possess reduced transfection efficiencies (Anchordoquy *et al.*, 1998). In contrast, two-syringe mixing is likely to result in a narrower distribution of polyplexes because the contact of the PLL and the DNA occurs simultaneously in the T-connector of the mixing equipment (Fig. 3.1). For these complexes at the charge ratios of 0.8 and 1.0, owing to the syringe mixing method, free DNA was more likely to be associated on the surface of the polyplexes, giving a less heterogeneous and more stable system. The following results (Fig. 4.7) demonstrate the presence of free DNA at these charge ratios. The contribution of heterogeneity to aggregation of the polyplexes is explained later in Section 4.2.2.3. Since using a charge ratio of 2.0 gave stable complexes wherein all the DNA was likely to be complexed to the PLL, further experiments were focused on the characterisation of formulations prepared at this charge ratio.

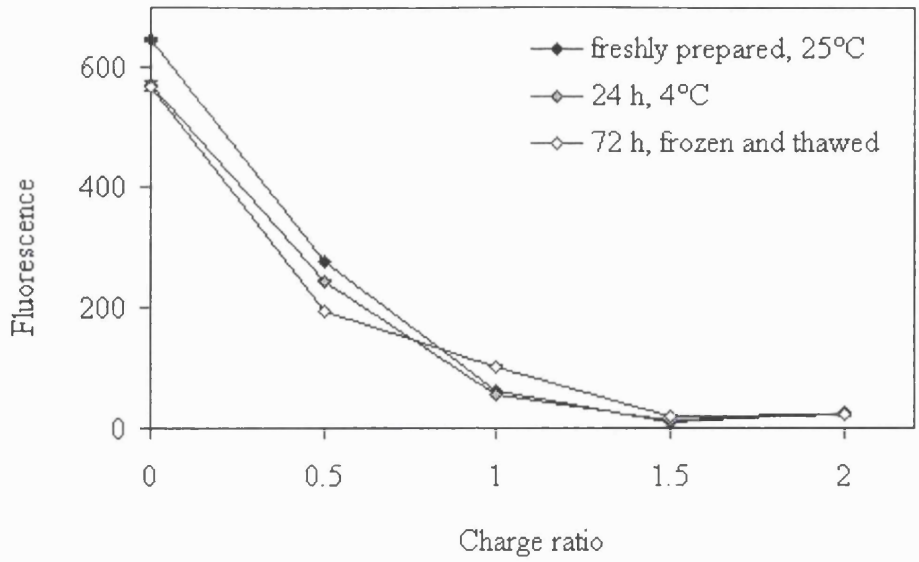

Figure 4.7 Effect of short-term storage on DNA accessibility of polyplexes, measured by the PicoGreen assay. PLL/DNA complexes were prepared from PLL (25,250 MW) and calf thymus DNA by the two-syringe mixing method (6 ml/min) at a DNA concentration of 12.5 µg/ml and various charge ratios in 20 mM HEPES pH 7.2. The polyplexes were then diluted to a final concentration of 0.5 µg/ml before the addition of PicoGreen working solution. After initial fluorescence measurements ("freshly prepared, 25°C"), the polyplexes were stored in a 4°C refrigerator overnight and measured ("24 h, 4°C"). The polyplexes were subsequently frozen at -20°C for three days and thawed for final fluorescence measurements ("72 h, frozen and thawed"). Values are the standard deviation for two separate experiments; note that for most data points error bars are eclipsed by the size of the symbol.

Fig. 4.7 shows the influence of short-term storage conditions on the fluorescence quenching for polyplexes formed between poly-L-lysine of molecular weight 25,250 and calf thymus DNA as a function of polyplex age. The relative binding efficiencies of PLL to DNA were examined using a PicoGreen-based quenching assay. Polyplexes were prepared at a DNA concentration of 12.5 µg/ml using the two-syringe mixing method and

diluted appropriately for the fluorescence assay as previously described in Section 3.12. The fluorescence of each sample was then measured in a fluorometer. It is observed that increasing amounts of PLL resulted in a decrease in fluorescence (Fig. 4.7). The same samples of polyplexes were then stored overnight in the refrigerator (4°C), assessed for fluorescence, and then frozen at -20°C for a subsequent 48 h before being analysed again. Details are given in the legend. Maximum quenching is first achieved between the theoretical charge ratio 1.0, where all of the DNA phosphate charge is expected to be neutralised, and the charge ratio of 1.5. The binding of polylysine-containing peptides to DNA has been found in other fluorescence quenching studies to also occur at charge ratios higher than 1.0 (Kwoh *et al.*, 1999; McKenzie *et al.*, 1999). In one study, the binding efficiency of PLL to DNA was also found to decrease at high ionic strength (150 mM NaCl) and when a targeting ligand was conjugated to the PLL chain (Kwoh *et al.*, 1999). Similarly for lipoplexes, the interaction between a cationic phospholipid and DNA was found to be decreased under physiological conditions (Kennedy *et al.*, 2000). These results would be critical in designing targeted complexes for *in vivo* gene delivery.

No difference in the appearance of the solution or the fluorescence quenching of the polyplexes was noted in all of the samples, confirming their storage stability (Fig. 4.7). Note that the final polyplexes prepared by the two-syringe mixing method at the 1.0 charge ratio were remarkably stable even after freeze-thawing, and did not precipitate out of the solution (Fig. 4.7), unlike polyplexes prepared by pipette mixing at charge ratio 1.0 where one component is added to the other followed by cold storage (Fig. 4.6).

Considering all of the results shown in this section (Section 4.1.2), it is concluded that polyplexes prepared using the two-syringe mixing method at a mixing rate of 6 ml/min, and at a charge ratio of 2.0, gave the most consistent results. At these conditions, the polyplexes demonstrated the best results in terms of physical stability, as shown by their particle size and DNA accessibility.

4.1.3 Influence of charge ratio and pH on zeta potential

Experiments were conducted to determine the surface charge of poly-L-lysine/calf thymus DNA complexes prepared at various charge ratios and pH conditions. Fig. 4.8 shows that the zeta potential of the PLL/DNA complexes is controlled by both the pH of the solution and the charge ratio. Unless indicated otherwise, all subsequent experiments were carried out at a charge ratio of 2.0 indicating a positively charged polyplex suspension. Decreasing the pH of this system increased the protonation of the lysine amino groups which have an intrinsic pK_a value of 11.1 (Creighton, 1993). The expected effect is an increase in the stability of the suspension, which is supported by the data shown later in Fig. 4.9 and the theoretical predictions of the total potential energy of interaction based on Eqs. (4.3) to (4.10), as shown later in Section 4.2.1. Additionally, at the lower pH, the crossover from a negative to a positive zeta potential occurs before the charge ratio value of 1.0. This is in agreement with work elsewhere (Tang and Szoka, 1997; Xu *et al.*, 1998) and suggests that the environment of the lysine residues has an influencing role in their interactions with the phosphate groups of the DNA.

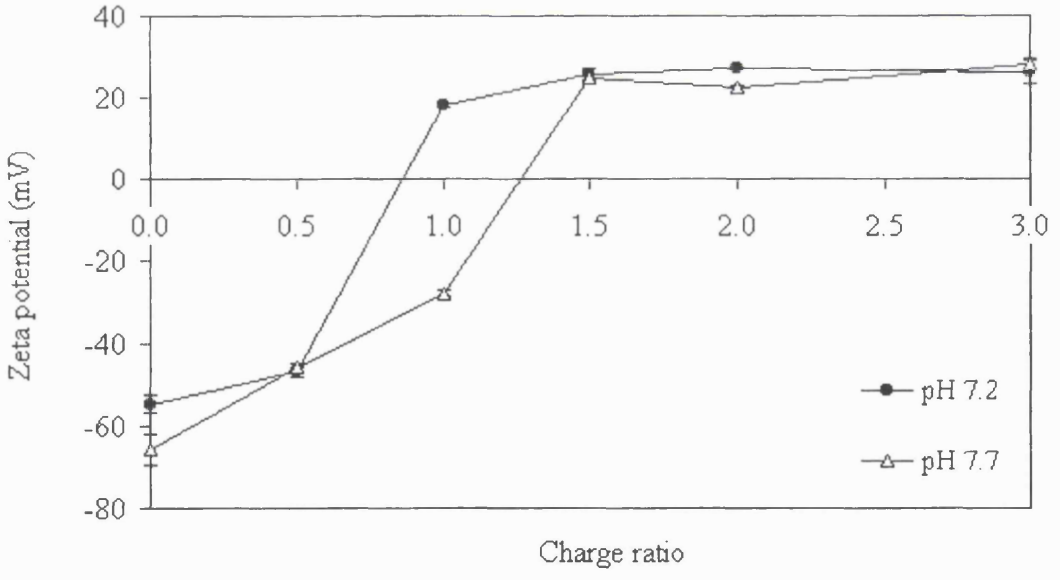

Figure 4.8 Zeta potentials of poly-L-lysine/calf thymus DNA complexes as a function of the charge ratio. Data refer to polyplexes in 20 mM HEPES pH 7.2 (filled symbols) and pH 7.7 (open symbols). The polyplex formulation was prepared by mixing equal volumes of calf thymus DNA (25 μg/ml) and polylysine

of the appropriate concentration by the two-syringe mixing method as described in Section 3.7.

4.1.4 Influence of ionic strength and pH on polyplex stability

The colloidal aggregation processes associated with effects of ionic strength in polymer solutions have long been studied by photon correlation spectroscopy (PCS) for a variety of materials such as hematite (Amal *et al.*, 1990), protein-coated polystyrene particles (Molina-Bolívar *et al.*, 1998; Molina-Bolívar *et al.*, 1999) and human transferrin receptor (Schüler *et al.*, 1999). In order to understand the aggregation properties (described later in Sections 4.2 and 4.3) of the PLL/DNA system, it is important to study the colloidal stability of the polyplexes. Dynamic light scattering (DLS) was used to monitor the aggregation of PLL/DNA complexes in buffers both containing sodium chloride or to which the NaCl was added. The results are discussed below.

4.1.4.1 PLL/calf thymus DNA complexes

Fig. 4.9 shows the variation in the mean particle size of PLL/calf thymus DNA complexes with solution salt concentration (ionic strength) and pH. The polyplexes were prepared using the two-syringe mixing method with a fixed mixing rate of 6 ml/min. The data in Fig. 4.9 show that ionic strength and pH of the suspension critically determine the physical stability of the PLL/DNA complexes. PLL of molecular weight 25,250 was used. With the exception of the suspension at a concentration of 10 mM NaCl at the lowest pH, all systems examined showed an increase in the z-average hydrodynamic diameter as a function of time. The rate of aggregation increased with increasing ionic strength and increasing pH. At a pH of 8.0, even the suspension containing 10 mM NaCl exhibited a degree of aggregation as shown in Fig. 4.9C.

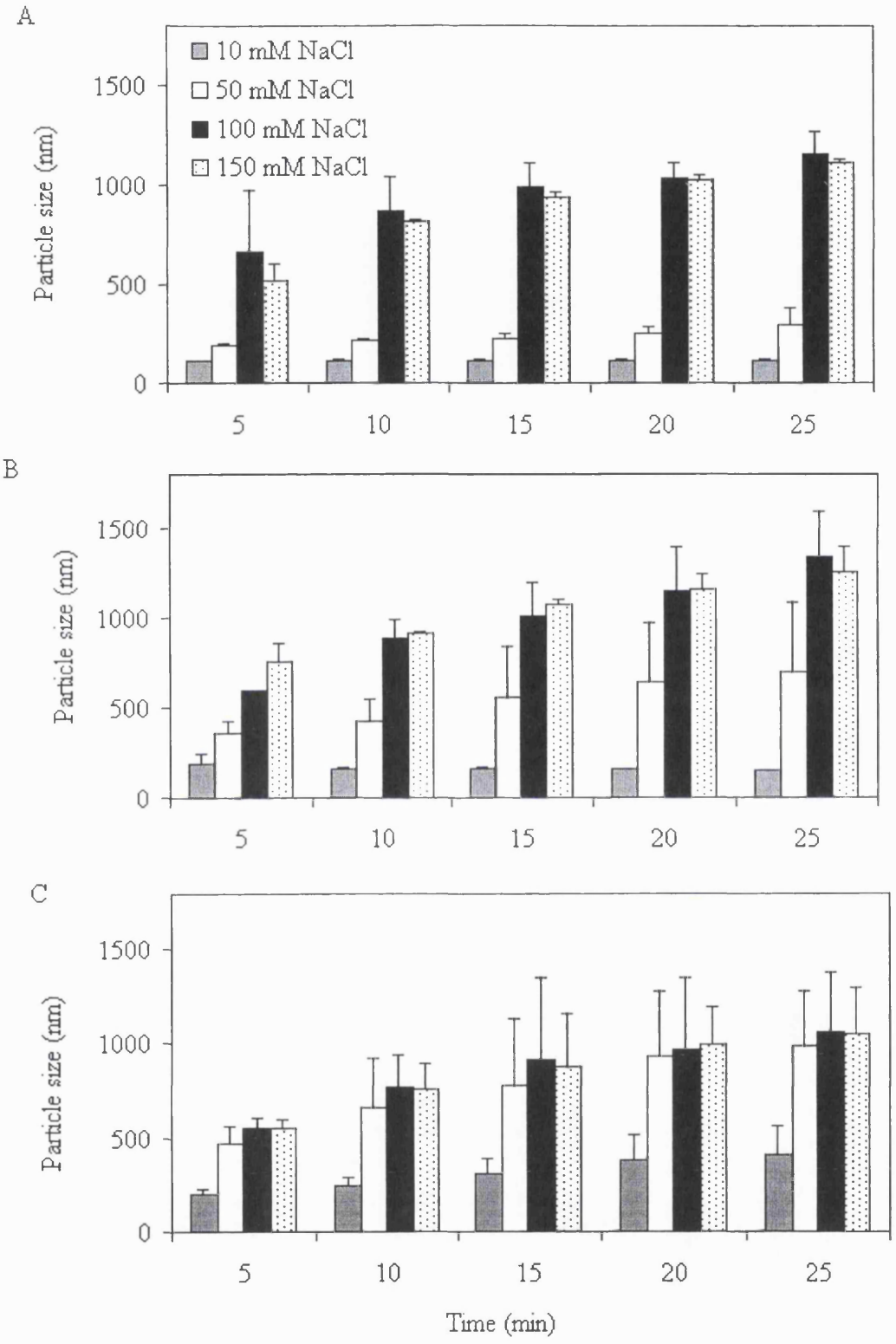

Figure 4.9 Particle size of poly-L-lysine/calf thymus DNA complexes as a function of time for different salt concentrations and pH. The polyplexes were prepared at a mixing rate of 6 ml/min and a charge ratio of 2.0 in 20 mM HEPES: (A) pH 7.2,

(B) pH 7.7 and (C) pH 8.0. The data are expressed as the mean hydrodynamic diameter and standard deviation obtained from two independent experiments.

As shown in Fig. 4.9, the larger sizes (greater than 500 nm) of polyplexes formed immediately after mixing (t = 0) at higher ionic strengths (100 and 150 mM NaCl) confirmed that rapid aggregation occurred in the initial five minutes following preparation of the polyplexes, i.e. during the data acquisition time. Although DNA delivery systems of such sizes have been used in the transfection of cultured cells with satisfactory gene expression levels, *in vivo* gene delivery would impose limitations on the size of the polyplexes so that they may pass through biological barriers such as the vascular endothelium and blood-brain barrier, diffuse through tissues, and be efficiently internalised by the cells (Pouton, 1999). Furthermore, higher DNA concentrations ($\geq$ 330 μg/ml) are essential for clinical applications (Zelphati *et al.*, 1998a). It will be shown later (Chapter 5) that the aggregation of DNA complexes increases dramatically as the DNA concentration is increased.

Fig. 4.10 summarises the comparison of particle size distributions for two different samples of PLL/DNA complexes as a function of time after preparation. The polyplexes were prepared by the two-syringe mixing method at a 2.0 charge ratio in 20 mM HEPES: (A) pH 7.2, 10 mM NaCl and (B) pH 8.0, 150 mM NaCl. The data refer to the systems shown in Fig. 4.9: (A) 10 mM NaCl and (C) 150 mM NaCl, respectively. Comparison of Figs. 4.10A and B demonstrates that the physical stability of the polyplexes is acutely sensitive to the salt concentration. The extreme instability of the system at physiological ionic strength, as shown by samples at 100 and 150 mM NaCl in Fig. 4.9, is well supported by the distinct shift and broadening in the size distributions shown in Fig. 4.10B.

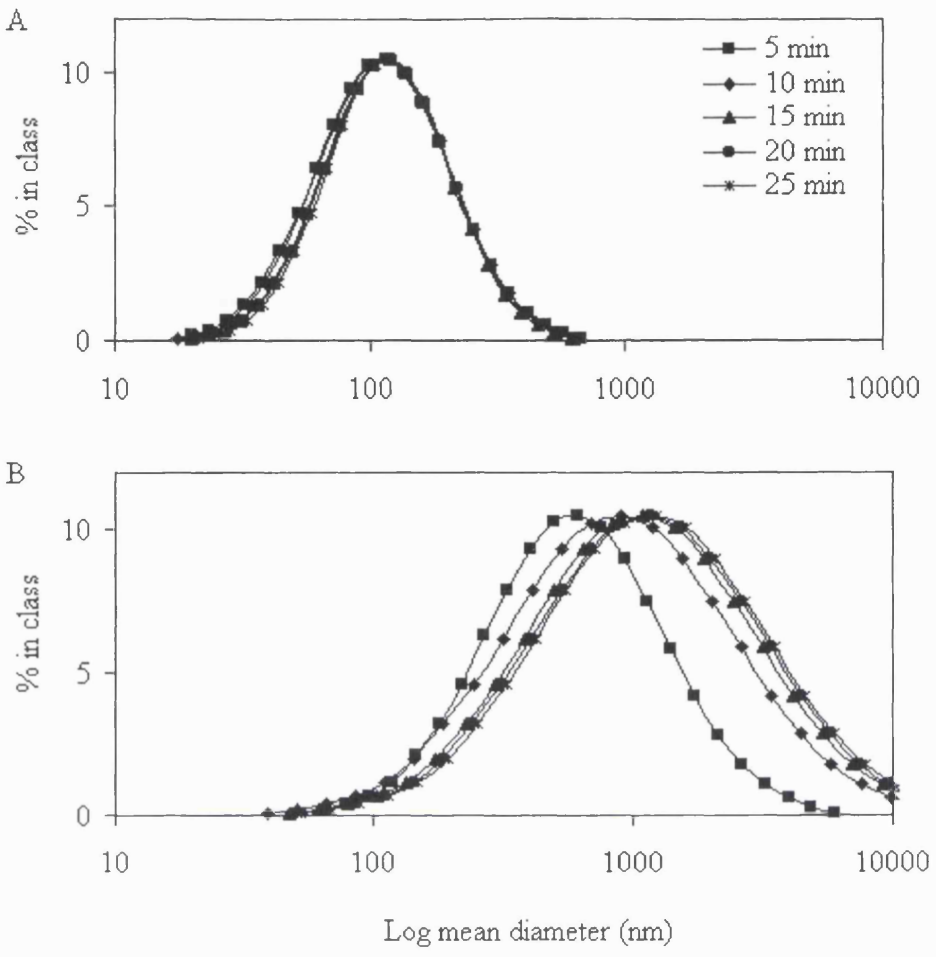

Figure 4.10 Particle size distributions of poly-L-lysine/calf thymus DNA complexes at a charge ratio of 2.0 in 20 mM HEPES: (a) pH 7.2, 10 mM NaCl [corresponds to Fig. 4.9(A) 10 mM NaCl] and (B) pH 8.0, 150 mM NaCl [corresponds to Fig. 4.9(C) 150 mM NaCl], as a function of time after preparation. Size distributions were determined as mean of diameter on the basis of intensity of scattered light at 90°. The data shown were obtained from a single representative sample.

As previously shown in Fig. 4.2, the results from the Malvern Zetasizer gives intensity, mass and number weighted size distributions (Fig. 4.2A), as well as *z*-average diameter and polydispersity index (Fig. 4.2B). The broadening of the size distribution as a function of time corresponds to increasing polydispersity of the sample, which is associated with

the variance of the population (Rustemeier and Killmann, 1997). The polydispersity index, estimated by cumulants analysis of the DLS data, has a maximum value of 1.0, with a nominal value of 0.7 representing a highly polydisperse distribution. The polydispersity indices of about 0.2-0.3, for all size distributions of the system at a low salt concentration (Fig. 4.10A) and for the initial distribution ("5 min") of the system at the high salt concentration (Fig. 4.10B), indicate fairly narrow size distributions of the polyplexes. In contrast, the polydispersity values for subsequent measured distributions in Fig 4.10B increased from 0.4 at 10 min to beyond 0.7 for a sample analysed nearly 30 minutes after polyplex formation. It will be shown later (in Section 4.2.2.3) that aggregation in polydisperse systems is particularly marked.

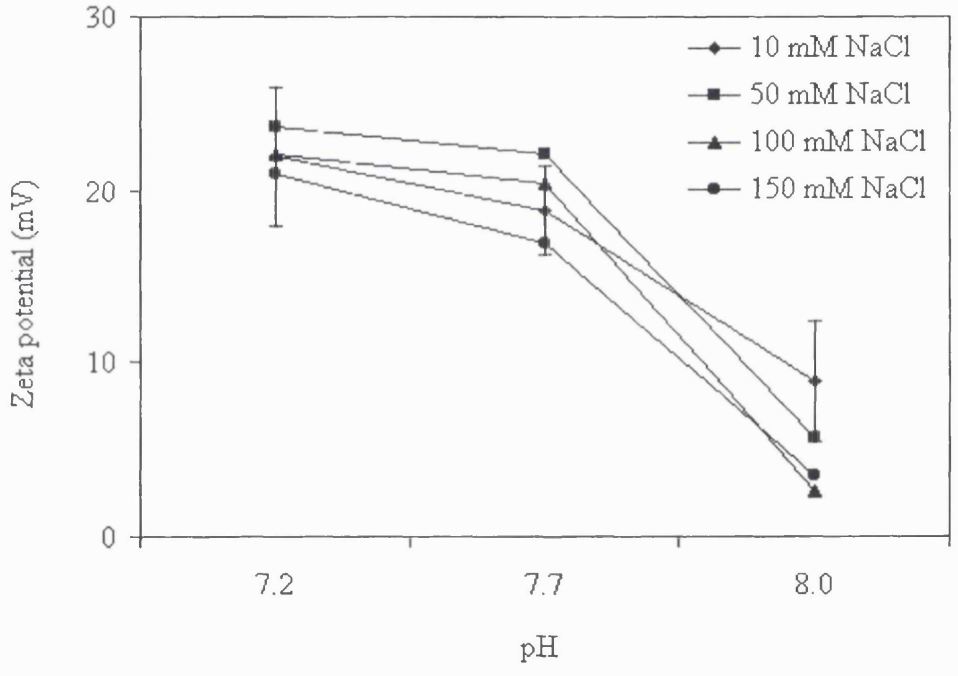

Figure 4.11 Effect of buffer pH and sodium chloride concentration on the measured zeta potential of complexes formed between polylysine and calf thymus DNA. Polyplexes were prepared using the two-syringe mixing method (6 ml/min mixing rate) in 20 mM HEPES buffer at a charge ratio of 2.0. Bars indicate the value of standard deviation of two separate experiments. For the sake of clarity only deviations for polyplex samples at 10 mM NaCl are shown.

The surface charge of the polyplexes can be quantitatively inferred from mobility measurements and is given by the measured zeta potential (see Sections 3.8 and 4.2.1.1). The zeta potential of the PLL/calf thymus DNA complexes whose particle size distributions are shown in Figs. 4.9 and 4.10 were tested. The zeta potentials of the polyplexes were observed to decrease with increasing solution pH, as shown in Fig. 4.11. The results indicate that at higher pH values, the polyplexes are less positively charged, and consequently, more likely to interact with each other. These observations (Fig. 4.11) are in good agreement with the physical instability of polyplexes in buffers of higher pH as shown previously (Fig. 4.9). Polyplexes prepared at higher pH values had zeta potentials close to zero, indicating the tendency of the system to aggregate in a basic environment (pH $\geq$ 8.0 in this case), and the presence of more titratable groups close to the isoelectric point (IEP, the pH at which the zeta potential becomes zero). The zeta potentials remained fairly constant over a range of ionic strengths for a given pH, which is in disagreement with findings by other groups, where an increase in the salt concentration resulted in a decrease in the zeta potential (Son *et al.*, 2000; Xu *et al.*, 1998). The zeta potential measurements in Fig. 4.11 were performed after the size measurements, i.e. when most of the polyplexes were observed to have aggregated (Fig. 4.9), hence possibly contributing to this dissimilarity.

4.1.4.2 PLL/pSVβ complexes

All experiments detailed so far referred to polyplexes formed with calf thymus DNA, not plasmid DNA. Here, two sets of experiments were conducted for polyplexes formed between poly-L-lysine of average molecular weight 34,300 and the plasmid pSVβ, each one using a range of NaCl concentrations. Polyplexes were formed either in HEPES buffer (pH 7.2) with the desired salt concentration, or in salt-free buffer to which salt was added. The salt concentrations ranged from 10 to 150 mM for the former case and from 10 to 500 mM for the latter.

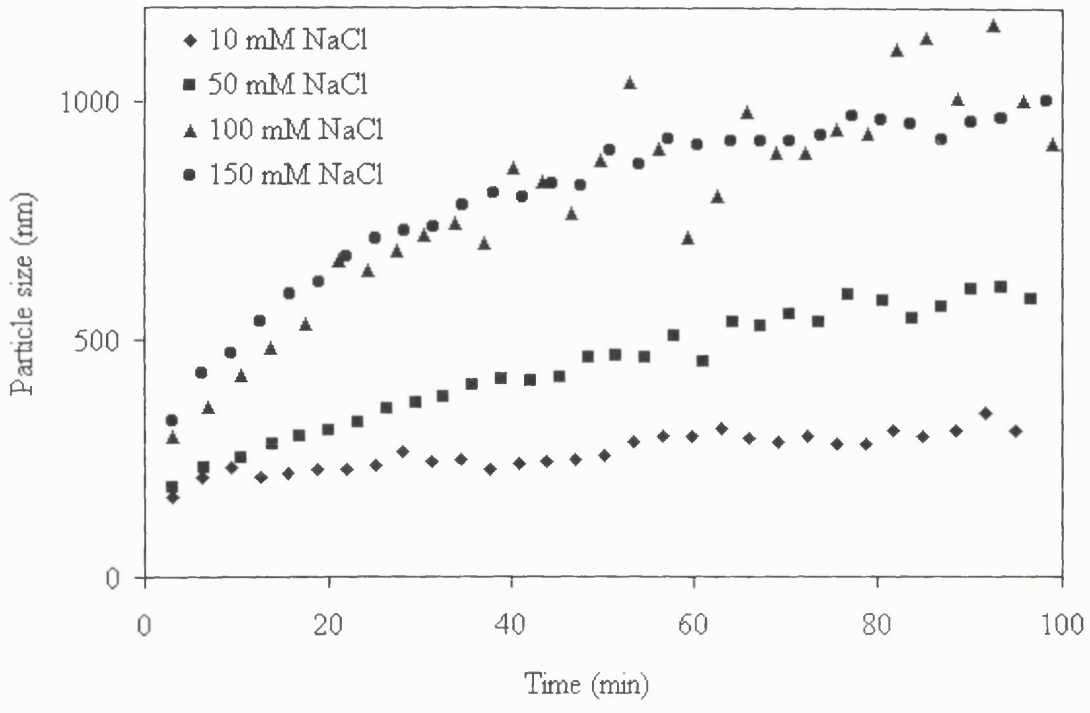

Figure 4.12 Time evolution of average hydrodynamic diameter of complexes between poly-L-lysine (MW 34,400) and pSVβ plasmid. The polyplexes were prepared under a mixing rate of 6 ml/min using the two-syringe mixing method. Freshly prepared polyplexes at 2.0 charge ratio in 20 mM HEPES pH 7.2 buffer with different ionic strengths (10 to 150 mM NaCl) were analysed by dynamic light scattering. The data shown are representative of at least two experiments.

Fig. 4.12 shows the variation of the measured mean hydrodynamic diameter (*z*-average size) of poly-L-lysine/pSVβ complexes with time for salt concentrations in the range between 10 and 150 mM. As was shown previously in experiments using calf thymus DNA (Fig. 4.9A), it can be seen that at pH 7.2, polyplex growth is extremely sensitive to NaCl concentration in the range 50-150 mM. The increase in the strong small molecule electrolytes, Na^+ and Cl^-, balanced the surface charge of the polyplexes and hence reduces the repulsion between them. The polydispersity indices of the polyplexes also increased largely as aggregation proceeded, for example, in the 100 mM NaCl sample, from 0.3-0.4 immediately after mixing to 0.9-1.0 after about 90 minutes. Again, the instability of polyplexes such as these and other gene delivery systems at the

physiological ionic strength of 150 mM remains a considerable challenge for successful gene transfer, especially *in vivo*, where the positive surface charge of the polyplexes promotes interactions with serum proteins.

Experiments were also carried out with the Malvern Autosizer 4700 photon correlation spectroscopy system. The particle size distributions of PLL/pSVβ complexes in HEPES buffer (pH 7.2) containing no added salt were measured and found to be stable, as shown earlier in this chapter (Sections 4.1.2 and 4.1.3). After 5 consecutive particle size measurements (~ 15 min) of the non-aggregating polyplexes, a small predetermined volume of concentrated NaCl solution was then quickly pipetted into the polyplex sample to induce aggregation, without removing the polyplex sample from the spectrophotometer cell. During the *in situ* NaCl addition, particle size measurements by the instrument were allowed to proceed automatically. The particle size data were recorded continuously during the aggregation process by the software for up to 3 hours.

Fig. 4.13A shows the variation of the measured size of PLL/pSVβ complexes with time. Aggregation was initiated at a range of NaCl concentrations (10-500 mM). In the case of 10 mM NaCl, aggregate growth is not observed. At higher electrolyte concentrations, the polyplexes display considerable physical instability. The aggregation rate was found to increase with increasing NaCl concentrations. The data in Fig. 4.13A can be replotted differently to show clearly this trend (Fig. 4.13B). Fig. 4.13B, which refers to the same samples seen in Fig. 4.13A, shows the mean particle size measured at various time intervals (30, 60, 90 and 120 min) for the polyplex systems at different ionic strengths. In Fig. 4.13B, the data on the left of the plot illustrates how stable the polyplexes at 10 mM NaCl are. In contrast, at salt concentrations of 25 mM and above, the same system is highly unstable. Fifteen minutes following addition of NaCl (denoted by "30 min" in Fig. 4.13B), aggregation is evident. The time intervals at which the particle size was measured are approximate due to the manner of collection of light scattering data by the instrument.

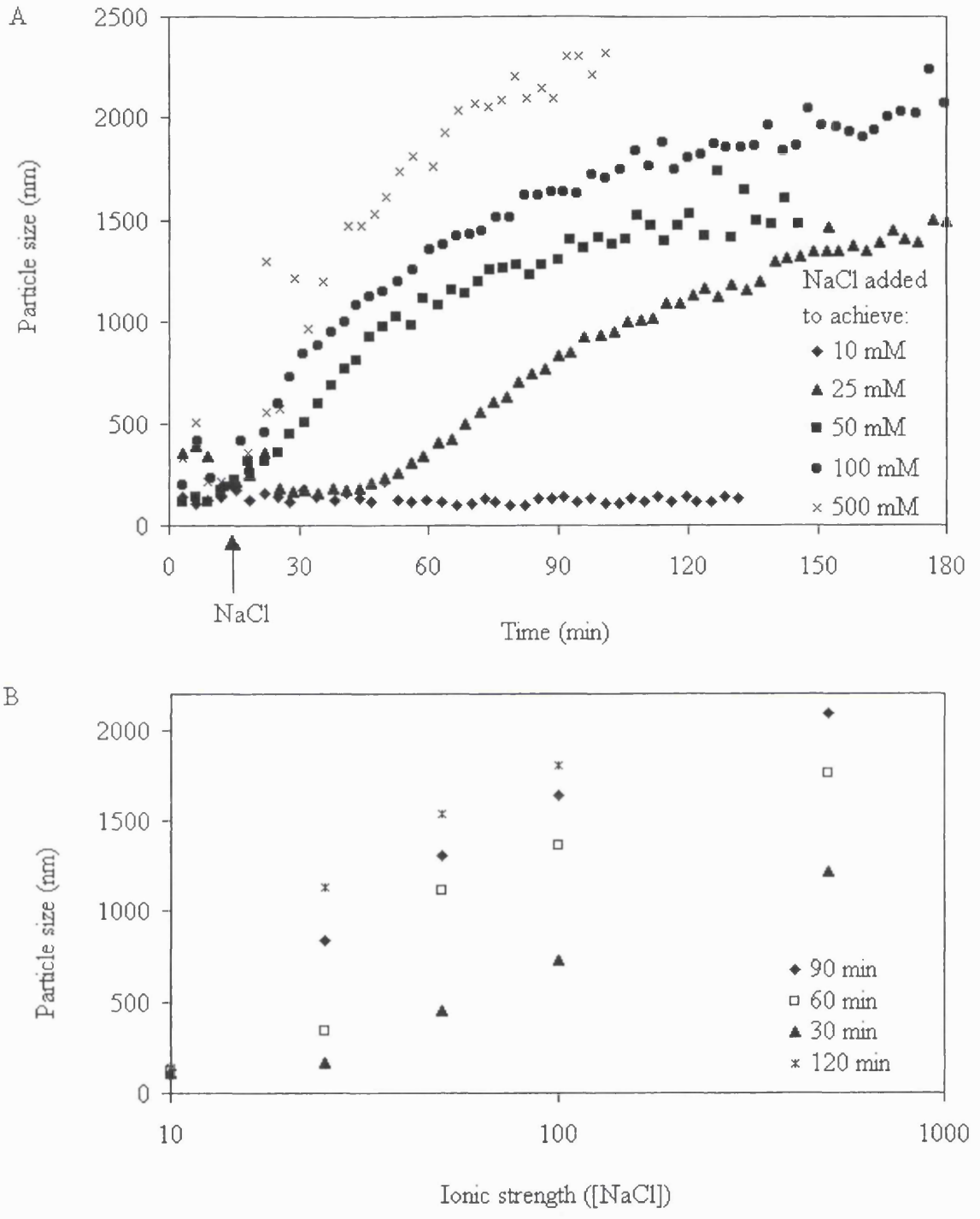

Figure 4.13 Mean hydrodynamic diameter of complexes between poly-L-lysine (MW 34,300) and pSVβ plasmid prepared in 20 mM HEPES pH 7.2 buffer and different ionic strengths. Aggregations were induced by adding 3 M NaCl to the

stable samples after 15 minutes of dynamic light scattering analysis of the initial particle diameter. The final salt concentration was between 10 and 500 mM NaCl. The salt solution was rapidly mixed into the sample cell containing the stable dispersion using a pipette tip; this occurred over less than 3 s. (A) Time evolution of particle size as a function of salt concentration. (B) Variation of particle size with salt concentration as a function of time after initial polyplex formation.

The "0 min" plot in Fig. 4.14A shows a monodisperse distribution with an average hydrodynamic diameter of about 130 nm, for PLL/pSVβ complexes before the addition of NaCl to the desired molarity of 10 mM, as seen in Fig. 4.13A. Following NaCl addition, the measured diameters remain in the same size range, i.e. 130 ± 30 nm (Fig. 4.14A). In contrast, Fig. 4.14B shows rapid aggregation of the polyplexes, where the hydrodynamic diameter increased rapidly immediately following the addition of NaCl to 500 mM. Polyplexes with a hydrodynamic diameter of nearly 3000 nm and polydispersity index of 0.9-1.0 were formed 70 minutes after NaCl addition.

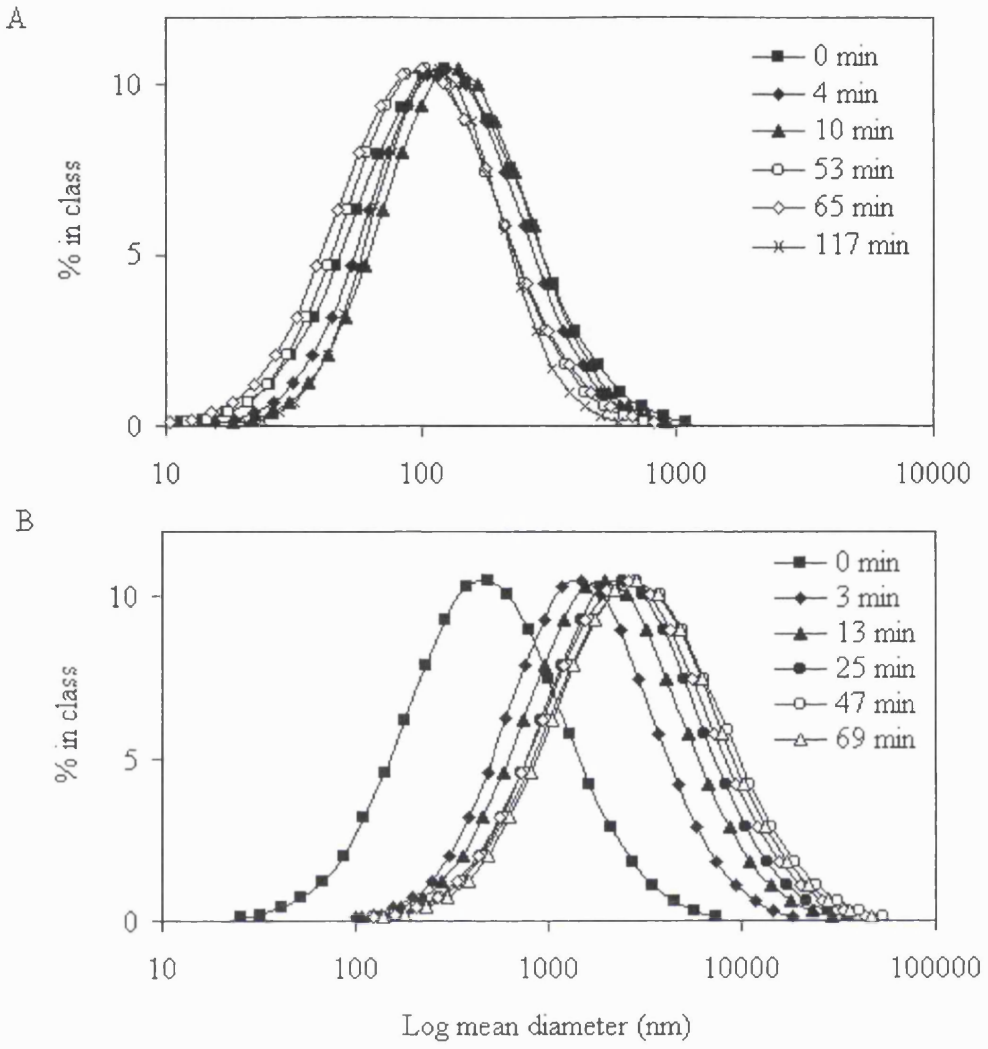

Figure 4.14 Size distribution data obtained using dynamic light scattering analysis of poly-L-lysine/pSVβ complexes. The polyplexes were prepared using the two-syringe mixing method (6 ml/min mixing rate) and at a 2.0 charge ratio in 20 mM HEPES, pH 7.2 ("0 min"). Aggregation was immediately induced by rapid addition of 3 M NaCl to the stable dispersion in order to obtain the desired ionic strength: (A) 10 mM NaCl and (B) 500 mM NaCl. The size distributions, shown as the percentage of particles in each class as a function of the particle size, were determined as mean of diameter based on the scattered light intensity at 90°C.

The PCS software displays the monomodal distribution obtained from cumulants analysis as a log-Gaussian plot based on the mean (*z*-average diameter) and width (polydispersity). Cumulants is a good description of monomodal and monodisperse distributions. Although the monomodal distribution obtained from cumulants was not recommended for the polyplex systems under consideration here, which tend to have high polydispersities, i.e. greater than 0.7-0.8, monomodal analysis was nonetheless employed for simplicity and the ease of obtaining a mean diameter. The experimental data was regularly also analysed by one of the recommended "distribution" algorithms, CONTIN, to ensure that the *z*-average size obtained by both methods closely agreed.

4.1.4.3 Comparison of polyplexes as a function of their DNA compositions

In Fig. 4.15, the *z*-average hydrodynamic diameter is plotted against the elapsed time following the mixing of the PLL solution with the DNA (calf thymus or plasmid) using the two-syringe mixing method. Concentrated NaCl was injected into the sample cell *in situ* immediately after the first measurement to induce aggregation of the polyplex system. The pSVβ plasmid (6.9 kb) used in these experiments was condensed and supercoiled (confirmed by agarose gel electrophoresis, results not shown), whilst the calf thymus DNA, as claimed by the manufacturer (Sigma-Aldrich UK, personal communication), was a heterogeneous sample of linear single- and double-stranded DNA of various lengths (15-23 kb). The results demonstrate that polyplexes composed of DNA of different topologies, calf thymus DNA and plasmid DNA, have similar aggregating characteristics, although PLL/plasmid DNA complexes appear to aggregate less quickly than their calf thymus DNA counterparts. However, it has been found that DNA topology affects transfection efficiency, with supercoiled DNA giving higher activity than open-circular and linear DNA (Cherng *et al.*, 1996).

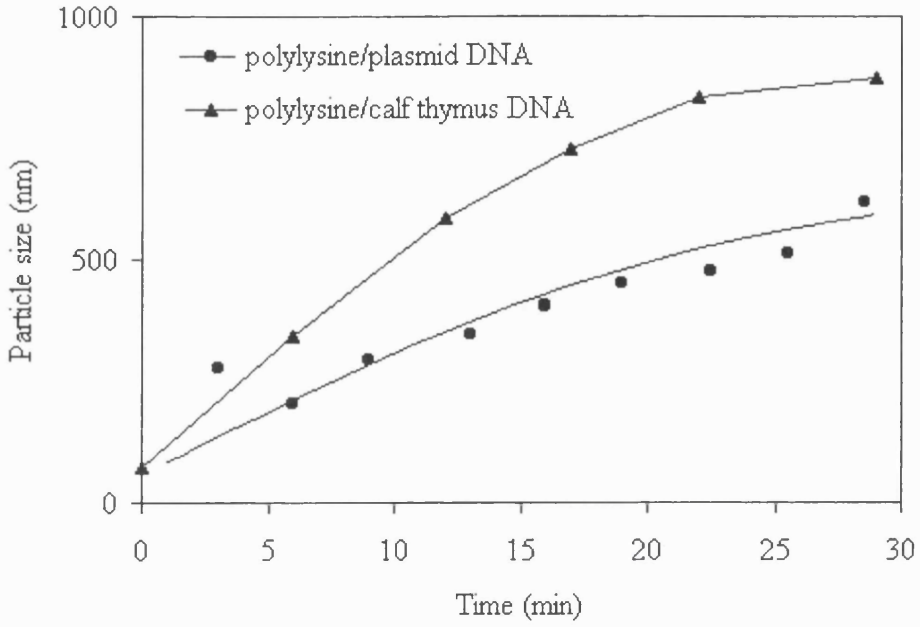

Figure 4.15 Particle size of polyplexes composed of DNA of different topologies (calf thymus DNA and plasmid DNA, pSVβ) and poly-L-lysine as a function of time. The polyplexes were prepared in 20 mM HEPES pH 7.2 at a charge ratio of 2.0 and mixing rate of 6 ml/min. The appropriate amount of 3 M NaCl was pipetted into the cell immediately after the first measurement to adjust the molarity to 150 mM NaCl.

Fig. 4.16 summarises the comparison between the aggregation processes of polyplexes composed of DNA of different types. The data refers to experiments carried out using the two-syringe mixing method and preparation of the polyplexes in buffer containing the predetermined amount of salt. At the lower salt concentrations of 10 and 50 mM NaCl, the aggregation rates of both polyplex systems for a given molarity are comparable. At higher NaCl concentrations, however, there is a marked increase in the aggregation rate of PLL/calf thymus DNA compared to that of PLL/pSVβ. This trend is most likely due to a structural factor, for example, the linear double-stranded form of calf thymus DNA, which was obtained as a heterogeneous population with an average size of 15-23 kb, as compared with the relatively monodisperse plasmid molecules. The heterogeneity of PLL/DNA complexes also influences the colloidal stability, and will be discussed later in

Section 4.3. Nonetheless, for the results illustrated in Fig. 4.16, the hypothesis that the rate of aggregation depends on the forms of DNA requires further experiments for its verification.

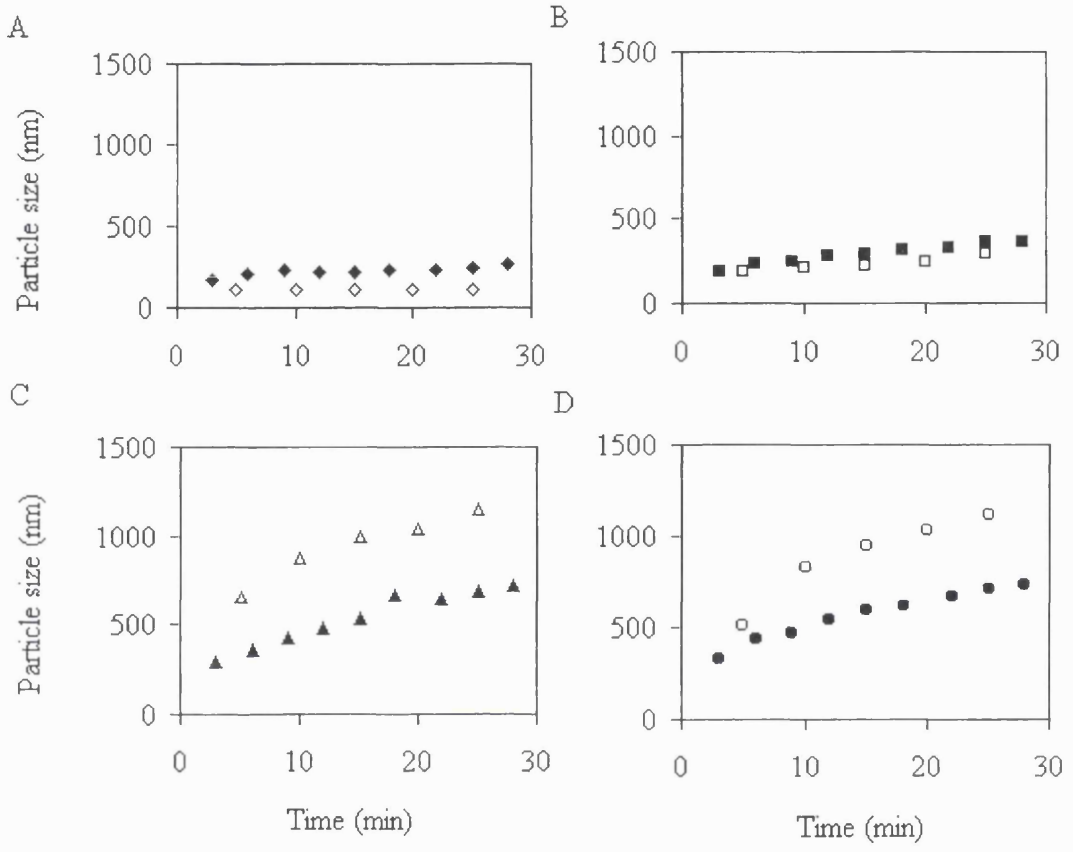

Figure 4.16 Time evolution of mean diameter of poly-L-lysine/DNA complexes (open symbols, calf thymus DNA; filled symbols, pSVβ plasmid). Polyplexes were prepared at a charge ratio of 2.0 and in 20 mM HEPES pH 7.2 buffer with varying ionic strengths: (A) 10 mM NaCl, (B) 50 mM NaCl, (C) 100 mM NaCl, and (D) 150 mM NaCl, immediately before analysis.

4.1.5 Shear of polyplexes

Plasmid DNA is easily damaged by shear and interfacial effects, resulting in a significant decrease in the supercoiled plasmid content. This sensitivity of plasmid DNA has been observed to be even more marked for plasmids greater than 20 kb in size (Levy *et al.*, 1999a). This poses an impediment to the application of gene delivery by aerosolisation or nebulisation into the lung (Alton *et al.*, 1999; Crook *et al.*, 1996). To assess the degree of protection afforded by condensing and complexing of the plasmid with cationic polymers, shear experiments were conducted with a 29 kb plasmid. A small (~20 ml) rotating disk device capable of generating specifiable shear rates from 1.0×10^5 s^{-1} to 1.3×10^6 s^{-1} was employed. The plasmid or polyplex solution (~20 ml) was injected into the chamber of the shearing device, completely surrounding the flat shearing disk. Rotation of the disk subjected the material to a steady shear flow at a controlled rate of shear (1×10^6 s^{-1}). After the shear run, the polyplexes were siphoned out, dissociated and analysed by agarose gel electrophoresis. Further experimental details are given in Section 3.11 and elsewhere (Levy *et al.*, 1999a; Levy *et al.*, 1999b).

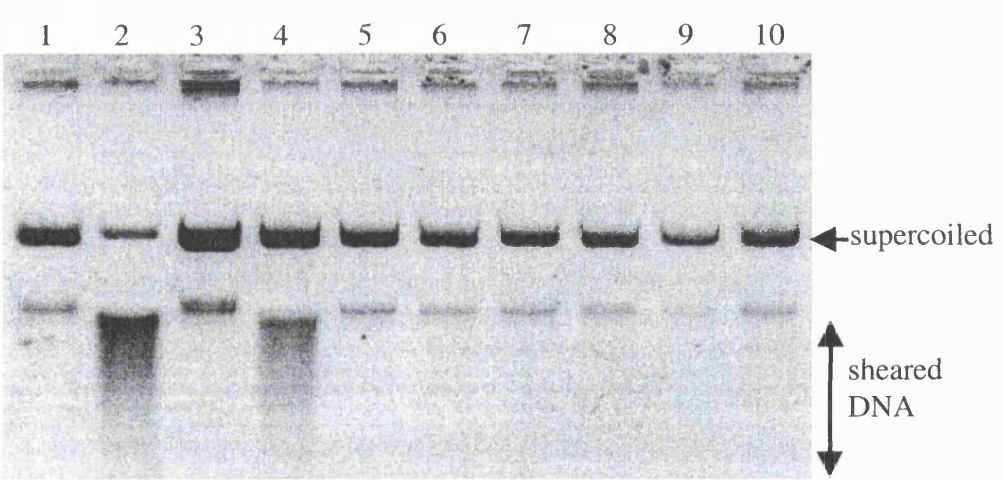

Figure 4.17 Effect of shear on PLL/pMT103 complexes. The polyplexes were mixed at a charge ratio of 1.5 using the two-syringe mixing method, and sheared using the rotating disk device operated at a shear rate of 1×10^6 s^{-1} for 5 s. The sheared polyplexes and unsheared controls were treated with trypsin before agarose gel electrophoresis analysis, as described in Section 3.11. Lanes: (1,2)

unsheared and sheared plasmid (pMT103; 29 kb) in TE buffer; (3,4) unsheared and sheared pMT103 plasmid in TE buffer at 150 mM NaCl; (5, 6) unsheared and sheared PLL (25,900 MW)/pMT103 in TE buffer; (7,8) unsheared and sheared PLL (25,900 MW)/pMT103 in TE buffer at 150 mM NaCl; and (9,10) unsheared and sheared PLL (99,500 MW)/pMT103 in TE buffer.

Fig. 4.17 shows the results from shear experiments with a 29 kb plasmid, pMT103, condensed by poly-L-lysine of two molecular weights, i.e. 25,900 and 99,500. The samples were analysed by agarose gel electrophoresis followed by scanning of the gel. After 5 s at 27,700 rpm, corresponding to a shear rate of 1×10^6 s^{-1}, detectable breakage of plasmid DNA in TE buffer without added salt (Lane 2) was the most marked, as shown by heavy smearing at the bottom of the gel. An additional degree of protection from shear damage of the plasmid was provided by the presence of salt (Lane 4). However, PLL, which complexed and condensed the plasmid, provided virtually complete protection from shear damage. Additionally, shearing in the presence of an air-liquid interface, which is generally more damaging, was similarly performed on a 7 ml solution of polyplexes formed between PLL of molecular weight 2,900 and pMT103 (data not shown). No difference was detected between polyplex samples of different PLL molecular weights, with and without the addition of salt, as well as with and without an air-liquid interface. Further experiments involving higher shear speeds for longer duration would be necessary to discern any difference between the degree of protection conferred upon plasmid DNA by cationic polymers of various molecular weights.

Other groups have investigated other mechanical methods of testing the stability of polyplexes. Sonication of PLL/DNA complexes resulted in no damage (Adami *et al.*, 1998) or extensive fragmentation (Capan *et al.*, 1999) of the plasmid DNA. Obviously, further experiments must be performed under more controlled conditions to confirm these findings.

4.2 Colloidal stability of poly-L-lysine/DNA complexes

There is no shortage of publications that detail the development and characterisation of formulations of gene delivery systems but the mathematical descriptions of the conditions influencing their stability have received less attention. Aqueous suspensions of DNA complexes, with average sizes of 25 nm to a few microns, are colloid systems. The surface properties and overall surface charge of DNA complexes are important because they govern the interactions of the complexes with plasma proteins, their circulation times and their distribution following *in vivo* administration. In this section, well-established and simple equations according to the Derjaguin-Landau-Verwey-Overbeek (DLVO) theory that describe the electrokinetic and colloidal stability of colloidal dispersions are briefly described. The equations are also applied to the poly-L-lysine/DNA system in order to understand particle-particle interaction and the influence of the presence of electrolytes on their aggregation characteristics. The hypothetical effects of temperature and hydration force on stability are also examined.

4.2.1 Forces in colloidal interactions

According to classical colloidal theory, the surface charge of polyplex particles is a significant parameter in controlling aggregation behaviour. The charge neutralisation mechanism of aggregation involves essentially the reduction of repulsive charges between colloidal particles, which leads to their destabilisation and subsequent aggregate-forming collisions between the primary particles. According to the widely used DLVO theory, the main forces involved in coagulation are electrical repulsion and the London-van der Waals attraction (Gregory, 1993; Hogg *et al.*, 1966; Israelachvili, 1992). The total interaction energy, V_T, between the particles is obtained by summing the repulsive double layer electrostatic potential, V_R, and the van der Waals attractive potential, V_A:

$$V_T = V_R + V_A \tag{4.1}$$

The equation assumes that the particles are soft objects with an effective volume that is increased by the double layer, giving rise to the measured hydrodynamic diameter, which is larger than the actual particle diameter.

4.2.1.1 Surface charge and electrical double layers

In Eq. (4.1), V_R represents the interaction energy between the overlapping diffuse electrical double layers that surround the particles. The electric potential ψ_d at the Stern plane or inner boundary of the diffuse layer (which separates a layer of specifically adsorbed ions close to the particle surface from an outer layer of less closely associated ions) is important in determining V_R, and falls away rapidly with distance, at a decay length of $1/\kappa$ (Fig. 4.18).

At high ionic strengths, the double layer is compressed, causing a corresponding increase in the diffuse layer thickness or reciprocal Debye-Hückel screening length, $1/\kappa$. This reduces the range of V_R, so that the particles must approach closely before they repel each other considerably. Conversely, at low electrolyte concentrations, the repulsion forces can be felt at larger distances due to the extended diffuse layer. For aqueous electrolytes containing more than one dissolved salt, the Debye-Hückel parameter κ is given by:

$$\kappa = \sqrt{\frac{8\pi c e^2 z^2}{\varepsilon k T}} \tag{4.2}$$

where c is the concentration of the ionic species in solution, e the elementary charge, z the valency of the ions, ε the permittivity of the medium, k the Boltzmann constant, and T the absolute temperature. It can be seen that the Debye screening length $1/\kappa$ is inversely proportional to the square root of the solution ionic strength. For an aqueous solution of a symmetrical z-z electrolyte at 25°C, converting the ion concentration into molar terms (mol/dm^3 or M) yields:

$$\kappa = 0.329 \times 10^{10} \sqrt{c z^2} \qquad (\mathrm{m}^{-1}) \tag{4.3}$$

The thickness of the diffuse double layer, $1/\kappa$, in many typical solutions have values in the range 1-100 nm (Elimelich *et al.*, 1995).

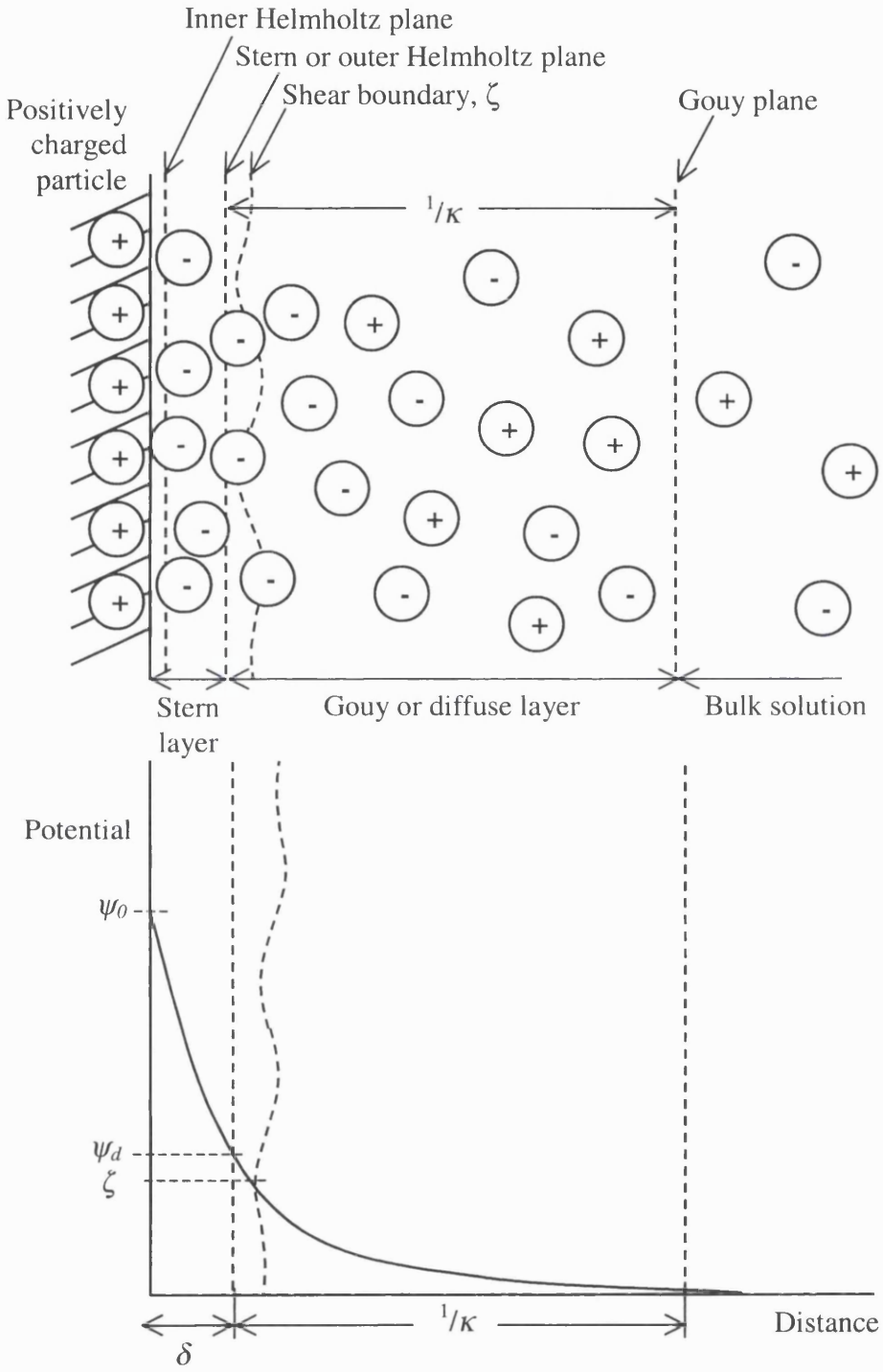

Figure 4.18 Schematic representation of diffuse double layer structure proposed by Stern and Grahame. δ = thickness of Stern layer; ζ = zeta potential; κ = Debye-Hückel parameter; ψ_0 = surface potential; ψ_d = Stern potential. Sources: Elimelich et al., 1995; Shaw, 1992.

Since actual measurement of ψ_d is impractical, most workers exploit the electrokinetic potential of the shear boundary located just outside of the Stern layer. The shear plane, which is actually a region of rapidly changing viscosity, separates the "fixed" charge in the Stern layer from the "mobile" counterions of the electrical double layer (Fig. 4.18). The electrokinetic potential, also known as the zeta (ζ) potential, is a reasonable approximation of ψ_d and can be measured by electrokinetic methods, such as electro-osmosis, particle electrophoresis and streaming potential. In this work, particle electrophoresis was used to measure the electrophoretic mobility, to which the zeta potential is related.

Assuming the separation distance H between two spherical particles of radii a_1 and a_2 is relatively large, i.e. $\exp[-\kappa H] << 1$, V_R can be expressed as a function of H:

$$V_R = \frac{64\pi\varepsilon a_1 a_2 k^2 T^2 \gamma_1 \gamma_2}{(a_1 + a_2) e^2 z^2} \exp[-\kappa H] \tag{4.4}$$

The dimensionless functions, $\gamma_1$and γ_2, of the zeta potentials ζ_1 and ζ_2, respectively, are given by:

$$\gamma_i = \frac{\exp[ze\zeta/2kT]-1}{\exp[ze\zeta/2kT]+1} \tag{4.5}$$

In the case of identical particles ($a_1 = a_2 = a$; $\gamma_1 = \gamma_2 = \gamma$) and small zeta potentials, Eq. (4.5) simplifies to:

$$V_R = 2\pi\varepsilon a \zeta^2 \exp[-\kappa H] \tag{4.6}$$

This model assumes that only the charges on the particle surface are significant and that the surface is impermeable to electrolyte ions. Other factors that contribute to the stability of a colloidal dispersion include solvation forces and steric interactions.

4.2.1.2 Van der Waals interactions

The van der Waals attractive potential is another substantial long-range interaction in colloidal dispersions. Neglecting retardation effects between atoms, the van der Waals force due to the London dispersion interaction energy between spherical molecules of similar composition, separated by a minimum distance H, is given by:

$$V_A = -\frac{A}{12}\left[\frac{y}{x^2+xy+x} + \frac{y}{x^2+xy+x+y} + 2\ln\left(\frac{x^2+xy+x}{x^2+xy+x+y}\right)\right] \tag{4.7}$$

where $x = \dfrac{H}{a_1 + a_2}$ and $y = a_1/a_2$ (Elimelich *et al.*, 1995).

H is the separation distance between the surfaces of two spherical particles of radii a_1 and a_2. A, the Hamaker constant, is a measure of the magnitude of the force between the materials (Israelachvili, 1992). This parameter is dependent on the refractive indices and the dielectric constants of the interacting materials, as well as the medium between them, and the polarizability of atoms. For materials 1 and 2, interacting across medium 3, it can be approximated by:

$$A_{132} \approx \left(\sqrt{A_{11}} - \sqrt{A_{33}}\right)\left(\sqrt{A_{22}} - \sqrt{A_{33}}\right) \tag{4.8}$$

or for similar materials:

$$A_{131} \left(\sqrt{A_{11}} - \sqrt{A_{33}}\right)^2 \tag{4.9}$$

in which case the force is attractive and V_A has a negative value. For equal spheres, Eq. (4.7) reduces to:

$$V_A = -\frac{A}{12}\left[\frac{1}{x(x+2)} + \frac{1}{(x+1)^2} + 2\ln\left(\frac{x(x+2)}{(x+1)^2}\right)\right] \tag{4.10}$$

and at sufficiently small separation distances ($H << a$),

$$V_A = -\frac{Aa}{12H} \tag{4.11}$$

The value of the Hamaker constant may be determined mathematically from the optical properties of the material under consideration, or experimentally, but many workers have adapted it to conform to experimental data. Typically of the order kT, values of A fall in the range 10^{-19}-10^{-20} J. For example, the Hamaker constant for a hexane-water-hexane system is 0.360×10^{-20} J (Hunter, 1987) The presence of an electrolyte in the aqueous vehicle of the suspended particles tends to lower the value of the Hamaker constant, though this effect is insignificant for $A > 10^{-20}$ J (Elimelich *et al.*, 1995).

4.2.1.3 Total interaction energy profiles

As stated in Eq. (4.1), the total energy of interaction, V_T, is given by the sum of the double layer and London dispersion forces, and results in energy-separation curves, such as the one illustrated in Fig. 4.19. For irreversible coagulation, the particles must overcome a potential barrier (maximum V_T/kT) in order to approach very small separations, where the value of V_A increases significantly and drags V_T into a theoretical and infinitely deep primary minimum. In the absence of mixing, i.e. under the influence of Brownian motion only, energy barrier heights greater than the order of 20 times the thermal energy of the particles (20 kT) cannot be easily surmounted and the suspension is stable (Gregory, 1993). At very large interparticle distances V_A exerts more influence on the behaviour of the total potential energy of interaction than V_R does, giving rise to a secondary minimum in the potential energy curve. Particles at such separation distances (approximately $7 \times 1/\kappa$) may form loose aggregates. The secondary minimum is more distinct for dispersions of particles greater than ~1000 nm, fairly high ionic strengths and/or in the presence of an adsorbed polymer layer. At a depth of the order kT, it is usually associated with reversible flocculation.

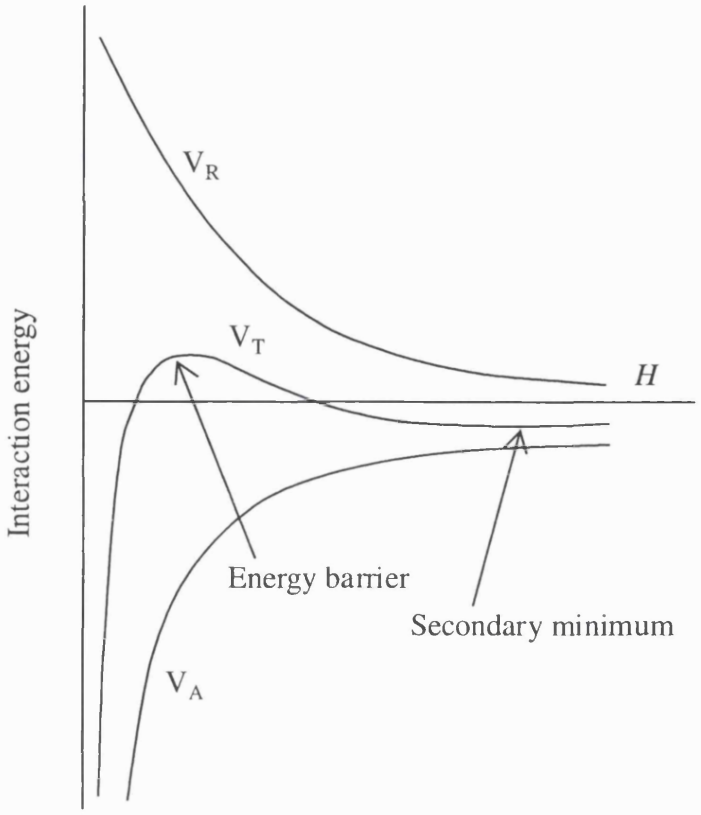

Figure 4.19 Hypothetical potential energy between two equal spherical particles. The net potential profile (V_T) is a superposition of the van der Waals potential (V_A) and the repulsive double layer potential (V_R).

4.2.1.4 Hydration effects

The repulsive behaviour of certain hydrophilic particles in aqueous environments of high ionic strengths contradicts the classical DLVO theory which predicts strong adhesion or coagulation in a primary minimum (Israelachvili, 1992). This colloidal stability, though not completely understood, can be explained by the existence of a repulsive structural force known as the hydration force. Several workers have found that hydration forces, which are exponentially repulsive, play an important role in the stabilisation of colloidal systems, particularly those containing particles with hydrophilic surfaces (Molina-Bolívar *et al.*, 1999). These hydration forces originate from the water molecules that bind to the surface of charged macromolecules such as lipid bilayers and biological membranes, as

well as any ionic, zwitterionic or H-bonding peptides, polysaccharides and other functional groups at the surface of these materials. For these particles to contact or approach each other closely, some dehydration of their surfaces and ionic groups must occur. This raises the free energy of the system, leading to an anomalous repulsion between the particles even when they are exposed to high electrolyte concentrations. The hydration effects can be significant, acting at ranges comparable to the electrical double layer repulsion, even in very high salt environments (Butt, 1991; Healy *et al.*, 1978).

The hydration force between two spherical particles can be approximated by:

$$V_h = \pi a \lambda_h^2 P_0 \exp(-H/\lambda_h) \qquad (4.12)$$

where the hydration radius, λ_h, of the cations is assumed to be 0.363 nm, and the value of the constant, P_0, to be 10^7 Nm^{-2} (Ninham, 1985; Rand and Parsegian, 1989). The inclusion of hydration forces in the classical DLVO theory results in the following equation for the total potential energy of interaction between two particles:

$$V_T = V_R + V_A + V_h \qquad (4.13)$$

Experimental studies have shown that hydration forces generally exist between negatively charged biological entities only (Pashley, 1981; Petsev *et al.*, 2000). For solutions of negatively charged protein-covered latex particles at various salt concentrations (Molina-Bolívar *et al.*, 1999) and apoferritin molecules that were negatively charged at pH 5.0 (Petsev *et al.*, 2000), non-classical DLVO stabilisation was observed and attributed to the induction of hydration repulsion by Na^+ ions. This is explained by the greater degree of hydration of Na^+ compared to Cl^-. The hydration repulsion also increases with increasing hydration of the small counterions, with the order of increasing counterion hydration being $Mg^{2+} > Ca^{2+} > Li^+ \approx Na^+ > K^+ > Cs^+$ (Elimelich *et al.*, 1995; Israelachvili, 1992; Pashley and Israelachvili, 1984). Conversely, for a positively charged system of lysozyme molecules in sodium acetate ($NaOOCCCH_3$) at pH 4.7, hydration repulsion was not induced (Muschol and Rosenberger, 1995; Petsev

and Vekilov, 2000). In this system the counterions were the larger negative acetate ions, which had both hydrophobic and hydrophilic ends.

4.2.1.5 Steric effects

At short distances between molecules with adsorbed layers, such as surface-grafted polymers, steric interactions can contribute to colloidal stability. Although, theoretically, intermolecular distances do not govern the stabilisation action, these repulsive forces operate at distances of the order of 1 to 10 nm, depending on the molecular weight and density of the adsorbed polymeric layer. In synthetic gene delivery systems, the most commonly used polymers are hydrophilic linear chains of polyethylene glycol (PEG) of various chain lengths. Various groups have reported that the grafting of PEG chains onto the surface of the colloidal vector systems decrease interactions with plasma proteins and prolong circulation times (Choi *et al.*, 1999; Huwyler *et al.*, 1996; Kwoh *et al.*, 1999; Meyer *et al.*, 1998; Maruyama *et al.*, 1997; Ogris *et al.*, 1999; Verbaan *et al.*, 2001; Wheeler *et al.*, 1999; Wolfert and Seymour, 1996; Zhang *et al.*, 1999). Another advantage is that this method of stabilising the formulations is independent of the salt concentration. However the lack of agreement between investigators, the complexity of the chemistry of such systems and possible toxicity arising from the use of PEG in drug formulations necessitate further research to assess the effects of steric protection conferred by these PEG chains.

4.2.2 Application of the DLVO theory to PLL/DNA complexes (simulation results)

In the following section, the basic DLVO theory was used to simulate approximately the energy barriers for poly-L-lysine/calf thymus DNA complexes under different physicochemical conditions. The total potential energy of interaction, V_T, between the particles was calculated from the appropriate expressions for the repulsion and attractive energies, given in Sections 4.2.1.1 and 4.2.1.2, respectively. The summation of Eqs. (4.6) and (4.10) was taken as a suitable approximation for V_T. Experimental determination of the properties of the poly-L-lysine/calf thymus DNA (PLL/DNA) system, described in

Chapter 3 (Materials and methods) and illustrated in Figs. 4.8, 4.9 and 4.11, contributed to the general character of the potential energy diagrams. These measured experimental parameters included (initial) particle size and zeta potential. The potential energy curves, illustrated in the following sections, were plotted as V_T against the separation distance, *H*. Both EXCEL and Mathematica (Ver. 3.0; Wolfram Research, Champaign, IL) packages were used to produce the V_T mathematical models, but EXCEL was the main program used throughout this research project and for the results shown in this work.

The following simulations attempt to describe some of the results in the previous section (Section 4.1) from a theoretical viewpoint. They are also instructive in guiding process design for creating stable formulations with acceptable shelf lives. In the absence of any previous information, a value for the Hamaker constant (5×10^{-21} J) within the range recommended for biological materials (Gregory, 1993) was used in the equation for van der Waals forces of attraction between two particles, Eq. (4.10). The Hamaker constant was assumed to be constant for all systems considered in this study. It was assumed that the polyplexes were reasonably compact and spherical. Visual observations based on atomic force microscopy (Golan *et al.*, 1999; Hansma *et al.*, 1998; Wolfert and Seymour, 1996) and electron microscopy (Laemmli, 1975; Wagner *et al.*, 1991) suggest that this assumption is likely to give rise to some uncertainty regarding the absolute values of the calculated total potential energy of interaction between the particles.

4.2.2.1 Influence of pH

The interaction energies between equal spherical particles of 120 nm suspended in a solution at 150 mM NaCl and different pH values (7.2, 7.7, and 8.0) are shown in Fig. 4.20. These physicochemical conditions are similar to those for experiments with poly-L-lysine/calf thymus DNA complexes described earlier (Section 4.1.4.1). Experiments involving light scattering and electrophoretic mobility measurements gave particle size (Fig. 4.9) and zeta potential (Fig. 4.11) results, respectively, that were required for the calculation of the interaction energies. In Fig. 4.20, the energy barriers, indicated by the maxima of the curves, must be overcome by the colliding particles in order for

aggregation to occur. As discussed in Section 4.2.1.3, the barrier heights shown in Fig. 4.20 are less than ~20 *kT*, which predict that the systems should coagulate. Indeed, experimental data in Fig. 4.9 showed that PLL/DNA complexes at 150 mM NaCl and all pH values studied are fast aggregating systems. Both diagrams (Figs. 4.9 and 4.20) show that the stability of the system depends to a large extent on pH, becoming more unstable with increasing pH.

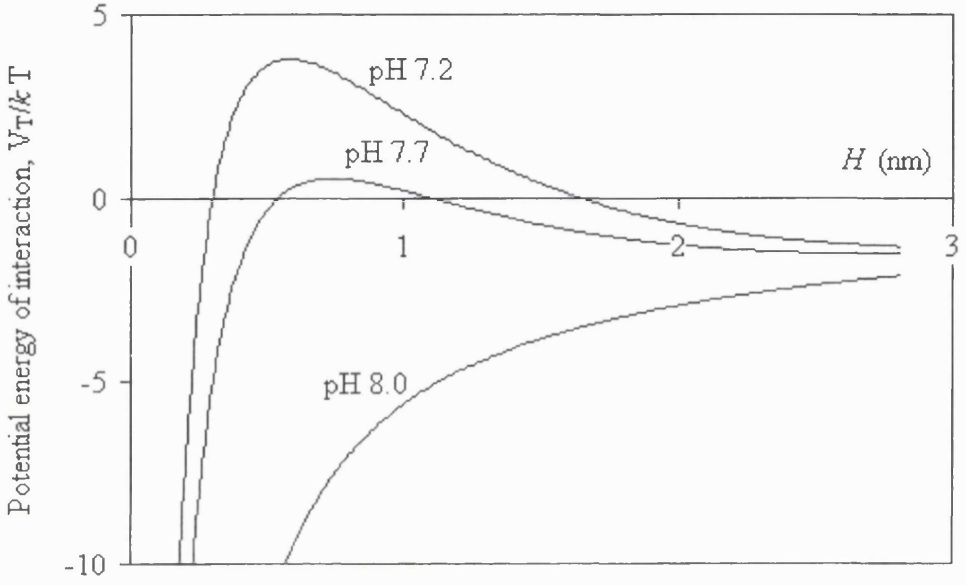

Figure 4.20 Influence of pH on the dimensionless total potential energy of interaction between two spherical particles of 120 nm diameter; salt concentration 150 mM NaCl, as a function of the distance H between their surfaces. pH 7.2, 7.7 and 8.0 correspond to the experimentally ascertained zeta potentials of 22, 19 and 5 mV, respectively.

4.2.2.2 Influence of ionic strength

The theoretical total interaction energy curves predicted for mono-size particles with an initial mean diameter of 120 nm suspended in solutions containing 10, 50, 100 and 150 mM NaCl are shown in Fig. 4.21. Calculations, using Eqs. (4.2) to (4.3), and shown as

the insert in Fig. 4.21, indicate that as the ionic strength is increased, the electrical double layer around the particles, given by the Debye-Hückel length, decreases. Evidence from other sources also indicates that with increasing electrolyte concentration the surface charges are screened (Rustemeier and Killmann, 1997). These effects cause the repulsive force between the particles to decrease. Consequently, the total potential energy barrier between the particles decreases and the system becomes more aggregating. This is consistent with the data shown in Fig. 4.9.

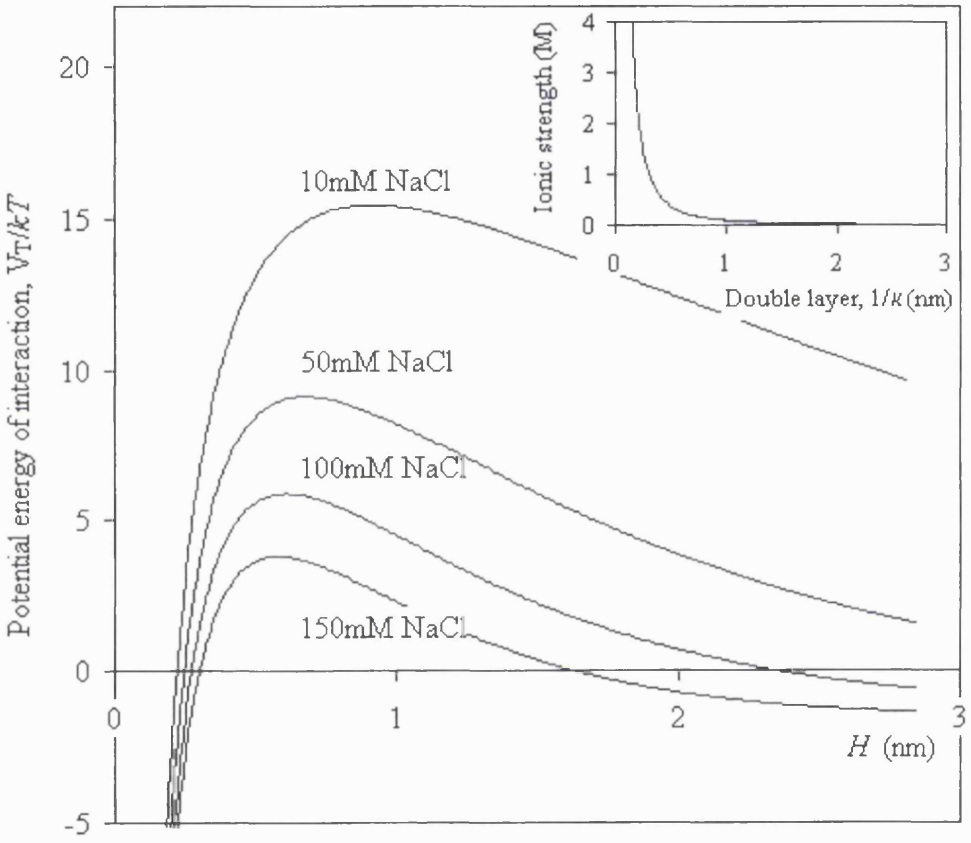

Figure 4.21 Influence of electrolyte concentration on the dimensionless total potential energy of interaction between two spherical particles of 120 nm diameter, at pH 7.2 (zeta potential = 22 mV), as a function of the distance H between their surfaces. The inset shows ionic strength dependence of the thickness of the double layer according to the DLVO theory.

4.2.2.3 Influence of particle size

In the presence of a population of polyplexes of different sizes, it is of considerable interest to analyse the tendency for aggregation. A typical example would be the case of the PLL/DNA systems shown in Fig. 4.10. Theoretical potential energy curves are shown in Fig. 4.22 for two such cases. Fig. 4.22A refers to binary aggregation involving two particles, each with a diameter of 50 nm, and between a 50 nm particle and larger ones of 120 nm, 500 nm and 900 nm. Fig. 4.22B is a similar plot showing binary aggregation for a 120 nm particle. It is notable that aggregation is particularly strong between particles of 50 nm and 120 nm in diameter. At values of potential energy of interaction less than about 5 kT to 10 kT, colloidal aggregation becomes noticeable (Hunter, 1981). According to the plots in Fig. 4.22, therefore, interactions between the 50 nm particle and all of the other particles are likely to cause aggregation although the lowest potential energies are observed between the smallest particles. Interaction energies greater than $15kT$, such as those occurring between the 120 nm particles and particles of 500 nm and 900 nm, render aggregation between these particles unlikely. These simulations are instructive in guiding process design for creating stable formulations with acceptable shelf life. For example, they suggest that the aggregation between small particles is expected to be rapid and the largest particles with their high surface area, if present, act as strong particle "collectors", sweeping the smallest particles quickly from the system. The elimination of such large particles from the formulation and the stabilisation of small particles against aggregation must therefore be a priority in the design of preparation methods for DNA-based drug formulations.

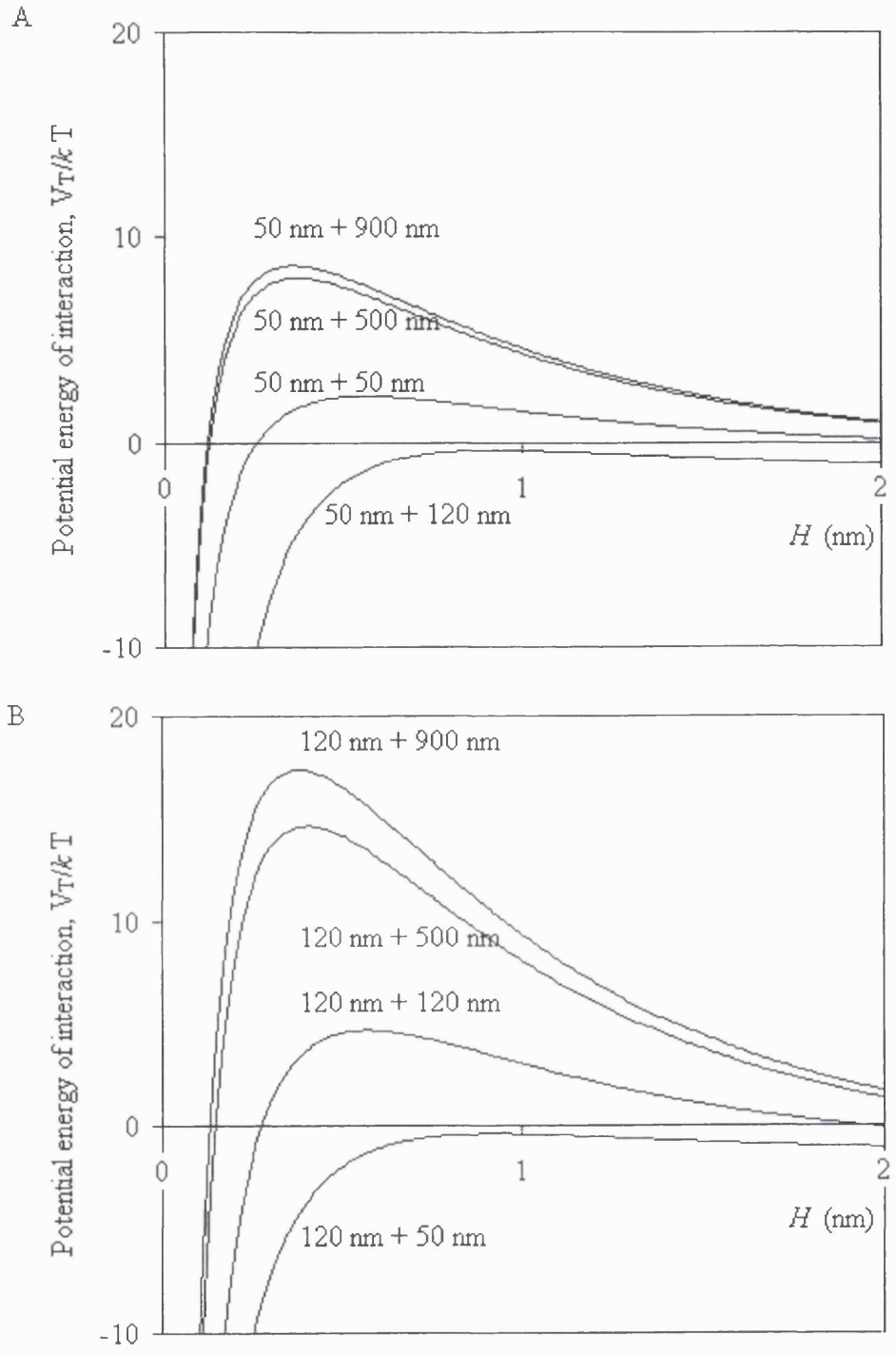

Figure 4.22 Influence of particle diameter on the dimensionless total potential energy of interaction between two spherical particles of: (A) 50 nm and (B) 120 nm diameter at pH 7.2 (zeta potential 22 mV), 150 mM NaCl.

Comparison of the plots shown in Figs. 4.22A and 4.22B for equal size particles shows that the potential energy barrier falls as particle diameter decreases. Additionally, binary aggregation between small particles of different diameters, e.g. between 50 nm and 120 nm particles, is particularly strong. It is therefore important to reduce the probability of aggregation of the small particles in the formulation. The data plotted in Fig. 4.9, and the simulations in Fig. 4.21, indicate that preparation under conditions of low ionic strength can significantly reduce aggregation. However, once injected into the patient, aggregation is expected to occur in response to the elevated ionic strength corresponding to physiological conditions in the body, this being generally about 150 mM and pH 7.4 representative of the environment in the cytoplasm.

4.2.2.4 Influence of temperature (hypothetical)

Examination of Eqs. (4.2) to (4.10) provides further insight into possible ways for controlling the physical stability of the formulation. For example, according to Eq. (4.4), lowering the temperature increases the repulsion barrier between all particles, resulting in a reduction of their tendencies for aggregation. The calculated total interaction potentials are shown in Fig. 4.23. In this work, the effect of temperature on the physical stability of the polyplex particles was not experimentally determined. However, the implication of the simulations shown in Fig. 4.23 is that lowering the temperature during the mixing step as well as maintaining a low temperature during transportation and storage can confer a degree of stability on the formulation. Nevertheless, considering the kT values plotted in Fig. 4.23, low temperature alone is unlikely to eliminate aggregation completely. Lyophilization of polyplex formulations, or their freezing in the presence of excipients, has been suggested as a means of avoiding aggregation during shipping and storage. This method of preparation is still unlikely to be satisfactory on a large scale and has the risk of damaging the supercoiled plasmid upon thawing (Anchordoquy, 1999a; Anchordoquy, 1999b).

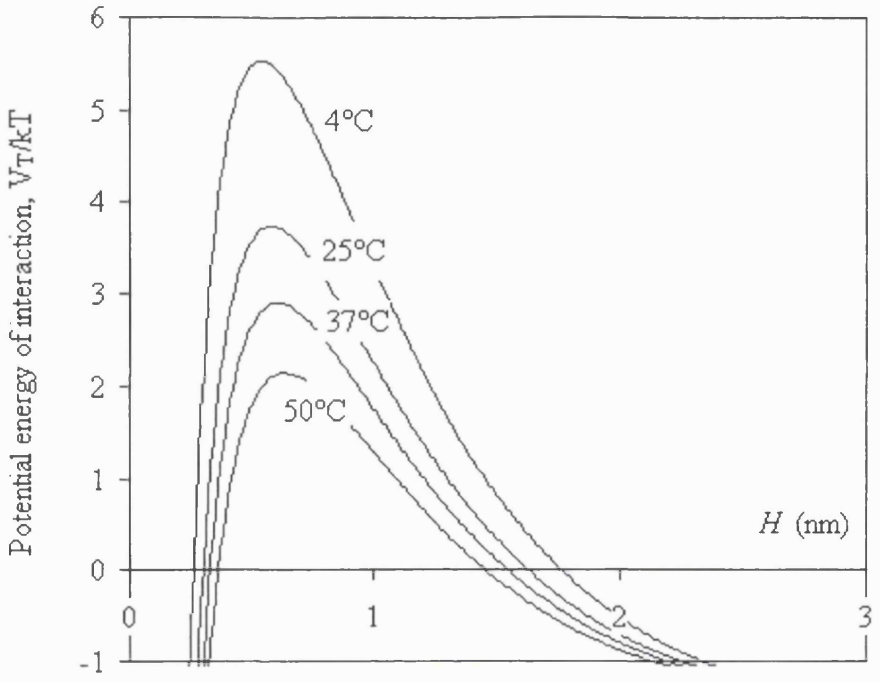

Figure 4.23 Influence of temperature on the dimensionless total potential energy of interaction between two particles of 120 nm diameter at pH 7.2 (zeta potential 22 mV), 150 mM NaCl.

4.2.2.5 Inclusion of hydration force (hypothetical)

Fig. 4.24 incorporates the repulsive hydration force into the classic DLVO theory for the computation of the interaction energy curves. The values of P_0 and λ previously reported in Section 4.2.1.4, as well as Eqs. (4.12) and (4.13), were employed in the calculation of V_{hyd}. Results from experiments with the positively charged PLL/DNA complexes (Section 4.1) cannot be applied to these plots because the presence of hydration repulsion in that system is not possible in practice. Hence for the purpose of these simulations, it was assumed that the system under consideration was negatively charged at any given ionic strength. Values for the particle radii (a = 60 nm), zeta potential (ζ = -22 mV), suspension temperature (T = 298 K) and Hamaker constant ($A = 5 \times 10^{-21}$ J) were assumed, and fitted to the theoretical data to estimate the interaction energy curves. The

screening length, 1/κ, for the 10 mM NaCl system is ~3 nm whereas that for the 150 mM NaCl system is ~0.8 nm. In the latter case, the compression of the double layer corresponds to a decrease in the interparticle repulsion energy and increased aggregation tendencies. The inclusion of the hydration force in the DLVO treatment of the above plots drives the energy barriers up so that the system with an ionic strength of 150 mM NaCl appears physically stable.

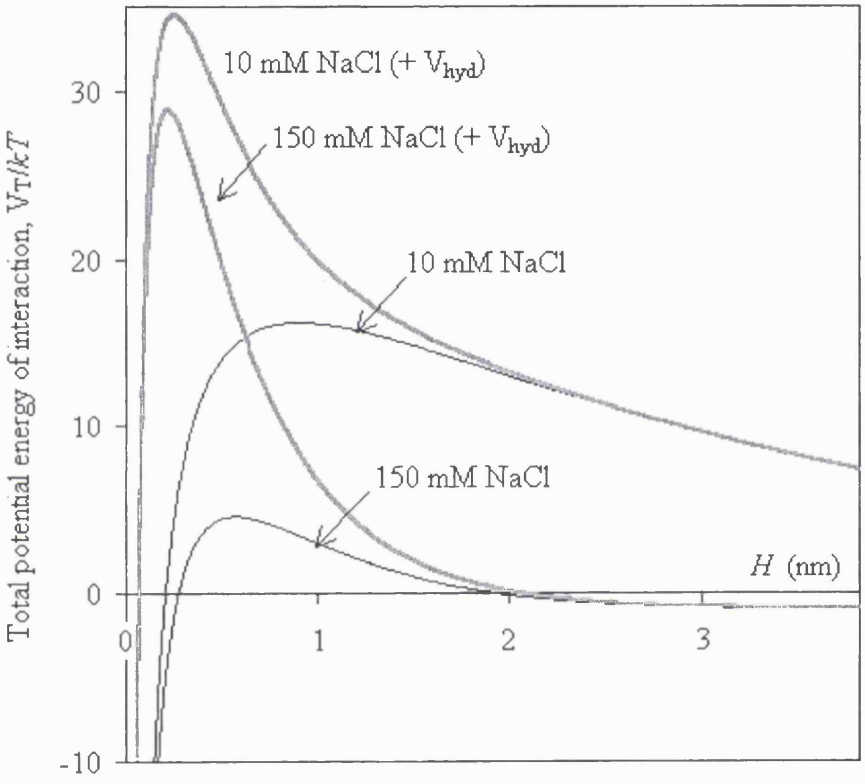

Figure 4.24 Influence of the repulsive hydration potential on the dimensionless total potential energy of interaction between two spherical particles. The following parameters were assumed: diameter = 120 nm, zeta potential = -22 mV, temperature = 298 K, Hamaker constant = 5×10^{-21} J. The data refer to potential energy curves calculated both without (black lines) and with (grey lines) the inclusion of the hydration force, V_{hyd}.

Various assumptions, described in Section 4.2.2, were made in the handling of the above interaction potentials. Nevertheless, the simulations provide a basis for the comparison of the stability of different systems. More importantly, the DLVO theory allows the assessment of the superimposed effect of important process and material parameters affecting the stability of the formulation. This is very difficult to envisage intuitively given the large number of parameters that are known to influence the stability of the polyplex formulations. These parameters include the initial or primary particle size, ionic strength and pH of the solution, zeta potential of the polyplexes, temperature, and presence of any protective colloids.

Another factor that may impact the interaction potential between the polyplexes is the viscous drag force on the polyplexes. This force arises as a result of the mixing of the colloidal suspension. The effect of this force on the stability of the polyplexes will depend on the ratio of the viscous drag force to the total interaction force between the condensed particles (Wilson and French, 1978). Slow mixing characterised by a relatively low viscous drag force can cause the polyplex particles to aggregate by increasing the frequency of collisions between them. In contrast, intense mixing can give rise to viscous drag forces sufficiently high to break the aggregates. In the discussion of the above results, it was assumed that viscous drag forces were absent during the measurements and the only hydrodynamic force causing aggregation was due to the Brownian motion of the polyplex particles. This was thought to closely represent the actual formulation in a vial under storage and transportation, and was therefore selected as the focus of attention in the present investigation. The effects of the viscous drag force on the physical stability of polyplexes will necessitate further work, beyond the scope of this thesis.

Finally, according to the classical theories of colloid science, stabilisation of the polyplexes may be achieved by modification of the surface properties of the particles by, for example, steric interaction. The molecular weight of the poly-L-lysine used in our experiments was ~25,000, relatively low for steric stabilisation to have an effect.

Experiments with charged latex particles stabilised by poly-L-lysine of different molecular weights have been reported (Rustemeier and Killmann, 1997). These experiments showed that at molecular weights of poly-L-lysine greater than about 100,000 steric interaction was caused by the poly-L-lysine molecules, resulting in the stabilisation of the suspension against aggregation. Additionally, measurements of size and zeta potential have shown that high molecular weight adsorbed particles, such as neutral polyethylene oxides and its co-polymers, have the potential to stabilise charged latex nanoparticles (Killmann and Sapuntzjis, 1994; Vandorpe *et al.*, 1996). As described earlier in Section 4.2.1.5, recent experiments with various formulations of gene delivery systems containing polyethylene glycol have been reported which suggest that stabilisation of the polyplex particles may be possible by this mechanism.

The content of this section (Section 4.2) showed that it was possible to reasonably describe the stability of simple gene delivery formulations through established equations of colloid science. Theoretical descriptions of the forces controlling interactions of colloidal suspensions, such as the poly-L-lysine/DNA complexes studied in this work, were introduced and simulated. Models of the potential energies of interaction were calculated using well-established equations based on the DLVO theory and experimentally ascertained parameters such as particle size and surface charge density. Results from the modelling of the colloidal stability of the PLL/DNA system were presented as potential energy curves and were in agreement with the experimental data. These show that formulations are susceptible to aggregation, especially under physiological conditions of the body. However, during processing and storage, the physical stability of the formulations can be enhanced significantly by the creation of conditions that lead to monodisperse particles in a low pH, ionic strength, and temperature environment. To more accurately depict the electrostatic forces that control these interactions, the models must address other characteristics typical of biological entities such as the polyplexes studied here, e.g. the non-uniform distribution of charges, and the irregularity of the molecular surface.

4.3 Fractal dimension of poly-L-lysine/DNA complexes

4.3.1 Fractal aggregates and measurement techniques

In Section 4.1.4.2, dynamic light scattering (DLS) was employed to measure the particle size and monitor the aggregation process of the poly-L-lysine/plasmid DNA aggregates in aqueous solution containing added salt. The polyplexes were shown to be stable in salt-free solutions or low ionic strength buffers. When formed in buffers of higher ionic strength, aggregation of the polyplexes was observed. Data was provided in Figs. 4.13 and 4.14, among others, that showed aggregation could be induced by the addition of a small amount of salt to a salt-free solution. These were in good agreement with results reported by different authors (Anchordoquy, 1999a; Ogris *et al.*, 1998; Ross and Hui, 1999).

Although polycation complexes with DNA have been studied by different groups (Bloomfield and Rau, 1980; Choi *et al.*, 1999; Deshmukh and Huang, 1997; Duncan *et al.*, 1998; Geall *et al.*, 1999; Laemmli, 1975; Schaffer *et al.*, 2000; Zauner *et al.*, 1997), there appears to be no reports in the literature on the theoretical aspects relating to the internal structure and aggregation mechanism of such systems. The objective of the work contained in this section is to provide some preliminary data on the fractal properties of these colloidal aggregates. Poly-L-lysine/pSVβ was chosen as model particles for these experiments. The pH of 7.2 and ionic strength of 150 mM NaCl were included in these experiments since this is thought to closely represent normal blood pH (7.4) and salt concentration (9 g/L). The concentrations of extracellular Na^+ and Cl^- in the body are 145 and 110 mM, respectively (Alberts *et al.*, 1994).

The fractal dimension, D_f, which characterises the internal structure of aggregates formed from colloidal particles, was evaluated by static light scattering (SLS). Both dynamic and static light scattering have been used for the real-time monitoring of the aggregation kinetics of biomolecules or nanoparticles (Bloomfield, 2000; Derrendinger and Sposito,

2000; Hagiwara *et al.*, 1996; Kerker, 1969; Magazu *et al.*, 1989; Molina-Bolívar *et al.*, 1998; Tirado-Miranda *et al.*, 2000). In dynamic light scattering, the average particle size is determined based on the translational movement of the particles in suspension, whereas in static light scattering, the absolute intensity of light that is scattered by particles in solution is measured as a function of the scattering angle to determine the fractal dimension. The results obtained from both techniques yield information on the colloidal aggregation and structure formation of the aggregates.

Numerous groups have used fractals to describe the various highly disordered and complex structures formed by colloidal biomolecules and other macromolecules during aggregation processes (Amal and Raper, 1993; Ayazi Shamlou *et al.*, 1996; Bohr *et al.*, 1997; Magazu *et al.*, 1989; Molina-Bolívar *et al.*, 1998). Scientists and engineers model and characterise the internal organisation of these systems through their fractal properties. The fractal dimension, D_f, can throw light on the spatial structure or space-filling capacity and aggregation regime of the aggregation process. Briefly, two distinct regimes of aggregation exist for such colloidal dispersions. Reaction-limited colloidal aggregation (RLCA) generally occurs at low particle concentrations. Under these conditions compact structures with a high value of fractal dimension ($D_f \geq 2.1$) are formed slowly between a small portion of particles. Diffusion-limited colloidal aggregation (DLCA) occurs more rapidly and at high particle concentrations, whereby all particles collide to form loose tenuous structures with fractal dimensions close to 1.8 (Lin *et al.*, 1989).

Fractals may also be categorised by the structures they define. Mass fractals have randomly-oriented but connected structures, in which both mass and surface are self-similar and scale alike. They tend to be formed from random aggregation processes and scattering occurs from the bulk of the aggregate, with D_f lying in the interval $1 \leq D_f \leq 3$. Surface fractals are self-affine objects in which only the surface is fractal or self-similar, with $2 \leq D_f < 3$ (Schmidt, 1989).

The theory of light scattering to determine the fractal dimension has been reviewed in several publications (Meakin, 1988; Schmidt, 1989; Sorensen, 2001), so only a very basic introduction to the methods is given here. Two methods exist for the measurement of the fractal dimension of aggregates, i.e. static light scattering (SLS) and dynamic light scattering (DLS). In this study, only SLS was found to be an effective method for obtaining the fractal dimension of PLL/DNA complexes. The other technique, DLS, was found to be unreliable and therefore the results are not included here. The fractal dimension (D_f) values obtained from studying the aggregation kinetics of PLL/DNA complexes using DLS were outside the range, $1 \leq D_f \leq 3$, specified for fractal aggregates. Both methods are described below.

4.3.1.1 Probing of fractal structure by SLS

In these experiments, the scattered intensity $I(q)$ from the randomly oriented particles in suspension is measured as a function of the scattering angle, θ. The magnitude of the scattering vector, q, measured in reciprocal length, is given by

$$q = \frac{4\pi n \sin(\theta/2)}{\lambda} \tag{4.14}$$

where n is the refractive index of the solution and λ the incident wavelength of the light in a vacuum. For the scattering from a mass fractal, the scattered intensity $I(q)$ obeys a power-law function:

$$I(q) \propto q^{-D_f} \tag{4.15}$$

providing $1/l \leq q \leq 1/a$, where a is the radius of a rigid and spherically symmetric scatterer within the aggregate under consideration, and l is the characteristic length, typically the maximum aggregate hydrodynamic radius, or, alternatively, the radius of gyration (Amal and Raper, 1993; Schmidt, 1989). Hence the inverse wave vector q^{-1} is a measure of the scaling range for analysis by light scattering techniques. By measuring the angle dependence of the scattered intensity (photoncounts) and plotting $I(q)$ versus q on a log-log scale, the fractal dimension can be obtained from the negative of the slope in the power-law region. To assure the validity conditions of Eq. (4.15), the angular range 12° ≤

$\theta \leq 68°$ was chosen for determination of the power-law exponents in our experiment ($0.2 < qa < 1$), where a was taken to be 50 nm.

It has been shown that the magnitude of the slope in the power-law region is less than 3 for mass fractals and between 3 and 4 for surface fractals (Schmidt, 1989). Hence the power-law scattering exponents for mass and surface fractals are D_f and $6\text{-}D_f$, respectively.

4.3.1.2 Probing of aggregation kinetics by DLS

It has been shown that the growth kinetics of colloidal systems, when observed by DLS, can yield information on the fractal dimensions (Brunner *et al.*, 1997; Lin *et al.*, 1989; Schüler *et al.*, 1999). For aggregation according to an RLCA mechanism, the aggregates display an exponential time-dependence of the average cluster size,

$$D_H \propto \exp(At) \tag{4.16}$$

where D_H is the hydrodynamic diameter and A is a constant dependent on experimental conditions such as the sticking probability and the time between collisions. On the other hand, DLCA type aggregates grow according to a power law,

$$D_H \propto t^{1/D_f} \tag{4.17}.$$

Hence the fractal dimension can be determined: for an RLCA mechanism, from the slope of a semi-logarithmic plot of the hydrodynamic diameter against time, and for a DLCA mechanism, from the slope of a double-logarithmic plot of the hydrodynamic diameter against time. However, in this study, attempting to fit cluster-size kinetics curves for polyplexes on both semi-logarithmic time scales (RLCA) and on double-logarithmic time scales (DLCA) did not yield slopes corresponding to reported values of fractal dimension, i.e. the slopes were not in the range 1.0–3.0. These results, which are essentially different interpretations of the plots in Figs. 4.12 and 4.13A, are not shown.

4.3.2 Static light scattering of PLL/pSVβ complexes

Complexes of plasmid DNA (pSVβ) with poly-L-lysine (average MW = 34,300) at 2.0 charge ratio and salt concentrations of 50, 100, 150 and 1000 mM NaCl were prepared using the pipette-mixing method. At this charge ratio, pipette mixing and twin-syringe mixing was previously shown (in Section 4.1.2.3) to produce polyplexes of approximately similar particle size (~100 nm). To avoid contamination of the sample by dust, which would have introduced potential errors, special precautions including rinsing all glassware with particle free water and performing sample preparation in a laminar flow cabinet had to be taken (see Section 3.5). The intensity of light scattered by the PLL/pSVβ complexes was measured at angles ranging from 12° to 68° using the Malvern Autosizer 4800 computer controlled spectrometer. The details of the static light scattering (SLS) experiments can be found in Section 3.10.

Fig. 4.25 shows some typical SLS curves (scattered intensity $I(q)$ versus magnitude of the scattering vector q) obtained at successive times following the preparation of polyplexes in 20 mM HEPES pH 7.2: (A) 50 mM NaCl, (B) 100 mM NaCl, (C) 150 M NaCl, and (D) 1 M NaCl. These polyplexes aggregate as shown previously in Section 4.1.4.2. Fig. 4.12 showed that under the physiologically compatible conditions of 100 and 150 mM NaCl, aggregation of the polyplexes was especially pronounced. The physical instability of such systems has been well-documented and is a major problem in gene delivery since aggregation of DNA complexes profoundly affects *in vitro* and *in vivo* transfection (Ogris *et al.*, 1998; Tang and Szoka, 1997; Zelphati *et al.*, 1998b; Ziady *et al.*, 1999). It was impossible to make meaningful light scattering measurements at an NaCl concentration of 1 M. The results indicate that the high salt concentration promoted spontaneous and extensive aggregation of the polyplexes upon their formation, so that they became larger than about 3 μm, i.e. not in the detection range of the instrument. Such large particle sizes could not be measured accurately using DLS.

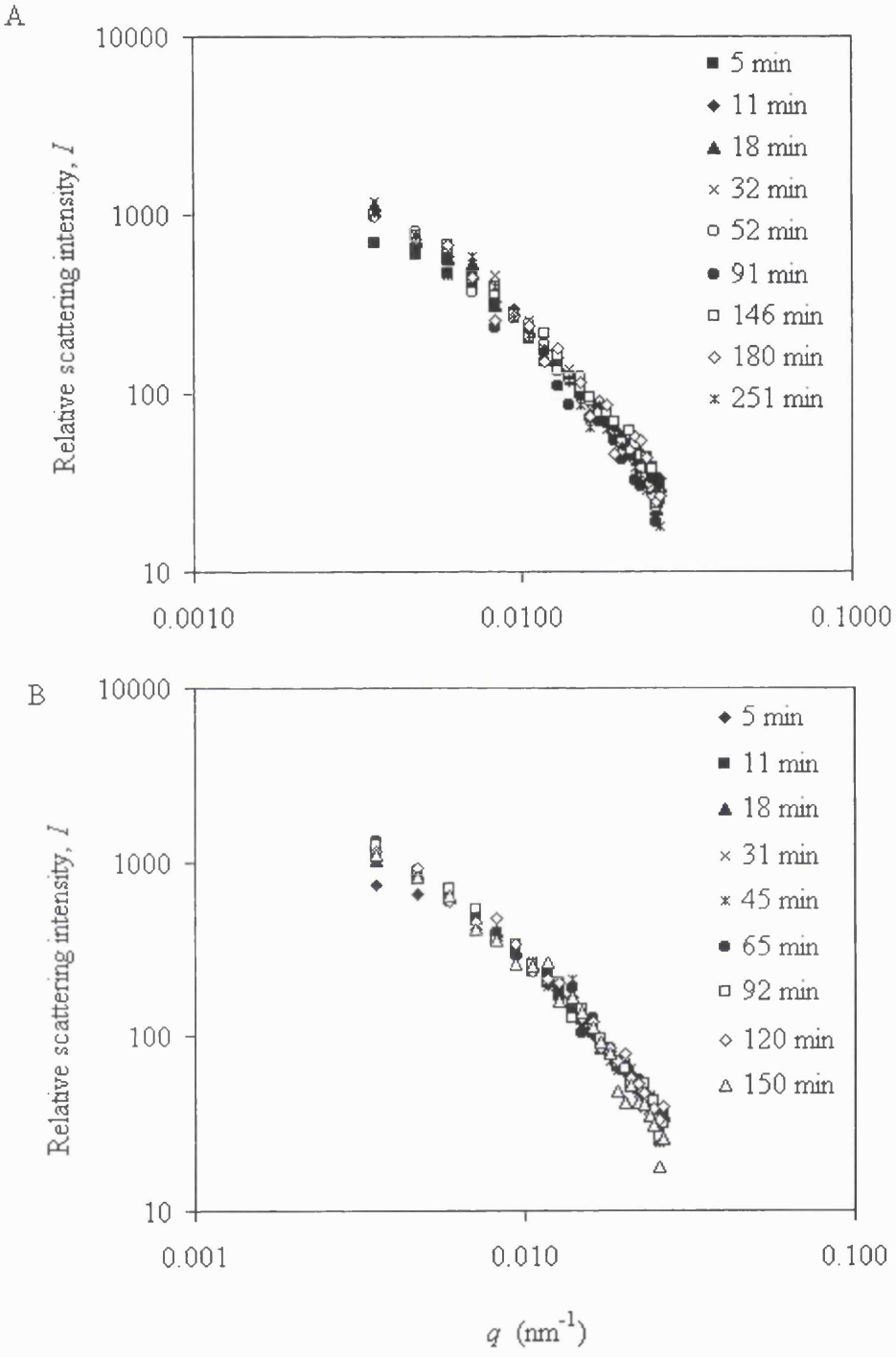
A
10000
1000
100
10
Relative scattering intensity, I
0.0010
0.0100
0.1000
5 min
11 min
18 min
32 min
52 min
91 min
146 min
180 min
251 min
B
10000
1000
100
10
Relative scattering intensity, I
0.001
0.010
0.100
q (nm-1)
5 min
11 min
18 min
31 min
45 min
65 min
92 min
120 min
150 min

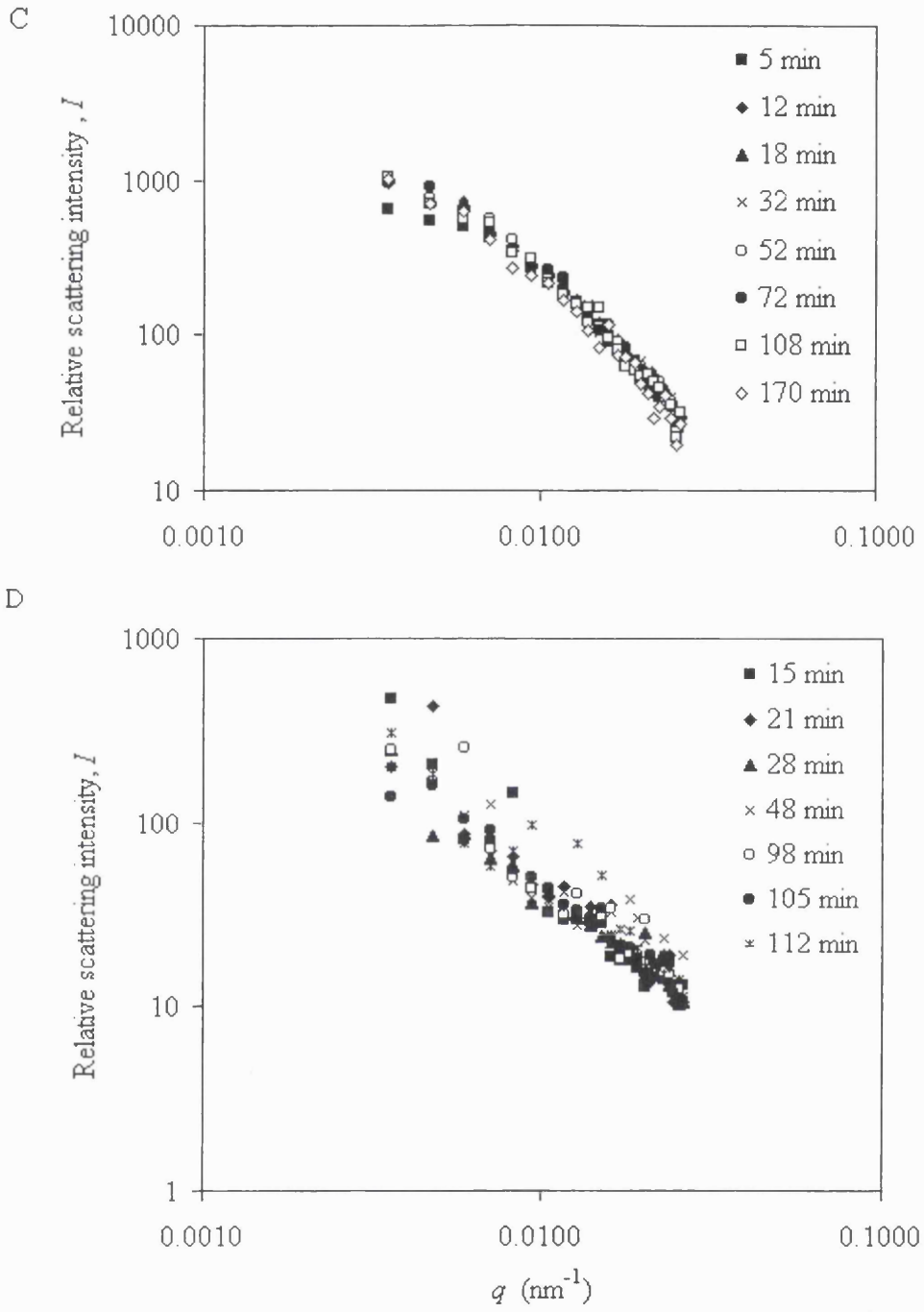

Figure 4.25 Static light scattering results. Log–log plot of I(q) collected at various times during the run for the poly-L-lysine/pSVβ complexes in 20 mM HEPES pH 7.2: (A) 50 mM NaCl, (B) 100 mM NaCl, (C) 150 M NaCl, and (D) 1 M NaCl (n = 1). For the sake of clarity, only selected data sets are displayed.

4.3.3 Measurement of polyplex fractal dimension

Eq. (4.15) implies that the slope of a log-log plot of the scattered light intensity $I(q)$ versus q yields the fractal dimension of the polyplex aggregates, under the condition that $a << 1/q << l$ for all clusters. Considering the curves in Fig. 4.25, they can be fit to straight lines throughout the aggregation process for $q > 0.008$. Within the scaling range $1/l < q < 1/a$ of wave vector q, which corresponds to the condition that $50 < 1/q < 1500$ or $0.0007 < q < 0.02$, the ln I (photoncounts) vs. ln q (nm^{-1}) plots in the power-law region lead to straight lines. Hence, the fractal dimensions for the polyplex samples as shown in Fig. 4.25 were obtained as shown in Fig. 4.26. At a given NaCl concentration, and with increasing particle size, the overall constancy of the slopes of these lines and the associated fractal dimensions suggests the formation of similar cluster structures throughout the aggregation process. The fractal dimension, averaged from the slopes obtained for the polyplexes at 50, 100 and 150 mM NaCl (Fig. 4.26), was approximately 2.20. Note that at the physiological salt concentration range of 100 to 150 mM NaCl, no substantial differences in fractal dimension were observed between the formulations.

It has been shown by other groups that for colloidal materials including illite colloids in NaCl solution, protein-covered polystyrene spheres and emulsions, the scattering curves such as those shown in Fig. 4.25 move toward higher intensity at small values of q at the earlier stages of aggregation (Derrendinger and Sposito, 2000; Molina-Bolívar *et al.*, 1998; Poulin *et al.*, 1999; Tirado-Miranda *et al.*, 2000). The scattering curves then display asymptotic behaviour as aggregation proceeds, and converge to yield straight lines with slopes corresponding to the true fractal dimension. This observation may be explained by the time required for the internal structure of the clusters to be resolved. Furthermore, the clusters must reach a sufficiently large size to be probed for fractal structure, as determined by the conditions for Eq. (4.15). In this study, such asymptotic behaviour is noticed only for the initial two scans in the case of the polyplexes at 50, 100 and 150 mM NaCl (Figs. 4.25A, B and C). The results indicate the presence or rapid formation of an ordered system even at the earliest stages of aggregation, as well as the apparent lack of cluster restructuring during the aggregation process.

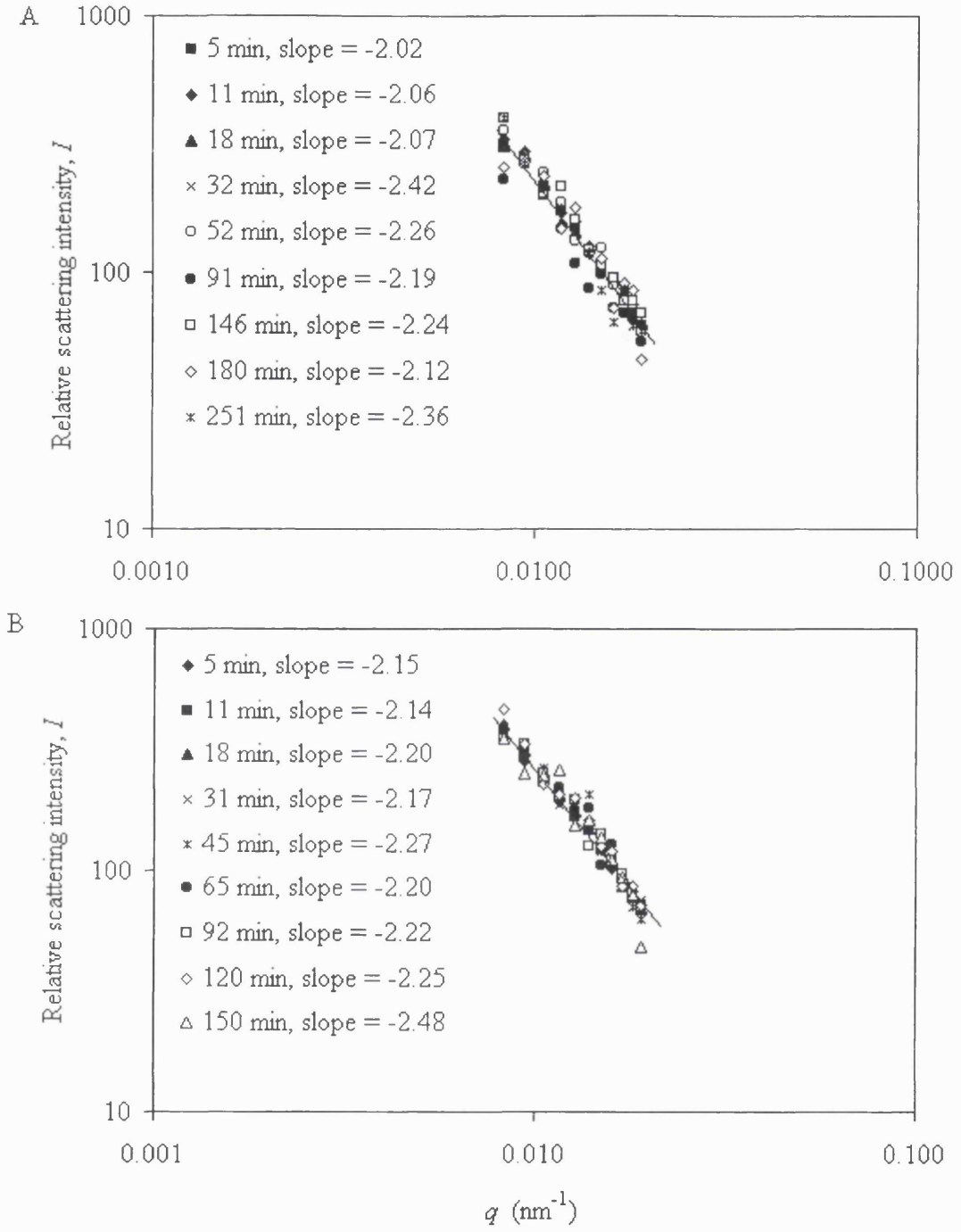
A
1000
100
10
Relative scattering intensity, I
5 min, slope = -2.02
11 min, slope = -2.06
18 min, slope = -2.07
32 min, slope = -2.42
52 min, slope = -2.26
91 min, slope = -2.19
146 min, slope = -2.24
180 min, slope = -2.12
251 min, slope = -2.36
0.0010
0.0100
0.1000
B
1000
100
10
Relative scattering intensity, I
5 min, slope = -2.15
11 min, slope = -2.14
18 min, slope = -2.20
31 min, slope = -2.17
45 min, slope = -2.27
65 min, slope = -2.20
92 min, slope = -2.22
120 min, slope = -2.25
150 min, slope = -2.48
0.001
0.010
0.100
q (nm-1)

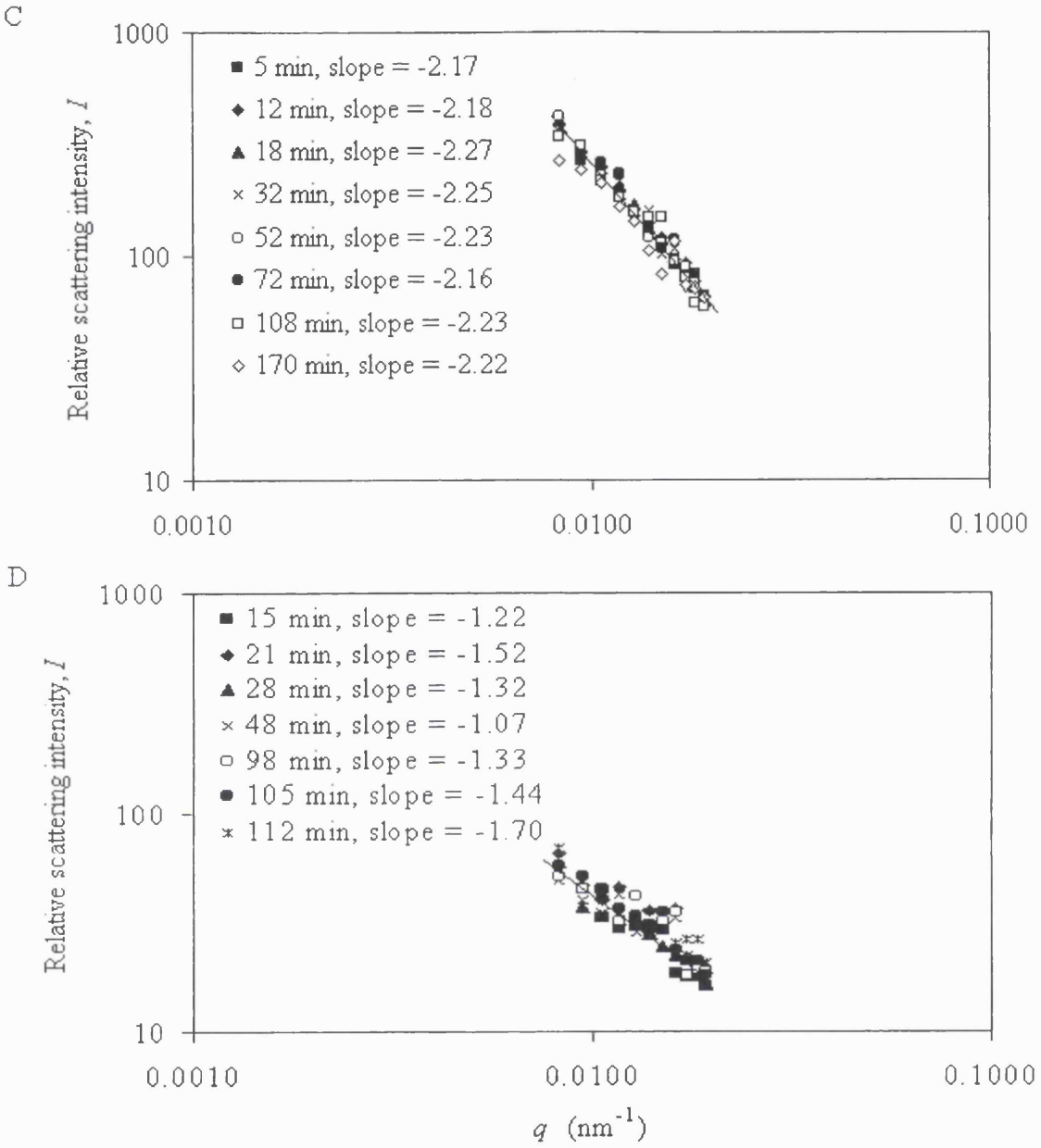

Figure 4.26 Determination of the fractal dimensions. Log–log plot of I(q) collected at various times during the run for the poly-L-lysine/pSVβ complexes in 20 mM HEPES pH 7.2: (A) 50 mM NaCl, (B) 100 mM NaCl, (C) 150 M NaCl, and (D) 1000 mM NaCl (n =1). The power-law exponents shown on the plot were obtained from the slopes of the regression lines fitted by EXCEL. For the sake of clarity, only selected data sets are displayed.

4.3.4 Diffusion- and reaction-limited regimes of aggregation

The fractal dimensions obtained from the straight line slopes of the intensity profiles for all the scans performed (Fig. 4.25; method shown in Fig. 4.26) are summarised for comparative purposes in Table 4.1 and shown in Fig. 4.27. As can be seen in Fig. 4.27, the scattering exponents obtained from the light scattering curves have values less than 3.0, indicating that the poly-L-lysine/pSVβ complexes in this study are mass fractals and have connected structures. Note that there is no decrease in the mean fractal dimension from 50 mM NaCl to 150 mM NaCl. Therefore, it is apparent that in this range, at the lower ionic strengths, the polyplex structures and aggregation regimes do not differ significantly between one another. At the highest electrolyte concentration of 1000 mM NaCl, the fractal dimension is significantly decreased. The results suggest that the polyplexes under this condition have a different aggregation regime.

Table 4.1 Effect of ionic strength on the fractal dimension of poly-L-lysine/pSVβ complexes in 20 mM HEPES pH 7.2.

NaCl concentration	Fractal dimension, D_f			
(mM)	Min.	Max.	Mean	Median
50	1.83	2.50	2.22	2.22
100	2.10	2.48	2.22	2.20
150	1.97	2.35	2.22	2.24
1000	1.07	1.70	1.44	1.44

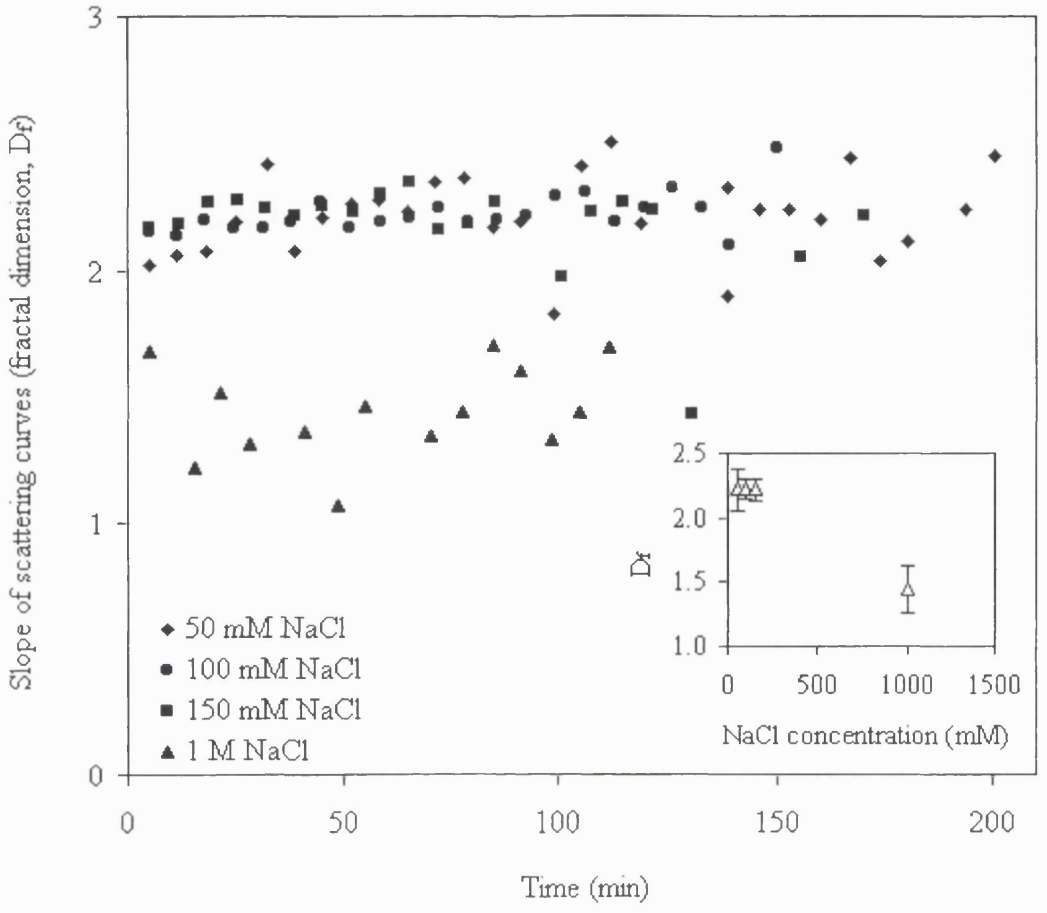

Figure 4.27 Evolution of the fractal dimensions obtained from the slope of ln I vs. ln q plots (Fig. 4.26), as a function of salt concentration for the poly-L-lysine/pSVβ aggregates. Inset: Mean fractal dimension (D_f) as a function of NaCl concentration in the polyplex suspensions. Vertical bars indicate standard deviations calculated using the Excel worksheet function.

Table 4.1 lists the minimum, maximum, mean and mode values of mass fractal dimensions obtained from the data illustrated in Fig. 4.27. As each system had a representative fractal dimension, it was possible to clearly identify two irreversible aggregation regimes. The aggregation kinetics of these systems depend on a balance of attractive van der Waals and repulsive double-layer electrostatic forces between the

colloidal polyplexes. Fractal dimensions around 2.2, such as those observed for the polyplexes at ionic strengths between 50 and 150 mM NaCl, are characteristic of the slow reaction-limited kinetics (RLCA), where not every collision of two polyplex particles or clusters results in aggregation. Other groups investigated the effect of NaCl concentration on fractal dimension for various colloids (Derrendinger and Sposito, 2000; Molina-Bolívar *et al.*, 1998) and found similar results in terms of fractal dimension values. In comparison, the fractal dimension of the polyplexes at 1 M NaCl was determined to be 1.44 ± 0.19. The smaller fractal dimension is characteristic of diffusion-limited colloidal aggregation (DLCA). It has been shown that electrostatic interactions are weakened by addition of salt (Lee *et al.*, 2001; Molina-Bolívar *et al.*, 1998). Therefore, while the attractive van der Waals force is largely unaffected by the salt, the double-layer repulsion increases with increasing salt concentration. The decrease in repulsive forces results in aggregation occurring upon every collision between particles. The fast DLCA mechanism leads to the formation of polyplex aggregates that are tenuous fractal structures with a greater tendency for restructuring than RLCA type aggregates.

The fractal dimensions obtained for the polyplexes at lower electrolyte concentrations remain fairly constant with time (see Fig. 4.27), suggesting that the slower aggregation conditions yield polyplex structures, although not cluster sizes, that are fairly stable and do not undergo significant structural rearrangement, for at least a few hours. On the other hand, the fractal dimensions of the polyplexes at 1 M NaCl exhibit a more marked deviation from the average value of 1.44 throughout the aggregation process.

The upper limit of particle size measured by photon correlation spectroscopy is usually about 3 μm. This condition is dependent on the density of the sample and the onset of sedimentation. In the case of PLL/pSVβ complexes at 1 M NaCl, it was expected that the polyplexes aggregated very rapidly, and reached mean hydrodynamic diameters greater than 3 μm after only minutes. Note that the static light scattering measurements were made even after the polyplexes were larger than 3 μm. This was acceptable since the intensity of the scattered light remains constant at a given scattering angle as aggregation

proceeds. Furthermore, the recorded scattered intensity was directly found by the photomultiplier and not subjected to analysis by the instrument software, as is the case in size measurements (Stephen Ward-Smith, personal communication).

The fractal structure of a colloid of relatively large particles, induced to aggregate by a simple salt, was analysed. Two regimes of irreversible aggregation were found to exist, each giving different fractal dimensions. It is suggested, therefore, that the analytical methods presented here for a relatively simple well-characterised system provide potentially useful approaches to more complicated biologically relevant DNA complexes.

CHAPTER 5

RESULTS AND DISCUSSION: LIPOFECTIN/INTEGRIN-TARGETING PEPTIDE/DNA (LID) COMPLEXES

This chapter is concerned with the investigation of the physicochemical properties and related transfection efficiency of a novel targeted non-viral gene delivery system. After a brief introduction, the influence of parameters such as the mixing method, complex charge ratio, ionic strength of solution, DNA concentration and concentration of added albumin on the particle size and surface charge are described. Subsequently, the correlation of complex size and charge ratio with *in vitro* gene expression is discussed. The chapter is concluded by simulation results from a colloidal model, based on the DLVO theory, of the total interaction potentials between the complexes.

5.1 Introduction

Integrins are a class of heterodimeric transmembrane surface receptors, anionic proteoglycans on the cell surface that are involved in mediating cell-cell adhesion and promoting interactions between cells and extracellular matrices (Hynes, 1987; Hynes, 1992). They also provide a means of entry into cells such as airway fibroblasts and epithelial cells. Integrin-mediated cell binding and entry is a process exploited by many microbial pathogens, making the process attractive for the cell-targeted transfer of therapeutic genes (Horton, 1996; Horton, 1999). Developed by the Molecular Immunology Unit at the Institute of Child Health, Great Ormond Street Hospital, London, for use in clinical trials of gene therapy for immunodeficiencies, cancers and cystic fibrosis, the Lipofectin/integrin-targeting peptide/DNA (LID) vector has shown high transfection efficiency, low toxicity and the ability to package large DNA molecules. Recent studies have demonstrated integrin-mediated transfection by the LID vector in various cell lines, including corneal endothelial cells (Hart *et al.*, 1998), keratinocytes (Compton *et al.*, 2000), bronchial and alveolar cells in the lungs of rats (Jenkins *et al.*, 2000), and fibroblasts from patients with lysosomal storage diseases (Estruch *et al.*, 2001).

The LID formulation consists of a cationic liposome, Lipofectin, an integrin-targeting peptide, and plasmid DNA. Affinity for integrins is conferred upon the peptide by a cyclic integrin-binding domain containing the arginine-glycine-aspartic acid (RGD) peptide motif, which in turn is crosslinked to a short 16-lysine tail that mediates DNA-binding and compaction. These peptides can be synthesised and chemically modified fairly easily. The peptide used in these studies, peptide 6, is $\alpha5\beta1$ integrin-specific. The inclusion of a widely used cationic lipid mixture, Lipofectin, a 1:1 (w/w) mixture of the cationic lipid *N*-[1-(2,3,-dioleyloxy)propyl]-*N,N,N*-trimethylammonium chloride (DOTMA) and the neutral lipid dioleoyl phosphatidylethanolamine (DOPE), also enhances transfection efficiency by destabilisation of endosomal membranes. The following is a report on the characterisation of the size and structure of LID complexes

(lipopolyplexes), their surface charge under varying conditions, and the correlation with *in vitro* transfection efficiency.

5.2 Physicochemical characterisation

5.2.1 Influence of mixing method

Plasmid DNA (D) condensation was observed in the presence of the lipid/peptide (LI) components under all conditions, as evidenced by the formation of relatively dense cores that were detected by photon correlation spectroscopy (PCS) immediately after mixing of the formulation components. Time evolution studies utilising dynamic light scattering (DLS) analysis showed that the average diameters of the LID complexes (lipopolyplexes) increased rapidly with time. Such observations of aggregation have also been noted for other gene delivery systems (Bally *et al.*, 1997; Kennedy *et al.*, 2000; Ogris *et al.*, 1998; Ogris *et al.*, 1999; Pouton *et al.*, 1998; Tang and Szoka, 1997; Turek *et al.*, 2000; Zelphati *et al.*, 1998a). LID complexes were prepared at a charge ratio of 6.8 and DNA concentration of 5 μg/ml (Section 3.6). In order to optimise the preparation of the LID complexes, initial mixing of the plasmid DNA (D) and Lipofectin/integrin-targeting peptide (LI) solutions were carried out using the two-syringe mixing method, described in Section 3.7, to mix the D and LI solutions in a reproducible manner and to eliminate any variability arising from different handling procedures. Both the two-syringe mixing method at four mixing flow rates and the pipette mixing method (addition of DNA to LI) were used. Immediately after mixing, their mean light scattering hydrodynamic diameters were obtained at various time intervals using DLS.

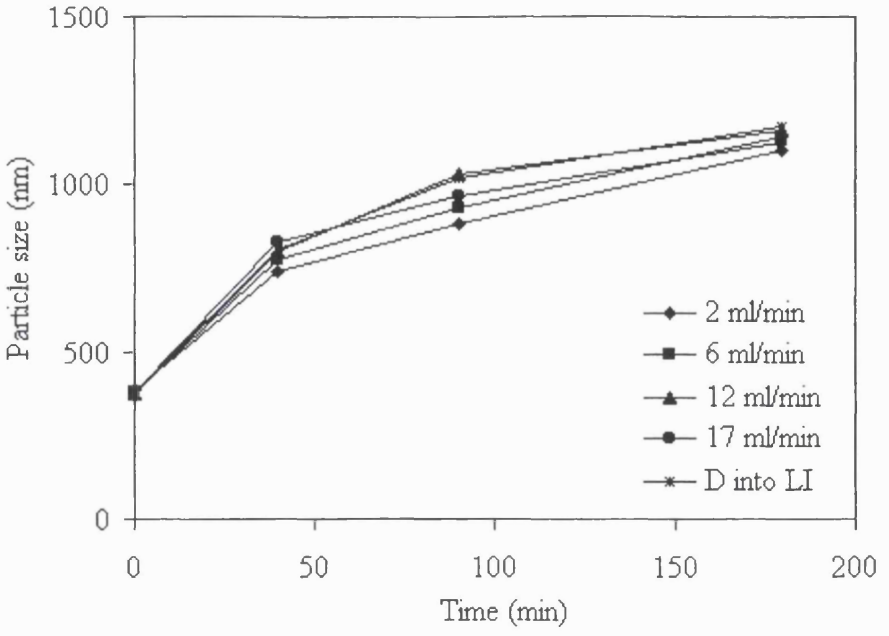

Figure 5.1 Mean particle size of Lipofectin/integrin-targeting peptide/pSVβ (LID) complexes as a function of time for different mixing rates. Lipopolyplexes were prepared in Opti-MEM at a charge ratio of 6.8 and a DNA concentration of 5 μg/ml.

As shown in Fig. 5.1, the LID complexes aggregated rapidly, from an initial mean size of approximately 400 nm to almost 1200 nm in 3 h. Correspondingly, PCS data exhibited a decreased photoncount rate (data not shown), presumably due to the sedimentation of large aggregates. In addition, the polydispersity (Section 3.9) increased to greater than 0.7, indicating the growing heterogeneity of the population of lipopolyplexes. After approximately 3 h, the aggregation rate decreased. This agrees with previous results (Section 4.2.2.3), where the presence of smaller particles exhibits a greater tendency for aggregation with larger particles. Around this time point, the samples tend to be very heterogeneous, with polydispersity factors of 1.0 (standard deviations of nearly 100%).

Fig. 5.1 also shows that there is a lack of distinguishable differences between the particle growth behaviour of the lipopolyplexes prepared by both methods. The results are a

departure from the findings of other workers (Zelphati *et al.*, 1998a), who noted that the order of addition of DNA and the cationic component had a significant effect on the particle size of the complexes formed and could influence the aggregation behaviour. Although not relevant in this study, wherein the LI solution was always prepared before being mixed with DNA, it is interesting to note that adding Lipofectin to the other two formulation components resulted in lower transfection efficiencies (Hart *et al.*, 1998). This indicates that the formation of LID complexes is not greatly dependent on the preparation path. Subsequent experiments were performed to investigate the influence of other kinetic and thermodynamic factors, e.g. concentration and ionic strength, on the stability of LID complexes.

In addition, it was found that lipopolyplexes composed of different plasmids, i.e. pSVβ (6.9 kb), pEGFP (4.7 kb) or pCI-luc (5.7 kb), showed similar behaviour in terms of particle size, aggregation and zeta potential. This is consistent with the data obtained by Kreiss *et al.* (Kreiss *et al.*, 1999). In their work the plasmid size range was wider, i.e. between 3.7 and 52.5 kb. Similar data is also shown for pSVβ and linear calf thymus DNA of 15-23 kb (average size) in Section 4.1.4.3, and a previous work (Lee *et al.*, 2001). Unless otherwise mentioned, all LID complexes were prepared with pCI-luc.

5.2.2 Influence of DNA concentration and formulation buffer

Many workers allow an incubation time of several minutes up to an hour after preparation of the formulation before measurements. Unless the colloidal suspensions are stable, changes in diameter, count rate and polydispersity may affect the reproducibility of the results.

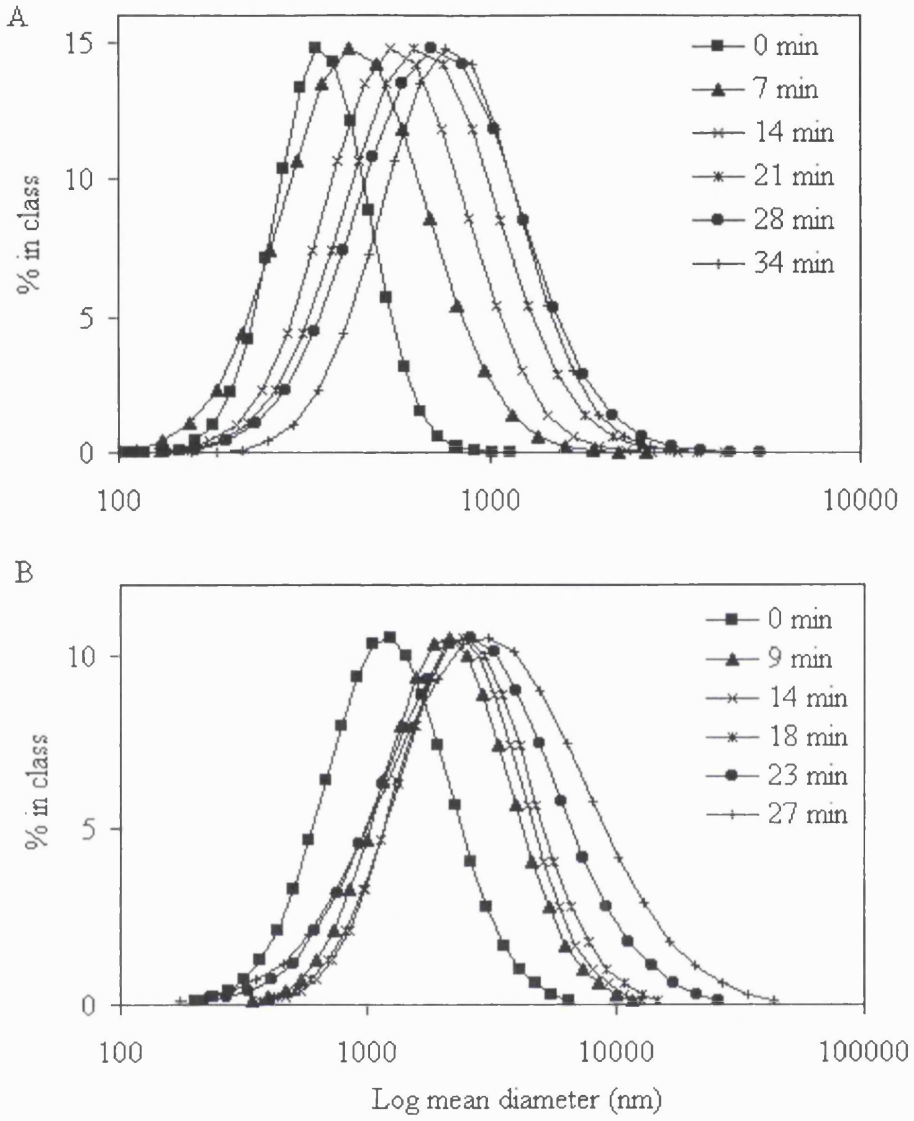

Figure 5.2 Comparison of particle size distributions for LID complexes prepared at DNA concentrations of (A) 5 μg/ml and (B) 160 μg/ml. The software determined the distributions as mean of diameter based on intensity of scattered light at 90°. The data plots are shown as individual measurements at various time periods after complex preparation. Lipopolyplexes were formed in phosphate-buffered saline (PBS) at a charge ratio of 6.8. as described in Section 3.6.

Figs. 5.2A and B show typical size distribution data obtained from DLS measurements for the LID complexes at plasmid concentrations of 5 μg/ml and 160 μg/ml, respectively. The data refer to experiments carried out with the 5.7 kb pCI-luc, and in each case, measurements were performed as a function of time immediately after pipette mixing of the solution of plasmid (D) into the lipid/peptide (LI) solution. Additional experimental details are shown in the caption. In both cases the plots demonstrate a continuous shift in the size distribution towards the right-hand-side as a function of time, indicating that aggregation of the complexes occurs practically as soon as the components are mixed. Comparison of the particle sizes (x-axis) in Fig. 5.2A with those in Fig. 5.2B shows that the extent of aggregation is critically dependent on plasmid concentration. This is a substantial problem since high DNA concentrations (300-1300 μg/ml) are often essential for *in vivo* studies and clinical use (Zelphati *et al.*, 1998a).

Fig. 5.3 shows the particle sizing data for LID complexes prepared in different buffers, all of which are at physiological salt conditions (100 to 150 mM NaCl) except for distilled water. For buffers with physiological salt conditions, the aggregation curves did not show any significant difference at similar plasmid DNA concentrations. The plots confirm the highly aggregative nature of the LID complexes prepared in phosphate-buffered saline (PBS) and high salt concentration buffers. The presence of an electrolyte brought about compression of the electrical double layers surrounding the particles, thus reducing the repulsion barrier between them and inducing aggregation. The increase in plasmid DNA concentration from 5 μg/ml to 160 μg/ml also had a significant impact on aggregation of the lipopolyplexes. For example, in the case of lipopolyplexes formed in PBS at a DNA concentration of 160 μg/ml, the z-average size of the complexes increased to a value of about 3000 nm after approximately 40 minutes. The polydispersity also increased, in the case of data in Fig. 5.3, from a value of about 0.5 at the start of the measurements to a value of 0.7-1.0 after about 40 minutes. Particles greater about 3000 nm in diameter are too large to be accurately sized by DLS and were not included in the plots. It was not possible to make any meaningful light scattering measurements for LID complexes formed in distilled water at a plasmid concentration of 5 μg/ml.

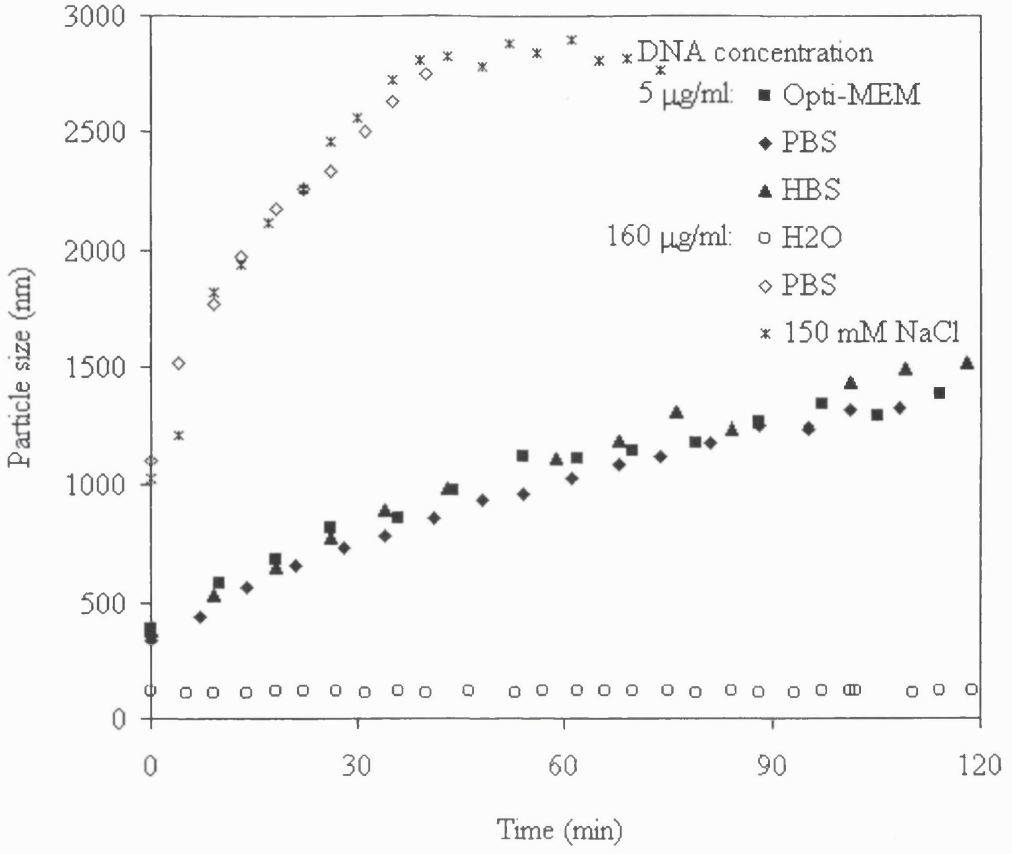

Figure 5.3 Growth of LID complexes in different buffers with time. Lipopolyplexes were formed at a DNA concentration of 5 μg/ml by the two-syringe mixing method (2 ml/min mixing rate; closed symbols) or 160 μg/ml by pipette mixing (addition of DNA to LI; open symbols). The data shown are a single representative sample from at least two separate experiments.

Lipopolyplexes prepared in PBS and normal saline at a DNA concentration of 160 μg/ml resulted in comparable aggregation profiles, as did all lipopolyplexes at 5 μg/ml. This indicated that even in the presence of other constituents in the solution environment, as in the case of Opti-MEM, for example, the concentration of salt determined the likelihood of aggregation occurring. Compared with other buffer conditions shown in Fig. 5.3, preparation in distilled water resulted in physically stable LID complexes with an initial mean hydrodynamic diameter of 110 nm ± 35 nm which was relatively consistent throughout the experiment, and with polydispersities no greater than 0.3. Measurements

carried out on samples prepared in distilled water confirmed that these lipopolyplexes remained stable for at least one week when stored at 4°C (data not shown). One major advantage to the use of LID complexes in water, besides their physical stability, is the hypotonic nature of the formulation. Since a drug solution that is hypotonic, when administered to the lung, will have a greater tendency to move from the pulmonary space into the alveoli for more rapid absorption and therapeutic effect (www.paddocklabs.com/publications/secundum/secart63.html, 1997), the LID vector in water should exhibit higher transfection efficiency in the lung than its PBS counterpart. This has been verified in *in vivo* studies in the lungs of mice (Jenkins *et al.*, 2001).

5.2.3 Influence of charge ratio

The particle growth data of LID complexes formed at various charge ratios in the transfection buffer Opti-MEM are plotted in Fig. 5.4. Extensive aggregation of the lipopolyplexes at all charge ratios was observed. Particle size measurements were also carried out for lipopolyplexes (LKD) in which the integrin-targeting peptide (peptide 6) was substituted for a similar peptide incorporating a longer oligolysine domain (K_{36}). The supplementary LKD data showed that a longer DNA-binding lysine tail neither conferred stability nor increased aggregation. The aggregation profiles of lipopolyplexes at charge ratios 0.5 when the lipopolyplex was not yet fully formed, and 1.0 when the lipopolyplex was theoretically neutral, appeared no different than those at net positive charge ratios. This suggests that at these charge ratios free plasmid DNA was present in the formulation. On the other hand, since the aggregation profiles at charge ratios higher than 1.0 were not significantly different, excess Lipofectin and integrin-targeting peptide may have been present in the solution.

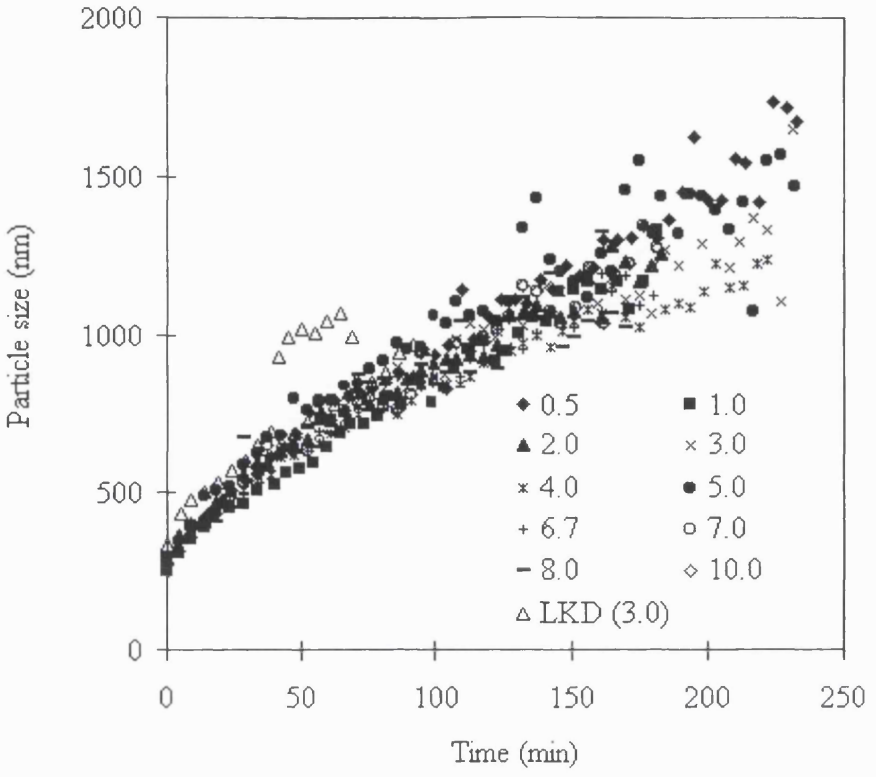

Figure 5.4 Mean particle size of LID and LKD complexes as a function of the charge ratio. LKD complexes were prepared at a charge ratio of 3. All lipopolyplexes were prepared in Opti-MEM by the two-syringe mixing method (2 ml/min mixing rate) and at a final DNA concentration of 5 μg/ml. This is a representative data plot from three experiments.

The PicoGreen assay (Section 3.12) was used as a highly sensitive and accurate method to quantify free DNA, i.e. DNA not complexed by Lipofectin or integrin-targeting peptide. Fig. 5.5 shows the effect of the complex charge ratio on the particle surface charge, given by the zeta potential (open symbols), and the accessibility of plasmid DNA to PicoGreen intercalation (closed symbols). The data refer to experiments carried out with pCI-luc, the 5.7 kb plasmid DNA. The lipopolyplexes were prepared at a DNA concentration of 5 μg/ml using the two-syringe mixing method as described in Section 3.7. In contrast to the constant aggregation profiles for all charge ratios in Fig. 5.4, the zeta potentials at charge ratios less than 1.0 were strongly negative, showing incomplete

charge neutralisation of the DNA (Fig. 5.5). The zeta potentials reached a value of approximately 25 mV at a charge ratio of 3-4 and remained relatively unchanged even with the addition of more peptide. Accordingly, the fluorescence progressively decreased through the range over which the zeta potentials were negative, and reached a plateau value also at the charge ratio 3-4, at which point the DNA became inaccessible to the dye.

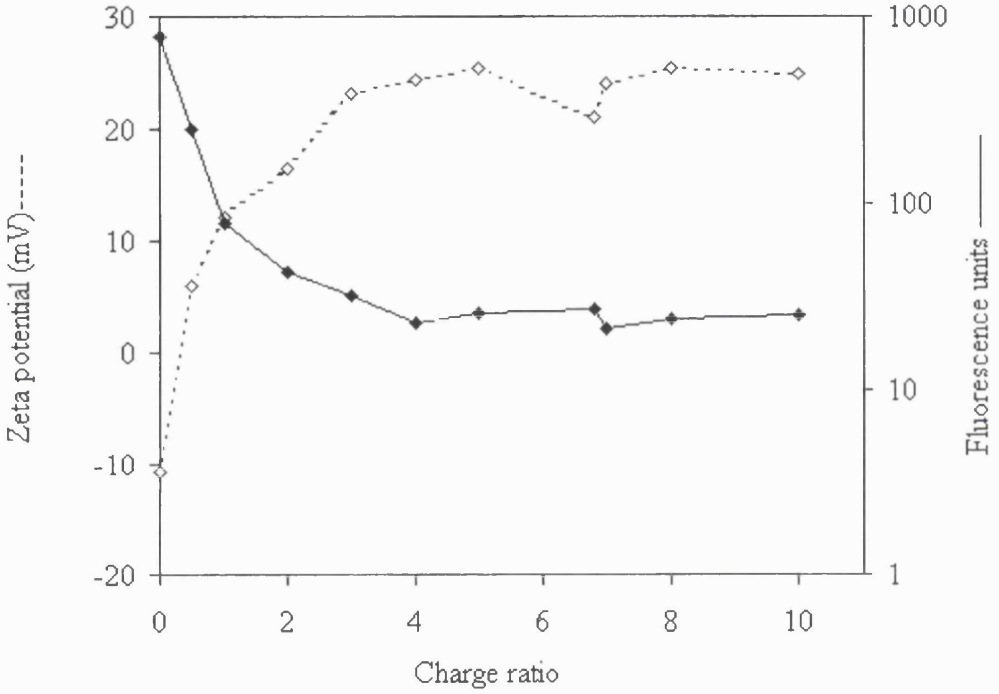

Figure 5.5 Zeta potentials and DNA accessibility of the LID complexes as a function of the charge ratio (varying amounts of integrin-targeting peptide). The complexes were prepared in PBS at a final DNA concentration of 5 μg/ml by the two-syringe mixing method (2 ml/min mixing rate), and their zeta potentials were immediately measured. For the fluorescence assay, the complexes were prepared in Opti-MEM at 5 μg/ml DNA concentration and diluted in TE buffer, as described in Section 3.12. Representative data plots from two experiments are shown.

Note that the maximum zeta potential was reached at a charge ratio greater than that of charge neutrality (Fig. 5.5). This may be due to the masking of charges on the oligolysine domain of the peptide by the cyclic integrin-targeting ligand (Kwoh *et al.*, 1999). In addition, it has been shown in other fluorescence dye exclusion assays that the ionic strength of the solution may increase the accessibility of DNA in the complex to the dye (Eastman *et al.*, 1997; Ferrari *et al.*, 2001). Eastman *et al.* suggested that the salt concentration influenced both lipoplex formation and pre-existing lipoplexes by enhancing extension of the DNA from the complex structure into the solution environment (Eastman *et al.*, 1997). This may explain the results shown in Fig. 5.5, where the lipopolyplexes were formed in PBS. The presence of charge shielding effects brought about by polyanions in the buffer may also account for the weaker electrostatic interaction between the DNA and the cationic components (LI), leading to an increased amount of peptide required to reach the maximum zeta potential.

Since *in vitro* transfection experiments, subsequently shown in Section 5.3, were performed in Opti-MEM, it would have been relevant to measure the zeta potentials and fluorescence signal with LID complexes in Opti-MEM. Nevertheless, this was not possible because zeta potentials of complexes in Opti-MEM could not be measured accurately; the quality of data obtained from the zeta potential measurements was very poor and hence unreliable (data not shown). This has been observed elsewhere for poly-L-lysine/DNA complexes in Opti-MEM and is thought to be due to an artefact of the method rather than a property of the complexes (Pouton *et al.*, 1998). For the PicoGreen assay, the LID complexes were diluted into a simple buffer, i.e. TE buffer (10 mM TrisCl pH 8.0, 1 mM EDTA), rather than a transfection buffer such as Opti-MEM, because this was recommended in the Product Information Sheet supplied with PicoGreen reagent. Furthermore, it was important to minimise contamination by any salts, enzymes and other compounds found in Opti-MEM that may influence the PicoGreen signal (Singer *et al.*, 1997).

5.2.4 Influence of LID vector composition

Dynamic light scattering was used to determine the influence of the components of the LID vector on the particle size. Lipopolyplexes were formed in distilled water, PBS and 5% dextrose at a charge ratio of 6.8 and a DNA concentration of 160 μg/ml. Complexes without the lipid component, in the case of ID complexes, or the peptide, in the case of LD complexes, were also prepared. Comparison of data for complexes prepared in PBS buffer (Fig. 5.6) indicate that the potential cause of aggregation in these systems is the presence of the integrin-targeting peptide (I) in the formulation. Its removal from the vector formulation resulted in the formation of (LD) aggregates with a size of approximately 400 nm that remained stable in PBS for more than 3 hours. However, the integrin-targeting peptide is an essential component of the formulation because it condenses the plasmid DNA efficiently, provides the cationic charge to the overall vector, and plays an important role in integrin recognition, hence facilitating cell targeting (Hart, 1999; Parkes and Hart, 2000). When included into the vector along with Lipofectin (LID), the integrin-targeting peptide produced significantly greater expression compared to LD complexes (Estruch *et al.*, 2001; Hart *et al.*, 1998; Jenkins *et al.*, 2000; Scott *et al.*, 2001). Similar results were also obtained in the transfection of cystic fibrosis and noncystic fibrosis tracheal epithelial cells *in vitro* using an integrin-targeted peptide and Lipofectamine (Colin *et al.*, 1998). Correspondingly, Lipofectin is also an important component of the vector since it enhances the transfection efficiency (Compton *et al.*, 2000; Hart *et al.*, 1998). It is thought to facilitate endosomal membrane destabilisation and subsequent DNA release to the cytoplasm (DOPE), and may contribute to the cationic charge of the vector (DOTMA).

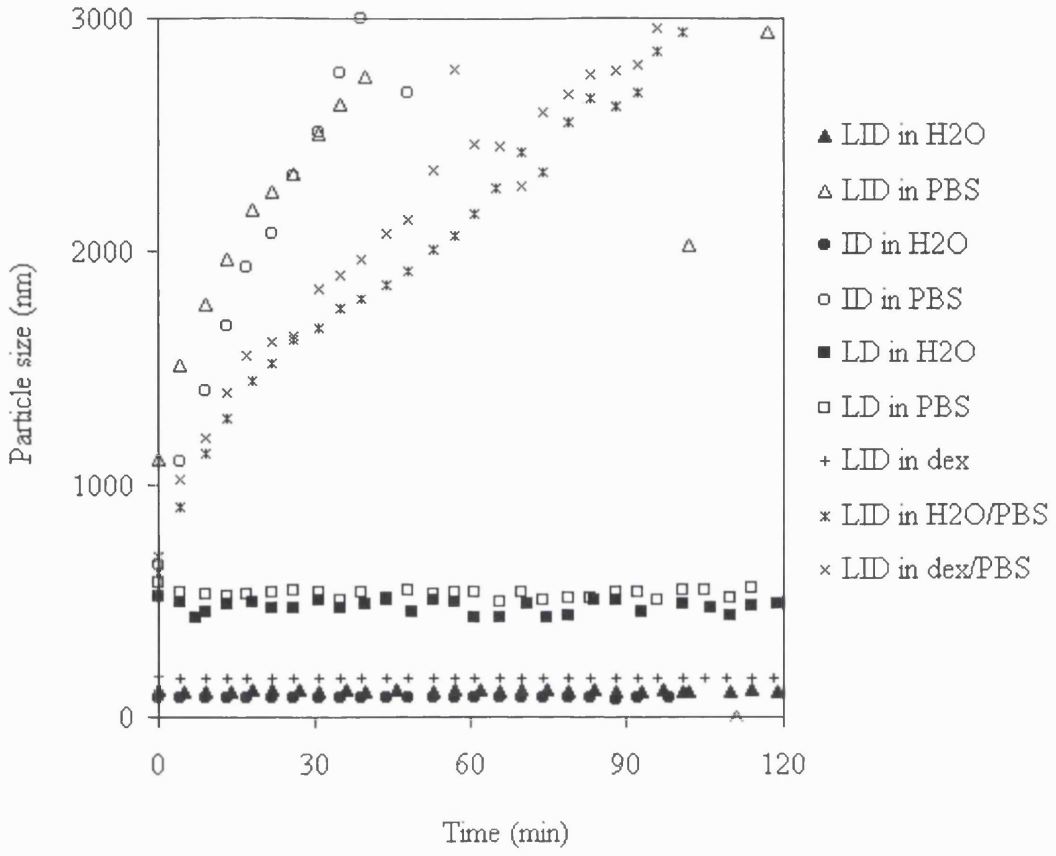

Figure 5.6 Time evolution of mean particle size of complexes in distilled water (H2O, closed symbols), phosphate-buffered saline (PBS, open symbols) and 5% dextrose solution (dex, + and ×): (▲, Δ, +) Lipofectin/integrin-targeting peptide/DNA (LID); (●, O) integrin-targeting peptide/DNA (ID); (■, □) Lipofectin/DNA (LD). The LID vector complex was formed by adding the plasmid pCI-luc to the LI mixture followed by pipette mixing. Lipopolyplexes were prepared at a charge ratio of 6.8. For ID and LD complexes, the L and I components were substituted by the appropriate volume of buffer. All of the samples were prepared at a final DNA concentration of 160 μg/ml, and their particle sizes were immediately measured by dynamic light scattering, except for LID in H2O/PBS (✶) and dex/PBS (×). LID complexes formed in distilled water (▲) or 5% dextrose (+) were found to be small, homogenous and relatively stable, with an average diameter of 110 ± 35 nm or 145 ± 35 nm, respectively. Those complexes were diluted in PBS to a final DNA concentration of 37.5 μg/ml before

subsequent measurement of their hydrodynamic diameters (✶ and ×, respectively). Representative data plots from two experiments are shown.

Both LID and ID complexes prepared in distilled water have a mean light scattering hydrodynamic diameter of about 110 nm (Fig. 5.6). Analysis of the LID and ID in water by atomic force microscopy (AFM) also showed that they were similar in size, albeit with a mean diameter of approximately 44 ± 8 nm (Hart *et al.*, 1998). The difference in size reported for both cases can be attributed to the sample handling process and analytical methods used. In the study by Hart *et al.*, the complexes were deposited on mica and dried. The dehydration presumably contributed to the observed smaller size. Considering the larger size of LD complexes (Fig. 5.6), it appears that most of the DNA condensation in LID complexes is due to the integrin-targeting peptide rather than the cationic lipid DOTMA in Lipofectin.

An isotonic solution of normal saline (154 mM or 0.9% NaCl) is frequently used for intravenous fluid administration, including *in vivo* gene delivery, because it has the same osmotic pressure as plasma (www.studentbmj.com/back_issues/0497/data/0497ed1.htm, 1997). Since the lipopolyplexes have been shown to aggregate in the presence of salt (Section 5.2.2), an alternative solution for potential administration of the formulation was considered. A solution of 5% dextrose, with an osmolality of 253 mOsm/l, is another isotonic solution that is commonly used as a maintenance and sometimes replacement fluid (Terry and Hedrick, 1995). Other groups have also used 5% dextrose in the preparation of lipoplexes for *in vivo* administration (Hong *et al.*, 1997; Li and Huang, 1997; Liu *et al.*, 2001; Templeton *et al.*, 1997; Zhu *et al.*, 1993). As shown in Fig. 5.6, LID complexes formed in 5% dextrose (5% w/v dextrose in distilled water with no salts added) gave small particle sizes (approximately 145 nm) and stable behaviour similar to that observed for lipopolyplexes in distilled water. Note that that subsequent addition of PBS to lipopolyplexes prepared in distilled water had a highly destabilising effect as shown by the rapid increase in the *z*-average values. Similarly, lipopolyplexes prepared in dextrose solution were also stable but aggregated when PBS was added. Nevertheless, the

stable nature of the lipopolyplexes in 5% dextrose suggests that they can be prepared a few hours (or longer, though this was not investigated) before administration for further manipulation or storage. This can be advantageous in many cases where water would not be a suitable transfection buffer, for example, the experiment discussed later in Section 5.3.1. The possibility of maintaining a stable suspension of LID complexes under isotonic conditions opens prospects for transfection studies (not pursued in this project).

5.2.5 Effects of interaction with proteins

It has been shown that the LID vector system has the potential for application in pulmonary gene therapy (Jenkins *et al.*, 2000; Jenkins *et al.*, 2001). In these studies, efficient gene delivery to the lungs of mice and rats by intratracheal instillation of LID complexes was achieved. Gene delivery to the lung is particularly advantageous for pulmonary ailments, such as cystic fibrosis, because of the relatively non-invasive procedure compared to systemic administration, easy accessibility to the lung via the airway, and the large surface area available for transfection (Pouton, 1999; Wheeler *et al.*, 1996). To study the effects of proteins in the airway surface fluid (ASF, the thin layer of liquid that overlays the lung epithelial cells) on the stability of the LID vector system, the lipopolyplexes were formed in distilled water and incubated with increasing concentrations of bovine serum albumin (BSA) (Fig. 5.7). BSA was used as an experimentally useful model system for these experiments. Little is known about the proteins of the ASF, owing to difficulties in measuring the protein concentrations in the tiny ASF volume. The albumin concentration in the local microenvironment of the lung is thought to be typically of the order of 0.2 mg/ml. Albumin is also the primary protein found in serum, comprising 50 to 55% of all blood plasma protein, and is found at a concentration of 35 to 50 g/l (Yokouchi *et al.*, 2001).

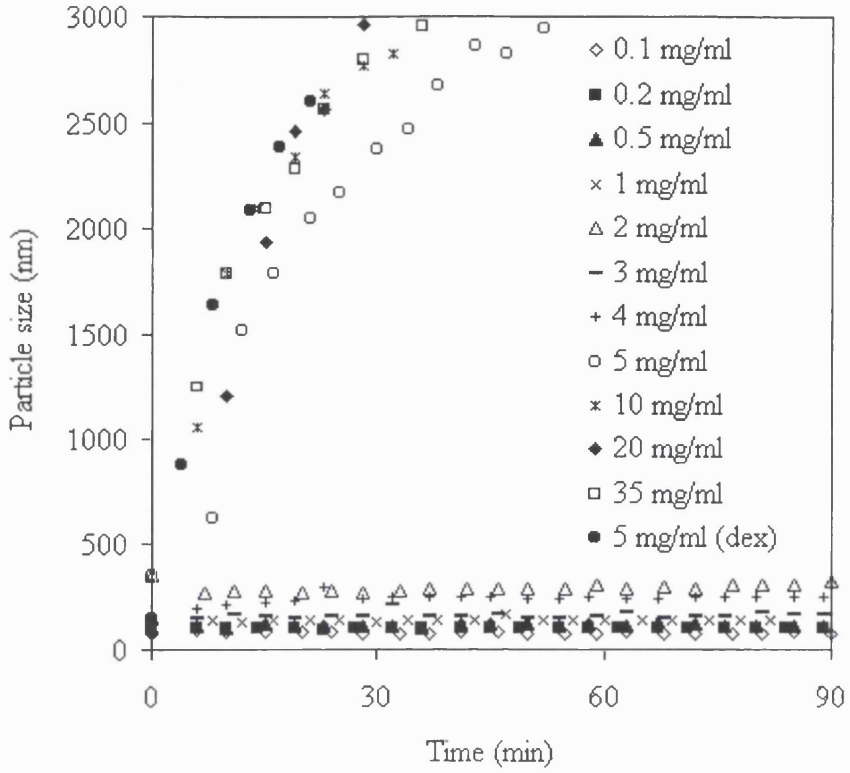

Figure 5.7 Time evolution of mean particle size of LID complexes as a function of the final concentration of bovine serum albumin (BSA). LID complexes were prepared in distilled water or 5% dextrose solution at a charge ratio of 6.8 and DNA concentration of 160 μg/ml. The lipopolyplexes were found to be stable, with an average diameter of 110 ± 35 nm or 145 ± 35 nm, in water or 5% dextrose, respectively, and are shown as single particle sizes at t = 0 min. Immediately after the first size measurement, an equal volume of BSA solution, that was of a concentration required to attain the final BSA concentrations shown in the plot, was added, and the kinetics of lipopolyplex aggregation monitored. BSA was dissolved at the required concentration in distilled water or 5% dextrose solution (●). The data in the plot corresponds to a fixed DNA concentration of 80 μg/ml and BSA concentrations as shown, except at t = 0 min.

Fig. 5.7 shows the time evolution of particle size of the LID complexes formed at a charge ratio of 6.8 in distilled water, to which BSA was added systematically to achieve various final BSA concentrations to cover the physiological range of interest. The data refer to experiments in which the initial DNA concentration of the complexes was 160 μg/ml. In each experiment stable complexes were prepared in distilled water as described previously. Immediately after the first size measurement (t = 0 min), an equal volume of distilled water containing a predetermined amount of BSA was added, resulting in complexes with a final DNA concentration of 80 μg/ml. As shown in Fig. 5.5, the addition of albumin to the complexes above a final BSA concentration of 5 mg/ml resulted in an increase in particle size from about 100 nm before the addition of BSA to more than 3 μm in less than an hour. This suggests that following intravenous administration, significant binding of the lipopolyplexes to serum proteins (opsonization) occurs in the bloodstream and prevents efficient cellular uptake. It has also been shown elsewhere that albumin promotes physical instability of DNA complexes (Cherng *et al.*, 1996; Dash *et al.*, 1999; Muller *et al.*, 1986; Verbaan *et al.*, 2001; Zelphati *et al.*, 1998b). However, the albumin concentration in the lung is low enough so that LID complexes in water (which were stable) gave substantially higher and prolonged transfection efficiency in the lungs of mice compared to LID complexes in PBS (which were unstable) (Jenkins *et al.*, 2001).

The plot in Fig. 5.8 indicates that the presence of BSA in the sample decreased the zeta potential of the complexes nearly exponentially from a value of about 27 mV at a BSA concentration of 1.0 mg/ml to a value approaching 8 mV at a BSA concentration of 5 mg/ml. The reduction in the potential energy barrier between the complexes was sufficient to cause the complexes to aggregate. These results, taken with those in Fig. 5.7, are well in agreement with observations of protein absorption on other complexes, leading to reduced transfection efficiency (Dash *et al.*, 1999). Studies on liposomes have shown that BSA, which is negatively charged under physiological conditions (pH 7.4), adsorb on negatively charged liposomes by hydrophobic interactions (Tsunoda *et al.*, 2001; Yokouchi *et al.*, 2001). Since the adsorption of proteins onto DNA complexes

depends on surface properties such as hydrophobicity and charge density (Lück *et al.*, 1998), modification of the surface chemistry would result in a decrease in the binding of serum proteins. A possible strategy to overcome protein binding would be to use a hydrophilic polymer to form complexes with reduced hydrophobicity and surface charge, in order to minimise the van der Waals interactions and Coulomb forces, respectively, between the complex surface and serum proteins. Another solution, shown to be successful, involves the formation of cross-linked hydrophilic shields on the complex surface that are resistant to protein interaction (Dash *et al.*, 2000).

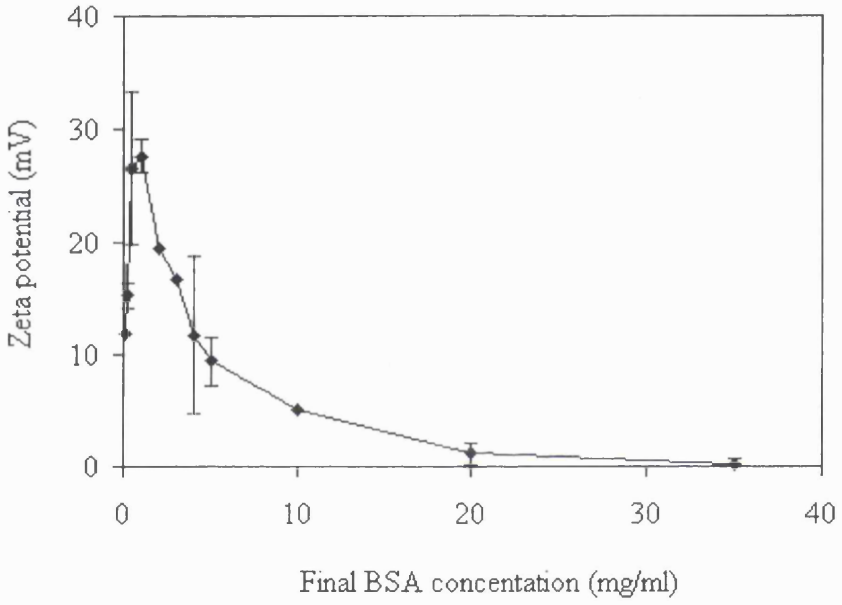

Fig. 5.8 Zeta potentials of the LID lipopolyplexes as a function of the bovine serum albumin (BSA) concentration. Stable LID complexes, with sizes of approximately 110 ± 35 nm, were generated by pipette mixing of D and LI components in distilled water at 6.8 charge ratio and 160 μg/ml DNA concentration. The final volume was 500 μl. The complexes were then diluted with the same volume of BSA solution at a given concentration to attain the BSA concentrations shown in the plot. After approximately two hours following addition of BSA, the complexes were further diluted with deionised water to a final concentration of 37.5 μg/ml for the zeta potential measurements. Data represent the mean ± standard deviation (n = 2).

5.3 *In vitro* transfection efficiency

5.3.1 Influence of formulation buffer

Fig. 5.9 shows the results for *in vitro* transfection of COS-7 cells using LID complexes (pEGFP plasmid complexed with Lipofectin/integrin-targeting peptide) prepared in three different formulation vehicles at a charge ratio of 6.8. The time axis represents the maturation time of the complexes before transfection was initiated. The transfection efficiency of LID complexes in water could not be determined because cell death occurred, possibly due to an osmotic effect of water being drawn into the cell. The transfection efficiency of LID complexes in PBS and HBS decreased sharply with complex maturation time (Fig. 5.9), whereas that for LID complexes prepared in Opti-MEM appear to be unaffected by complex maturation. The decrease in transfection efficiency of the LID complexes prepared in HBS and PBS buffers were in agreement with what was expected from the physical instability of these systems shown previously in Fig. 5.3. However, the apparent lack of change in the transfection efficiency over time for the LID complexes in Opti-MEM was unexpected since these complexes also aggregated (Fig. 5.3). Opti-MEM, a proprietary serum-free medium for cultivating mammalian cells *in vitro*, contains HEPES buffer, sodium bicarbonate, hypoxanthine, thymidine, sodium pyruvate, L-glutamine, trace elements (selenium, zinc), growth factors, insulin, transferrin and phenol red (www.lifetech.com/Content/Tech-Online/cell_culture/pps_manuals/2017.pdf, 2001). It is likely that the presence of some of these components in the transfection buffer provided conditions that were optimised for cell transfection. These observations (Fig. 5.9) may also be cell type and cell line specific.

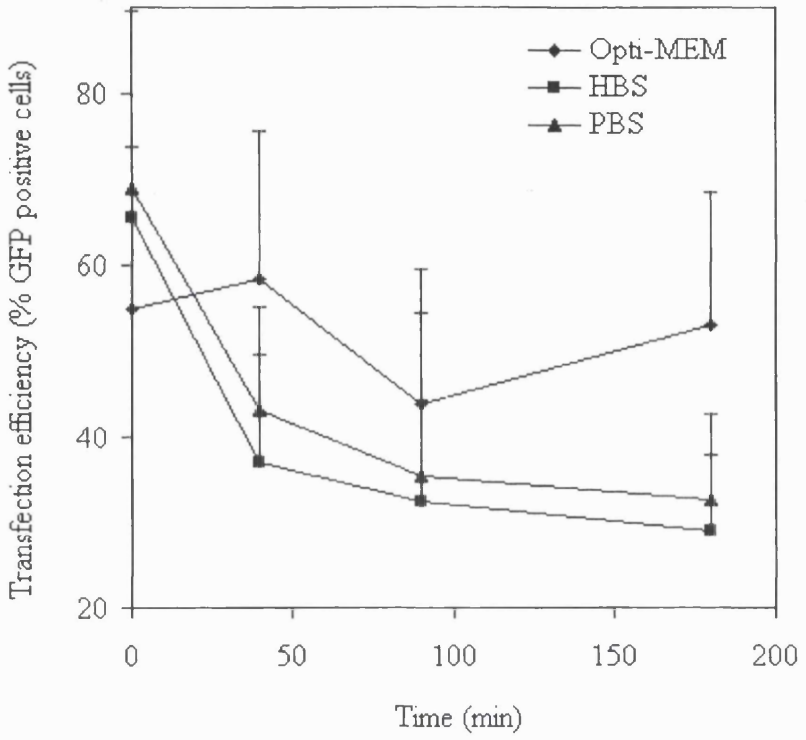

Figure 5.9 Transfection efficiency as a function of buffer at various times during the aggregation of LID complexes. COS-7 cells were transfected with LID complexes prepared at a charge ratio of 6.8 using the two-syringe mixing method (2 ml/min mixing rate) as described in Section 3.7. The data show the percentage of cells expressing GFP after 48 h. Data are the median and standard deviation of three separate experiments.

As shown in Fig. 5.3, the initial size of the lipopolyplexes in HBS and PBS (~350 nm) are larger than the typical values recommended for *in vivo* transfections, i.e. 100-200 nm for internalisation via receptors and diffusion through the vascular system and hepatic fenestrations (Ogris *et al.*, 1998). However, in cell culture experiments, where the complexes are directly added to the cells, cellular uptake and intracellular barriers may impose different size restrictions on the passage of the complexes. Fig. 5.9 shows that cells transfected with LID complexes of about 350 nm (t = 0 min) demonstrated some level of gene expression. The subsequently increased size of the complexes had a

detrimental effect on the transfection efficiency. Interestingly, lipoplexes of DNA complexed with the cationic lipid 1,2-dioleoyl-3-trimethylammonium-propane (DOTAP) and DOPE (1:1) in serum-containing media that were aggregated (> 2000 nm) showed increased gene expression in Chinese hamster ovary cells compared to smaller freshly prepared lipoplexes (~500 nm) (Ross and Hui, 1999). It has also been shown that plasmid DNA complexed with transferrin-conjugated polyethylenimine in saline buffer gave larger particles (300-600 nm) that transfected neuroblastoma cells at higher levels compared to the same polyplexes in water, which were smaller (30-60 nm) (Ogris *et al.*, 1998). The differences in these transfection results may be due, in part, to the cell association and uptake mechanism, which, in turn, are dependent on the cell line and DNA complex used. Turek *et al.* showed that the presence or absence of serum during transfection had an effect on the correlation between particle size and transfection activity, which may provide an explanation for the inconsistencies between these results (Turek *et al.*, 2000).

5.3.2 Influence of charge ratio

Given the charge-dominated similarities between the surface charge and accessible pEGFP plasmid shown in Fig. 5.5, it was anticipated that the transfection efficiency of the LID complexes would also depend strongly on the charge ratio. Supporting the fact that apparent binding of the DNA occurs beyond a charge ratio of 1.0, the data in Fig. 5.10 shows the correlation between the zeta potential of LID complexes with the transfection activity as a function of charge ratio. Complete DNA binding occurred when the zeta potential (Figs. 5.5 and 5.10) and fluorescence quenching of DNA (Fig. 5.5) reached a plateau, i.e. at the charge ratio of 3.0 to 4.0. In the lipopolyplexes, the ratio of primary amines to negatively charged nucleotides may be less than the charge ratio owing to suppression of protonation by closely spaced charged groups (Tang and Szoka, 1997).

As shown in Fig. 5.10, it is evident that the positively charged lipopolyplexes were more biologically active than naked plasmid DNA, which corresponds to a charge ratio of 0.0.

Maximum transfection efficiency is observed at a charge ratio of 3.0 to 4.0. Increasing the concentration of the integrin-targeting peptide did not correspondingly raise the transfection activity of the lipopolyplex. The reporter gene expression observed beyond a charge ratio of 3.0 to 4.0, notably around 7.0, was reduced. In contrast, it has previously been shown that LID complexes at a charge ratio of 7 were more efficient at *in vivo* gene delivery than those at a 3.5 charge ratio (Jenkins *et al.*, 2001). This underscores the ineffectiveness of determining the performance of the vector *in vivo* based on *in vitro* studies. It is likely that the different environments of *in vivo* systems and cell culture experiments presented different barriers that were inhibitory to gene delivery.

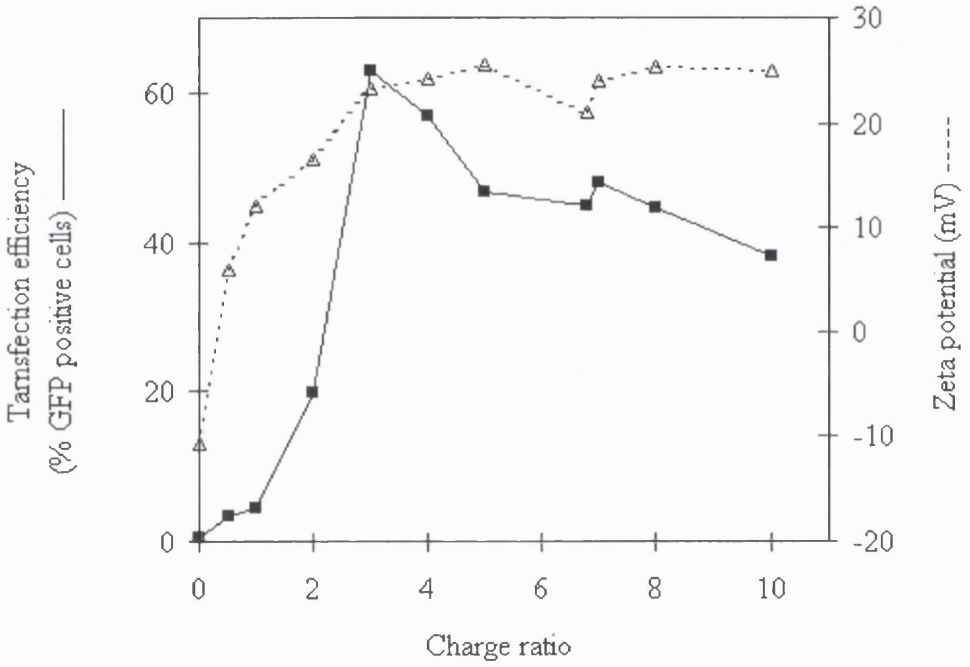

Figure 5.10 Transfection efficiency and zeta potential of LID complexes as a function of the charge ratio. COS-7 cells were transfected with LID complexes formed in Opti-MEM at a DNA concentration of 5 μg/ml by the two-syringe mixing method (2 ml/min mixing rate). The data show the percentage of cells expressing GFP after 48 h. For zeta potential analysis the complexes were prepared in phosphate-buffered saline (PBS). The zeta potential data was previously shown in Fig. 5.5. Both the transfection and zeta potential results shown are, in each case, a representative of two experiments.

There are several possible reasons for the lack of correlation of peptide concentration with charge ratio shown in Fig. 5.10, two of which follows. Since polylysine has potent cytotoxicity, the reduced transfection efficiency as peptide concentration is increased is presumably due to the lysine moiety of the integrin-targeting peptide. Another possible explanation is that the excess peptide was not complexed with DNA, and competed with the complexed lipid/peptide/DNA for binding sites (free peptide not detected by photon correlation spectroscopy). An alternative explanation that was ruled out is that at the higher charge ratios, electrostatic interactions of the lipopolyplexes with cell membranes led to non-specific uptake, at the expense of integrin-mediated uptake. This hypothesis is unlikely, since it is not supported by the zeta potential data, which indicated that increased peptide concentration did not increase the surface charge of the complexes. These proposed mechanisms of gene transfection behaviour were not pursued in this work and remains to be explained.

5.4 Colloidal stability of LID complexes

By combining experimental data and the DLVO theory that describes the colloidal stability of colloidal dispersions (Section 4.2), the dynamic stabilities of the LID, ID and LD complexes as shown in Fig. 5.6 can be described by theoretical simulations. These dynamic stabilities, shown in Fig. 5.11, are determined by the superimposed effects of the physicochemical properties of the formulation buffer including the pH and ionic strength, the size distribution and concentration of the complexes, as well as factors such as temperature and local fluid flow environment. The experiments were carried out at a constant temperature of 25°C, and the local flow conditions were such that aggregation was determined solely by the physical laws governing Brownian motion of colloidal particles (Elimelich *et al.*, 1995; Wilson and French, 1978).

Table 5.1 Parameter values for results shown in Fig. 5.11. The interaction energies were calculated according to equations detailed in Section 4.2.1.

Parameter	*Value*	*Units (SI)*
Hamaker constant	5×10^{-21}	J
Relative dielectric constant	78.5	-
Absolute temperature	298	K
Valency of ions	1	-

The measured zeta potential values for the different systems shown in Fig. 5.6, along with the corresponding *z*-average size of the initial complexes, were used to estimate the theoretical total potential energies of interaction for LID, ID and LD complexes. A description of the simulation results for interaction potentials of another system (poly-L-lysine/DNA complexes) was described in Section 4.2.2 and in another publication (Lee *et al.*, 2001). Calculations based on the classical DLVO theory, detailed in Section 4.2.1, were used to describe the stability of the suspensions of LID, ID and LD complexes in Fig. 5.11. Additional parameters of interest for the interaction potentials shown in Fig. 5.11 are summarised in Table 5.1. Typical predictions, based on binary interaction energy calculations between complexes of equal size (Fig. 5.11), confirm the stability of LID complexes in distilled water. This is given by the "LID in H2O" barrier height, which is the maximum value of the DLVO interaction energy (> 100 *kT*). Such a large energy barrier is expected to produce extremely stable systems because the rate of particles possessing sufficient energy to surmount the energy barrier is very low. In contrast, the "LID in PBS" system, for example, has a very low energy barrier and is likely to be spontaneously aggregating. The instability of this system can be inferred from its low zeta potential (1 mV), which is due to the small surface charge and weak double layer repulsion of the particles.

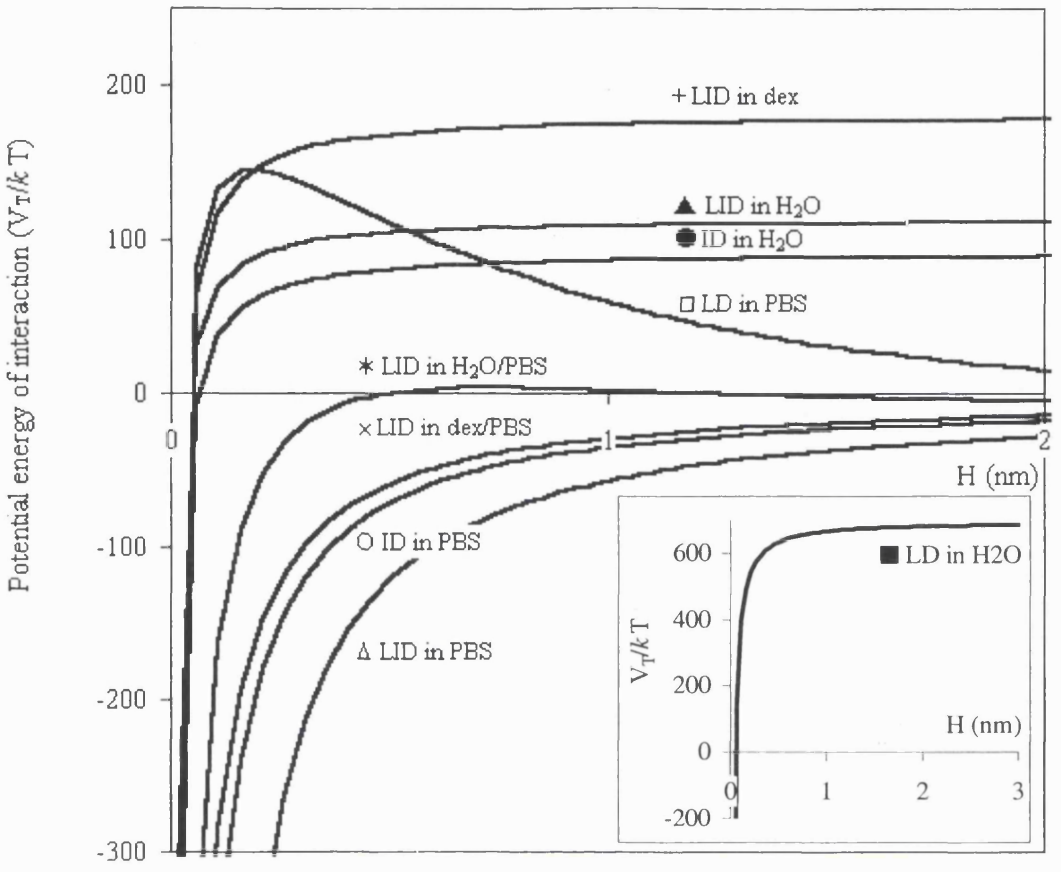

Figure 5.11 Interaction energy profiles (V_T in kT units) for some of the measured samples: LID, ID and LD complexes in distilled water (closed symbols), phosphate-buffered saline (PBS, open symbols), and 5% dextrose solution (dex, + and ×). The particle size and zeta potential were experimentally determined. Lipofectin/integrin-targeting peptide/DNA (LID): (▲) particle size = 100 nm, zeta potential = 50 mV; (Δ) 1100 nm, 1 mV; (+) 140 nm, 54 mV. Integrin-targeting peptide/DNA (ID): (●) 120 nm, 40 mV; (O) 800 nm, 6 mV. Lipofectin/DNA (LD): (■) 660 nm, -48 mV; ( ) 170 nm, -57 mV. LID in H2O/PBS: (✶) 550 nm, 19 mV. LID in 5% dextrose/PBS: (×) 635 nm, 4.4 mV. More details of the calculated total interaction potentials (V_T) can be found in Section 4.2.1.

The asymptotic form of the potential energy of interaction for two LID particles in a salt-free environment, such as in dextrose or water, as well as "ID in H2O", can be attributed to the high colloidal stability of these systems. In fact, when viewed in light of the possible interparticle distances between the complexes, a secondary minimum is evident, as shown for the "LID in H2O" system in Fig. 5.12.

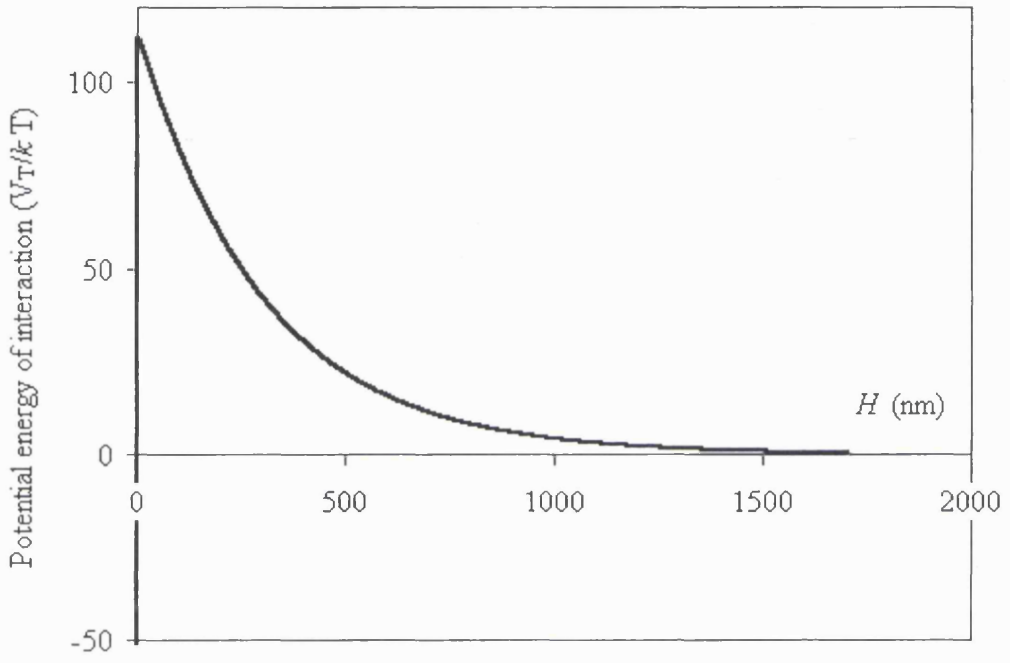

Figure 5.12 DLVO interaction potential for the stable suspension of LID in distilled water (particle size = 100 nm, zeta potential = 50 mV). This plot corresponds to "LID in H2O" (▲) seen in Fig. 5.11.

The application of the DLVO theory can be considered a useful tool when developing aqueous suspensions of LID complexes. The plots illustrate clearly the relative colloidal stabilities of the LID, ID and LD systems, which may, in some cases, reflect the transfection efficiencies of these systems.

CHAPTER 6

CONCLUSIONS AND RECOMMENDATIONS

This work presents a comprehensive experimental and theoretical investigation of the effects of various physicochemical parameters on the biophysical properties of DNA complexes. The characterisation of a novel gene delivery system with great potential for therapeutic use and its biological activity in an *in vitro* system is also described.

Poly-L-lysine (PLL) served as a model DNA condensing agent for investigating the reproducibility of complex preparation using a scaleable, controlled two-syringe pump flow system to mix the PLL and DNA solutions simultaneously. Mixing rates between 6 and 12 ml/min were found to be optimal for reproducibly producing PLL/calf thymus DNA complexes of ~100 nm. The PicoGreen assay for free DNA quantitation and zeta potential measurements were conducted on polyplex formulations at several charge ratios. Maximal DNA condensation by PLL occurred after a charge ratio (+/-) of 1, consistent with other workers. Polyplexes prepared by the two-syringe method were all very similar in size after short-term storage at 4°C. Aggregation was most pronounced for pipette mixed polyplexes at a charge ratio of 1, a result presumably of the heterogeneity

of the polyplex population. Relevant to the processing and delivery of complexes in pharmaceutical solutions, PLL of different molecular weights (2,900-99,500) protected a 29 kb plasmid from shear damage, even in the absence of salt and a gas-liquid interface.

Dynamic light scattering (DLS) experiments were conducted to monitor the aggregation kinetics of PLL/DNA complexes at various NaCl concentrations. Different DNA topology (linear calf thymus DNA, supercoiled pSVβ plasmid) of the polyplexes did not affect their aggregation kinetics. The rate of aggregation increased with ionic strength and pH. A rapid increase in polyplex size over time was observed upon addition of concentrated salt solution. For example, when aggregation was initiated at 100 mM NaCl, the average hydrodynamic diameter of PLL/pSVβ complexes increased from ~150 nm to ~1500 nm over 100 min. Hence, even if formulations of DNA complexes are stable in a single vial before administration, they may readily form aggregates as quickly as they are injected into patients. Stabilisation mechanisms for DNA complexes at physiological ionic strength remains a challenge that must be overcome for their development as pharmaceutical agents.

The stability of the PLL/DNA system was investigated theoretically using a new technique based on the well-known DLVO theory that describes interparticle interaction in a colloidal suspension. The simulations were useful for understanding the influence of variable input parameters (e.g. ionic strength, pH, reactant concentration, particle size, and temperature) on the material properties of PLL/calf thymus DNA complexes. The theoretical predictions were in excellent agreement with the experimental results. The simulations predicted an increase in the tendency towards aggregation under conditions of high pH, ionic strength and temperature, and increased particle size polydispersity. Assumptions made include the value for the Hamaker constant, a population of monodisperse spherical particles undergoing Brownian motion, and reduction of the many-body to a two-body problem. Future work on the model must address the stability factor, *W*, which is a measure of the effectiveness of collisions leading to aggregation. *W* allows the useful critical coagulation concentration and the effects of more than one

variable input parameter to be evaluated. The aggregation kinetics of DNA complexes under other mixing conditions besides Brownian diffusion, for example, transport under fluid flow, are also worth investigating. These can be computed using rate equations for the formation of aggregates, known as population balance equations.

The fractal approach to aggregate characterisation is another new method presented in this work for investigating the structures of gene delivery systems. Static light scattering experiments showed that the aggregating PLL/pSVβ complexes formed mass fractals with highly ordered internal structures whose fractal dimensions depended on the ionic strength. Plots of the angular dependence of the scattered intensity gave a mean fractal dimension of 2.22 for polyplexes at NaCl concentrations between 50 and 150 mM, indicating slow aggregation kinetics (RLCA), where interparticle aggregation occurs only after many collision attempts and results in the formation of compact aggregates with very little restructuring. A fractal dimension of 1.44 for polyplexes at 1 M NaCl suggested rapid aggregation kinetics (DLCA), where every collision is effective and results in tenuous structures with a substantial degree of restructuring. This is in agreement with the results of other workers for protein-coated polystyrene spheres (Molina-Bolívar *et al.*, 1998) and illite colloids (Derrendinger and Sposito, 2000). Determination of the fractal dimension from aggregation kinetics of the polyplexes was found to be unreliable, giving unrealistic fractal dimensions, a point worth further investigation.

In parallel with studies on the PLL/DNA system, the biophysical properties of Lipofectin/integrin-targeting peptide/DNA (LID) complexes were determined by similar analytical methods (DLS, zeta potential measurements and PicoGreen-based DNA quantitation) as well as an *in vitro* assay of biological activity. This is in contrast to earlier works on the LID vector system (Compton *et al.*, 2000; Hart *et al.*, 1998; Jenkins *et al.*, 2000), which had focused on biologically based assays. Important new results were obtained from this detailed analysis and summarised as follows. There are important

issues beyond the scope of this thesis that were not answered, and which deserve further investigation.

1. Under physiological ionic strength, LID complexes at 6.8 charge ratio rapidly aggregated to mean hydrodynamic diameters of 1500-3000 nm, while *in vitro* transfection activity in COS-7 cells decreased, inconsistent with findings elsewhere (Ross and Hui, 1999). A correlation between particle size and transfection activity was not observed for lipopolyplexes in Opti-MEM, presumably due to buffer constituents that affected delivery efficiency.
2. High DNA concentrations are necessary for *in vivo* transfections and clinical use. Under physiological ionic strength, increasing DNA concentration (150 μg/ml) yielded a corresponding increase in aggregation rate. In addition, LID complexes that were stable (100-150 nm) in both distilled water and 5% dextrose, the latter being an acceptable isotonic transfection buffer, also aggregated upon dilution with saline.
3. Increasing the concentration of peptide led to higher levels of transfection until a charge ratio of 3.0 to 4.0 was reached. Beyond this point, the increased peptide concentration decreased bioactivity. This inhibitory effect may be due to toxicity of the peptide and/or competition with uncomplexed peptide for binding to integrin receptors on the cell surface.
4. Albumin-induced aggregation of the LID complexes was observed at serum albumin concentrations of 5 mg/ml and greater. Surprisingly, zeta potential analysis showed no correlation between lipopolyplex surface charge and the tendency to interact with albumin.

The stabilisation and accurate biophysical characterisation of LID complexes provides particular challenges to overcome in order to gain significantly improved delivery properties and for their use as pharmaceuticals. Further work, including peptide chemistry and analysis of receptor-mediated targeted gene delivery, is needed to clarify the above results.

The simulation of interaction potentials and the measurement of fractal dimensions for the characterisation of DNA complexes are new simple methodologies that would be generally applicable to most synthetic gene delivery systems. The development of such methods are particularly relevant for theoretical interpretation of experimental formulation results, and offer the potential of complementing or even replacing measurements of biological activity.

CHAPTER 7

REFERENCES

Adami,R.C., W.T.Collard, A.A.Gupta, K.Y.Kwok, J.Bonadio, and K.G.Rice. 1998. Stability of peptide-condensed plasmid DNA formulations. *Journal of Pharmaceutical Sciences* 87:678-683.

Alberts,B., D.Bray, J.Lewis, M.Raff, K.Roberts, and J.D.Watson. 1994. Molecular biology of the cell. Garland Publishing, Inc., New York, NY.

Alton,E.W., M.Stern, R.Farley, A.Jaffe, S.L.Chadwick, J.Phillpis, J.Davies, S.N.Smith, J.Browning, M.G.Davies, M.E.Hodson, S.R.Durham, D.Li, P.K.Jeffery, M.Scallan, R.Balfour, S.J.Eastman, S.J.Cheng, A.E.Smith, D.Meeker, and D.M.Geddes. 1999. Cationic lipid-mediated CFTR gene transfer to the lungs and nose of patients with cystic fibrosis: A double-blind placebo-controlled trial. *Lancet* 353:947-954.

Amal,R., J.R.Coury, J.A.Raper, W.P.Walsh, and T.D.Waite. 1990. Structure and kinetics of aggregating colloidal hematite. *Colloids and Surfaces* 46:1-19.

Amal,R. and J.A.Raper. 1993. Measurement of aggregate fractal dimension using static light scattering. *Part. Part. Syst. Charact.* 10:239-245.

Anchordoquy,T.J., L.G.Girouard, J.F.Carpenter, and D.J.Kroll. 1998. Stability of lipid/DNA complexes during agitation and freeze-thawing. *Journal of Pharmaceutical Sciences* 87:1046-1051.

Anchordoquy,T.J. 1999b. Nonviral gene delivery systems, Part 1: Physical stability. *Biopharm* 12:42 (6 pages).

Anchordoquy,T.J. 1999a. Nonviral gene delivery systems, Part 2: Physical characterisation. *Biopharm* 12:46 (4 pages).

Anderson,W.F. 1998. Human gene therapy. *Nature* 392 (Suppl):25-30.

Andreadis,S., D.A.Brott, A.O.Fuller, and B.O.Palsson. 1997. Moloney murine leukemia virus-derived retroviral vectors decay intracellularly with a half-life in the range of 5.5 to 7.5 hours. *Journal of Virology* 71:7541-7548.

Andreadis,S.T., C.M.Roth, J.M.Le Doux, J.R.Morgan, and M.L.Yarmush. 1999. Large scale processing of recombinant retroviruses for gene therapy. *Biotechnol. Prog.* 15:1-11.

Aronsohn,A.I. and J.A.Hughes. 1998. Nuclear localization signal peptides enhance cationic liposome-mediated gene therapy. *Journal of Drug Targeting* 5:163-169.

Arscott,P.G., A.-Z.Li, and V.A.Bloomfield. 1990. Condensation of DNA by trivalent cations. 1. Effects of DNA length and topology on the size and shape of condensed particles. *Biopolymers* 30:619-630.

Ayazi Shamlou,P., S.Stavrinides, and N.J.Titchener-Hooker. 1996. Turbulent breakage of protein precipitates in mechanically stirred bioreactors. *Bioprocess Engineering* 14:237-243.

Bally,M.B., Y.-P.Zhang, F.M.P.Wong, S.Kong, E.Wasan, and D.L.Reimer. 1997. Lipid/DNA complexes as an intermediate in the preparation of articles for gene transfer: an alternative to cationic liposome/DNA aggregates. *Advanced Drug Delivery Reviews* 24:275-290.

Bassi,F.A., G.Arcovito, M.De Spirito, A.Mordente, and G.E.Martorana. 1995. Self-similarity properties of alpha-crystallin supramolecular aggregates. *Biophysical Journal* 69:2720-2727.

Baumann,C.B. and V.A.Bloomfield. 1995. Large-scale purification of plasmid DNA for biophysical and molecular biology studies. *BioTechniques* 19:884-890.

Bielinska,A.U., C.Chen, J.Johnson, and J.R.Baker, Jr. 1999. DNA complexing with polyamidoamine dendrimers: implications for transfection. *Bioconjugate Chemistry* 10:843-850.

Blagbrough,I.S., D.Al-Hadithi, and A.J.Geall. 2000. Cheno-, urso- and deoxycholic acid spermine conjugates: relative binding affinities for calf thymus DNA. *Tetrahedron* 56:3439-3447.

Bloomfield,V.A. 1991. Condensation of DNA by multivalent cations: Considerations on mechanism. *Biopolymers* 31:1471-1481.

Bloomfield,V.A. 1996. DNA condensation. *Current Opinion in Structural Biology* 6:334-341.

Bloomfield,V.A. 2000. Static and dynamic light scattering from aggregating particles. *Biopolymers* 54:168-172.

Bloomfield,V.A. and D.C.Rau. 1980. Polyelectrolyte effects in DNA condensation by polyamines. *Biophysical Chemistry* 11:339-343.

Bohr,H., A.Kühle, A.H.Sørensen, and J.Bohr. 1997. Hierarchical organization in aggregates of protein molecules. *Zeitschrift Für Physik D* 40:513-515.

Boulikas,T. 1998. Nucleocytoplasmic trafficking: implications for the nuclear import of plasmid DNA during gene therapy. *Gene Ther. Mol. Biol.* 1:713-740.

Boussif,O., F.Lezoualc'h, M.A.Zanta, M.D.Mergny, D.Scherman, B.Demeneix, and J.-P.Behr. 1995. A versatile vector for gene and oligonucleotide transfer into cells in culture and *in vivo*: polyethyleneimine. *Proc. Natl. Acad. Sci. USA* 92:7297-7301.

Braas,G., P.F.Searle, N.K.H.Slater, and A.Lyddiatt. 1996. Strategies for the isolation and purification of retroviral vectors for gene therapy. *Bioseparation* 6:211-228.

Branden,L., A.Mohamed, and C.Smith. 1999. A peptide nucleic acid–nuclear localization signal fusion that mediates nuclear transport of DNA. *Nature Biotechnology* 17:784-787.

Brunner,R., S.Gall, W.Wilke, and M.Zrinyi. 1997. A dynamic light scattering study on aggregation of rodlike colloidal particles. *Physica A* 239:477-485.

Butt,H.-P. 1991. Measuring electrostatic, van der Waals, and hydration forces in electrolyte solutions with an atomic force microscope. *Biophysical Journal* 60:1438-1444.

Capan,Y., B.Y.Woo, S.Gebrekidan, S.Ahmed, and P.P.DeLuca. 1999. Stability of poly(L-lysine)-complexed plasmid DNA during mechanical stress and DNase I treatment. *Pharmaceutical Development and Technology* 4:491-498.

Caplen,N.J., E.W.F.W.Alton, P.G.Middleton, J.R.Dorin, B.J.Stevenson, X.Gao, S.J.Durham, P.K.Jeffrey, M.E.Hodson, C.Coutelle, L.Huang, D.J.Porteous, R.Williamson, and D.M.Geddes. 1995. Liposome-mediated CFTR *gene* transfer to the nasal epithelium of patients with cystic fibrosis. *Nature Medicine* 1:39-46.

Carter,B.J. 2000. Gene therapy as drug development. *Molecular Therapy* 1:211-212.

Cavazzana-Calvo,M., S.Hacein-Bey, G.de Saint Basile, F.Gross, E.Yvon, P.Nusbaum, F.Selz, C.Hue, S.Certain, J.-L.Casanova, P.Bousso, F.Le Deist, and A.Fischer. 2000. Gene therapy of human severe combined immunodeficiency (SCID)-X1 disease. *Science* 288:669-672.

Cherng,J.-Y., N.M.E.Schuurmans-Niewwenbroek, W.Jiskoot, H.Talsma, N.J.Zuidam, W.E.Hennink, and D.J.A.Crommelin. 1999. Effect of DNA topology on the transfection efficiency of poly((2-dimethylamino)ethyl methacrylate)-plasmid complexes. *Journal of Controlled Release* 60:343-353.

Cherng,J.-Y., P.Van der Wetering, H.Talsma, D.J.A.Crommelin, and W.E.Hennink. 1996. Effect of size and serum proteins on transfection efficiency of poly(2-dimethylamino)ethyl methacrylate-plasmid nanoparticles. *Pharmaceutical Research* 13:1038-1042.

Chesnoy,S. and L.Huang. 2000. Structure and function of lipid-DNA complexes for gene delivery. *Annu. Rev. Biophys. Biomol. Struct.* 29:27-47.

Choi,Y.H., F.Liu, J.S.Choi, S.W.Kim, and J.S.Park. 1999. Characterization of a targeted gene carrier, lactose- polethylene glycol-grafted poly-L-lysine, and its complex with plasmid DNA. *Human Gene Therapy* 10:2657-2665.

Chonn,A. and P.R.Cullis. 1998. Recent advances in liposome technologies and their applications for systemic gene delivery. *Advanced Drug Delivery Reviews* 30:73-83.

Cohen,J. 2001. AIDS research: Merck reemerges with a bold AIDS vaccine effort. *Science* 292:24-25.

Colin,M., R.P.Harbottle, A.Knight, M.Kornprobst, R.G.Cooper, A.D.Miller, G.Trugnan, J.Capeau, C.Coutelle, and M.C.Brahimi-Horn. 1998. Liposomes enhance delivery and expression of an RGD-oligolysine gene transfer vector in human tracheal cells. *Gene Therapy* 5:1498.

Colin,M., M.Maurice, G.Trugnan, M.Kornprobst, R.P.Harbottle, A.Knight, R.G.Cooper, A.Miller, J.Capeau, C.Coutelle, and M.C.Brahimi-Horn. 2000. Cell delivery, intracellular trafficking and expression of an integrin-mediated gene transfer vector in tracheal epithelial cells. *Gene Therapy* 7:139-152.

Colton,R.J., D.R.Baselt, Y.F.Dufrêne, J.-B.D.Green, and G.U.Lee. 1997. Scannning probe microsopy. *Current Opinion in Chemical Biology* 1:370-377.

Compton,S.H., S.Mecklenbeck, J.E.Mejía, S.L.Hart, M.Rice, R.Cervini, Y.Barrandon, Z.Larrin, E.R.Levy, L.Bruckner-Tuderman, and A.Hovnanian. 2000. Stable

integration of large (>100kb) PAC constructs in HaCaT keratinocytes using an integrin-targeting peptide delivery system. *Gene Therapy* 7:1600-1605.

Creighton,T.E. 1993. Proteins: structure and molecular properties. W. H. Freeman and Company, New York.

Crook,K., G.McLachlan, B.J.Stevenson, and D.J.Porteous. 1996. Plasmid DNA molecules complexed with cationic liposomes are protected from degradation by nucleases and shearing by aerosolisation. *Gene Therapy* 3:834-839.

Crystal,R.G. 1995. Transfer of genes to humans: early lessons and obstacles to success. *Science* 270:404-410.

Dash,P.R., M.L.Read, L.B.Barrett, M.A.Wolfert, and L.W.Seymour. 1999. Factors affecting blood clearance and in vivo distribution of polyelectrolyte complexes for gene delivery. *Gene Therapy* 6:643-650.

Dash,P.R., M.L.Read, K.D.Fisher, K.A.Howard, M.Wolfert, A.Oupiky, V.Subr, J.Strohalm, K.Ulbrich, and L.W.Seymour. 2000. Decreased binding to proteins and cells of polymeric gene delivery vectors surface modified with a multivalent hydrophilic polymer and retargeting through attachment of transferrin. *Journal of Biological Chemistry* 275:3793-3802.

Davis,H.L. 1999. Gene-based vaccines. *In* Advanced gene delivery: from concepts to pharmaceutical products. A.Rolland, editor. Harwood Academic Publishers, Amsterdam. 213-33.

De Smedt,S.C., J.Demeester, and W.E.Hennink. 2000. Cationic polymer based gene delivery systems. *Pharmaceutical Research* 17:113-126.

Deng,H. and V.A.Bloomfield. 1999. Structural effects of cobalt-amine compounds on DNA condensation. *Biophysical Journal* 77:1556-1561.

Derrendinger,L. and G.Sposito. 2000. Flocculation kinetics and cluster morphology in illite/NaCl suspensions. *Journal of Colloid and Interface Science* 222:1-11.

Deshmukh,H.M. and L.Huang. 1997. Liposome and polylysine mediated gene transfer. *New Journal of Chemistry* 21:113-124.

Donnelly,J.J., J.B.Ulmer, J.W.Shiver, and M.A.Liu. 1997. DNA vaccines. *Annu. Rev. Immunol.* 15:617-648.

Duncan,R., N.Malik, S.Richardson, and P.Ferruti. 1998. Polymer conjugates for anti-cancer agent and DNA delivery. *Proceedings of the American Chemical Society* 39:180.

Dunlap,D., A.Maggi, M.R.Soria, and L.Monaco. 1997. Nanoscopic structure of DNA condensed for gene delivery. *Nucleic Acids Research* 25:3095-3101.

Dyer,M.R. and P.L.Herrling. 2000. Progress and potential for gene-based medicines. *Molecular Therapy* 1:213-224.

Eastman,S.J., C.Siegel, J.Tousignant, A.E.Smith, S.H.Cheng, and R.K.Scheule. 1997. Biophysical characterization of cationic lipid:DNA complexes. *Biochim. Biophys. Acta* 1325:41-62.

Elimelich,M., J.Gregory, X.Jia, and R.A.Williams. 1995. Particle deposition and aggregation: measurement, modelling and simulation. Butterworth-Heinemann Ltd, Oxford.

Estruch,E.J., S.L.Hart, C.Kinnon, and B.G.Winchester. 2001. Non-viral, integrin-mediated gene transfer into fibroblasts from patients with lysosomal storage diseases. *Journal of Gene Medicine* 3:488-497.

Felgner,P.L., Y.Barenholz, J.P.Behr, S.H.Cheng, P.Cullis, L.Huang, J.A.Jessee, L.Seymour, F.Szoka, A.R.Thierry, E.Wagner, and G.Wu. 1997. Nomenclature for synthetic gene delivery systems. *Human Gene Therapy* 8:511-512.

Felgner,P.L., O.Zelphati, and X.Liang. 1999. Advances in synthetic gene-delivery system technology. *In* The development of human gene therapy. T.Friedmann, editor. Cold Spring Harbor Laboratory Press, NY. 241-60.

Ferrari,M.E., C.M.Nguyen, O.Zelphati, Y.Tsai, and P.L.Felgner. 1998. Analytical methods for the characterization of cationic lipid-nucleic acid complexes. *Human Gene Therapy* 9:341-351.

Ferrari,M.E., D.Rusalov, J.Enas, and C.J.Wheeler. 2001. Trends in lipoplex physical properties dependent on cationic lipid structure, vehicle and complexation procedure do not correlate with biological activity. *Nucleic Acids Research* 29:1539-1548.

Friedmann,T. and R.Roblin. 1972. Gene therapy for human genetic disease? *Science* 175:949-955.

Fry,J.W. and K.J.Wood. 1999. Gene therapy: potential applications in clinical transplantation. *Expert Reviews in Molecular Medicine.*

Gamon,B.L., J.W.Virden, and J.C.Berg. 1989. The aggregation kinetics of an electrostatically stabilized dipalmitoyl phophatidylcholine vesicle system. *Journal of Colloid and Interface Science* 132:125-138.

Gautam,A., C.L.Densmore, B.Xu, and J.Clifford Waldrep. 2000. Enhanced gene expression in mouse lung after PEI–DNA aerosol delivery. *Molecular Therapy* 2:63-70.

Geall,A., M.A.W.Eaton, T.Baker, C.Catterall, and I.S.Blagbrough. 1999. The regiochemical distribution of positive charges along cholesterol polyamine carbamates plays significant roles in modulating DNA binding affinity and lipofection. *FEBS* 459:337-342.

Geall,A.J. and I.S.Blagbrough. 2000. Rapid and sensitive ethidium bromide fluorescence quenching assay of polyamine conjugate-DNA interactions for the analysis of lipoplex formation in gene therapy. *Journal of Pharmaceutical and Biomedical Analysis* 22:849-859.

Gill,D.R., K.W.Southern, K.A.Mofford, T.Seddon, L.Huang, F.Sorgi, A.Thomson, L.J.MacVinish, R.Ratcliff, D.Bilton, D.J.Lane, J.M.Littlewood, A.K.Webb, P.G.Middleton, W.H.Colledge, A.W.Cuthbert, M.J.Evans, C.F.Higgins, and S.C.Hyde. 1997. A placebo controlled study of liposome-mediated gene transfer to the nasal epithelium of patients with cystic fibrosis. *Gene Therapy* 4:199-209.

Godbey,W.T., M.A.Barry, P.Saggau, K.K.Wu, and A.G.Mikos. 2000. Poly(ethylenimine)-mediated transfection: a new paradigm for gene delivery. *J of Biomed Mater Res* 51:321-328.

Godbey,W.T. and A.G.Mikos. 2001. Recent progress in gene delivery using non-viral transfer complexes. *Journal of Controlled Release* 72:115-125.

Godbey,W.T., K.K.Wu, and A.G.Mikos. 1999. Tracking the intracellular delivery path of poly(ethylenimine)/DNA complexes for gene delivery. *Proc. Natl. Acad. Sci. USA* 96:5177-5181.

Golan,R., L.I.Pietrasanta, W.Hsieh, and H.G.Hansma. 1999. DNA toroids: stages in condensation. *Biochemistry* 38:14069-14076.

Gosule,L.C. and J.A.Schellman. 1976. Compact form of DNA induced by spermidine. *Nature* 259:333-335.

Goula,D., C.Benoist, S.Mantero, G.Merlo, G.Levi, and B.A.Demeneix. 1998. Polyethyleneimine-based intravenous delivery of transgenes to mouse lung. *Gene Therapy* 5:1291-1295.

Gregoriadis,G., R.Saffie, and J.B.de Souza. 1997. Liposome-mediated DNA vaccination. *FEBS Letters* 402:107-110.

Gregory,J. 1993. Stability and flocculation of suspensions. *In* Processing of solid-liquid suspensions. P.Ayazi Shamlou, editor. Butterworth-Heinemann Ltd, Oxford. 59-92.

Grisham,J. 2000. Changes to RAC. *Nature Biotechnology* 18:811.

Guan,J., T.D.Waite, and R.Amal. 1998. Rapid structure characterisation of bacterial aggregates. *Environmental Science & Technology* 32:3735-3742.

Guy,J., D.Drabek, and M.Antoniou. 1995. Delivery of DNA into mammalian cells by receptor-mediated endocytosis and gene therapy. *Mol. Biotechnol.* 3:237-248.

Hafez,I.M., S.Ansell, and P.R.Cullis. 2000. Tunable pH-sensitive liposomes composed of mixtures of cationic and anionic lipids. *Biophysical Journal* 79:1438-1446.

Hagiwara,T., H.Kumagai, and K.Nakamura. 1996. Fractal analysis of aggregates formed by heating dilute BSA solutions using light scattering methods. *Biosci Biotechnol Biochem* 60:1757-1763.

Han,S.-O., R.I.Mahato, Y.K.Sung, and S.W.Kim. 2000. Development of biomaterials for gene therapy. *Molecular Therapy* 2:302-317.

Hansma,H.G., M.Bezanilla, F.Zenhausern, M.Adrian, and R.L.Sinsheimer. 1993. Atomic force microscopy of DNA in aqueous solutions. *Nucleic Acids Research* 21:505-512.

Hansma,H.G., R.Golan, W.Hsieh, C.P.Lollo, P.Mullen-Ley, and D.Kwoh. 1998. DNA condensation for gene therapy as monitored by atomic force microscopy. *Nucleic Acids Research* 26:2481-2487s.

Harries,D., S.May, W.M.Gelbart, and A.Ben-Shaul. 198. Structure, stability, and thermodynamics of lamellar DNA-lipid complexes. *Biophysical Journal* 159:159-173.

Hart,S. 1999. Use of adhesion molecules for gene delivery. *Experimental Nephrology* 7:193-199.

Hart,S.L. 2000. Synthetic vectors for gene therapy. *Exp. Opin. Ther. Patents* 10:199-208.

Hart,S.L., C.V.Arancibia-Cárcamo, M.A.Wolfert, C.Mailhos, N.J.O'Reilly, R.R.Ali, C.Coutelle, D.F.P.Larkin, R.J.Levinsky, L.W.Seymour, A.J.Thrasher, and C.Kinnon. 1998. Lipid-mediated enhancement of transfection by a nonviral integrin-targeting vector. *Human Gene Therapy* 9:575-585.

Healy,T.W., A.Homola, and R.O.James. 1978. Coagulation of amphoteric latex colloids: reversibility and specific ion effects. *Faraday Disc. Chem. Soc.* 65:156-163.

Heinz,W.F. and J.H.Hoh. 1999. Spatially resolved force spectroscopy of biological surfaces using the atomic force microscope. *Trends in Biotechnology* 17:143-150.

Highfield, R. Gene trial frees babies from sterile 'bubbles'. The Daily Telegraph, 7. 4-28-2000. London. Ref Type: Newspaper

Hogg,R., T.W.Healy, and D.W.Fuerstenau. 1966. Mutual coagulation of colloidal dispersions. *Trans. Faraday Soc.* 62:1638-1651.

Hong,K., W.Zheng, A.Baker, and D.Papahadjopoulos. 1997. Stabilization of cationic liposome-plasmid DNA complexes by polyamines and poly(ethylene glycol)-phospholipid conjugates for efficient in vivo gene delivery. *FEBS Letters* 400:233-237.

Hope,M.J., B.Mui, S.Ansell, and Q.F.Ahkong. 1998. Cationic lipids, phosphatidylethanolamine and the intracellular delivery of polymeric, nucleic acid-based drugs (Review). *Molecular Membrane Biology* 15:1-14.

Horton,M.A. 1996. Cell adhesion receptors and their ligands as therapeutic targets. *In* Adhesion receptors as therapeutic targets. M.A.Horton, editor. CRC Press, Boca Raton, FL. London. 1-8.

Horton,M.A. 1999. Arg-Gly-Asp (RGD) peptides and peptidomimetics as therapeutics: relevance for renal diseases. *Experimental Nephrology* 7:178-184.

Huebner,S., B.J.Battersby, R.Grimm, and G.Cevc. 1999. Lipid-DNA complex formation: reorganization and rupture of lipid vesicles in the presence of DNA as observed by cryoelectron microscopy. *Biophysical Journal* 76:3158-3166.

Hunter,R.J. 1981. Zeta potential in colloid science. Academic Press.

Hunter,R.J. 1987. Foundations of colloid science. Oxford University Press, New York.

Hutchins,B. 2000. Characterization of plasmids and formulations for non-viral gene therapy. *Current Opinion in Molecular Therapeutics* 2:131-135.

Huwyler,J., D.Wu, and W.M.Pardridge. 1996. Brain drug delivery of small molecules using immunoliposomes. *Proc. Natl. Acad. Sci. USA* 93:14164-14169.

Hynes,R.O. 1987. Integrins: a family of cell surface receptors. *Cell* 48:549-554.

Hynes,R.O. 1992. Integrins: versatility, modulation, and signaling in cell adhesion. *Cell* 69:11-25.

Israelachvili,J.N. 1992. Intermolecular and surface forces. Academic Press Ltd, London.

Jenkins,R.G., S.E.Herrick, Q.-H.Meng, C.Kinnon, G.J.Laurent, R.J.McAnulty, and S.L.Hart. 2000. An integrin-targeted, non-viral vector for pulmonary gene therapy. *Gene Therapy* 7:393-400.

Jenkins,R.G., Q.-H.Meng, R.-H.Hodges, L.K.Lee, G.J.Laurent, D.Willis, P.Ayazi Shamlou, R.J.McAnulty, and S.L.Hart. 2001. Formation of LID vector complexes in hypotonic solution alters physico-chemical properties and enhances pulmonary gene expression *in vivo*. *Human Gene Therapy* Submitted for publication (see Appendix F – Publications)

Jones,N.A., I.R.C.Hill, S.Stolnik, F.Bignotti, S.S.Davies, and M.C.Garnett. 2000. Polymer chemical structure is a key determinant of physicochemical and colloidal properties of polymer-DNA complexes for gene delivery. *Biochim. Biophys. Acta* 1517:1-18.

Kabanov,A.V. 1999. Taking polycation gene delivery systems from *in vitro* to *in vivo*. *PSST* 2:365-372.

Kay,M.A., C.S.Manno, M.V.Ragni, P.J.Larson, L.B.Couto, A.McClelland, B.Glader, A.J.Chew, S.J.Tai, R.W.Herzog, V.Arruda, F.Johnson, C.Scallan, E.Skarsgard, A.W.Flake, and K.A.High. 2000. Evidence for gene transfer and expression of factor IX in haemophilia B patients treated with an AAV vector. *Nature Genetics* 24:257-261.

Kennedy,M.T., E.V.Pozharski, V.A.Rakhmanova, and R.C.MacDonald. 2000. Factors governing the assembly of cationic phospholipid-DNA complexes. *Biophysical Journal* 78:1620-1633.

Kerker,M. 1969. The scattering of light and other electromagnetic radiation. Academic Press, New York.

Killmann,E. and P.Sapuntzjis. 1994. Dynamic light scattering of polystyrene latex and silica with adsorbed poly(ethylene oxide) layers - influence of ionic strength and coverage. *Colloids and Surfaces A: Physicochemical and Engineering Aspects* 86:229-238.

Kim,J.-S., A.Maruyama, T.Akaike, and S.W.Kim. 1998. Terplex DNA delivery system as a gene carrier. *Pharmaceutical Research* 15:116-121.

Kircheis,R., S.Schüller, S.Brunner, M.Ogris, K.-H.Heider, W.Zauner, and E.Wagner. 1999. Polycation-based DNA complexes for tumor-targeted gene delivery in vivo. *Journal of Gene Medicine* 1:11-120.

Koltover,I., T.Salditt, and C.R.Safinaya. 1999. Phase diagram, stability, and overcharging of lamellar cationic lipid–DNA self-assembled complexes. *Biophysical Journal* 77:915-924.

Koping-Hoggard,M., I.Tubulekas, H.Guan, K.Edwards, M.Nilsson, K.M.Varum, and P.Artursson. 2001. Chitosan as a nonviral gene delivery system. Structure-property relationships and characteristics compared with polyethylenimine in vitro and after lung administration in vivo. *Gene Therapy* 8:1108-1121.

Kreiss,P., B.Cameron, R.Rangara, P.Mailhe, O.Aguerre-Charriol, M.Airiau, D.Scherman, J.Crouzet, and B.Pitard. 1999. Plasmid DNA size does not affect the physicochemical properties of lipoplexes but modulates gene transfer efficiency. *Nucleic Acids Research* 27:3792-2798.

Kukowska-Latallo,J.F., A.U.Bielinska, J.Johnson, R.Spindler, D.A.Tomalia, and J.R.Baker, Jr. 1996. Efficient transfer of genetic material into mammalian cells using Starburst polyamidoamine dendrimers. *Proc. Natl. Acad. Sci. USA* 93:4897-4902.

Kwoh,D.Y., C.C.Coffin, C.P.Lollo, J.Jovenal, M.G.Banaszczyk, P.Mullen, A.Phillips, A.Amini, J.Fabrycki, R.M.Bartholomew, S.W.Brostoff, and D.J.Carlo. 1999. Stabilization of poly-L-lysine/DNA polyplexes for in vivo gene delivery to the liver. *Biochim. Biophys. Acta* 1444:171-190.

Kyriakidis,A.S., S.G.Yiantsios, and A.J.Karabelas. 1997. A study of colloidal particle brownian aggregation by light scattering techniques. *Journal of Colloid and Interface Science* 195:299-306.

Laemmli,U.K. 1975. Characterization of DNA condensates induced by poly(ethylene oxide) and polylysine. *Proc. Natl. Acad. Sci. USA* 72:4288-4292.

Lai,E. and J.H.van Zanten. 2001. Monitoring DNA/poly-L-lysine polyplex formation with time-resolved multiangle laser light scattering. *Biophysical Journal* 80:864-873.

Lai,W.C. and M.Bennett. 1998. DNA vaccines. *Critical Reviews in Immunology* 18:449-484.

Langer,R. 1998. Drug delivery and targeting. *Nature* 392 (Suppl):5-10.

Laquerre,S., D.B.Anderson, D.B.Stolz, and J.C.Glorioso. 1998. Recombinant herpes simplex virus type 1 engineered for targeted binding to erythropoietin receptor-bearing cells. *Journal of Virology* 72:9683-9697.

Lasic,D.D. and N.S.Templeton. 2000. Bioorganic colloids: macromolecules, DNA, self-assembled particles, and their complexes. *In* Gene therapy: therapeutic mechanisms and strategies. N.S.Templeton and D.D.Lasic, editors. Marcel-Dekker, Inc., NY. 241-66.

Le Bon,C., T.Nicolai, and D.Durand. 1999. Growth and structure of aggregates of heat-denatured β-lactoglobulin. *International Journal of Food Science and Technology* 34:451-465.

Ledley,F.D. 1996. Pharmaceutical approach to somatic gene therapy. *Pharmaceutical Research* 13:15595-15613.

Lee,K.Y., I.C.Kwon, Y.-H.Kim, W.H.Jo, and S.Y.Jeong. 1998. Preparation of chitosan self-aggregates as a gene delivery system. *Journal of Controlled Release* 51:213-220.

Lee,L.K., C.N.Mount, and P.Ayazi Shamlou. 2001. Characterisation of the physical stability of colloidal polycation-DNA complexes for gene therapy and DNA vaccines. *Chemical Engineering Science* 56:3163-3172. See also Appendix F – Publications.

Lee,R.J. and L.Huang. 1996. Folate-targeted, anionic liposome-entrapped polylysine-condensed DNA for tumor cell-specific gene transfer. *Journal of Biological Chemistry* 271:8481-8487.

Lee,R.J. and L.Huang. 1997. Lipidic vector systems for gene transfer. *Critical Reviews in Therapeutic Drug Carrier Systems* 14:173-206.

Leitner,W.W., H.Ying, and N.P.Restifo. 2000. DNA and RNA-based vaccines: principles, progress and prospects. *Vaccine* 18:765-777.

Levy,E.R., R.O'Kennedy, M.Y.Lo-Yim, and P.Ayazi Shamlou. 2000b. Quantitation of supercoiled circular content in plasmid DNA solutions using a fluorescence-based method. *Nucleic Acids Research* 28:e57.

Levy,M.S., L.A.S.Ciccolini, S.S.S.Yim, J.T.Tsai, N.Titchener-Hooker, P.Ayazi Shamlou, and P.Dunnill. 1999b. The effects of material properties and fluid flow intensity on plasmid DNA recovery during cell lysis. *Chemical Engineering Science* 54:3171-3178.

Levy,M.S., I.J.Collins, J.T.Tsai, P.Ayazi Shamlou, J.M.Ward, and P.Dunnill. 2000c. Removal of contaminant nucleic acids by nitrocellulose filtration during pharmaceutical-grade plasmid DNA processing. *Journal of Biotechnology* 76:197-205.

Levy,M.S., I.J.Collins, S.S.Yim, J.M.Ward, N.Titchener-Hooker, P.Ayazi Shamlou, and P.Dunnill. 1999a. Effect of shear on plasmid DNA in solution. *Bioprocess Engineering* 20:7-13.

Levy,M.S., R.D.O'Kennedy, P.Ayazi-Shamlou, and P.Dunnill. 2000a. Biochemical engineering approaches to the challenges of producing pure plasmid DNA. *Trends in Biotechnology* 18:296-305.

Lewis,R.N.A.H. and R.N.McElhaney. 2000. Surface charge markedly attenuates the nonlamellar phase-forming propensities of lipid bilayer membranes: calorimetric and 31 P-nuclear magnetic resonance studies of mixtures of cationic, anionic, and zwitterionic lipids. *Biophysical Journal* 79:1455-1464.

Li,S. and L.Huang. 1997. In vivo gene transfer via intravenous administration of cationic lipid-protamine-DNA (LPD) complexes. *Gene Therapy* 4:891-900.

Li,S., W.-C.Tseng, D.Beer Stolz, S.-P.Wu, S.C.Watkins, and L.Huang. 1999. Dynamic changes in the characteristics of cationic lipidic vectors after exposure to mouse serum: implications for intravenous lipofection. *Gene Therapy* 6:585-594.

Liang,K.W., E.P.Hoffman, and L.Huang. 2000. Targeted delivery of plasmid DNA to myogenic cells via transferrin-conjugated peptide nucleic acid. *Molecular Therapy* 1:236-243.

Lin,M.Y., H.M.Lindsay, D.A.Weitz, R.C.Ball, R.Klein, and P.Meakin. 1989. Universality of fractal aggregates as probed by light scattering. *Proceedings of the Royal Society of London A* 423:71-87.

Linden,R.M. and S.L.Woo. 1999. AAVant-garde gene therapy. *Nature Medicine* 5:21-22.

Liu,Y., L.C.Mounkes, H.D.Liggitt, C.S.Brown, I.Solodin, T.D.Heath, and R.J.Debs. 2001. Factors influencing the efficiency of cationic liposome-mediated intravenous gene delivery. *Nature Biotechnology* 15:167-173.

Lockie,T., H.Herweijer, G.Zhang, V.Budker, and J.A.Wolff. 1999. Intravascular delivery of naked plasmid DNA. *In* Advanced gene delivery: from concepts to pharmaceutical products. A.Rolland, editor. Harwood Academic Publishers, Amsterdam. 236-51.

Lu,Y., J.Carraher, J.Armstrong, J.Lerner, W.P.Rogers, and M.S.Steiner. 1999. Delivery of adenoviral vectors to the prostate for gene therapy. *Cancer Gene Therapy* 6:64-72.

Luo,D. and W.M.Saltzman. 2000. Synthetic DNA delivery systems. *Nature Biotechnology* 18:33-37.

Lück,M., B.-R.Paulke, W.Schröder, and R.H.Müller. 1998. Analysis of plasma protein adsorption on polymeric nanoparticles with different surface characteristics. *J Biomed Mater Res* 39:478.

Lyddiatt,A. and D.A.O'Sullivan. 1998. Biochemical recovery and purification of gene therapy vectors. *Current Opinion in Biotechnology* 9:177-185.

Lyubchenko,Y.L. and L.S.Shlyakhtenko. 1997. Visualisation of supercoiled DNA with atomic force microscopy. *Proc. Natl. Acad. Sci. USA* 94:496-501.

Ma,C. and V.A.Bloomfield. 1994. Condensation of supercoiled DNA induced by MnCl2. *Biophysical Journal* 67:1678-1681.

MacDonald,R.C., G.W.Ashley, M.M.Shida, V.A.Rakhmanova, Y.S.Tarahovsky, D.P.Pantazatos, M.T.Kennedy, E.V.Pozharski, K.A.Baker, R.D.Jones, H.S.Rosenzweig, K.L.Choi, R.Qiu, and T.J.McIntosh. 1999. Physical and biological properties of cationic triesters of phosphatidylcholine. *Biophysical Journal* 77:2612-2629.

Magazu,S., G.Maisano, and F.Mallamace. 1989. Growth of fractal aggregates in water solutions of macromolecules by light scattering. *Physical Review A* 39:4195-4200.

Mahato,R.I. 1999. Non-viral peptide-based approaches to gene delivery. *Journal of Drug Targeting* 7:249-268.

Mahato,R.I., O.D.Monera, L.C.Smith, and A.Rolland. 1999. Peptide-based gene delivery. *Current Opinion in Molecular Therapeutics* 1:226-243.

Mahvi,D.M., M.J.Sheehy, and N.Yang. 1997. DNA vaccines: a gene gun approach. *Immunol. Cell Biol.* 75:456-460.

Marquet,M., N.A.Horn, and J.A.Meek. 1995. Process development for the manufacture of plasmid DNA vectors for use in gene therapy. *Biopharm-Manuf.* 8:26-36.

Marquet,M., N.A.Horn, and J.A.Meek. 1997a. Characterization of plasmid DNA vectors for use in human gene therapy, Part 1. *Biopharm-Manuf.* 10:42-45.

Marquet,M., N.A.Horn, and J.A.Meek. 1997b. Characterization of plasmid DNA vectors for use in human gene therapy, Part 2. *Biopharm-Manuf.* 10:40-50.

Maruyama,K., N.Takahashi, T.Tagawa, K.Nagaike, and M.Iwatsu. 1997. Immunoliposomes bearing polyethyleneglycol-coupled Fab' fragment show prolonged circulation time and high extravasation into targeted solid tumors in vivo. *FEBS* 413:177-180.

May,S., D.Harries, and A.Ben-Shaul. 2000. The phase behavior of cationic lipid–DNA complexes. *Biophysical Journal* 78:1681-1697.

McKenzie,D.L., W.T.Collard, and K.G.Rice. 1999. Comparative gene transfer efficiency of low molecular weight polylysine DNA-condensing peptides. *Journal of Peptide Research* 54:311-318.

Meakin,P. 1988. Fractal aggregates. *Advances in Colloid and Interface Science* 28:249-331.

Meyer,O., D.Kirpotin, K.Hong, B.Sternberg, J.W.Park, M.C.Woodle, and D.Papahadjopoulos. 1998. Cationic liposomes coated with polyethylene glycol as carriers for oligonucleotides. *Journal of Biological Chemistry* 273:15621-15627.

Middaugh,C.R., R.K.Evans, D.L.Montgomery, and D.R.Casimiro. 1998. Analysis of plasmid DNA from a pharmaceutical perspective. *Journal of Pharmaceutical Sciences* 87:130-146.

Molina-Bolívar,J.A., F.Galisteo-González, and R.Hidalgo-Álvarez. 1998. Cluster morphology of protein-coated polymer colloids. *Journal of Colloid and Interface Science* 298:445-454.

Molina-Bolívar,J.A., F.Galisteo-González, and R.Hidalgo-Álvarez. 1999. The role played by hydration forces in the stability of protein-coated particles: non-classical DLVO behaviour. *Colloids and Surfaces B: Biointerfaces* 14:3-17.

Mor,G. 1998. Plasmid DNA: a new era in vaccinology. *Biochemical Pharmacology* 55:1151-1153.

Morris,M.C., L.Chaloin, J.Méry, F.Heitz, and G.Divita. 1999. A novel potent strategy for gene delivery using a single peptide vector as carrier. *Nucleic Acids Research* 27:3510-3517.

Mountain,A. 2000. Gene therapy: the first decade. *Trends in Biotechnology* 18:119-128.

Muller,R.H., S.S.Davies, L.Illum, and E.Mak. 1986. Particle charge and surface hydrophobicity of colloidal drug carriers. *In* Targeting of Drugs with Synthetic Systems. G.Gregoriadis, J.Senior, and G.Poste, editors. Plenum Press, New York. 239-63.

Mumper,R.J. and S.L.Klakamp. 1999. Polymeric gene delivery systems for *in vivo* gene therapy. *In* Advanced gene delivery: from concepts to pharmaceutical products. A.Rolland, editor. Harwood Academic Publishers, Amsterdam. 143-73.

Murphy,E.A., A.J.Waring, J.C.Murphy, R.C.Wilson, and K.J.Longmuir. 2001. Development of an effetive gene delivery system: a study of complexes composed

of a peptide-based amphiphilic DNA compaction agent and phospholipid. *Nucleic Acids Research* 29:3694-3704.

Muschol,M. and F.Rosenberger. 1995. Interactions in undersaturated and supersaturated lysozyme solutions: static and dynamic light scattering results. *Journal of Chemical Physics* 103:10424-10432.

Niidome,T., K.Takaji, M.Urakawa, N.Ohmori, A.Wada, T.Hirayama, and H.Aoyagi. 1999. Chain length of cationic α-helical peptide sufficient for gene delivery into cells. *Bioconjugate Chemistry* 10:773-780.

Ninham,B.W. 1985. The background to hydration forces. *Chemica Scripta* 25:3-6.

Nishikawa,M. and L.Huang. 2001. Nonviral vectors in the new millenium: delivery barriers in gene transfer. *Human Gene Therapy* 12:861-870.

Noites,I.S., R.D.O'Kennedy, M.S.Levy, N.Abidi, and E.Keshavarz-Moore. 1999. Rapid quantitation and monitoring of plasmid DNA using an ultrasensitive DNA-binding dye. *Biotechnology and Bioengineering* 66:196-201.

O'Malley,B.W., Jr. and M.E.Couch. 1999. Gene therapy for cancer: strategies and review of clinical trials. *In* Advanced gene delivery: from concepts to pharmaceutical products. A.Rolland, editor. Harwood Academic Publishers, Amsterdam. 281-309.

Oberle,V., U.Bakowsky, I.S.Zuhorn, and D.Hoekstra. 2000. Lipoplex formation under equilibrium conditions reveals a three-step mechanism. *Biophysical Journal* 79:1447-1454.

Ogris,M., S.Brunner, S.Schüller, R.Kircheis, and E.Wagner. 1999. PEGylated DNA/transferrin-PEI complexes: reduced interaction with blood components, extended circulation in blood and potential for systemic gene delivery. *Gene Therapy* 6:595-605.

Ogris,M., P.Steinlein, M.Kursa, K.Mechtler, R.Kircheis, and E.Wagner. 1998. The size of DNA/transferrin-PEI complexes is an important factor for gene expression in cultured cells. *Gene Therapy* 5:1433.

Pack,D.W., D.Putnam, and R.Langer. 2000. Design of imidazole-containing endosomolytic biopolymers for gene delivery. *Biotechnology and Bioengineering* 67:217-223.

Palu,G., R.Bonaguro, and A.Marcello. 1999. In pursuit of new developments for gene therapy of human diseases. *Journal of Biotechnology* 68:1-13.

Pardoll,D.M. 1993. Cancer vaccines. *TiPS* 14:202-208.

Parkes,R.J. and S.L.Hart. 2000. Adhesion molecules and gene transfer. *Advanced Drug Delivery Reviews* 44:135-152.

Pashley,R.M. 1981. Hydration forces between mica surfaces in aqueous electrolyte solutions. *Journal of Colloid and Interface Science* 80:153-162.

Pashley,R.M. and J.N.Israelachvili. 1984. DLVO and hydration forces between mica surfaces in Mg^{2+}, Ca^{2+}, Sr^{2+}, and Ba^{2+} chloride solutions. *Journal of Colloid and Interface Science* 97:446-455.

Peng,K.-W. and S.J.Russell. 1999. Viral vector targeting. *Current Opinion in Biotechnology* 10:454-457.

Perales,J.C., T.Ferkol, M.Molas, and R.W.Hanson. 1994. An evaluation of receptor-mediated gene transfer using synthetic DNA-ligand complexes. *Eur. J. Biochem.* 226:255-266.

Perales,J.C., G.A.Grossmann, M.Molas, G.Liu, T.Ferkol, J.Harpst, H.Oda, and R.W.Hanson. 1997. Biochemical and functional characterization of DNA complexes capable of targeting genes to hepatocytes via the asialoglycoprotein receptor. *Journal of Biological Chemistry* 272:7398-7407.

Petsev,D.N., B.R.Thomas, S.-T.Yau, and P.G.Vekilov. 2000. Interactions and aggregation of apoferritin molecules in solution: effects of added electrolytes. *Biophysical Journal* 78:2060-2069.

Petsev,D.N. and P.G.Vekilov. 2000. Evidence for non-DLVO hydration interactions in solutions of the protein apoferritin. *Physical Review Letters* 84:1339-1342.

Planck,C., K.Zatloukal, M.Cotten, K.Mechtler, and E.Wagner. 1992. Gene transfer into hepatocytes using asialoglycoprotein receptor mediated endocytosis of DNA complexes with an artificial tetra-antennary galactose ligand. *Bioconjugate Chemistry* 3:533-539.

Plank,C., M.X.Tang, A.R.Wolfe, and F.C.Szoka, Jr. 1999. Branched cationic peptides for gene delivery: role of type and number of cationic residues in formation and *in vitro* activitiy of DNA polyplexes. *Human Gene Therapy* 10:319-332.

Plum,G.E., P.G.Arscott, and V.A.Bloomfield. 1990. Condensation of DNA by trivalent cations. 2. Effect of cation structure. *Biopolymers* 30:643.

Podgornik,R., H.H.Strey, and V.A.Parsegian. 2000. Molecular interactions in lipids, DNA, and DNA-lipid complexes. *In* Gene therapy: therapeutic mechanisms and strategies. N.S.Templeton and D.D.Lasic, editors. Marcel-Dekker, Inc., NY. 209-39.

Poeschla,E.M., F.Wong-Staal, and D.J.Looney. 1998. Efficient transduction of non-dividing human cells by feline immunodeficiency virus lentiviral vectors. *Nature Medicine* 4:354-357.

Porteous,D.J., J.R.Dorin, G.MacLachlan, H.Davidson-Smith, H.Davidson, B.J.Stevenson, A.D.Carothers, W.A.H.Wallace, S.Moralee, C.Hoenes, G.Kallmeyer, U.Michaelis, K.Naujoks, L.-P.Ho, J.M.Samways, M.Imrie, A.P.Greening, and A.J.Innes. 1997. Evidence for the safety and efficacy of DOTAP cationic liposome mediated *CFTR* gene transfer to the nasal epithelium of patients with cystic fibrosis. *Gene Therapy* 4:210-218.

Poulin,P., J.Bibette, and D.A.Weitz. 1999. From colloidal aggregation to spinodal decomposition in sticky emulsions. *The European Physical Journal B* 7:277-281.

Pouton,C.W. 1999. Biological barriers to gene transfer. *In* Advanced gene delivery: from concepts to pharmaceutical products. A.Rolland, editor. Harwood Academic Publishers, Amsterdam. 66-102.

Pouton,C.W., P.Lucas, B.J.Thomas, A.N.Uduehi, D.A.Milroy, and S.H.Moss. 1998. Polycation-DNA complexes for gene delivery: a comparison of the biopharmaceutical properties of cationic polypeptides and cationic lipids. *Journal of Controlled Release* 53:289-299.

Pouton,C.W. and L.W.Seymour. 1998. Key issues in non-viral gene delivery. *Advanced Drug Delivery Reviews* 34:3-19.

Provencher,S.W. 1979. Inverse problems in polymer characterization; direct analysis of polydispersity with photon correlation spectroscopy. *Makromol. Chem.* 180:201-209.

Provencher,S.W. 1982a. A constrained regularization method for inverting data represented by linear algebraic equations. *Comp. Phys. Com.* 27:213-227.

Provencher,S.W. 1982b. CONTIN: a general purpose constrained regularization program for inverting data represented by noisy linear algebraic and integral equations. *Comp. Phys. Com.* 27:229-242.

Ramsay,E., J.Hadgraft, J.Birchall, and M.Gumbleton. 2000. Examination of the biophysical interaction between plasmid DNA and the polycations, polylysine and polyornithine, as a basis for their differential gene transfection in-vitro. *International Journal of Pharmaceutics* 210:97-107.

Rand,R.P. and V.A.Parsegian. 1989. Hydration forces between phospholipid bilayers. *Biochim. Biophys. Acta Biomembranes Reviews* 988:351-376.

Riddell,S. 1996. T-cell mediated rejection of gene-modified HIV-specific cytotoxic T lymphocytes in HIV-infected patients. *Nature Medicine* 2:216-223.

Rolland, A., Duguid, J., Barron, M., Gong, L., Levin, J., and Eastman, E. Characterization of non-viral gene medicines. 21, 240-241. 1994. Controlled Release Society, Inc. Proceed. Intern. Symp. Control. Rel. Bioact. Mater. Ref Type: Conference Proceeding

Ross,P.C. and S.W.Hui. 1999. Lipoplex size is a major determinant of in vitro lipofection efficiency. *Gene Therapy* 6:651-659.

Roth,C.L. and M.L.Yarmush. 1999. Nucleic acid biotechnology. *Annu. Rev. Biomed. Eng.* 1:265-297.

Rouzina,I. and V.A.Bloomfield. 1996. Macroion attraction due to electrostatic correlation between screening counterions. 1. Mobile surface-adsorbed ions and diffuse ion cloud. *Journal of Physical Chemistry* 100:9977-9989.

Rouzina,I. and V.A.Bloomfield. 1997. Competitive electrostatic binding of charged ligands to polyelectrolytes — practical approach using the nonlinear Poisson-Boltzmann equation. *Biophysical Chemistry* 64:139-155.

Rustemeier,O. and E.Killmann. 1997. Electrostatic interactions and stability of poly-L-lysine covered polystyrene latex particles investigated by dynamic light scattering. *Journal of Colloid and Interface Science* 190:360-370.

Sambrook,J., E.F.Fritsch, and T.Maniatis. 1989. Molecular cloning: a laboratory manual. Cold Spring Harbor Laboratory Press, Cold Spring, New York.

Samulski,R.J., L.S.Chang, and T.Shenk. 1989. Helper-free stocks of recombinant adeno-associated viruses: normal integration does not requires viral gene expression. *Journal of Virology* 63:3822-3828.

Schaffer,D.V., N.A.Fidelman, N.Dan, and D.A.Lauffenburger. 2000. Vector unpacking as a potential barrier for receptor-mediated polyplex gene delivery. *Biotechnology and Bioengineering* 67:598-606.

Schaffer,D.V. and D.A.Lauffenburger. 1998. Optimization of cell surface binding enhances efficiency and specificity of molecular conjugate gene delivery. *Journal of Biological Chemistry* 273:28004-28009.

Scherman,D., M.Bessodes, B.Cameron, J.Herscovici, H.Hofland, B.Pitard, F.Soubrier, P.Wils, and J.Crouzet. 1998. Application of lipids and plasmid design for gene delivery to mammalian cells. *Current Opinion in Biotechnology* 9:480-485.

Schmidt,P.W. 1989. Use of scattering to determine the fractal dimension. *In* The fractal approach to heterogeneous chemistry: surfaces, colloids, polymers. D.Avnir, editor. John Wiley & Sons Ltd., New York. 67-79.

Schoen,P., L.Bijl, and J.Wilschut. 1998. Efficient encapsulation of plasmid DNA in anionic liposomes by a freeze/thaw-extrusion procedure. *Journal of Liposome Research* 8:485-497.

Schüler,J., J.Frank, W.Saenger, and Y.Georgalis. 1999. Thermally induced aggregation of human transferrin reporter studied by light scattering techniques. *Biophysical Journal* 77:1117-1125.

Scott,E.S., J.W.Wiseman, M.J.Evans, and W.H.Colledge. 2001. Enhanced gene delivery to human airway epithelial cells using an integrin-targeting lipoplex. *Journal of Gene Medicine* 3:125-134.

Shapiro,J.T., M.Leng, and G.Fesenfeld. 1969. Deoxyribonucleic acid-polylysine complexes. Structure and nucleotide specificity. *Biochemistry* 8:3219-3232.

Shaw,D.J. 1992. Introduction to colloid and surface chemistry. Butterworth-Heinemann, Oxford, UK.

Simões,S., V.Slepushkin, P.Pires, R.Gaspar, M.C.Pedroso de Lima, and N.Düzgünes. 1999. Mechanisms of gene transfer mediated by lipoplexes associated with targeting ligands or pH-sensitive peptides. *Gene Therapy* 6:1798-1807.

Singer,V.L., L.J.Jones, S.T.Yue, and R.P.Haugland. 1997. Characterization of PicoGreen reagent and development of a fluorescence-based solution assay for double-stranded DNA quantitation. *Analytical Biochemistry* 249:228-238.

Son,K.K., D.Tkach, and K.J.Hall. 2000. Efficient in vivo gene delivery by the negatively charged complexes of cationic liposomes and plasmid DNA. *Biochim. Biophys. Acta* 1468:6-10.

Sorensen,C.M. 2001. Light scattering by fractal aggregates: a review. *Aerosol Science and Technology* 35:648-687.

Stopeck,A.T., E.M.Hersh, E.T.Akporiaye, D.T.Harris, T.Grogan, E.Unger, J.Warneke, S.F.Schluter, and S.Stahl. 1997. Phase I study of direct gene transfer of an allogeneic histocompatibility antigen, HLA-B7, in patients with metastatic melanoma. *Journal of Clinical Oncology* 15:341-349.

Sudimack,J. and R.J.Lee. 2000. Targeted drug delivery via the folate receptor. *Advanced Drug Delivery Reviews* 41:147-162.

Tang,F. and J.A.Hughes. 1998. Introduction of a disulfide bond into a cationic lipid enhances transgene expression of plasmid DNA. *Biochemical and Biophysical Research Communications* 242:141-145.

Tang,M.X. and F.C.Szoka. 1997. The influence of polymer structure on the interactions of cationic polymers with DNA and morphology of the resulting complexes. *Gene Therapy* 4:823-832.

Tang,M.X. and F.C.Szoka, Jr. 1998a. Characterization of polycation complexes with DNA. *In* Self-assembling complexes for gene delivery: from laboratory to clinical trial. A.V.Kabanov, P.L.Felgner, and L.W.Seymour, editors. John Wiley & Sons, Ltd., 169-96.

Tang,M.X. and F.C.Szoka, Jr. 1998b. Structure of polycation-DNA complexes and theories of compaction. *In* Self-assembling complexes for gene delivery: from laboratory to clinical trial. A.V.Kabanov, P.L.Felgner, and L.W.Seymour, editors. John Wiley & Sons, Ltd., 27-50.

Tang,S., Y.Ma, and I.M.Sebastine. 2001. The fractal nature of *Escherichia coli* biological flocs. *Colloids and Surfaces B: Biointerfaces* 20:211-218.

Templeton,N.S., D.D.Lasic, P.M.Frederik, H.H.Strey, D.D.Roberts, and G.N.Pavlakis. 1997. *Nature Biotechnology* 15:647-652.

Terry,J. and C.Hedrick. 1995. Intravenous agents: parenteral fluids. *In* Intravenous therapy: clinical principles and practice. J.Terry, L.Baranowski, R.A.Lonsway, and C.Hedrick, editors. WB Saunders & Company, Philadelphia, PA. 156-7.

Thierry,A. and L.C.Mahan. 1999. Therapeutic applications of lipid-based gene delivery systems. *In* Advanced gene delivery: from concepts to pharmaceutical products. A.Rolland, editor. Harwood Academic Publishers, Amsterdam. 123-42.

Tirado-Miranda,M., A.Schmitt, J.Callejas-Fernández, and A.Fernández-Barbero. 2000. Dynamic scaling and fractal structure of small colloidal clusters. *Colloids and Surfaces A: Physicochemical and Engineering Aspects* 162:67-73.

Toda,M., S.D.Rabkin, H.Kojima, and R.L.Martuza. 1999. Herpes simplex virus as an in situ cancer vaccine for the induction of specific anti-tumor immunity. *Human Gene Therapy* 10:385-393.

Trubetskoy,V.S., A.Loomis, J.E.Hagstrom, V.G.Budker, and J.A.Wolff. 1999. Layer-by-layer deposition of oppositely charged polyelectrolytes on the surface of condensed DNA particles. *Nucleic Acids Research* 27:3090-3095.

Tsai,J.T., E.Keshavarz-Moore, J.M.Ward, M.Hoare, P.Ayazi Shamlou, and P.Dunnill. 1999. Characterisation of plasmid DNA conjugates as a basis for their processing. *Bioprocess Engineering* 21:279-286.

Tsunoda,T., T.Imura, M.Kadota, T.Yamazaki, H.Yamauchi, K.O.Kwon, S.Yokoyama, H.Sakai, and M.Abe. 2001. Effects of lysozyme and bovine serum albumin on membrane characteristics of dipalmitoylphosphatidylglycerol liposomes. *Colloids and Surfaces B: Biointerfaces* 20:155-163.

Turek,J., C.Dubertret, G.Jaslin, K.Antonakis, D.Scherman, and B.Pitard. 2000. Formulations which increase the size of lipoplexes prevent serum-associated inhibition of transfection. *Journal of Gene Medicine* 2.

Valsesia-Wittmann,S., F.J.Morling, B.H.Nilson, Y.Takeuchi, and S.J.Russell. 1996. Improvement of retroviral retargeting by using amino acid spacers between an additional binding domain and the N terminus of Moloney murine leukemia virus SU. *Journal of Virology* 70:2059-2064.

Vandorpe,J., E.Schacht, S.Stolnik, M.C.Garnett, M.C.Davies, L.Illum, and S.S.Davies. 1996. Poly(organo phosphazene) nanoparticles surface modified with poly(ethylene oxide). *Biotechnology and Bioengineering* 52:89-95.

Verbaan,F.J., C.Oussoren, I.M.van Damm, Y.Takakura, M.Hashida, D.J.A.Crommelin, W.E.Hennink, and G.Storm. 2001. The fate of poly(2-dimethyl amino ethyl)methacrylate-based polyplexes after intravenous administration. *International Journal of Pharmaceutics* 21:99-101.

Verma,I.M. and N.Somia. 1997. Gene therapy - promises, problems and prospects. *Nature* 389:239-242.

Wagner,E. 1998b. Effects of membrane-active agents in gene delivery. *Journal of Controlled Release* 53:155-158.

Wagner,E., M.Cotten, R.Foisner, and M.L.Brinstiel. 1991. Transferrin-polycation-DNA complexes: the effect of polycations on the structure of the complex and DNA delivery to cells. *Proc. Natl. Acad. Sci. USA* 88:4255-4259.

Wagner,E., M.Zenke, M.Cotten, H.Beug, and M.H.Birnstierl. 1990. Transferrin-polycation DNA conjugates as carriers for DNA uptake into cells. *Proc. Natl. Acad. Sci. USA* 87:3410-3414.

Wagner,J.A. 1998a. Efficient and persistent gene transfer of AAV-CFTR in maxillary sinus. *Lancet* 351:1702-1703.

Wahren,B. 1996. Gene vaccines. *Immunotechnology* 2:77-83.

Wang,C.-Y. and L.Huang. 1987. pH-sensitive immuonoliposomes mediate target-cell-specific delivery and controlled expression of a foreign gene in mouse. *Proc. Natl. Acad. Sci. USA* 84:7851.

Watkins,S.J., V.V.Mesyanzhinov, L.P.Kurochkina, and R.E.Hawkins. 1997. The 'adenobody' approach to viral targeting: specific and enhanced adenoviral gene delivery. *Gene Therapy* 4:1004-1012.

Wells,J.M., L.H.Li, A.Sen, G.P.Jahreis, and S.W.Hui. 2000. Electroporation-enhanced gene delivery in mammary tumors. *Gene Therapy* 7:541-547.

Wheeler,C.J., P.L.Felgner, J.T.Tsai, J.Marshall, L.Sukhu, S.G.Doh, J.Hartikka, J.Nietupski, M.Manthorpe, M.Nichols, M.Plewe, X.Liang, J.Norman, A.Smith, and S.H.Cheng. 1996. A novel cationic lipid greatly enhances plasmid DNA delivery and expression in mouse lung. *Proc. Natl. Acad. Sci. USA* 93:11454-11459.

Wheeler,J.J., L.Palmer, M.Ossanlou, I.MacLachlan, R.W.Graham, Y.P.Zhang, M.J.Hope, P.Scherrer, and P.R.Cullis. 1999. Stabilized plasmid-lipid particles: construction and characterization. *Gene Therapy* 6:271-281.

Wickham,T.J., E.Tzeng, L.L.2.Shears, P.W.Roelvink, Y.Li, G.M.Lee, D.E.Brough, A.Lizonova, and I.Kovesdi. 1997. Increased *in vitro* and *in vivo* gene transfer by adenovirus vectors containing chimeric fiber proteins. *Journal of Virology* 71:8221-8229.

Wilson,D.J. and R.H.French. 1978. Kinetic and equilibrium aspects of floc coagulation. II. Slow mixing criteria. *Separation Science and Technology* 13:95-106.

Wilson,R.W. and V.A.Bloomfield. 1979. Counterion-induced condensation of deoxyribonucleic acid. A light-scattering study. *Biochemistry* 18:2192-2196.

Wolfert,M.A. and L.W.Seymour. 1996. Atomic force microscopic analysis on the influence of the molecular weight of poly(L)lysine on the size of polyelectrolyte complexes formed with DNA. *Gene Therapy* 3:269-273.

Wolff,J.A., J.Ludtke, G.Acsadi, P.Williams, and A.Jani. 1992. Long-term persistence of plasmid DNA and foreign gene expression in mouse muscle. *Hum. Mol. Genet.* 1:363-369.

Wolff,J.A., R.Malone, P.Williams, W.Chong, G.Acsadi, A.Jani, and P.Felgner. 1990. Direct gene transfer into mouse muscle *in vivo*. *Science* 247:1468.

Wu,G.Y. and C.H.Wu. 1987. Receptor-mediated *in vitro* gene transformation by a soluble DNA carrier system. *Journal of Biological Chemistry* 262:4429-4432.

www.lifetech.com/Content/Tech-Online/cell_culture/pps_manuals/2017.pdf. Opti-MEM® I Reduced Serum Medium: modification of MEM (Eagle's). World Wide Web. 2001. Ref Type: Electronic Citation

www.paddocklabs.com/publications/secundum/secart63.html. Secundum Artem: current and practical compounding information for the pharmacist — inhalation products. World Wide Web. 1997. Ref Type: Electronic Citation

www.studentbmj.com/back_issues/0497/data/0497ed1.htm. Student BMJ April 1997: Education — understanding fluid balance: types of intravenous fluids. World Wide Web. 1997. Ref Type: Electronic Citation

www.wiley.co.uk/genmed/clinical. Gene Therapy Vectors Website. World Wide Web. 2001. Ref Type: Electronic Citation

www4.ncbi.nlm.nih.gov/PubMed/. MEDLINE database. World Wide Web. 2001. Ref Type: Electronic Citation

Xu,B., S.Wiehle, J.A.Roth, and R.J.Cristiano. 1998. The contribution of poly-L-lysine, epidermal growth factor and streptavidin to EGF/PLL/DNA polyplex formation. *Gene Therapy* 5:1235-1243.

Xu,Y., S.-W.Hui, P.Frederik, and Jr.F.C.Szoka. 1999. Physicochemical characterization and purification of cationic lipoplexes. *Biophysical Journal* 77:341-353.

Xu,Y. and Jr.F.C.Szoka. 1996. Mechanism of DNA release from cationic liposome/DNA complexes used in cell transfection. *Journal of Biological Chemistry* 35:5616-5623.

Yang,J.-P. and L.Huang. 1996. Direct gene transfer to mouse melanoma by intratumor injection of free DNA. *Gene Therapy* 3:542-548.

Yokouchi,Y., T.Tsunoda, T.Imura, H.Yamauchi, S.Yokohama, H.Sakai, and M.Abe. 2001. Effect of adsorption of bovine serum albumin on liposomal membrane characteristics. *Colloids and Surfaces B: Biointerfaces* 20:95-103.

Yoo,H. and R.L.Juliano. 2000. Enhanced delivery of antisense oligonucleotides with fluorophore-conjugated PAMAM dendrimers. *Nucleic Acids Research* 28:4225-4231.

Zabner,J., L.A.Couture, R.J.Gregory, S.M.Granham, and A.E.Smith. 1993. Adenovirus-mediated gene transfer transiently corrects the chloride transport defect in nasal epithelia of patients with cystic fibrosis. *Cell* 75:207-216.

Zauner,W., M.Ogris, and E.Wagner. 1997. Polylysine-based transfection systems utilizing receptor-mediated delivery. *Advanced Drug Delivery Reviews* 30:97-113.

Zelphati,O., C.Nguyen, M.Ferrari, J.Felgner, Y.Tsai, and P.L.Felgner. 1998a. Stable and monodisperse lipoplex formulations for gene delivery. *Gene Therapy* 5:1272-1282.

Zelphati,O., L.S.Uyechi, L.G.Barron, and F.C.Szoka, Jr. 1998b. Effect of serum components on the physico-chemical properties of cationic lipid/oligonucleotide complexes and on their interactions with cells. *Biochim. Biophys. Acta* 1390:119-133.

Zhang,Y.-P., L.Sekirov, E.G.Saravolac, J.J.Wheeler, P.Tardi, K.Clow, E.Leng, R.Sun, P.R.Cullis, and P.Scherrer. 1999. Stabilized plasmid-lipid particles for regional gene therapy: formulation and transfection properties. *Gene Therapy* 6:1438-1447.

Zhu,N., D.Liggitt, Y.Liu, and R.Debs. 1993. Systemic gene expression after intravenous DNA delivery into adult mice. *Science* 261:209-211.

Ziady,A.-G., T.Ferkol, D.V.Dawson, D.H.Perlmutter, and P.B.Davis. 1999. Chain length of the polylysine in receptor-targeted gene transfer complexes affects duration of reporter gene expression both *in vitro* and *in vivo*. *Journal of Biological Chemistry* 274:4908-4916.

CHAPTER 8

APPENDICES

Appendix A – Photon correlation spectroscopy (PCS)

This appendix contains a description of photon correlation spectroscopy (PCS) relevant to the work represented by this thesis. PCS, also known as quasielastic light scattering (QELS), is an establish technique for particle size analysis. It represents dynamic light scattering (DLS) in the time domain.

In PCS, the Brownian motion of colloidal particles are analysed and related to their size. A typical PCS experiment using the Malvern Autosizer 4700/4800 is shown in Fig. A.1. The Malvern Zetasizer 3000 apparatus is generally similar, except for the photomultiplier assembly that allows measurement at various angles. For the Zetasizer, measurements are carried out a single fixed angle of 90°, which is sufficient for interpretation of the size distribution. The Autosizer 4800 is also shown in Fig. A.2.

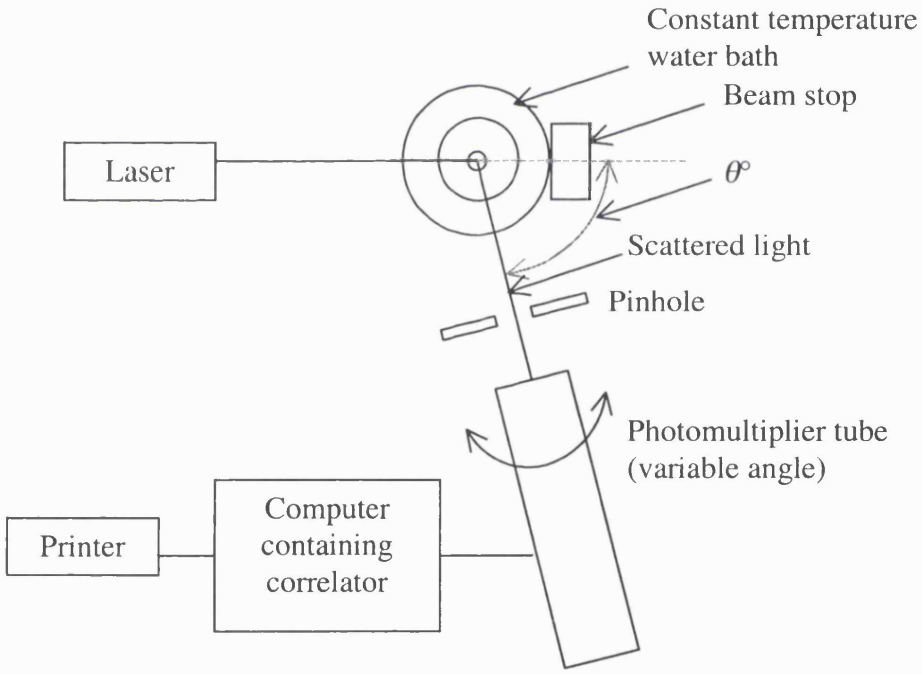

Figure A.1 Diagrammatic representation of the PCS apparatus.

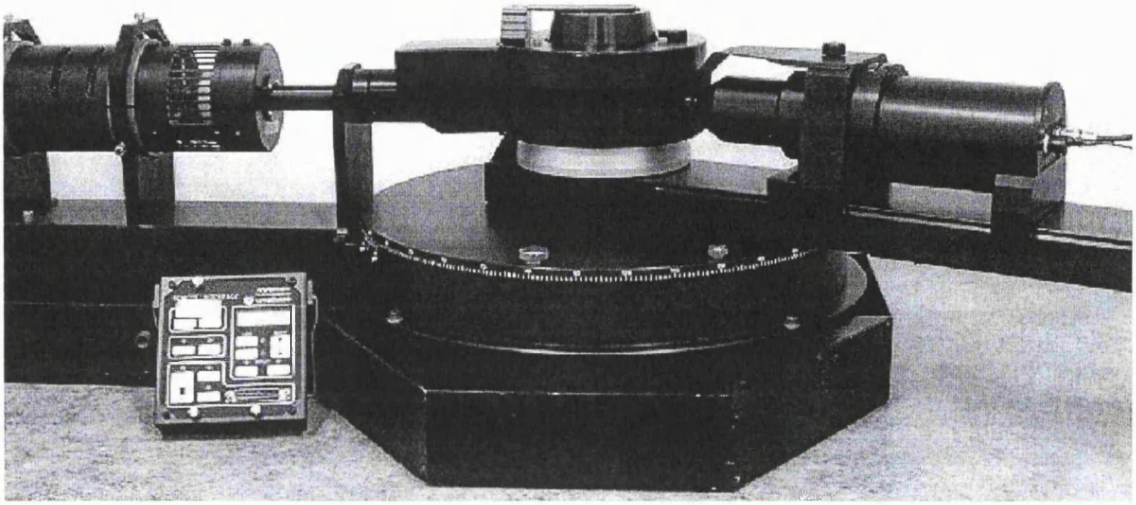

Figure A.2 The Malvern Autosizer 4800, photon correlation spectrometer. A series of baffles that can be removed for maintenance shields the operator from the scattered light. The system is mounted on a metal base for rigidity.

When a colloidal suspension is coherently illuminated by a laser light source, such as the 488 nm wavelength Argon ion laser in the Autosizer 4700 or the 633 nm He-Ne laser in Zetasizer 3000, the dynamic fluctuations in light scattered from different particles vary as the particles undergo Brownian motion, causing the intensity of scattered light at the small aperture, photon counting detector to fluctuate with time. The rate at which the intensity fluctuations occur depend on the size of the particles, with small particles possessing more rapid intensity fluctuations than large particles. Each randomly positioned particle in the scattering volume scatters the incident light with a random phase shift into the detector. Hence, the detected intensity of a signal at a particular point in time, t, can be compared to the intensity at a very small time later, $t + \delta t$, revealing a strong relationship or correlation between the two signals. Accordingly, this correlation will be stronger than one between two signals at t and $t + 2\delta t$, which, in turn, will be stronger than one between t and $t + 3\delta t$, and so on. The correlation is reducing with time.

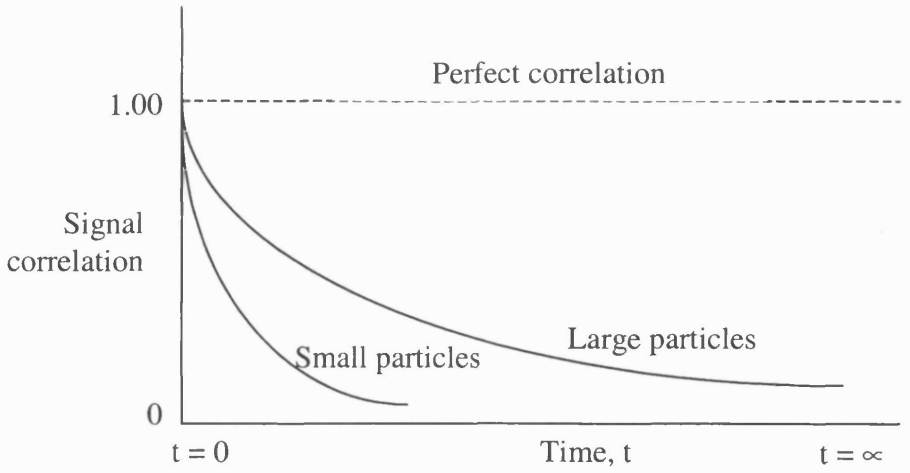

Figure A.2 Correlation curves showing exponential decay of the normalised correlation function. Large particles have a slower changing signal, giving a correlation that persists for a longer time. The correlation for smaller, rapidly moving particles will disappear more quickly.

A correlator measures the degree of similarity between two signals or one signal with itself at varying time intervals (Fig. A.2), and generates a correlation function of the scattered intensity. For a large number of monodisperse spherical particles undergoing Brownian motion, the normalised first-order autocorrelation function, $g^{(1)}(\tau)$, is a single exponential decaying function of the correlator time difference or sample time, τ:

$$g^{(1)}(\tau) = \exp(-\Gamma\tau)] \qquad \text{(A.1)}$$

The decay rate $\Gamma = Dq^2$ provides information about diffusion in the sample. Hence analysis of Eq. (A.1) yields the translational diffusion coefficient of the particle, D, which is related to the hydrodynamic diameter D_H by the Stokes-Einstein equation:

$$D = \frac{kT}{3\pi\mu D_H} \qquad \text{(A.2)}$$

where k is the Boltzmann constant, T is the absolute temperature of the sample, and μ is the dynamic viscosity. The hydrodynamic diameter D_H includes effects arising from shape and hydration, and is the diameter of a sphere undergoing the same hydrodynamic

drag as the particle under consideration. The magnitude of the scattering vector, q, is given by the Bragg formula:

$$q = \frac{4\pi n \sin(\theta/2)}{\lambda} \tag{A.3}$$

where n is the refractive index of the solution, θ the scattering angle, and λ the incident wavelength of the laser.

For polydisperse samples, $g^{(1)}(\tau)$ must be expressed as an integral of the exponential decays weighted over the distribution, $G(\Gamma)$, of decay rates:

$$g^{(1)}(\tau) = \int_0^\infty G(\Gamma) \exp(-\Gamma\tau)] d\Gamma \tag{A.4}$$

Appendix B – Shear rates vs. disk rotational speed

This appendix shows the estimated average shear rate as a function of disk rotational speed and the Reynolds number for the rotating shear device described in Sections 3.11 and 4.1.5. Further information on the equipment can be found in a previous publication by Levy *et al* (Levy *et al.*, 1999).

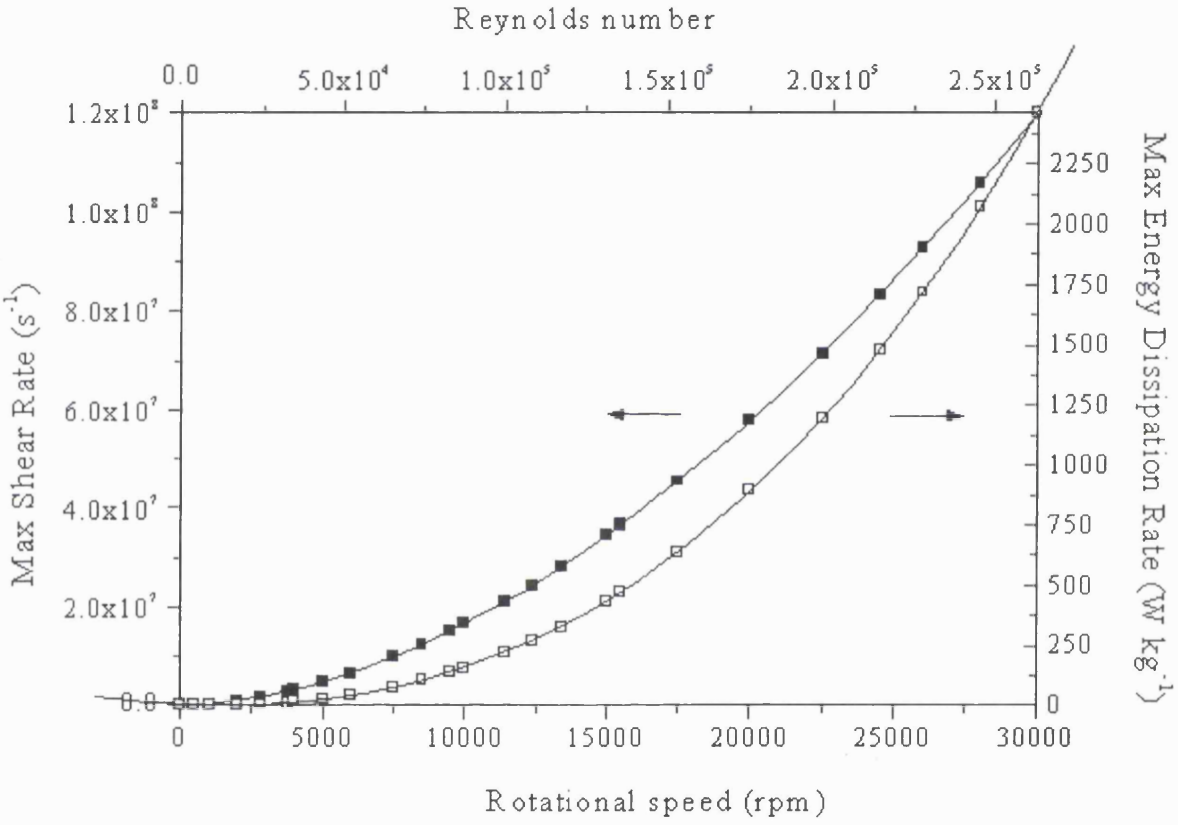

Figure B.1 Shear rate of rotating disk shear device as a function of Reynolds number and disk rotational speed.

The above plot was kindly provided by Michael Boychn. The assumption that the critical region where damage occurs is the boundary layer of the rotating disk was made in the calculation of the values.

Appendix C – Example calculation of the PLL/DNA and LID charge ratios

The charge ratios of PLL/DNA and LID complexes were determined from their molecular weight and charge parameters. The number of moles of negative charge per mole of DNA was calculated based on one negatively charged phosphate per base, multiplied by two for double-stranded DNA. Lipofectin, a 1:1 (w/w) mixture of the cationic lipid DOTMA (MW = 669.5) and the neutral lipid DOPE (MW = 744), contains a charge of +1. In the $[K]_{16}$GACRRETAWACG integrin-targeting peptide, the glutamic acid residue (E) contributes a charge of –1, while lysine (K) and arginine (R) each contributes a charge of +1. These details are summarised in the following table.

Table C.1 Some physical properties of materials used in calculations.

Materials	*Average MW*	*Charge*	*Charge per μg (nmol)*
Nucleotide	330	-1	3.03
Lysine ($C_6H_{12}N_2O$.HBr)	209	+1	4.78
DOTMA	669.5	+1	1.49
Integrin-targeting peptide	3331.5	+17	0.30

Using the values in Table C.1, the charge ratio for the PLL/DNA and LID complexes can be calculated:

$$\text{Charge ratio} = \frac{\left(\frac{\text{mass of lipid} \times \text{lipid charge}}{\text{lipid mol. wt.}}\right) + \left(\frac{\text{mass of peptide} \times \text{peptide charge}}{\text{peptide mol. wt.}}\right)}{\left(\frac{\text{mass of DNA} \times \text{nucleotide charge}}{\text{nucleotide mol. wt.}}\right)}$$

E.g. 1

Consider that we want to find out the amount of PLL required to prepare PLL/DNA complexes at a charge ratio of 2.0. Therefore, for 1 μg DNA, the amount of PLL required is: $\frac{209}{330}\times 1\times 10^{-6}\times 2.0 \approx 1.26$ μg.

E.g. 2

Consider that we have LID complexes at the weight ratio 0.75:4:1 (L:I:D). Hence, assuming 0.75 μg Lipofectin, 4 μg integrin-targeting peptide and 1 μg DNA were mixed, the charge ratio of the lipopolyplexes is: $\frac{\left(\frac{\frac{0.75}{2}\times 10^{-6}\times 1}{669.5}\right)+\left(\frac{4\times 10^{-6}\times 17}{3331.5}\right)}{\left(\frac{1\times 10^{-6}\times 1}{330}\right)} \approx 6.8.$

Note that the calculation of the charge contributed by Lipofectin was performed on the charged lipid, DOTMA.

Appendix D – Glossary

AAV	adeno-associated virus
Ad	adenovirus
AFM	atomic force microscopy
AGE	agarose gel electrophoresis
AIDS	acquired immunodeficiency syndrome
ASF	airway surface fluid
AsOR	asialoorosomucoid
ATP	adenosine triphosphate
BSA	bovine serum albumin
CD	circular dichroism
Da	dalton (approximately equal to hydrogen atom mass, 1.66×10^{-24} g)
DLCA	diffusion-limited colloidal aggregation
DLS	dynamic light scattering
DLVO	Derjaguin-Landau-Verwey-Overbeek
DMEM	Dulbecco's modified Eagle's medium
DMRIE	1,2-dimyristyloxypropyl-3-dimethyl-hydroxyammonium bromide
DNA	deoxyribonucleic acid
DOPE	dioleoyl phosphatidylethanolamine
DOSPA	2,3 dioleyloxy-*N*-[2(spermine carboxaminino)ethyl]-*N*,*N*-dimethyl-1-propanaminium trifluoroacetate
DOTAP	1,2-dioleoyl-3-trimethylammonium propane
DOTMA	*N*-[1-(2,3-dioleyloxy)propyl]-*N*,*N*,*N*-trimethylammonium chloride

E. coli	*Escherichia coli*
ECACC	European Collection of Cell Cultures
EM	electron microscopy
FCS	fetal calf serum
FDA	Food and Drug Administration (US)
GFP	green fluorescent protein
GMP	good manufacturing practice
h	hour
H^+	hydrogen ion
HBS	HEPES-buffered saline (20 mM HEPES, 150 mM NaCl)
He-Ne	helium-neon
HEPES	*N*-[2-hydroxyethyl] piperazine-*N*'-[2-ethanesulfonic acid]
HIV	human immunodeficiency virus (the human AIDS virus)
HSV	herpes simplex virus
ICH	Institute of Child Health
IEP	isoelectric point
K	lysine
kb	kilobase
LDV	laser Doppler velocimetry
LID	Lipofectin/integrin-targeting peptide/DNA
l	litre
ln	natural logarithm (base e)
M	molar (gram molecule/litre)
MALLS	multiangle laser light scattering

Max.	maximum
min	minutes
Min.	minimum
MW	molecular weight
NaCl	sodium chloride (salt)
NCBI	National Centre for Biotechnology Information
NIH	National Institutes of Health (NIH)
NLS	nuclear localisation signal
N/P	nitrogen/phosphate ratio (+/-)
Opti-MEM	optimal minimal essential media
PAMAM	polyamidoamine
PBS	phosphate-buffered saline
PCS	photon correlation spectroscopy
PEG	polyethylene glycol
PEI	polyethyleneimine
PLL	poly-L-lysine
PTFE	polytetrafluoroethylene
QA	quality assurance
QC	quality control
QELS	quasielastic light scattering
RAC	Recombinant DNA Advisory Committee
RGD	Arg-Gly-Asp (arginine-glycine-aspartic acid)
RLCA	reaction-limited colloidal aggregation
RNA	ribonucleic acid

rpm	revolutions per minute
Rv	retrovirus
SALLS	small angle laser light scattering
SCID	severe combined immune deficiency
SLS	static light scattering
UCL	University College London
WHO	World Health Organization

Appendix E – Notation

Latin symbols

a	*(m)*	particle radius
A	(J)	Hamaker constant
c	(mol/dm^3)	ionic concentration
D	(m^2/s)	diffusion coefficient
D_f	(-)	fractal dimension
D_H	(m)	particle hydrodynamic diameter
e	(C)	elementary charge (1.6×10^{-19} C)
H	(m)	separation distance between two particles
k	(J/K)	Boltzmann constant (1.381×10^{-23} J/K)
P_0	(N/m^2)	hydration force parameter
t	(s)	time
T	(K)	absolute temperature
V_A	(J)	London-van der Waals (dispersion) energy
V_{hyd}	(J)	energy due to hydration forces
V_R	(J)	electrostatic interaction energy
V_T	(J)	total interaction potential
x	(-)	$\frac{H}{a_1 + a_2}$
y	(-)	a_1/a_2
z	(-)	valency (charge number) of ions

Greek symbols

δ	(m)	thickness of Stern layer
ε	(-)	relative dielectric constant or permittivity
γ	(-)	$\frac{\exp[ze\zeta/2kT]-1}{\exp[ze\zeta/2kT]+1}$
κ	(m^{-1})	Debye-Hückel parameter
λ	(m)	wavelength
λ_h	(m)	hydration radius
μ	(kg/ms)	viscosity
θ	(°)	angle
ψ_0	(V)	surface potential
ψ_d	(V)	Stern potential
ζ	(V)	zeta potential (shear boundary)

Appendix F – Publications

1. Lee,L.K., C.N.Mount, and P.Ayazi Shamlou. 2001. Characterisation of the physical stability of colloidal polycation-DNA complexes for gene therapy and DNA vaccines. *Chemical Engineering Science* 56:3163-3172.

2. Lee,L.K., E.K.Siapati, R.G.Jenkins, R.J.McAnulty, S.L.Hart, and P.Ayazi Shamlou. Biophysical characterization of an integrin-targeted non-viral vector for pulmonary gene delivery. *Biotechnology and Bioengineering* (submitted).

3. Jenkins,R.G., Q.-H.Meng, R.-H.Hodges, L.K.Lee, G.J.Laurent, D.Willis, P.Ayazi Shamlou, R.J.McAnulty, and S.L.Hart. Formation of LID vector complexes in hypotonic solution alters physico-chemical properties and enhances pulmonary gene expression *in vivo*. *Human Gene Therapy* (submitted).

4. Lee,L.K. and P.Ayazi Shamlou. The fractal structure of polycation-DNA complexes (in progress).

PERGAMON

Chemical Engineering Science 56 (2001) 3163–3172

Chemical Engineering Science

www.elsevier.nl/locate/ces

Characterisation of the physical stability of colloidal polycation-DNA complexes for gene therapy and DNA vaccines

L. K. Lee, C. N. Mount, P. Ayazi Shamlou*

Department of Biochemical Engineering, The Advanced Centre for Biochemical Engineering, University College London, Torrington Place, London WC1E 7JE, UK

Received 17 April 2000; received in revised form 30 October 2000; accepted 2 December 2000

Abstract

Plasmid DNA is a potentially effective and safe means of in vivo delivery of exogenous genetic material to human cells and tissues. The lack of physical stability of plasmid formulations however continues to pose major challenges. These formulations tend to aggregate under conditions of interest, especially under physiological ones. Experimental data show that over a period of nearly 30 min after preparation, aggregates of poly-L-lysine-DNA grow to sizes above 1000 nm. This will severely reduce their diffusion rate through tissues and will have a detrimental effect on their uptake by cells. Our theoretical analysis shows that aggregation is a complex function of the physicochemical properties of the system with the initial particle size distribution, solution pH and ionic strength, and temperature being the most important parameters. These considerations show that conditions conducive to the formation of stable formulations are low pH, low ionic strength, a narrow size distribution and low temperature. Though these conditions can not be achieved in vivo they can be maintained during processing and the theoretical analysis lays the foundation for assessment of other complexes that may be able to meet in vivo requirements.

Keywords: Gene delivery; Plasmid DNA; Formulation; Mathematical modelling; Pharmaceuticals; Stability

1. Introduction

The capacity of plasmid DNA-based vectors to safely deliver genes to human cells and tissues offers the potential for novel therapy and vaccines in the new millennium (Anderson, 1998). Progress to a successful medicine however has been slow caused largely by poor targeting and low cellular uptake (Lai & Bennett, 1998; Luo & Saltzman, 2000), in in vivo administration (Hart, 1999; Hart, 2000). Plasmid DNA is relatively large, compared with, for example, proteins, and in its "naked" form it is susceptible to degradation by plasma and serum proteins in vivo (Adami et al., 1998). Naked plasmid DNA is also susceptible to damage by interfacial effects and mechanical forces (Levy et al., 1999a) that can occur in delivery devices including nebulizers and aerosolizers (Crook, McLachlan, Stevenson, & Porteous, 1996; Alton et al., 1999). Condensation of the plasmid DNA provides significant protection against both chemical degradation and mechanical damage (Tsai et al., 1999) and forms the basis for targeting of the vector and for improving its cellular uptake (Luo & Saltzman, 2000).

Condensing agents are small polycationic molecules that electrostatically bind to the negatively charged phosphate groups of the double-stranded polynucleotides, causing a significant reduction in the volume occupied by the plasmid DNA. Natural DNA condensing agents such as the polyamines, hexamine cobalt, spermidine and spermine, and many synthetic agents, for example, cationic lipids, polypeptides and dendrimers, have the capacity to spontaneously form complexes with plasmid DNA (Bloomfield & Rau, 1980; Bloomfield, 1991; Deng & Bloomfield, 1999; Deshmukh & Huang, 1997; Duguid et al., 1998; Gosule & Schellman, 1976; Tang & Szoka, 1997; Whitmore, Li, & Huang, 1999). However, condensation by charge neutralisation destabilises the DNA macromolecules, causing interparticle interaction, leading to aggregation (Pouton et al., 1998; Tsai et al., 1999). Aggregation of the lipid- or polymer–DNA complexes is a serious challenge limiting their widespread application in clinical trials and their

* Corresponding author. Tel.: +44-020-7679-3841; fax: +44-020-7616-3943.

E-mail address: p.shamlou@ucl.ac.uk (P. Ayazi Shamlou).

0009-2509/01/$-see front matter
PII: S0009-2509(00)00545-5

eventual use for human gene delivery, therapy and vaccines (Rolland, 1998; Ross & Hui, 1999).

We previously studied the condensation of plasmid DNA by poly-L-lysine of different molecular weights. Photon-correlation spectroscopy (PCS) was used to show that over a period of less than an hour the size of the resulting polyplexes increased from about 200 nm to over 1000 nm (Tsai et al., 1999). Others have made similar observations (Dunlap, Maggi, Soria, & Monaco, 1997; Kircheis et al., 1999). Aggregation of the polyplexes was noticeably reduced at DNA concentrations typically below 0.5 mg/ml. However, minimising aggregation by this method is unsatisfactory clinically because of the large volumes of material that are likely to be required, particularly for cases that necessitate repetitive dosing. Currently, problems associated with aggregation dictates that formulations be prepared immediately before delivery to patients (Zelphati et al., 1998). However, for regulated commercial products stable formulations are likely to be demanded. Additionally, the physiological conditions in the body normally favour aggregation. Therefore, if the long-term potential of plasmid DNA for gene therapy and vaccines is to be realised, formulation instability needs to be addressed. This provided the key motivation for the study presented here.

There is additional need to understanding the factors that control the physical stability of condensed plasmid DNA. This is because of the recognition of the potential of condensation for improving large-scale recovery and purification of plasmid DNA (Levy, O'Kennedy, Ayazi Shamlou, & Dunnill, 2000a). Chromatography is an essential purification step in the downstream recovery of biological macromolecules, but currently, its application to plasmid DNA is severely limited owing to the large size of plasmid DNA compared to the typical size of the pores of commercially available chromatographic column materials. Here, binding is often limited to the outer surface of the column material because the large macromolecules of DNA are unable to penetrate the pores of the matrix. Previous experimental studies (Levy et al., 2000a; Prazeres, Schluep, & Cooney, 1998) have shown that these macromolecules have binding capacities that are typically less than about 1% of values normally reported for proteins. Experimental evidence has been provided which suggests that condensation of the plasmid DNA has beneficial effects on its chromatographic separation (Horn, Marquet, Meek, & Budahazi, 1995).

The physical stability of gene delivery formulations has received little attention in terms of theoretical analysis to date although it is being recognised that the gene transfer capacity of these systems is seriously affected by it. In this investigation, we use the established DLVO theory of colloidal stability to analyse experimental data on aggregation of poly-L-lysine-DNA complexes, and polyplexes, for different physicochemical conditions and over a range of operating parameters. We demonstrate that such an approach provides a basis for analysing the complex interactions between material properties, process parameters and formulation stability. Parameters, such as the absolute value of the Hamaker constant, are not available for the systems of interest to this study. However, approximations are made and the theoretical predictions used to show the trends in aggregation. The methodology that is developed here will be applicable for the selection of process conditions that are likely to lead to the creation of stable formulations.

2. Materials and methods

Experiments were carried out with commercially available calf thymus DNA of average molecular weight 8 kb, and a 6.9 kb plasmid DNA, pSVβ (Clonetech, Palo Alto, CA, USA), cultured and purified in-house using techniques described fully elsewhere (Ciccolini, Ayazi Shamlou, Titchener-Hooker, Ward, & Dunnill, 1999; Levy et al., 1999a,b, 2000b; Noites, O'Kennedy, Levy, Abidi, & Keshavarz-Moore, 1999). Calf thymus DNA is a good, short, double-stranded DNA system that has been used (Deng & Bloomfield, 1999; Geall, Eaton, Baker, Catterall, & Blagbrough, 1999; Geall & Blagbrough, 2000; Shapiro, Leng, & Fesenfeld, 1969) to replicate the behaviour of plasmid DNA in terms of stability during formulation. In experiments reported here we used poly-L-lysine to condense plasmid DNA and calf thymus DNA in order to assess their physical stability. Poly-L-lysine has been used by many groups in the past for DNA condensation in studies involving in vitro and in vivo transfection although there is a degree of uncertainty over whether or not poly-L-lysine is immunogenic (Deshmukh & Huang, 1997; Pouton et al., 1998).

Unless otherwise stated, all reagents were obtained from Sigma (Poole, Dorset, UK). Poly-L-lysine (PLL) HBr (average molecular weight 25,250) and DNA were dissolved in autoclaved TE buffer (10 mM TrisCl pH 8.0, 1 mM EDTA) to concentrations of 5 and 1 mg/ml, respectively, for use as stock solutions. 20 mM HEPES (*N*-[2-hydroxyethyl] piperazine-*N'*-[2-ethanesulfonic acid]) buffer was titrated with NaOH to pH 7.2, 7.7 and 8.0. Concentrated NaCl was then added to the solutions to give final salt concentrations of 10, 50, 100 or 150 mM NaCl. Working solutions of PLL at a concentration of 31.67 μg/ml (for a polyplex charge ratio of 2.0) and DNA at a concentration of 25 μg/ml were prepared with 20 mM HEPES at predetermined solution pH and salt concentrations.

The poly-L-lysine and DNA solutions were mixed using a vertically mounted syringe pump (Harvard Apparatus, Holliston, MA, USA). The pump had the capacity to deliver flow rates between 0.2 and 100 ml/min. Two standard Becton–Dickinson plastic syringes were each fitted with a three-way luer-lock adapter and 0.8 mm

internal diameter silicone tubing (Bio-Rad, Hercules, CA, USA). Equal volumes of DNA and PLL solutions were loaded into separate syringes and driven by the pump through a *T*-mixer. The mixture was collected either in a 10 mm round quartz cell (PCS8400; Malvern Instruments Ltd., Malvern, Worcester, UK) for particle size analysis or in a polystyrene Universal container (201152; Greiner Labortechnik Ltd, Stonehouse, UK) for determination of zeta potentials. Mixing rates of the PLL and DNA solutions were in the range of 2–17 ml/min. Additional experiments were conducted to assess the effects of solution pH and salt concentration. For the calculation of the positive charge equivalents of the cationic amino groups to negative charge equivalents of the nucleic acid component (the charge ratio), the average molecular weight per nucleotide molecule was taken as 330. In the case of polycation, it was assumed that the lysine residues each contributed a charge of +1 per dry molecular weight of 209. Filtered MilliQ (Millipore Ltd., Bedford, MA, USA) water was used in all of the following preparations.

The zeta potential (ζ) of the polyplexes was determined by laser Doppler spectrometry using a Malvern ZetaSizer (Model: 3000, Malvern Instruments Ltd, UK). The instrument was calibrated with a −55 mV standard (DTS5050; Malvern Instruments Ltd.) between measurements. Measurements were performed 5 times at 25°C, within 5 h of mixing, using ~4 ml of a polyplex suspension at a final DNA concentration of 12.5 μg/ml.

The particle size distributions of polyplexes were measured by dynamic light scattering (DLS). Photon correlation spectroscopy (PCS) has long been utilised as a sensitive optical technique to monitor the aggregation kinetics of complex particles (Kerker, 1969; Van de Hulst, 1957). The intensity of light scattered at a given angle from a visible laser beam is related to the Brownian motion of the scattering particles in suspension and is measured by a photon detector. This temporal fluctuation is analysed by a correlator which computes, in real time, the autocorrelation function to yield the effective translational diffusion coefficient, δ_{trans}. The apparent hydrodynamic diameter, D_H, of the polyplex particles is then determined from the Stokes–Einstein relation

$$\delta_{\text{trans}} = \frac{kT}{3\pi\mu D_H}, \tag{1}$$

where k is Boltzmann's constant, T is the absolute temperature of the sample, and μ is the viscosity of the solution.

Particle size measurements were made with a Malvern PCS4700 system (Malvern Instruments Ltd.) at a scattering angle of 90°. The cumulant mean size or "z-average" representing the hydrodynamic diameter of the polyplex particles was calculated using the "moments" method by the autocorrelation function analysis software of the instrument. The laser used was a diode-pumped, frequency-doubled, single-frequency laser (Series 142, Lightwave Electronics, Elliot Scientific Ltd., Hertfordshire, UK) with an output power of a 100 mW and wavelength of 532 nm. Given the power of the laser and the sensitivity of the instrument, the practical lower limit of accurate particle size detection is approximately of the order of 10 nm and the upper limit is about 1500–2000 nm. The size distributions were obtained from light-scattering profiles reported as the intensity of light scattered by polyplex particles in each size class. For each sample, particle size distribution measurements were made five times in succession with a counting time of ~300 s per measurement. All measurements were made at a set temperature of 25°C. At least two duplicates were performed for each measurement.

3. Results and discussion

In what follows we used measurements of the hydrodynamic diameter and zeta potential to analyse the physical stability of polyplexes prepared under different conditions. In attempting to explain our results from a theoretical viewpoint we used the well-established DLVO equations (Gregory, 1993; Hogg, Healy, & Fuerstenau, 1966; Hunter, 1981). In the absence of any previous information, we used a value for the Hamaker constant in the equation for van der Waals forces of attraction between two particles recommended for biological particles. We further assumed the polyplexes to be reasonably compact and spherical. Visual observations based on atomic force microscopy (Golan, Hsieh, Hsieh, & Hansma, 1999; Hansma et al., 1998; Wolfert & Seymour, 1996) and electron microscopy (Laemmli, 1975; Wagner, Cotten, Foisner, & Brinstiel, 1991) suggest that these assumptions are likely to give rise to some uncertainty regarding the absolute values of the calculated total potential energy of interaction between the particles. Nevertheless, the simulations provide a basis for comparison of the stability of different systems. More importantly, the DLVO theory allows the assessment of the superimposed effect of important process and material parameters affecting the stability of the formulation. This is very difficult to envisage intuitively given the large number of parameters that are known to influence the stability of the polyplex formulations. These parameters include the initial particle size distribution, ionic strength and pH of the solution, zeta potential of the polyplexes, temperature and presence of any protective colloids. Another factor that can be important is the viscous drag forces on the polyplexes resulting from the mixing of the colloidal suspension. The effect of this force on the stability of the polycation-DNA complexes will depend on the ratio of the viscous drag force to the total interaction force between the condensed particles (Wilson & French,

1978). Slow mixing characterised by a relatively low viscous drag force can cause the polyplex particles to aggregate by increasing the frequency of collisions between them. In contrast, intense mixing can give rise to viscous drag forces sufficiently high to break the aggregates.

In the present investigation, following mixing of the DNA solution with the poly-L-lysine solution in the *T*-mixer of the syringe pump assembly, the suspension was collected and stored under quiescent conditions in a cuvette or universal for subsequent particle analysis. Initial experiments (data not shown) indicated that for flow rates between 2 and 17 ml/min the average hydrodynamic diameter of the polyplexes was effectively independent of flow rate. In the discussion that follows it is assumed that viscous drag forces were absent during our measurements and the only hydrodynamic force causing aggregation is due to the Brownian motion of the polyplex particles. This is thought to closely represent the actual formulation in a vial under storage and transportation and is therefore selected as the focus of attention in the present investigation. The effects of the viscous drag force on the physical stability of polycation-DNA complexes will be the subject of a separate publication.

The total interaction energy, V_T, between the particles was obtained by summing the van der Waals attractive potential, V_A, and the repulsive double-layer electrostatic potential, V_R. We used the following equation given by Elimelich et al. (Elimelich, Gregory, Jia, & Williams, 1995) to calculate V_A:

$$V_A = -\frac{A}{12}\left[\frac{y}{x^2+xy+x} + \frac{y}{x^2+xy+x+y} + 2\ln\left(\frac{x^2+xy+x}{x^2+xy+x+y}\right)\right], \tag{2}$$

where $x = (H/a_1 + a_2)$ and $y = a_1/a_2$. A is the Hamaker constant, assumed to have a value of 5×10^{-21} J, which is within the range recommended for biological materials (Gregory, 1993). In Eq. (2), H is the separation distance between the surfaces of two spherical particles of radii a_1 and a_2. The electrical double-layer repulsive force was calculated from the following expression (Gregory, 1993):

$$V_R = \frac{64\pi\varepsilon a_1 a_2 k^2 T^2 \gamma_1 \gamma_2}{(a_1 + a_2)e^2 z^2} \exp[-\kappa H], \tag{3}$$

where ε is the permittivity of the medium, k the Boltzmann constant, T the absolute temperature, and e the elementary charge. The dimensionless functions, γ_1 and γ_2, of the zeta potentials ζ_1 and ζ_2, respectively, are given by

$$\gamma_i = \frac{\exp[ze\zeta/2kT] - 1}{\exp[ze\zeta/2kT] + 1}. \tag{4}$$

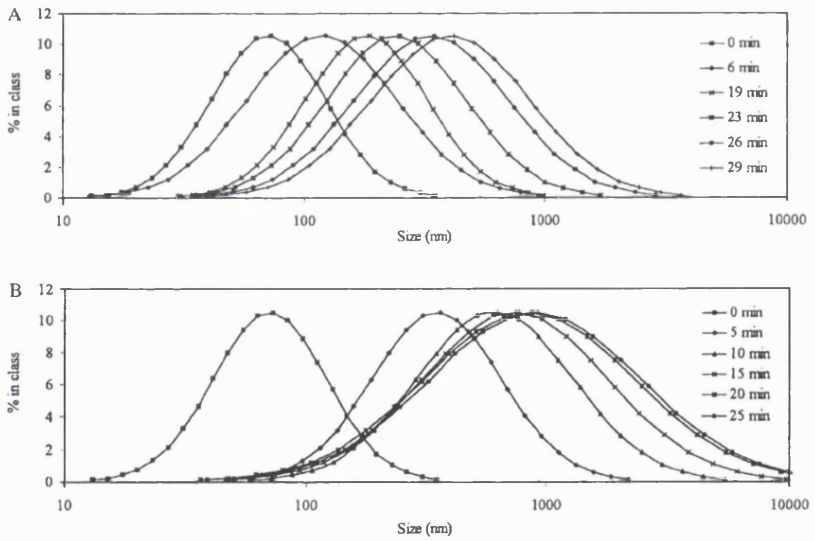

Fig. 1 . Size distributions of: (A) polylysine-pSVβ complexes and (B) polylysine-calf thymus DNA complexes after various time periods following addition of NaCl to a molarity of 150 mM. The polyplex sample was prepared in 20 mM HEPES pH 7.2 at a mixing rate of 6 ml/min, and the appropriate amount of 3 M NaCl was pipetted into the cell immediately after the first measurement (i.e. "0 min"). The data plots for a typical particle size distribution, determined by the software as mean of diameter based on intensity of scattered light, are shown. The size distributions show single 90° measurements.

In Eq. (3), κ is the Debye–Hückel reciprocal length given by

$$\kappa = 0.329 \times 10^{10} \sqrt{cz^2} \quad (\mathrm{m}^{-1}), \tag{5}$$

where c is the concentration of the ionic species in solution and z the valency of the ions (a symmetrical z–z electrolyte was assumed in the present study).

Typical size distribution plots obtained by PCS as a function of time following the mixing of a DNA solution with poly-L-lysine are shown in Fig. 1. The data refer to experiments carried out with both plasmid DNA (Fig. 1A) and calf thymus DNA (Fig. 1B). Details of the experimental conditions are given in the caption. The initial size distribution of the stable polyplex particles in HEPES buffer containing no added salt is represented by the data shown as "$t = 0$ min". Thereafter, the salt concentration of the sample was adjusted rapidly to the desired level by manually injecting the required volume of concentrated NaCl solution into the glass cell containing the sample in the PCS instrument. Measurements of particle size were made continually and the results displayed at fixed intervals shown in each plot. The data in Fig. 1 show that polyplexes in high salt concentration solutions are strongly aggregating. In each case, the experimental data were mathematically fitted, yielding the smooth curves drawn through the data point. For the purpose of assessing the particle size distributions, we conducted two sets of analysis based on the cumulants method and the CONTIN "constrained regularisation" algorithm (Provencher, 1979). The latter is recommended for broad, irregularly shaped distributions, where the method of cumulants is less applicable. Treatment of the experimental particle size distribution data using both methods yielded similar results indicating that the size distributions were practically monomodal. The broadening of the size distribution as a function of time corresponds to increasing polydispersity of the sample, which is associated with the variance of the population. The polydispersity index, estimated by cumulants analysis of the DLS data, has a maximum value of 1.0, with a value of 0.70 representing a highly polydisperse distribution. In Fig. 1, the polydispersity indices of about 0.2–0.3 for a sample analysed before addition of the concentrated NaCl, $t = 0$ min, and ~ 0.4 for the following measurement, $t = 6$ min in the case of data in Fig. 1A and $t = 5$ min for the case of Fig. 1B, indicate fairly narrow size distributions of the polyplexes. In contrast, the polydispersity values increased to about 0.7–0.9 for a sample analysed nearly 30 min after addition of the salt. It will be shown later that aggregation in polydisperse systems is particularly marked.

In the following discussion, the particle size distributions are plotted in terms of the z-average hydrodynamic diameter. In Fig. 2, the experimental z-average diameter data are plotted against the elapsed time following the mixing of the DNA solutions with the poly-L-lysine solution in the T-mixer of the syringe pump. Polyplexes composed of DNA of different types, that is, calf thymus DNA and plasmid DNA, have similar aggregating characteristics, although polylysine–plasmid DNA complexes aggregate less quickly than their calf thymus DNA counterparts. The data in Fig. 3 refer to experiments carried out at a fixed mixing rate of 6 ml/min and show that ionic strength and pH of the suspension critically determine the physical stability of the poly-L-lysine-DNA complexes. With the exception of the suspension containing the 10 mM NaCl at the lowest pH, all systems examined showed an increase in the z-average hydrodynamic diameter as a function of time. The rate of aggregation increased with increasing ionic strength and increasing pH. At a pH of 8.0, even the suspension containing 10 mM NaCl exhibited a degree of aggregation as shown in Fig. 3C.

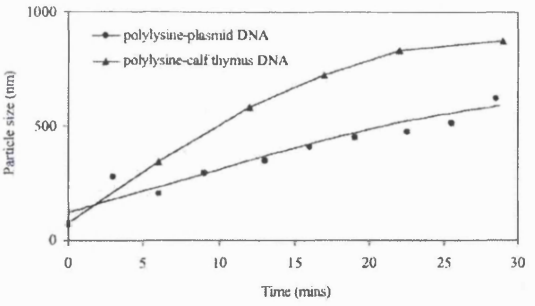

Fig. 2. Particle size of polyplexes composed of DNA of different types (calf thymus DNA and plasmid DNA, pSVβ) and poly-L-lysine as a function of time. The polyplexes were prepared in 20 mM HEPES pH 7.2 at a charge ratio of 2 and mixing rate of 6 ml/min. The appropriate amount of 3 M NaCl was pipetted into the cell immediately after the first measurement to adjust the molarity to 150 mM NaCl.

Measurements of particle size distributions were made on poly-L-lysine-DNA complexes of different charge ratios in 20 mM HEPES buffer at a pH of 7.7. These measurements (data not shown) demonstrated that the z-average hydrodynamic diameter of the polyplexes was about 140 nm ($\pm$ 20 nm) for a charge ratio of 1.0 and 90 nm ($\pm$ 20 nm) for a charge ratio of 2.0. Data plotted in Fig. 4 show that the zeta potentials of the polylysine-DNA complexes is controlled by both the pH of the solution and the charge ratio. All subsequent experiments including those plotted in Figs. 1 to 3 were carried out at a charge ratio of 2.0 indicating a positively charged polyplex suspension. Decreasing the pH of this system increased the protonation of the lysine amino groups which have an intrinsic pK_a value of 11.1 (Creighton, 1993). The expected effect is an increase in the stability of the suspension, which is supported by the data shown in Fig. 3 and the theoretical predictions of the total potential energy of interaction based on Eqs. (2)–(5), as shown in Fig. 5.

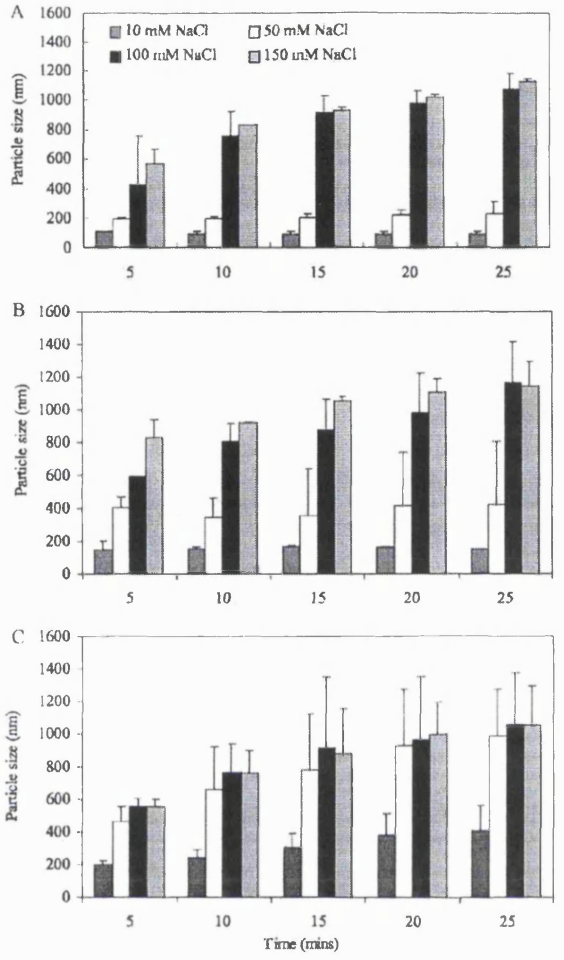

Fig. 3. Size of polylysine-calf thymus DNA complexes as a function of time with ionic strength as a parameter. The complexes were prepared in 20 mM HEPES at a mixing rate of 6 ml/min. Suspending solutions of: (A) pH 7.2, (B) pH 7.7, and (C) pH 8.0 were used. The mean ± standard error of two separate experiments is shown.

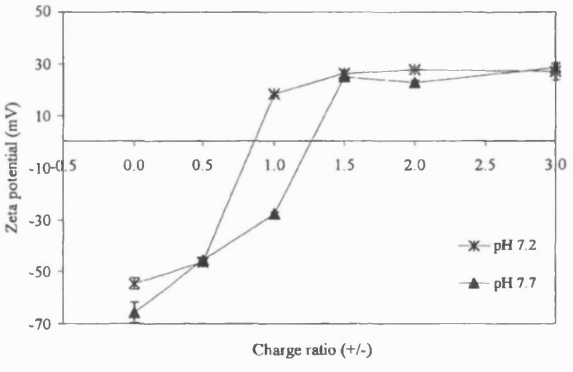

Fig. 4. Zeta potentials of polylysine-calf thymus DNA complexes as a function of the charge ratio. Data refer to polyplexes in 20 mM HEPES buffer of pH 7.2 (*) and pH 7.7 (▲). The polyplex formulation was prepared by mixing equal volumes of calf thymus DNA (25 μg/ml) and polylysine of the appropriate concentration.

The theoretical total interaction energy curves predicted for mono-size particles with an initial mean diameter of 120 nm suspended in solutions containing 10, 50, 100 and 150 mM NaCl are shown in Fig. 6. Calculations, using Eq. (5), and shown as the inset to Fig. 6, indicate that as the ionic strength is increased, the electrical double layer around the particles, given by the Debye–Hückel length, decreases. Evidence from other sources also indicates that with increasing electrolyte concentration the surface charges are screened (Rustemeier & Killmann, 1997). These effects cause the repulsive force between the particles to decrease. Consequently, the total potential energy barrier between the particles decreases and the system becomes more aggregating. This is consistent with the data shown in Fig. 3.

In the presence of a population of polyplexes of different sizes, for example, the case shown in Fig. 1, it is of considerable interest to analyse the tendency for aggregation. Theoretical potential energy curves are shown in Fig. 7 for two such cases. Fig. 7A refers to binary aggregation involving two particles each with a diameter of 50 nm and between a 50 nm particle and larger ones of 120, 500 and 900 nm. Fig. 7B is a similar plot showing binary aggregation for a 120 nm particle. It is notable that aggregation is particularly strong between particles of 50 and 120 nm in diameter. At values of potential energy of interaction less than about 5 to $10kT$, colloidal aggregation becomes noticeable (Hunter, 1981). According to the plots in Fig. 7, therefore, interactions between the 50 nm particle and all of the other particles are likely to cause aggregation although the lowest potential energies are observed between the smallest particles. Interaction energies greater than $15kT$, such as that occurring between the 120 nm particles and particles of 500 and 900 nm, render aggregation between these particles unlikely. These simulations are instructive in guiding process design for creating stable formulations with acceptable shelf life. For example, they suggest that the aggregation between small particles is expected to be rapid and the largest particles with their high surface area, if present, act as strong particle "collectors", sweeping the smallest particles quickly from the system. The elimination of such large particles from the formulation and stabilisation of small particles against aggregation must therefore be a priority in the design of preparation methods for gene-based drug formulations.

Comparison of the plots shown in Figs. 7A and B for equal size particles show that the potential-energy barrier falls as particle diameter decreases. Additionally, binary aggregation between small particles of different diameters, e.g. between 50 and 120 nm particles, is particularly strong. It is therefore important to reduce the probability of aggregation of the small particles in the formulation. The data plotted in Fig. 3, and the simulations in Fig. 6, indicate that preparation under conditions

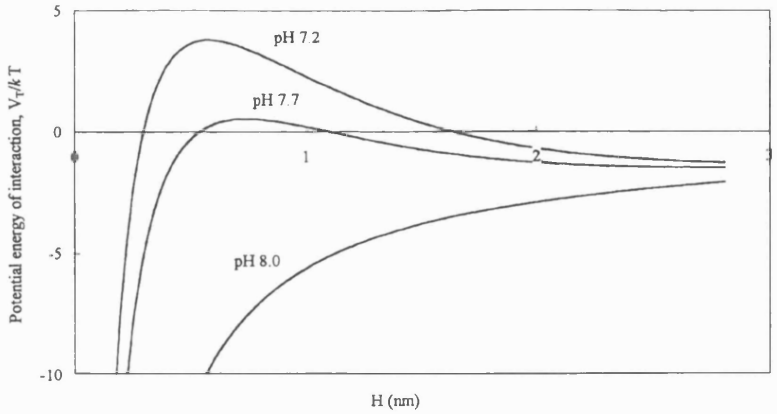

Fig. 5. Influence of pH on the dimensionless total potential energy of interaction between 2 spherical particles of 120 nm diameter; salt concentration 150 mM [NaCl]. pH 7.2, 7.7 and 8.0 correspond to the experimentally ascertained zeta potentials of 22, 19 and 5 mV, respectively.

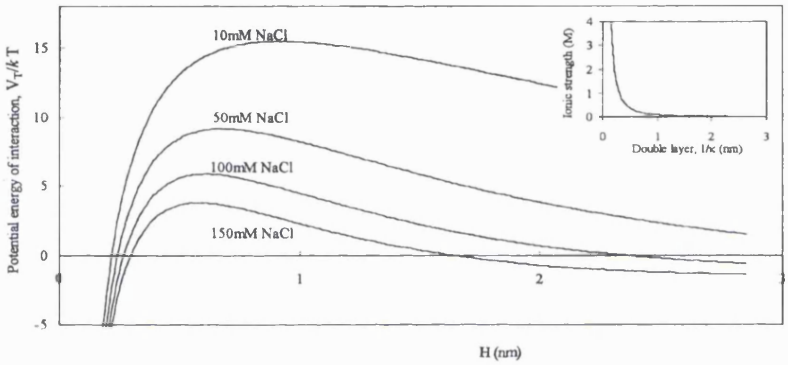

Fig. 6. Influence of electrolyte concentration on the dimensionless total potential energy of interaction between 2 spherical particles of 120 nm diameter, at pH 7.2 (ζ potential = 22 mV), as a function of the distance H between their surfaces. The inset shows ionic strength dependence of the thickness of the double layer according to the DLVO theory.

of low ionic strength can significantly reduce aggregation. However, once injected into the patient, aggregation is expected to occur in response to the elevated ionic strength corresponding to the physiological conditions in the body, this being generally about 150 mM and pH 7.4 representative of the environment in the cytoplasm.

Examination of Eqs. (2)–(5) provides further insight into possible ways for controlling the physical stability of the formulation. For example, according to Eq. (4), lowering the temperature increases the repulsion barrier between all particles, resulting in a reduction of their tendencies for aggregation. The theoretical interaction energy plots are shown in Fig. 8. In the present study, we did not measure the effect of temperature on the physical stability of the polyplex particles. However, the implication of the simulations shown in Fig. 8 is that lowering the temperature during the mixing step as well as maintaining a low temperature during transportation and storage can confer a degree of stability on the formulation. However, considering the kT values plotted in Fig. 8, low temperature alone is unlikely to eliminate aggregation completely. Lyophilization of polyplex formulations, or their freezing in the presence of excipients, has been suggested as a means of avoiding aggregation during shipping and storage. This method of preparation nevertheless is unlikely to be satisfactory on a large scale and has the risk of damaging the supercoiled plasmid upon thawing (Anchordoquy, 1999a,b).

Finally, according to the classical theories of colloid science, stabilisation of the polyplexes may be achieved by modification of the surface properties of the particles by, for example, steric interaction. The molecular weight of the poly-L-lysine used in our experiments was $\sim$ 25,000, relatively low for steric stabilisation to have an effect. Experiments with charged latex particles stabilised by poly-L-lysine (Rustemeier & Killmann, 1997) of different molecular weights have been reported. These experiments showed that at molecular weights of poly-L-lysine greater than about 100,000 steric interaction was caused by the poly-L-lysine molecules, resulting in the

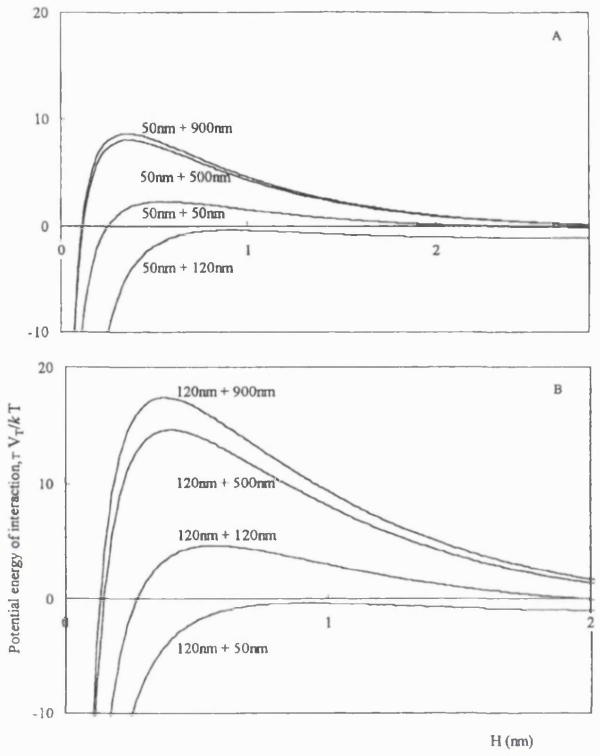

Fig. 7. Influence of particle diameter on the dimensionless total potential energy of interaction between two spherical particles of: (A) 50 nm and (B) 120 nm diameter at pH 7.2 (ζ potential 22 mV), 150 mM [NaCl].

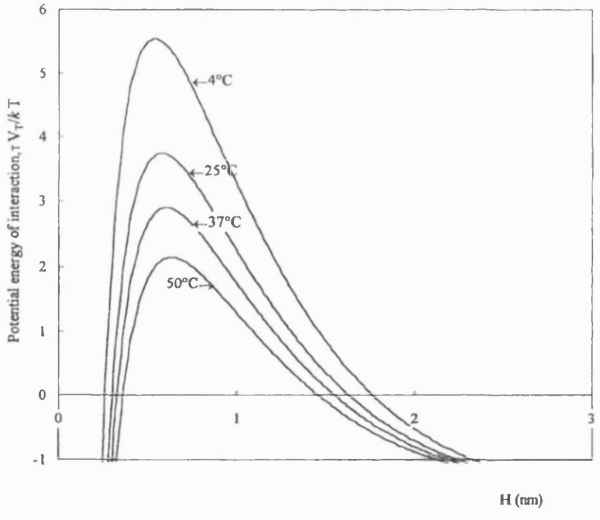

Fig. 8. Influence of the temperature on the dimensionless total potential energy of interaction between 2 particles of 120 nm diameter at pH 7.2 (ζ potential 22 mV), 150 mM [NaCl].

stabilisation of the suspension against aggregation. Additionally, measurements of size and zeta potential (Killmann & Sapuntzjis, 1994; Vandorpe et al., 1996) have shown that high molecular weight adsorbed particles, such as neutral polyethylene oxides and its copolymers, have the potential to stabilise charged latex nanoparticles. Recent experiments with various formulations of gene-delivery systems containing polyethylene glycol have been reported which suggest that stabilisation of the polyplex particles may be possible by this mechanism (Choi, Liu, Choi, Kim, & Park, 1999; Hisayasu et al., 1999; Ogris, Brunner, Schüller, Kircheis, & Wagner, 1999).

4. Conclusion

The capacity of plasmid DNA to deliver safely and efficiently exogenous genetic materials to human cells and tissues for therapy and vaccination is limited by many factors (Luo & Saltzman, 2000). One that is known to limit clinical applications is the stability of polycation-DNA formulations. In this paper we have presented experimental data and provided a theoretical basis for the assessment of factors that influence the physical stability of polyplexes as an example of a typical gene formulation. Our analysis shows that aggregation is a complex function of many parameters, including ionic strength and pH of the solution, and the initial size distribution of the particles. The stability of the gene delivery formulations may be described through established equations of colloid science. These show that formulations are susceptible to aggregation, especially under physiological conditions of the body. However, during processing and storage, the physical stability of the formulations can be enhanced significantly by the creation of conditions that lead to monodisperse particles in a low pH, ionic strength, and temperature environment. Experimental evidence from other sources (Maruyama, Takahashi, Tagawa, Nagaike, & Iwatsu, 1997; Ogris et al., 1999) indicates that formulation stability may be improved through steric interactions, for example by conjugation of stabilising agents such as polyethylene glycol to the polyplexes.

Notation

a_1, a_2	radii of primary particles 1 and 2, m
A	Hamaker constant, J
c	ionic concentration, M
D_H	particle hydrodynamic diameter, m
e	charge on electron (1.6×10^{-19} C)
H	separation distance between two primary particles, m
k	Boltzmann's constant (1.381×10^{-23} J/K)
T	absolute temperature, K
V_A, V_R, V_T	interaction energies (van der Waals' attraction, electrical repulsion and total interaction), J

x dimensionless ($= (H/a_1 + a_2)$)
y dimensionless ($= a_1/a_2$)
z valence (charge number) of the ionic species

Greek letters

γ_1, γ_2 dimensionless functions of zeta potentials in Eq. (4)
δ_{trans} translational diffusion coefficient, m^2/s
ε permittivity, dimensionless
ζ_1, ζ_2 zeta potentials of particles 1 and 2
κ Debye–Hückel parameter, defined in Eq. (5)
μ dynamic viscosity of liquid, kg/ms

References

Adami, R. C., Collard, W. T., Gupta, A. A., Kwok, K. Y., Bonadio, J., & Rice, K. G. (1998). Stability of peptide-condensed plasmid DNA formulations. *Journal of Pharmaceutical Sciences, 87*, 678–683.

Alton, E. W., Stern, M., Farley, R., Jaffe, A., Chadwick, S. L., Phillpis, J., Davies, J., Smith, S. N., Browning, J., Davies, M. G., Hodson, M. E., Durham, S. R., Li, D., Jeffery, P. K., Scallan, M., Balfour, R., Eastman, S. J., Cheng, S. J., Smith, A. E., Meeker, D., & Geddes, D. M. (1999). Cationic lipid-mediated CFTR gene transfer to the lungs and nose of patients with cystic fibrosis: A double-blind placebo-controlled trial. *Lancet, 353*, 947–954.

Anchordoquy, T. J. (1999a). Nonviral gene delivery systems, Part 1: Physical stability. *Biopharm, 12*, 42 (6 pages).

Anchordoquy, T. J. (1999b). Nonviral gene delivery systems, Part 2: Physical characterisation. *Biopharm, 12*, 46 (4 pages).

Anderson, W. F. (1998). Human gene therapy. *Nature, 392*(Suppl), 25–30.

Bloomfield, V. A. (1991). Condensation of DNA by multivalent cations: Considerations on mechanism. *Biopolymers, 31*, 1471–1481.

Bloomfield, V. A., & Rau, D. C. (1980). Polyelectrolyte effects in DNA condensation by polyamines. *Biophysical Chemistry, 11*, 339–343.

Choi, Y. H., Liu, F., Choi, J. S., Kim, S. W., & Park, J. S. (1999). Characterization of a targeted gene carrier, lactose–polyethylene glycol–grafted poly-L lysine, and its complex with plasmid DNA. *Human Gene Therapy, 10*, 2657–2665.

Ciccolini, L. A. S., Ayazi Shamlou, P., Titchener-Hooker, N. J., Ward, J. M., & Dunnill, P. (1999). Rheological properties of chromosomal and plasmid DNA during alkaline lysis reaction. *Bioprocess Engineering, 21*, 231–237.

Creighton, T. E. (1993). *Proteins: structure and molecular properties*. New York: W. H. Freeman and Company.

Crook, K., McLachlan, G., Stevenson, B. J., & Porteous, D. J. (1996). Plasmid DNA molecules complexed with cationic liposomes are protected from degradation by nucleases and shearing by aerosolisation. *Gene Therapy, 3*, 834–839.

Deng, H., & Bloomfield, V. A. (1999). Structural effects of cobalt–amine compounds on DNA condensation. *Biophysical Journal, 77*, 1556–1561.

Deshmukh, H. M., & Huang, L. (1997). Liposome and polylysine mediated gene transfer. *New Journal of Chemistry, 21*, 113–124.

Duguid, J. G., Shi, M., Logan, M. J., Alila, H., Rolland, A., Tomlinson, E., Sparrow, J. T., Smith, L. C., & Li, C. (1998). A physicochemical approach for predicting the effectiveness of peptide-based gene delivery systems for use in plasmid-based gene therapy. *Biophysical Journal, 74*, 2802–2814.

Dunlap, D., Maggi, A., Soria, M. R., & Monaco, L. (1997). Nanoscopic structure of DNA condensed for gene delivery. *Nucleic Acids Research, 25*, 3095–3101.

Elimelich, M., Gregory, J., Jia, X., & Williams, R. A. (1995). *Particle deposition and aggregation: measurement, modelling and simulation*. Oxford: Butterworth-Heinemann Ltd.

Geall, A., Eaton, M. A. W., Baker, T., Catterall, C., & Blagbrough, I. S. (1999). The regiochemical distribution of positive charges along cholesterol polyamine carbamates plays significant roles in modulating DNA binding affinity and lipofection. *FEBS, 459*, 337–342.

Geall, A. J., & Blagbrough, I. S. (2000). Rapid and sensitive ethidium bromide fluorescence quenching assay of polyamine conjugate-DNA interactions for the analysis of lipoplex formation in gene therapy. *Journal of Pharmaceutical and Biomedical Analysis, 22*, 849–859.

Golan, R., Hsieh, W., Hsieh, W., & Hansma, H. G. (1999). DNA toroids: stages in condensation. *Biochemistry, 38*, 14069–14076.

Gosule, L. C., & Schellman, J. A. (1976). Compact form of DNA induced by spermidine. *Nature, 259*, 333–335.

Gregory, J. (1993). Stability and flocculation of suspensions. In P. Ayazi Shamlou (Ed.), *Processing of solid–liquid suspensions*. pp. 59–92. Oxford: Butterworth-Heinemann Ltd.

Hansma, H. G., Golan, R., Hsieh, W., Lollo, C. P., Mullen-Ley, P., & Kwoh, D. (1998). DNA condensation for gene therapy as monitored by atomic force microscopy. *Nucleic Acids Research, 26*, 2481–2487s.

Hart, S. L. (1999). Integrin-mediated vectors for gene transfer and therapy. *Current Opinion in Molecular Therapeutics, 1*, 197–203.

Hart, S. L. (2000). Synthetic vectors for gene therapy. *Expert Opinions on Therapy Patents, 10*, 199–208.

Hisayasu, S., Miyauchi, M., Akiyama, K., Gotoh, T., Satoh, S., & Shimada, T. (1999). In vivo targeted gene transfer into liver cells mediated by a novel galactosyl-D-lysine/D-serine copolymer. *Gene Therapy, 6*, 689–693.

Hogg, R., Healy, T. W., & Fuerstenau, D. W. (1966). Mutual coagulation of colloidal dispersions. *Transactions of Faraday Society, 62*, 1638–1651.

Horn, N. A., Marquet, M., Meek, J. A., & Budahazi, G. (1995). [WO96/21729]. Ref Type: Patent.

Hunter, R. J. (1981). *Zeta potential in colloid science*. New York: Academic Press.

Kerker, M. (1969). *The scattering of light and other electromagnetic radiation*. New York: Academic Press.

Killmann, E., & Sapuntzjis, P. (1994). Dynamic light scattering of polystyrene latex and silica with adsorbed poly(ethylene oxide) layers — influence of ionic strength and coverage. *Colloids and Surfaces A: Physicochemical and Engineering Aspects, 86*, 229–238.

Kircheis, R., Schüller, S., Brunner, S., Ogris, M., Heider, K.-H., Zauner, W., & Wagner, E. (1999). Polycation-based DNA complexes for tumor-targeted gene delivery in vivo. *Journal of Gene Medicine, 1*, 11–120.

Laemmli, U. K. (1975). Characterization of DNA condensates induced by poly(ethylene oxide) and polylysine. *Proceedings of the National Academy of Science USA, 72*, 4288–4292.

Lai, W. C., & Bennett, M. (1998). DNA vaccines. *Critical Reviews in Immunology, 18*, 449–484.

Levy, M. S., Ciccolini, L. A. S., Yim, S. S. S., Tsai, J. T., Titchener-Hooker, N., Ayazi Shamlou, P., & Dunnill, P. (1999b). The effects of material properties and fluid flow intensity on plasmid DNA recovery during cell lysis. *Chemical Engineering Science, 54*, 3171–3178.

Levy, M. S., Collins, I. J., Tsai, J. T., Ayazi Shamlou, P., Ward, J. M., & Dunnill, P. (2000b). Removal of contaminant nucleic acids by nitrocellulose filtration during pharmaceutical-grade plasmid DNA processing. *Journal of Biotechnology, 76*, 197–205.

Levy, M. S., Collins, I. J., Yim, S. S., Ward, J. M., Titchener-Hooker, N., Ayazi Shamlou, P., & Dunnill, P. (1999a). Effect of shear on plasmid DNA in solution. *Bioprocess Engineering, 20*, 7–13.

Levy, M. S., O'Kennedy, R. D., Ayazi Shamlou, P., & Dunnill, P. (2000a). Biochemical engineering approaches to the challenges of producing pure plasmid DNA. *Trends in Biotechnology, 18*, 296–305.

Luo, D., & Saltzman, W. M. (2000). Synthetic DNA delivery systems. *Nature Biotechnology, 18*, 33–37.

Maruyama, K., Takahashi, N., Tagawa, T., Nagaike, K., & Iwatsu, M. (1997). Immunoliposomes bearing polyethyleneglycol-coupled Fab' fragment show prolonged circulation time and high extravasation into targeted solid tumors in vivo. *FEBS, 413*, 177–180.

Noites, I. S., O'Kennedy, R. D., Levy, M. S., Abidi, N., & Keshavarz-Moore, E. (1999). Rapid quantitation and monitoring of plasmid DNA using an ultrasensitive DNA-binding dye. *Biotechnology and Bioengineering, 66*, 196–201.

Ogris, M., Brunner, S., Schüller, S., Kircheis, R., & Wagner, E. (1999). PEGylated DNA/transferrin-PEI complexes: reduced interaction with blood components, extended circulation in blood and potential for systemic gene delivery. *Gene Therapy, 6*, 595–605.

Pouton, C. W., Lucas, P., Thomas, B. J., Uduehi, A. N., Milroy, D. A., & Moss, S. H. (1998). Polycation-DNA complexes for gene delivery: a comparison of the biopharmaceutical properties of cationic polypeptides and cationic lipids. *Journal of Controlled Release, 53*, 289–299.

Prazeres, D. M. F., Schluep, T., & Cooney, C. (1998). Preparative purification of supercoiled plasmid DNA using anion-exchange chromatography. *Journal of Chromatography A, 806*, 31–45.

Provencher, S. W. (1979). Inverse problems in polymer characterization; direct analysis of polydispersity with photon correlation spectroscopy. *Makromolekulare Chemie, 180*, 201–209.

Rolland, A. P. (1998). From genes to gene medicines: recent advances in nonviral gene delivery. *Critical Reviews and Therapy in Drug Carrier Systems, 15*, 143–198.

Ross, P. C., & Hui, S. W. (1999). Lipoplex size is a major determinant of in vitro lipofection efficiency. *Gene Therapy, 6*, 651–659.

Rustemeier, O., & Killmann, E. (1997). Electrostatic interactions and stability of poly-L-lysine covered polystyrene latex particles investigated by dynamic light scattering. *Journal of Colloid and Interface Science, 190*, 360–370.

Shapiro, J. T., Leng, M., & Fesenfeld, G. (1969). Deoxyribonucleic acid-polylysine complexes. Structure and nucleotide specificity. *Biochemistry, 8*, 3219–3232.

Tang, M. X., & Szoka, F. C. (1997). The influence of polymer structure on the interactions of cationic polymers with DNA and morphology of the resulting complexes. *Gene Therapy, 4*, 823–832.

Tsai, J. T., Keshavarz-Moore, E., Ward, J. M., Hoare, M., Ayazi Shamlou, P., & Dunnill, P. (1999). Characterisation of plasmid DNA conjugates as a basis for their processing. *Bioprocess Engineering, 21*, 279–286.

Van de Hulst, H. C. (1957). *Light scattering by small particles*. New York: Wiley.

Vandorpe, J., Schacht, E., Stolnik, S., Garnett, M. C., Davies, M. C., Illum, L., & Davies, S. S. (1996). Poly(organo phosphazene) nanoparticles surface modified with poly(ethylene oxide). *Biotechnology and Bioengineering, 52*, 89–95.

Wagner, E., Cotten, M., Foisner, R., & Brinstiel, M. L. (1991). Transferrin-polycation-DNA complexes: The effect of polycations on the structure of the complex and DNA delivery to cells. *Proceedings of the National Academy of Science USA, 88*, 4255–4259.

Whitmore, M., Li, S., & Huang, L. (1999). LPD lipopolyplex initiates a potent cytokine response and inhibits tumor growth. *Gene Therapy, 6*, 1867–1875.

Wilson, D. J., & French, R. H. (1978). Kinetic and equilibrium aspects of floc coagulation. II. Slow mixing criteria. *Separation Science and Technology, 13*, 95–106.

Wolfert, M. A., & Seymour, L. W. (1996). Atomic force microscopic analysis on the influence of the molecular weight of poly(L)lysine on the size of polyelectrolyte complexes formed with DNA. *Gene Therapy, 3*, 269–273.

Zelphati, O., Nguyen, C., Ferrari, M., Felgner, J., Tsai, Y., & Felgner, P. L. (1998). Stable and monodisperse lipoplex formulations for gene delivery. *Gene Therapy, 5*, 1272–1282.

BIOPHYSICAL CHARACTERIZATION OF AN INTEGRIN-TARGETED NON-VIRAL VECTOR FOR PULMONARY GENE DELIVERY

L. K. Lee, K. E. Siapati*, R. G. Jenkins†, R. J. McAnulty†, S. L. Hart*, P. Ayazi Shamlou
The Advanced Centre for Biochemical Engineering, Department of Biochemical Engineering, University College London, Torrington Place, London WC1E 7JE, England
* Molecular Immunology Unit, Institute of Child Health, University College London Medical School, 30 Guilford Street, London WC1N 0NN, England
† Centre for Cardiopulmonary Biochemistry and Respiratory Medicine, Royal Free and University College Medical School, University College London, Rayne Institute, 5 University Street, London WC1E 6JJ, England

ABSTRACT

Formulation of recombinant plasmid DNA carrying therapeutic genes for human gene therapy, gene replacement and DNA vaccination continues to be a major research goal with the aim of increasing the transfection efficiency. Here we present new data on the biophysical properties of an integrin-targeted plasmid DNA formulation and demonstrate the effects of these properties on *in vitro* transfection of COS-7 cells and *in vivo* transfection using a murine model. We provide experimental evidence for a significant increase in the level and duration of transgene expression for lipopolyplexes prepared in distilled water at DNA concentrations of up to 160 μg/ml and show strong evidence for the biophysical stability of these complexes. The albumin concentration in the local microenvironment of the lung is typically of the order of 0.2 mg/ml. Our results show that lipopolyplexes prepared in distilled water and containing bovine serum albumin (BSA) remain stable at BSA concentrations below 5 mg/ml. Additionally, our experimental data indicate that the presence of dextrose at 5% w/v in the transfection solution has no detectable effect on complex stability. The physical instability of lipopolyplexes prepared in buffers including phosphate-buffered saline is graphically illustrated by their aggregation profiles and is a major cause for their low transfection activity.

Keywords: mouse lung, photon correlation spectroscopy, gene therapy, colloidal interactions, lipopolyplex, integrin-mediated transfection

INTRODUCTION

Viral vectors have been popular in early research on delivery of therapeutic genes to cells because it has been possible to quickly progress to animal studies. However, non-viral systems are showing promise, and in particular their capacity to transfer large gene constructs and their ability to deliver these with a lower risk of immune response have made them the subject of intense research (Leitner *et al.*, 2000; Roth and Yarmush, 1999; Smith *et al.*, 1997). Additionally, gene therapy with large DNA molecules, including artificial chromosomes, is likely to grow to deal with the need for selective targeting and control of gene action. Artificial mammalian chromosomes also have the capacity to eliminate concerns of random insertion of genetic material by viral vectors and provide the motivation for continuing with efforts to overcome the problems of establishing synthetic gene delivery systems (Compton *et al.*, 2000; Willard, 1998).

Many different plasmid DNA-based delivery systems have been proposed over the past two decades and several are being actively pursued (Chesnoy and Huang, 2000; Kabanov, 1999; Luo and Saltzman, 2000; Tomlinson and Rolland, 1996). Cationic liposomes (Felgner *et al.*, 1994) are clinically well tolerated with few side effects and the resulting complexes have been used for *in vivo* transfection of cells in the lungs, arterial wall and brain, as well as ex vivo cultured primary cells derived from several tissues including cultured muscle cells (Armeanu *et al.*, 2000; Ennist, 1999; Kichler *et al.*, 1998; Kim *et al.*, 1997; Lam and Breakefield, 2001; Lee *et al.*, 1998). However, in comparison with recombinant viral vectors, transfection efficiencies have remained disappointingly low, typically 10% for primary hepatocytes and myoblasts (Chemin *et al.*, 1998; Liang *et al.*, 2000; Nishikawa *et al.*, 1998). In some cases, improvements in transfection have been achieved by the inclusion of other components into the formulation. For example, Hart *et al* (Hart *et al.*, 1998) have used the transfection agent Lipofectin which consists of a 1:1 (w/w) mixture of the cationic liposome DOTMA (*N*-[1-(2,3,-dioleyloxy)propyl]-*N*,*N*,*N*-trimethylammonium chloride) and DOPE (dioleoyl phosphatidylethanolamine). Further improvements in transfection have been achieved by providing cationic liposomes with a degree of cell specificity. For example, monoclonal antibodies that specifically recognise a cell-surface antigen have been used to produce a receptor-mediated gene delivery system with improved transfection (Ferkol and Davis, 2001; Wang and Huang, 1989). A host of cell-surface ligands including transferrin, asialoglycoproteins, immunoglobulins, sugars and insulin have been used while many different DNA-binding moieties including poly-L-lysine, protamines, histones, DNA intercalating agents and high-mobility group 1 proteins (HMG1) have been examined (Lee and Huang, 1996; Li *et al.*, 1998; McKee *et al.*, 1994; Wagner *et al.*, 1991).

Integrins are cell-surface glycoproteins that have been identified as potential targets for gene delivery (Aris *et al.*, 2000; Li *et al.*, 2000) because of their exploitation of cell entry by different viruses including adenovirus, echovirus and foot-and-mouth disease virus (Jackson *et al.*, 2000; McDonald *et al.*, 1999). We have developed a novel peptide containing a positively charged 16-lysine tail that binds and condenses DNA, and a cyclic domain that recognises $\alpha 5\beta 1$ integrins which are expressed on many cells including epithelial cells, airway fibroblasts, smooth muscle cells and hematopoetic cells (Hart *et al.*, 1995). The basic components of our synthetic vector are therefore the cationic liposome Lipofectin (L) which confers protection against endosomal degradation and the integrin-targeted peptide (I) with the 16-lysine tail. Mixing of the lipid and peptide solution with plasmid DNA (D) solution produces the LID vector complex (Hart *et al.*, 1998) which in preliminary transfection tests with animals have shown promising results (Jenkins *et al.*, 2000). Additionally, recent *in vitro* tests (Compton *et al.*, 2000) have indicated the capacity of this agent to transfer DNA constructs with a size larger than 100 kb to human keratinocytes.

Parallel studies carried out in our laboratories (Lee *et al.*, 2001; Tsai *et al.*, 1999) and elsewhere (Eastman *et al.*, 1997; Ross and Hui, 1999; Wheeler *et al.*, 1999) have suggested that one of the causes for the poor transfection of DNA delivery systems based on cationic agents is the physical instability of the complexes. These agents achieve DNA condensation by reducing the net negative charge on the plasmid DNA molecule. The reduction in the repulsive charge of the DNA causes it to collapse, producing complexes with physical dimensions typically of the order of 100 nm to 200 nm (Duguid *et al.*, 1998; Tsai *et al.*, 1999). However, charge neutralisation can induce physical instability causing aggregation of the complexes (Kennedy *et al.*, 2000; Lee *et al.*, 2001; Mahato *et al.*, 1997; Xu *et al.*, 1999). Additionally, physiological ionic strength favours aggregation (Bloomfield and Rau, 1980; He *et al.*, 2000; Lee *et al.*, 2001) and the presence of proteins may accelerate the rate of aggregation. For example, Zelphati *et al* (Zelphati *et al.*, 1998a) provide experimental data showing that interactions between bovine serum albumin (BSA), lipoproteins and macroglobulin with cationic lipid-nucleic acid complexes alter the physicochemical properties of complexes and suggest that their effects on transfection may be important.

In this paper, we combine data from photon correlation spectroscopy (PCS, or dynamic light scattering, DLS) capable of nanometer resolution for size measurements with laser Doppler spectrometry for the determination of electrophoretic mobility to assess the physical stability of

LID complexes under a variety of physicochemical conditions. These measurements are complemented with data from *in vivo* transfection experiments using a murine model and *in vitro* experiments using COS-7 cells to examine the relationship between the physical stability and the transfection capacity of the LID complex.

MATERIALS AND METHODS

Chemicals and Reagents

The peptide $[K]_{16}$GACRRETAWACG (MW 3,331; net molar positive charge 17) which contains a peptide sequence that specifically targets $\alpha5\beta1$ integrins, was synthesised by Zinsser Analytic (Maidenhead, UK) and dissolved in deionised water at a concentration of 2 mg/ml. Lipofectin, a cationic liposome composed of 1:1 (w/w) ratio of *N*-[1-(2,3,-dioleyloxy)propyl]-*N,N,N*-trimethylammonium chloride (DOTMA) and dioleoyl phosphatidylethanolamine (DOPE) at 1 mg/ml, Opti-MEM buffer and phosphate-buffered saline (PBS, calcium- and magnesium-free) were purchased from Life Technologies (Paisley, UK). N-[2-hydroxyethyl] piperazine-N'-[2-ethanesulfonic acid] (HEPES) was obtained from Sigma (Poole, UK). All materials were of the highest purity commercially available. All solutions were prepared with deionised water from a Millipore (18.2 MΩ) Milli-Q water system (Millipore Ltd., Bedford, MA, USA).

Plasmid DNA

Two plasmids coding for two different reporter genes were used in the experiments. These were a 4.7-kb plasmid, pEGFP-N1 (Clonetech, Palo Alto, CA), containing the gene for green fluorescent protein (GFP), and a 5.7-kb plasmid, pCI-luc (Promega, Madison, Wisconsin) containing the luciferase reporter gene under the control of the cytomegalovirus promoter-enhancer. Both were propagated in the *E. coli* DH5α strain and purified on Hybaid columns (Hybaid, Middlesex, UK) according to the manufacturer's instructions. After ethanol precipitation, the plasmid was resuspended in sterile non-pyrogenic water (Baxter, Thetford, UK).

Preparation of the LID complexes

The Lipofectin/integrin-binding peptide/DNA (LID) vector complex was prepared at both low (5 μg/ml) and high (160 μg/ml) DNA concentrations at a weight ratio of 0.75:4:1 (L:I:D, respectively) (Hart *et al.*, 1998), which corresponds to a positive molar charge ratio of 7. The LID vector was used at this charge ratio in all experiments except in cases where the aim was to assess the impact of lipopolyplex charge ratio on transfection efficiency and biophysical properties.

For the preparation of LID complexes at a DNA concentration of 5 μg/ml, plasmid DNA solution (10 μg/ml) was mixed with an equal volume, typically 1.5 to 3.0 ml, of Lipofectin/peptide solution to produce the LID complexes. The lipopolyplexes were prepared either by manual mixing or the semi-automated controlled mixing procedure as described previously (Lee *et al.*, 2001). Briefly, this entailed mixing the plasmid DNA (D) and Lipofectin/peptide (LI) solutions using a vertically mounted twin syringe pump (Harvard Apparatus, Holliston, MA, USA). Two standard plastic syringes (Becton-Dickinson Labware, Lincoln Park, NJ, USA) were fitted with 0.8 mm internal diameter silicone tubing and a T-mixer (Bio-Rad, Hercules, CA, USA). Equal volumes of DNA and LI solutions were loaded independently into separate syringes and driven by the pump through the T-mixer at 2 ml/min. The mixture was then collected in a polystyrene Universal container (201152; Greiner Labortechnik Ltd., Stonehouse, UK) for particle size analysis or for electrophoretic mobility measurements.

For experiments with lipopolyplexes prepared at a DNA concentration of 160 μg/ml, the DNA stock solution was first diluted into the appropriate buffer in an Eppendorf tube, after which it was added to the lipid and peptide solution in a sample cell to give a final DNA concentration of 160 μg/ml in a total volume of 500 μl. The DNA and lipid/peptide solutions were mixed briefly by pipetting the mixture up and down for approximately 5 seconds. The cell was then put into the Zetasizer light scattering sample holder and the particle size of the sample immediately measured by dynamic light scattering at 25°C.

Zeta potential measurements

Zeta potential measurements were carried out using the Malvern Zetasizer 3000, a laser-based particle electrophoresis analyser that measures the electrophoretic mobility and distribution of zeta potential of the particles in suspension. Measurements were performed at 25°C, and calibrated with negatively charged standards (DTS5050, Malvern Instruments Ltd., UK). The zeta potential values were calculated from the mean of five separate runs.

Dynamic light scattering

Dynamic light scattering (DLS) measurements were used to obtain information on the size distribution of the complexes. In DLS a monochromatic laser beam is employed to probe a small volume of diffusing particles in a dilute colloidal suspension. As the particles undergo Brownian motion, the temporal fluctuation of the intensity of the scattered light is detected and analysed using a correlator that yields, in real time, the autocorrelation function. This function is analysed

by the method of cumulants, which gives a statistically determined z-average diameter and a population distribution of the complexes. The first cumulant is directly related to the effective translational diffusion coefficient from which the hydrodynamic diameter of the complex is obtained through the Stokes–Einstein relation (Kerker, 1969; Van de Hulst, 1957).

DLS measurements were performed using a Malvern Zetasizer 3000 instrument (Malvern Instruments Ltd., UK) operating at a wavelength of 633 nm and a power output of 5 mW. All experiments were conducted at a constant temperature of 25°C and a scattering angle of 90°, and spectra were collected every 180s for at least 90 min. For broad, irregularly shaped distributions, where the method of cumulants was inappropriate, the CONTIN 'constrained regularisation' program (Provencher, 1979; Provencher, 1982) was used for data analysis.

PicoGreen assay

The total DNA concentration in the LID complexes was quantified by fluorescence using the DNA-intercalating PicoGreen reagent (Molecular Probes, Leiden, The Netherlands). The PicoGreen reagent (1:200 dilution in TE buffer) was prepared according to the manufacturer's instructions. The sensitivity of the PicoGreen assay required dilution of the complexes to DNA concentrations of 20 nM - 4μM. The appropriate volume of TE buffer was added to suspensions of LID complexes to a final DNA concentration of 1 μg/ml. 500 μl of the PicoGreen working solution was added to each 800 μl sample of the diluted complexes and pipette-mixed in polystyrene fluorometer cuvettes at room temperature. After 2 min, the fluorescence was measured using a TD-700 Laboratory Fluorometer (Turner Designs, Sunnyvale, CA, USA) at excitation and emission wavelengths of 489 and 520 nm, respectively. Measurements were corrected for background fluorescence from a solution of buffer and PicoGreen reagent. The results were presented as the average of three readings.

In vivo transfection experiments

The LID complex containing the reporter gene pCI-luc was used to determine cell transfection in a murine model. Luciferase activity was assessed biochemically in whole lung lysates as previously described (Jenkins *et al.*, 2000). The protein concentration of each lysate sample was determined with protein assay reagent (BioRad, Hemel Hempstead, UK) and the luciferase enzyme activity expressed in terms of relative light units per milligram of protein (RLU/mg). The luciferase activity data obtained were not normally distributed and were statistically analysed using Mann-Whitney U test. In all cases a p value <0.05 was considered significant.

In vitro transfection experiments

All *in vitro* transfection experiments were carried out with adherent COS-7 cells (SV-40 virus transformed monkey kidney epithelial cells) grown in Falcon 75 cm^2 plastic tissue culture flasks (Becton Dickinson Labware, Lincoln Park, NJ, USA) at 37°C in 95% air and 5% CO_2 in a water saturated atmosphere. The cells were maintained in Dulbecco's modified Eagle's medium (DMEM, Life Technologies) with 10% fetal calf serum (FCS), 2 mM L-glutamine, penicillin and streptomycin. For transfections, cells were harvested by trypsinisation, pelleted by centrifugation and resuspended in the culture medium in Falcon 48-well tissue culture plastic plates (Becton-Dickinson Labware) and incubated overnight at 37°C to reach cell confluency of more than 50%. Following incubation, the cells were washed with PBS to remove serum, and 200 µl of Opti-MEM buffer was added to the cells in each well. The LID complexes containing the reporter gene pEGFP-NI were prepared as described previously and 200 µl (1 µg DNA) immediately pipetted to triplicate wells. Cells were exposed to the complexes for 3 h at 37°C, followed by aspiration of the transfection media and addition of regular growth medium. After 48 h, cells were washed twice with PBS and detached from the tissue culture plastic by incubation in 1 × Trypsin-EDTA (Life Technologies, Paisley, UK) for 5 to 10 min at 37°C. The harvested cells were centrifuged, washed and resuspended in PBS containing 0.01% sodium azide. A fluorescence-activated cell sorter, FACSCalibur (Becton-Dickinson, Oxford, UK), was used to automatically analyse the GFP expression of individual cells. Each measured number of GFP positive cells was determined on the basis of one sample of pooled triplicates.

RESULTS AND DISCUSSION

Biophysical studies

Figure 1 shows the effect of complex charge ratio on the zeta potentials and the amount of unbound DNA as measured by the PicoGreen fluorescence assay. The data refer to experiments carried out with the 5.7-kb plasmid DNA complexes prepared in PBS buffer at a DNA concentration of 5 µg/ml. The components were mixed using the twin-syringe pump and the T-mixer as described in Materials and Methods. The PicoGreen data indicate that beyond a charge ratio of about 4 the plasmid DNA in the complex becomes effectively inaccessible to the dye and this is supported by the zeta potential profile for the system which peaks at about the same charge ratio. Experimental results discussed later indicate that optimum *in vivo* transfection results were achieved when the complexes were prepared at a charge ratio of 7. Unless otherwise stated, all subsequent experiments were performed at a charge ratio of 7.

Figures 2A and 2B show typical size distribution data obtained from DLS measurements for the LID complexes at plasmid concentrations of 5 μg/ml and 160 μg/ml, respectively. The data refer to experiments carried out with the 5.7-kb pCI-luc, and in each case, measurements were performed as a function of time immediately after the mixing of the solution of plasmid (D) into the lipid/peptide (LI) solution. Additional experimental details are shown in the caption. In both cases the plots show a continuous shift in the size distribution towards the right-hand-side as a function of time, indicating that aggregation of the complexes occurs practically as soon as the components are mixed. Additional experiments (data not shown) with the twin-syringe pump confirmed that at flow rates between 2 ml/min and 17 ml/min, the rate of complex aggregation and the final aggregate size distribution were independent of mixing flow rate.

The data in Figure 3 show the time evolution of the *z*-average size of the complexes prepared in different buffers. The plots confirm the highly aggregative nature of the LID complexes prepared in PBS and high salt concentration buffers. They also demonstrate the significant impact on aggregation of the increase in plasmid DNA concentration from 5 μg/ml to 160 μg/ml. For example, in the case of 160 μg/ml of DNA in PBS, the *z*-average size of the complexes continued to increase to a value of about 3000 nm after approximately 40 minutes. The polydispersity, which gives a measure of the degree of heterogeneity in the size distribution of the complexes, also increased, in the case of data in Figure 3, from a value of about 0.3 at the start of the measurements to a value approaching 0.7 after about 40 minutes. Particle sizes larger than 3000 nm fall outside the normal operating range of the DLS equipment and are not included in the plots. Compared with other buffer conditions shown in Figure 3, preparation in distilled water results in LID complexes with an initial and stable *z*-average size of 145 nm ± 35 nm, with a polydispersities no greater than 0.3. Measurements carried out on samples prepared in distilled water confirmed that these complexes remained stable for at least one week when stored at 4°C. It is notable that subsequent addition of PBS to complexes prepared in distilled water had a highly destabilising effect as shown by the rapid increase in the *z*-average values. Additionally, LID complexes prepared in a dextrose solution (5% w/v dextrose in distilled water, no salts added) were stable, similar to those prepared in distilled water, but aggregated when PBS was added to them.

Comparison of data for complexes prepared in PBS buffer (Figure 4) indicate that the potential cause of aggregation in these systems is the presence of the integrin-targeted peptide (I) in the

formulation. Its removal from the vector formulation resulted in the formation of (LD) aggregates with a size of approximately 400 nm that remained stable for up to 3 hours. However, in terms of cell binding, DNA condensation and transfection efficiency, the peptide is an essential component of the formulation (Compton *et al.*, 2000; Fortunati *et al.*, 2000; Vaysse *et al.*, 2000).

The dynamic stability of the complexes shown in Figures 3 and 4 are determined by the superimposed effects of the physicochemical properties of the transfection solution such as its pH and ionic strength, the size distribution and concentration of the complexes, as well as factors such as temperature and local fluid flow environment. The size measurements reported here were carried out at a constant temperature of 25°C, and the local flow conditions were such that aggregation was determined solely by the physical laws governing Brownian motion of colloidal particles (Elimelich *et al.*, 1995; Wilson and French, 1978). The measured zeta potential values for the different systems shown in Figures 3 and 4, along with the corresponding *z*-average sizes of the initial complexes, were used to estimate the theoretical total potential energies of interaction for the complexes as described in our previous publication (Lee *et al.*, 2001). Typical predictions, based on binary interaction energy calculations between complexes of equal size (Figure 5), confirm that the LID complexes in distilled water have a total potential energy of interaction in excess of 100 kT. Such a high interaction energy is expected to produce extremely stable systems. In contrast, the LID in PBS system, for example, has very low potential energy barriers and is likely to be spontaneously aggregating.

Proteins such as albumin found in most physiological fluids have the potential to cause physical instability of plasmid DNA complexes (Cherng *et al.*, 1996; Dash *et al.*, 1999; Muller *et al.*, 1986; Verbaan *et al.*, 2001; Zelphati *et al.*, 1998b). Albumin, the primary serum protein, occurs in varying concentrations, from about 0.2 mg/ml in the fluid lining the lungs to 40 - 44 mg/ml in the human plasma. Figure 6 shows the time evolution of the *z*-average size of LID complexes in distilled water (initially stable) to which BSA was added systematically to achieve various final BSA concentrations to cover the physiological range of interest. The data refer to experiments in which the initial DNA concentration of the complexes was 160 μg/ml. In each experiment stable complexes were prepared in distilled water as described previously. Immediately after the first size measurements (t = 0 min) an equal volume of distilled water containing a pre-determined amount of BSA was added, resulting in complexes with a final DNA concentration in each case of 80 μg/ml. The complexes remained stable as long as the final concentration of BSA in solution remained below about 5 mg/ml. Beyond this concentration, as demonstrated by the data,

significant complex instability is encountered. The plot in Figure 6 (inset) indicates that the presence of BSA in the sample decreased the zeta potential of the complexes nearly exponentially from a value of about 27 mV at a BSA concentration of 1.0 mg/ml to a value approaching 8 mV at a BSA concentration of 5 mg/ml. The reduction in the potential energy barrier between the complexes is sufficient to cause the complexes to aggregate.

Transfection studies

Initial experiments were performed to investigate the impact on luciferase activity of the LID complexes prepared by two different protocols and at various DNA dose concentrations. Mice lungs were instilled with 8 μg of plasmid in 50 μl of solution of the LID complexes, which corresponds to a plasmid concentration of 160 μg/ml. The complexes were prepared in PBS either by rapid mixing of a solution containing the lipid and peptide (LI) with the plasmid DNA solution (D) in a Falcon tube for five seconds before instillation, or by the slow addition of the lipid and peptide mixture to the plasmid solution in 10 μl aliquots over 20 minutes. The former method caused significant aggregation resulting in the formation of large precipitated particles that were visible to the eye but which dispersed to give a clear solution after repeated rapid pipetting. By the latter method, slow addition of the lipid/peptide mixture led to a gradual increase in turbidity which cleared with further addition of lipid/peptide, until the final solution was completely clear by eye. Luciferase activity in whole lung lysates one day after instillation for the two systems are plotted in Figure 7 where the horizontal bars represent the median value for each group. Statistical analysis of the data indicated a significant reduction in the transfection efficiency of samples prepared by the slow mixing method. All subsequent experiments were carried out using the rapid mixing protocol.

Luciferase activity in whole lung lysates was also measured one day following instillation for the LID complexes prepared in distilled water. The results (data not shown) indicated that activity increased as a function of plasmid DNA concentration in a fixed dose volume. In the experiments that follow we limited the DNA concentration to 8 μg per 50 μl dose, which has been shown in previous work to be appropriate (Jenkins *et al.*, 2000).

We also assessed the impact of complex charge ratio on the level of transgene expression, as shown in Figure 8, which shows significantly higher luciferase activity one day after instillation at a charge ratio of 7 compared to a charge ratio of 3.5.

Luciferase activity in whole lung lysates one day after instillation was determined for the LID complexes prepared in different transfection solutions. The transfection results (Figure 9) illustrate the capacity of the LID complexes prepared in distilled water to induce gene expression. Coupled with the physical stability (Figures 3 and 4) and small size, 145μm ± 35 nm, of these complexes, the transfection data indicate a strong correlation between the physical stability of the LID complexes prepared in distilled water and their capacity to transfect cells *in vivo*. Additional experiments (data reported elsewhere (Jenkins,R.G., Meng,Q.-H., Hodges,R.-H., Lee,L.K., Laurent,G.J., Willis,D., Ayazi Shamlou,P, McAnulty,R.J., Hart,S.L., submitted)) indicated that the physical properties of the complexes also impact the duration of transgene expression, with the LID in water complexes consistently performing better than other systems examined including the LID in PBS.

We also measured the transfection capacity of the LID complexes in Opti-MEM at different charge ratios using COS-7 cells. The measurements of GFP positive cells were obtained 48 h after transfection and the results shown in Figure 10. The transfection efficiency increased as zeta potential increased (Figure 1) and both profiles plateaued at a charge ratio of about 3.5. The *in vitro* transfection efficiency of complexes formed at charge ratios higher than 3.5 decreased as the charge ratio increased. There was however, no observable change in the zeta potential of the complexes beyond a charge ratio of 3.5. According to the results shown in Figure 8 optimum *in vivo* transfection occurred at a charge ratio of 7. The reason for the difference between the two systems is not clear. It is possible however that the decrease in *in vitro* transfection efficiency for charge ratios greater than 3.5 caused effects of toxicity induced in the cells by the presence of excess peptide.

In vitro transfection of COS-7 cells was also carried out using LID complexes prepared in three different buffers at a charge ratio of 7 and the results are shown in Figure 11. The time axis represents the maturation time of the complexes before transfection was initiated. *In vitro* experiments with the LID complexes prepared in water could not be carried out because in the absence of a suitable buffer such as Opti-MEM cell death occurred rapidly by osmotic rupture. The transfection efficiency of the LID complexes in PBS and HBS decreased sharply with complex maturation time (Figure 11) whereas the LID complexes prepared in Opti-MEM appear to be unaffected by maturation time. The decrease in transfection efficiency of the LID complexes prepared in HBS and PBS buffers is consistent with the aggregative nature of these systems. The transfection efficiency for the LID complexes in Opti-MEM however was

unexpected since these complexes also aggregated. Opti-MEM is a proprietary buffer and its detailed composition is unknown to the authors. It is possible that the presence of some of the minor components in the transfection solution may have had an overriding effect on *in vitro* transfection. It is hypothesised that these observations may be cell line specific. What is clear from our study is that there seems to be no correlation between *in vivo* and *in vitro* transfection results (Figures 1 and 8).

CONCLUSION

Our study suggests that the integration of vector chemistry, characterisation of interactions between gene delivery systems with the cellular physiological environment, and *in vivo* transfection is a prerequisite to understanding the cellular uptake of non-viral DNA complexes. We report experiments in which we have assessed the efficiency of local delivery into the lungs of mice of a novel integrin-targeting vector. We describe the main components of the vector and their function, and report recent data of stable transfection of bronchial and parenchymal cells with good levels of luciferase expression lasting up to seven days. We also present physicochemical data including size distributions by photon correlation spectroscopy and overall vector charge by electrophoretic mobility measurements. Using the DLVO theory we demonstrate the physical instability of DNA complexes in physiological buffers and use this approach to lay the foundation for the creation of stable complexes with satisfactory long-term stability and transfection properties.

ACKNOWLEDGEMENTS

We are grateful to Dr Aima Uduehi for crucial assistance with the particle sizing studies, Professor John Gregory for advice on the mathematical models of colloidal suspensions, and Professor Peter Dunnill and Dr Susana Levy for many useful suggestions and comments on the manuscript.

REFERENCES

Aris,A., J.X.Feliu, A.Knight, C.Coutelle, and A.Villaverde. 2000. Exploiting viral cell-targeting abilities in a single polypeptide, non-infectious, recombinant vehicle for integrin-mediated DNA delivery and gene expression. Biotechnology and Bioengineering 68:689-696.

Armeanu,S., J.Pelisek, E.Krausz, A.Fuchs, D.Groth, R.Curth, O.Keil, J.Quilici, P.H.Rolland, R.Reszka, and S.Nikol. 2000. Optimization of nonviral gene transfer of vascular smooth muscle cells in vitro and in vivo. Molecular Therapy 1:366-375.

Bloomfield,V.A. and D.C.Rau. 1980. Polyelectrolyte effects in DNA condensation by polyamines. Biophysical Chemistry 11:339-343.

Chemin,I., D.Moradpour, S.Wieland, W.B.Offensperger, E.Walter, J.-B.Berh, and H.E.Blum. 1998. Liver-directed gene transfer: a linear polyethylenimine derivative mediates highly efficient DNA delivery to primary hepatocytes in vitro and in vivo. J. Viral Hepat. 5:369-375.

Cherng,J.-Y., P.Van der Wetering, H.Talsma, D.J.A.Crommelin, and W.E.Hennink. 1996. Effect of size and serum proteins on transfection efficiency of poly(2-dimethylamino)ethyl methacrylate-plasmid nanoparticles. Pharmaceutical Research 13:1038-1042.

Chesnoy,S. and L.Huang. 2000. Structure and function of lipid-DNA complexes for gene delivery. Annu. Rev. Biophys. Biomol. Struct. 29:27-47.

Compton,S.H., S.Mecklenbeck, J.E.Mejía, S.L.Hart, M.Rice, R.Cervini, Y.Barrandon, Z.Larrin, E.R.Levy, L.Bruckner-Tuderman, and A.Hovnanian. 2000. Stable integration of large (>100kb) PAC constructs in HaCaT keratinocytes using an integrin-targeting peptide delivery system. Gene Therapy 7:1600-1605.

Dash,P.R., M.L.Read, L.B.Barrett, M.A.Wolfert, and L.W.Seymour. 1999. Factors affecting blood clearance and in vivo distribution of polyelectrolyte complexes for gene delivery. Gene Therapy 6:643-650.

Duguid,J.G., M.Shi, M.J.Logan, H.Alila, A.Rolland, E.Tomlinson, J.T.Sparrow, L.C.Smith, and C.Li. 1998. A physicochemical approach for predicting the effectiveness of peptide-based gene delivery systems for use in plasmid-based gene therapy. Biophysical Journal 74:2802-2814.

Eastman,S.J., C.Siegel, J.Tousignant, A.E.Smith, S.H.Cheng, and R.K.Scheule. 1997. Biophysical characterization of cationic lipid:DNA complexes. Biochim. Biophys. Acta 1325:41-62.

Elimelich,M., J.Gregory, X.Jia, and R.A.Williams. 1995. Particle deposition and aggregation: measurement, modelling and simulation. Butterworth-Heinemann Ltd, Oxford.

Ennist,D.L. 1999. Gene therapy for lung disease. Trends in Pharmacological Sciences 20:260-266.

Felgner,J.H., R.Kumar, N.Sridhar, C.J.Wheeler, Y.J.Tsai, R.Border, P.Ramsey, M.Martin, and P.L.Felgner. 1994. Enhanced gene delivery and mechanism studies with a novel series of cationic lipid formulations. Journal of Biological Chemistry 269:2550-2561.

Ferkol,T. and P.B.Davis. 2001. Single chain Fv: a ligand in receptor-mediated gene delivery. Gene Therapy 8:586-592.

Fortunati,E., E.Ehlert, N.D.van Loo, C.Wyman, J.A.Eble, F.Grosveld, and B.J.Scholde. 2000. A multi-domain protein for beta1 integrin-targeted DNA delivery. Gene Therapy 7:1505-1515.

Hart,S.L., C.V.Arancibia-Cárcamo, M.A.Wolfert, C.Mailhos, N.J.O'Reilly, R.R.Ali, C.Coutelle, D.F.P.Larkin, R.J.Levinsky, L.W.Seymour, A.J.Thrasher, and C.Kinnon. 1998. Lipid-mediated enhancement of transfection by a nonviral integrin-targeting vector. Human Gene Therapy 9:575-585.

Hart,S.L., R.P.Harbottle, R.Cooper, A.Miller, R.Williamson, and C.Coutelle. 1995. Gene delivery and expression mediated by an integrin-binding peptide. Gene Therapy 2:552-554.

He,S., P.G.Arscott, and V.A.Bloomfield. 2000. Condensation of DNA by multivalent cations: experimental studies of condensation kinetics. Biopolymers 53:329-341.

Jackson,T., D.Sheppard, M.Denyer, W.Blakemore, and A.M.King. 2000. The epithelial integrin αvβ6 is a receptor for foot-and-mouth disease virus. Journal of Virology 74:4949-4956.

Jenkins,R.G., S.E.Herrick, Q.-H.Meng, C.Kinnon, G.J.Laurent, R.J.McAnulty, and S.L.Hart. 2000. An integrin-targeted, non-viral vector for pulmonary gene therapy. Gene Therapy 7:393-400.

Kabanov,A.V. 1999. Taking polycation gene delivery systems from in vitro to in vivo. PSST 2:365-372.

Kennedy,M.T., E.V.Pozharski, V.A.Rakhmanova, and R.C.MacDonald. 2000. Factors governing the assembly of cationic phospholipid-DNA complexes. Biophysical Journal 78:1620-1633.

Kerker,M. 1969. The scattering of light and other electromagnetic radiation. Academic Press, New York.

Kichler,A., W.Zauner, and E.Wagner. 1998. Influence of the DNA complexation medium on the transfection efficiency of lipospermine/DNA particles. Gene Therapy 5:855-860.

Kim,J.-S., A.Maruyama, T.Akaike, and S.W.Kim. 1997. In vitro gene expression on smooth muscle cells using a terplex delivery system. Journal of Controlled Release 47:51-59.

Lam,P.Y.P. and X.O.Breakefield. 2001. Potential of gene therapy for brain tumours. Human Molecular Genetics 10:777-787.

Lee,L.K., C.N.Mount, and P.Ayazi Shamlou. 2001. Characterisation of the physical stability of colloidal polycation-DNA complexes for gene therapy and DNA vaccines. Chemical Engineering Science 56:3163-3172.

Lee,R., C.H.R.Boasquevisque, M.M.Boglione, M.Hiratsuka, R.K.Scheule, J.D.Cooper, and G.A.Patterson. 1998. Isolated lung liposome-mediated gene transfer produces organ-specific transgenic expression. Annals of Thoracic Surgery 66:903-907.

Lee,R.J. and L.Huang. 1996. Folate-targeted, anionic liposome-entrapped polylysine-condensed DNA for tumor cell-specific gene transfer. Journal of Biological Chemistry 271:8481-8487.

Leitner,W.W., H.Ying, and N.P.Restifo. 2000. DNA and RNA-based vaccines: principles, progress and prospects. Vaccine 18:765-777.

Li,J.M., L.Collins, X.Zhang, K.Gustafsson, and J.W.Fabre. 2000. Efficient gene delivery to vascular smooth muscle cells using a nontoxic, synthetic peptide vector system targeted to membrane integrins: a first step toward the gene therapy of chronic rejection. Transplantation 70:1616-1624.

Li,S., M.A.Rizzo, S.Bhattacharya, and L.Huang. 1998. Characterization of cationic lipid-protamine-DNA (LPD) complexes for intravenous gene delivery. Gene Therapy 5:930-937.

Liang,K.W., E.P.Hoffman, and L.Huang. 2000. Targeted delivery of plasmid DNA to myogenic cells via transferrin-conjugated peptide nucleic acid. Molecular Therapy 1:236-243.

Luo,D. and W.M.Saltzman. 2000. Synthetic DNA delivery systems. Nature Biotechnology 18:33-37.

Mahato,R.I., Y.Takakura, and M.Hashida. 1997. Nonviral vectors for in vivo gene therapy: Physicochemical and pharmacokinetic considerations. Critical Reviews in Therapeutic Drug Carrier Systems 14:133-172.

McDonald,G.A., G.Zhu, Y.Li, I.Kovesdi, T.J.Wickham, and V.P.Sukhatme. 1999. Efficient adenoviral gene transfer to kidney cortical vasculature utilizing a fiber modified vector. Journal of Gene Medicine 1:103-110.

McKee,T.D., M.E.DeRome, G.Y.Wu, and M.A.Findeis. 1994. Preparation of asialoosoromucoid-polylysine conjugates. Bioconjugate Chemistry 5:306-311.

Muller,R.H., S.S.Davies, L.Illum, and E.Mak. 1986. Particle charge and surface hydrophobicity of colloidal drug carriers In Targeting of Drugs with Synthetic Systems. G.Gregoriadis, J.Senior, and G.Poste, editors. Plenum Press, New York. 239-63.

Nishikawa,M., S.Takemura, Y.Takakura, and M.Hashida. 1998. Targeted delivery of plasmid DNA to hepatocytes in vivo: optimization of the pharmacokinetics of plasmid DNA/galactosylated poly(l-lysine) complexes by controlling their physicochemical properties. The Journal of Pharmacology and Pharmaceutical Therapeutics 287:408-415.

Provencher,S.W. 1979. Inverse problems in polymer characterization; direct analysis of polydispersity with photon correlation spectroscopy. Makromol. Chem. 180:201-209.

Provencher,S.W. 1982. CONTIN: a general purpose constrained regularization program for inverting data represented by noisy linear algebraic and integral equations. Comp. Phys. Com. 27:229-242.

Ross,P.C. and S.W.Hui. 1999. Lipoplex size is a major determinant of in vitro lipofection efficiency. Gene Therapy 6:651-659.

Roth,C.L. and M.L.Yarmush. 1999. Nucleic acid biotechnology. Annu. Rev. Biomed. Eng. 1:265-297.

Smith,J., Y.Zhang, and R.Niven. 1997. Toward development of a non-viral gene therapeutic. Advanced Drug Delivery Reviews 26:135-150.

Tomlinson,E. and A.P.Rolland. 1996. Controllable gene therapy pharmaceutics of nonviral gene delivery systems. Journal of Controlled Release 39:357-372.

Tsai,J.T., E.Keshavarz-Moore, J.M.Ward, M.Hoare, P.Ayazi Shamlou, and P.Dunnill. 1999. Characterisation of plasmid DNA conjugates as a basis for their processing. Bioprocess Engineering 21:279-286.

Van de Hulst,H.C. 1957. Light scattering by small particles. John Wiley & Sons, New York.

Vaysse,L., I.Burgelin, J.P.Merlio, and B.Arvelier. 2000. Improved transfection using epithelial cell line-selected ligands and fusogenic peptides. Biochim. Biophys. Acta 1475:369-376.

Verbaan,F.J., C.Oussoren, I.M.van Damm, Y.Takakura, M.Hashida, D.J.A.Crommelin, W.E.Hennink, and G.Storm. 2001. The fate of poly(2-dimethyl amino ethyl)methacrylate-based polyplexes after intravenous administration. International Journal of Pharmaceutics 21:99-101.

Wagner,E., M.Cotten, R.Foisner, and M.L.Brinstiel. 1991. Transferrin-polycation-DNA complexes: the effect of polycations on the structure of the complex and DNA delivery to cells. Proc. Natl. Acad. Sci. USA 88:4255-4259.

Wang,C.-Y. and L.Huang. 1989. Highly efficient DNA delivery mediated by pH-sensitive immunoliposomes. Biochemistry 28:9508-9514.

Wheeler,J.J., L.Palmer, M.Ossanlou, I.MacLachlan, R.W.Graham, Y.P.Zhang, M.J.Hope, P.Scherrer, and P.R.Cullis. 1999. Stabilized plasmid-lipid particles: construction and characterization. Gene Therapy 6:271-281.

Willard,H.F. 1998. Human artificial chromosomes coming into focus. Nature Biotechnology 16:415-417.

Wilson,D.J. and R.H.French. 1978. Kinetic and equilibrium aspects of floc coagulation. II. Slow mixing criteria. Separation Science and Technology 13:95-106.

Xu,Y., S.-W.Hui, P.Frederik, and Jr.F.C.Szoka. 1999. Physicochemical characterization and purification of cationic lipoplexes. Biophysical Journal 77:341-353.

Zelphati,O., C.Nguyen, M.Ferrari, J.Felgner, Y.Tsai, and P.L.Felgner. 1998a. Stable and monodisperse lipoplex formulations for gene delivery. Gene Therapy 5:1272-1282.

Zelphati,O., L.S.Uyechi, L.G.Barron, and F.C.Szoka, Jr. 1998b. Effect of serum components on the physico-chemical properties of cationic lipid/oligonucleotide complexes and on their interactions with cells. Biochim. Biophys. Acta 1390:119-133.

Figure legends

Fig. 1. The open symbols show the zeta potential of LID complexes formed with different amounts of integrin-targeting peptide. The complexes were prepared in phosphate-buffered saline (PBS) at a final DNA concentration of 5 μg/ml. In the case of the PicoGreen assay (solid symbols), a series of LID solutions were diluted in TE buffer (10 mM Tris-HCl, 1 mM EDTA, pH 8) buffer to a final DNA concentration of 1 μg/ml before addition of the PicoGreen dye.

Fig. 2. Particle size distributions of LID complexes, determined by PCS measurements at 25°C. Lipopolyplexes were formulated in phosphate-buffered saline (PBS, pH 7.4) at a molar charge ratio of + 7, and (A) 5 μg/ml and (B) 160 μg/ml DNA concentration, by adding the plasmid pCI-luc into the lipid/peptide mixture followed by pipette-mixing. The data are shown as individual measurements at various time periods after complex preparation: (A): (■) 0 minutes, (▲) 7 min., (×) 14 min., (✲) 21 min., (●) 28 min., (+) 34 min.; (B): (■) 0 min., (▲) 9 min., (×) 14 min., (✲) 18 min., (●) 23 min., (+) 27 min.

Fig. 3. Time evolution of *z*-average particle size of LID complexes in different buffers determined by PCS at 25°C. The complexes were formed either at 5 μg/ml DNA concentration using a controlled mixing method: (■) Opti-MEM, (◆) PBS and (▲) HBS; or at 160 μg/ml DNA concentration by rapid pipette-mixing: (O) distilled water, (◊) PBS, (+) 5% dextrose and (−) 150mM NaCl. LID complexes formed in distilled water or 5% dextrose were very stable (O and +, respectively), but aggregated rapidly when diluted in PBS to a final DNA concentration of 37.5 μg/ml (✶ and ×, respectively).

Fig. 4. Time evolution of z-average size of LID complexes showing the impact of complex composition on aggregation. Data refer to experiments in different buffers: distilled water (▲), PBS (Δ) and 5% dextrose (+); ID complexes in PBS (O); and LD complexes in PBS ( ). The LID complexes were prepared by adding the plasmid pCI-luc to the peptide/Lipofectin mixture followed by pipette-mixing. The L:I:D weight ratio was 0.75:4:1. For particle size analysis of ID and LD complexes, the L and I components were substituted by the appropriate volume of buffer, respectively. All of the samples were mixed at a final DNA concentration of 160 μg/ml, and the particle sizes were immediately measured by PCS technique. LID complexes formed in distilled water or 5% dextrose (▲ and +, respectively) were stable, with an average diameter of 110 ± 35

nm or 145 ± 35 nm, respectively. Both systems when diluted in PBS (to a final DNA concentration of 37.5 μg/ml) exhibited strong aggregation (✶ and ×, respectively).

Fig. 5. Calculated total interaction potential energies (V_T in kT units) versus separation distance H between two equal-sized particles for the LID, ID and LD complexes in distilled water (closed symbols), phosphate-buffered saline (PBS, open symbols), and 5% dextrose solution (dex, + and ×). Data refer to the following conditions. LID: (▲) particle size = 100 nm, zeta potential = 50 mV; (Δ) 1100 nm, 1 mV; (+) 140 nm, 54 mV. Integrin-targeting peptide/DNA (ID): (O) 800 nm, 6 mV. Lipofectin/DNA (LD): ( ) 170 nm, -57 mV. LID in H2O/PBS: (✶) 550 nm, 19 mV. LID in 5% dextrose/PBS: (×) 635 nm, 4.4 mV. The particle size and zeta potential data were experimentally determined. The interaction potential energies were calculated as described in Materials and Methods.

Fig. 6. Time evolution of z-average LID particle size with the concentration of bovine serum albumin (BSA) as a parameter. Stable LID complexes were generated as described in Materials and Methods (pipette-mixing of D and LI components in deionised water or 5% dextrose solution at a charge ratio of 6.7, DNA concentration of 160 μg/ml and final volume of 500 μl). At t= 0 min, stable LID complexes with an average diameter of 110 ± 35 nm or were generated in distilled water. Immediately after the first size measurement (t=0 min), an equal volume of BSA in distilled water was added to give the final BSA concentrations shown in the plot: (◊) 0.1 mg/ml, (■) 0.2 mg/ml, (▲) 0.5 mg/ml, (×) 1 mg/ml, (Δ) 2 mg/ml, (–) 3 mg/ml, (+) 4 mg/ml, (O) 5 mg/ml, (✶) 10 mg/ml, (◆) 20 mg/ml, ( ) 35 mg/ml. (●) refers to BSA in 5% dextrose added to a final concentration of 5 mg/ml in an initially stable system (particle size of 145 ± 35 nm) of LID in 5% dextrose.

Fig. 6. Inset: Zeta potentials of the LID complexes as a function of the bovine serum albumin (BSA) concentration. Stable LID complexes, with sizes of approximately 100 ± 20 nm, were generated as described in Materials and Methods (pipette-mixing of D and LI components in deionised water at a charge ratio of 6.7, DNA concentration of 160 μg/ml and final volume of 500 μl). 500 μl of BSA solution at a given concentration was quickly added and pipette-mixed to attain the final BSA concentrations shown in the plot. After approximately two hours following the BSA addition, the complexes prepared as above were diluted in buffer (deionised water) to a final concentration of 37.5 μg/ml for the zeta potential measurements measured.

Fig. 7. The impact of speed of LID complex preparation on *in vivo* transfection efficiency of murine lung. The complexes were formed in phosphate buffered saline (PBS) either by quick mixing or slow mixing as described in Materials and Methods. Briefly, to prepare LID complexes by quick mixing the plasmid (D) was added directly to the Lipofectin/Integrin-targeting peptide (LI) and pipette-mixed vigorously for five seconds. Slow mixing entailed addition of the LI component to the DNA in 5 μl aliquots over twenty minutes. 50 μl (containing 8 μg DNA) of the complexes were instilled intratracheally immediately after each sample was prepared without any incubation.

Fig. 8. Effect of complex charge ratio on levels of gene expression in murine lung. LID complexes were prepared in distilled water by the quick mixing method as described in Materials and Methods at a DNA concentration of 160 μg/ml, and charge ratios of 3.5 (L:I:D weight ratio of 0.75:2:1) and 7 (L:I:D weight ratio of 0.75:4:1). 50 μl of the complexes was instilled intratracheally, and luciferase activity in whole lung lysates was measured after 24 h.

Fig. 9. Luciferase activity in the whole lung lysates of mice one day after transfection with the LID vector in water and in PBS. The complexes were prepared by the quick mixing method as described in Materials and Methods.

Fig. 10. Effect of charge ratio on *in vitro* transfection efficiency. The complexes were formed at a DNA concentration of 5 μg/ml in Opti-MEM by a controlled mixing method. COS-7 cells plated onto 48-well plates were transfected at a density of 2.5×10^4 cells per well with 1 μg per well of freshly complexed DNA at the indicated charge ratios in the presence of an equal volume of Opti-MEM. Evaluation of the green fluorescent protein (GFP) expression was carried out after 48 h following transfection. Cells from triplicate transfections were pooled, trypsinised and analysed for GFP expression by FACS using a Becton-Dickinson FACSCalibur flow cytometer. All experiments were repeated at least three times and representative data from one experiment are plotted.

Fig. 11. *In vitro* transfection efficiency of LID in different buffers at various time periods following complex preparation: (◆) Opti-MEM, (▲) PBS and (■) HBS. COS-7 cells were seeded on to 48-well plates at a density of 2.5×10^4 cells per well and grown overnight before transfection. The lipid/peptide (LI) mixture was complexed with plasmid encoding the green

fluorescent protein (GFP) reporter gene under a controlled mixing rate of 2 ml/min and at 6.7 charge ratio. Then the cells were incubated with 200 µl of Opti-MEM and 200 µl of LID complexes (1 µg DNA) per well for 3 h at 37°C. At 48h after transfection, cells from triplicate transfections were pooled, trypsinised and analysed for GFP expression by FACS using a Becton-Dickinson FACSCalibur flow cytometer. All experiments were repeated at least three times and representative data from one experiment are plotted.

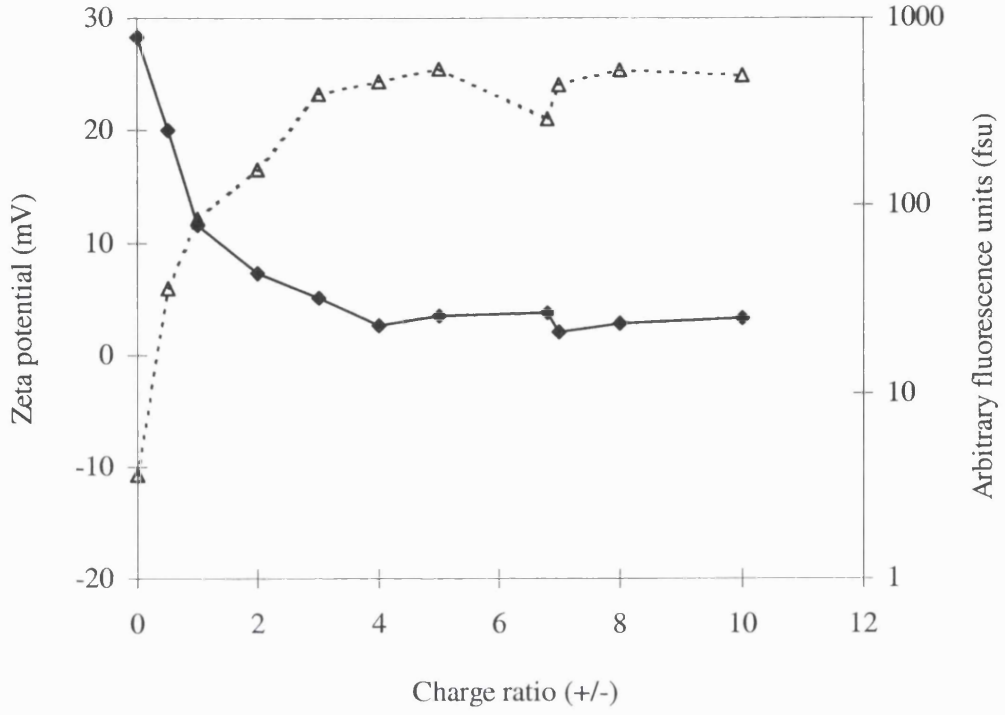
30
20
10
0
-10
-20
1000
100
10
1
0
2
4
6
8
10
12
Zeta potential (mV)
Arbitrary fluorescence units (fsu)
Charge ratio (+/-)

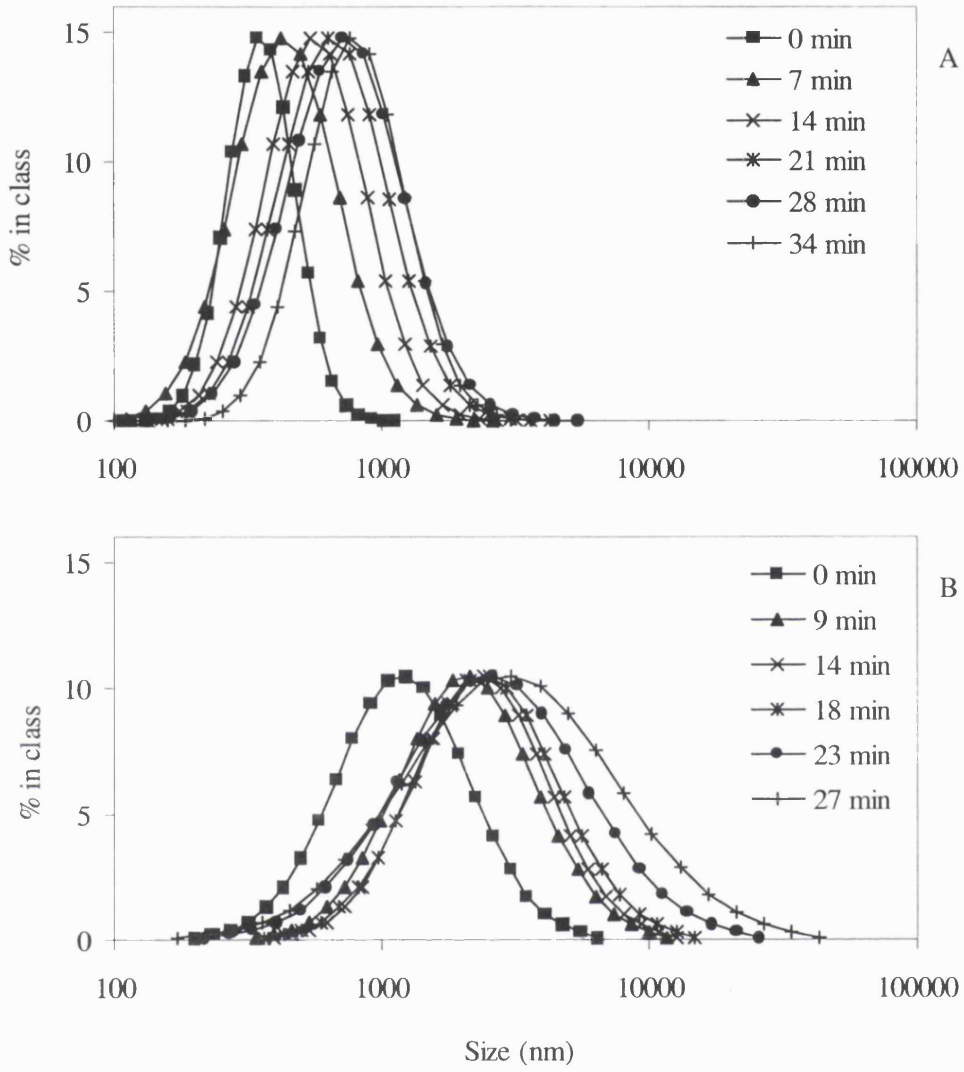
15
10
5
0
% in class
100
1000
10000
100000
0 min
7 min
14 min
21 min
28 min
34 min
A
15
10
5
0
% in class
100
1000
10000
100000
0 min
9 min
14 min
18 min
23 min
27 min
B
Size (nm)

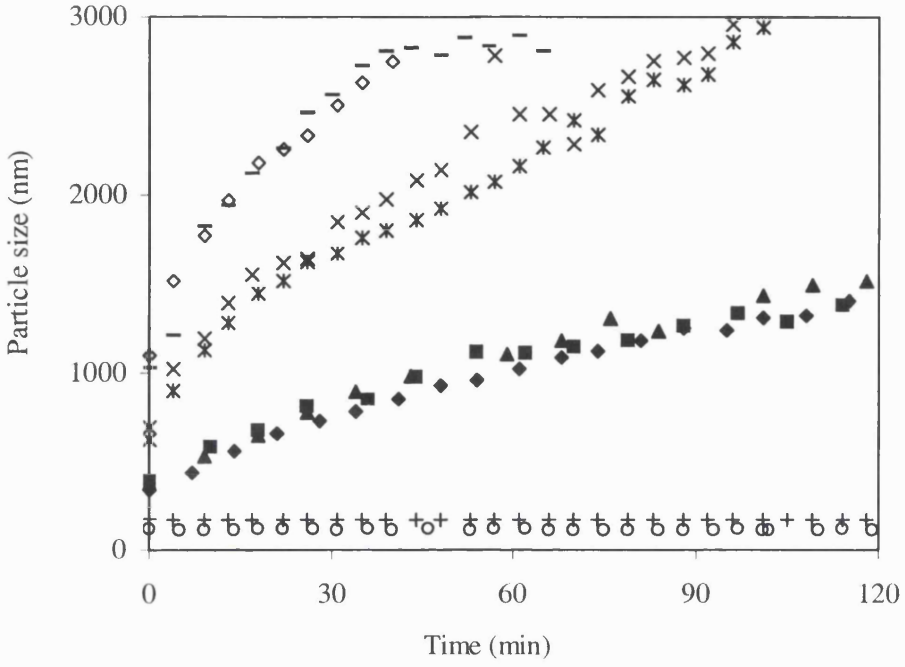
3000
2000
1000
0
Particle size (nm)
0
30
60
90
120
Time (min)

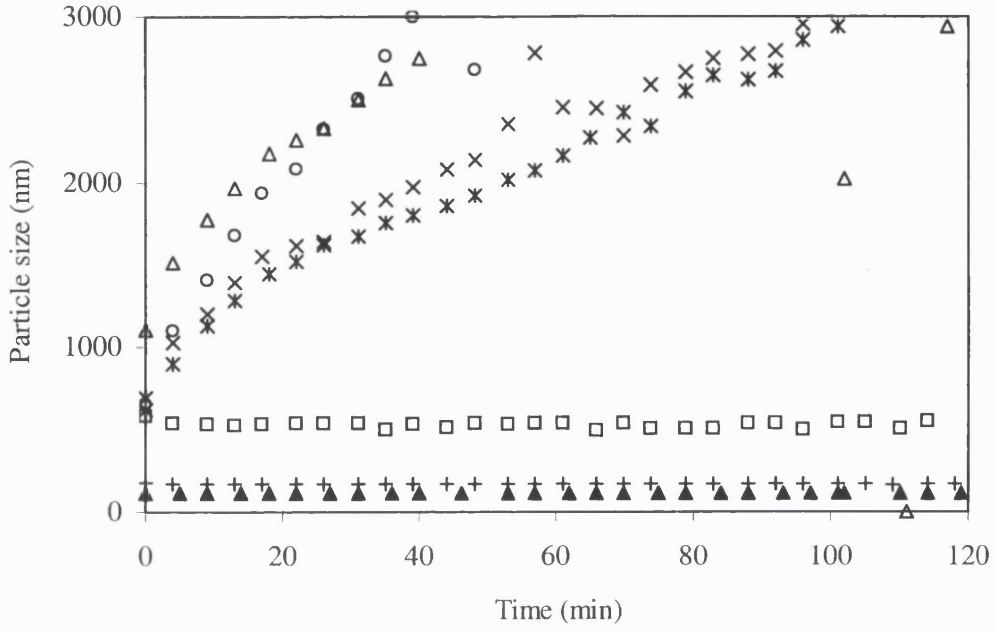
3000
2000
1000
0
Particle size (nm)
0
20
40
60
80
100
120
Time (min)

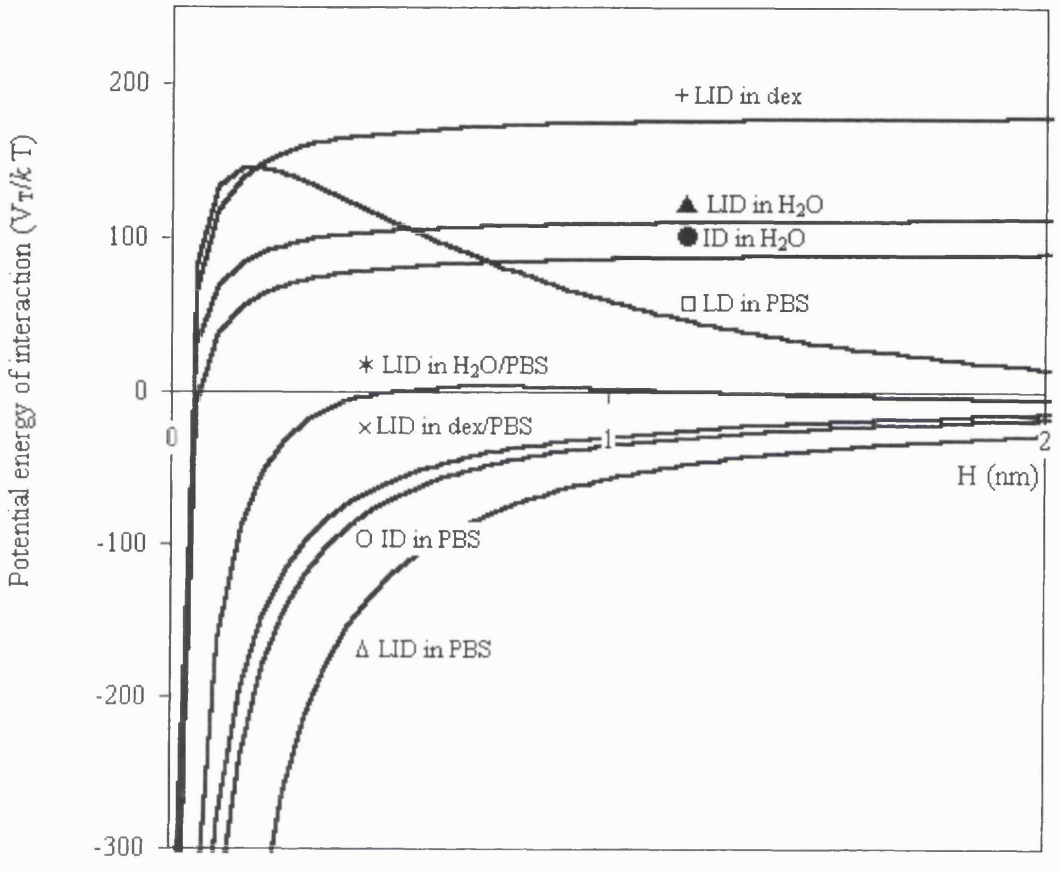

Lee et al., submitted

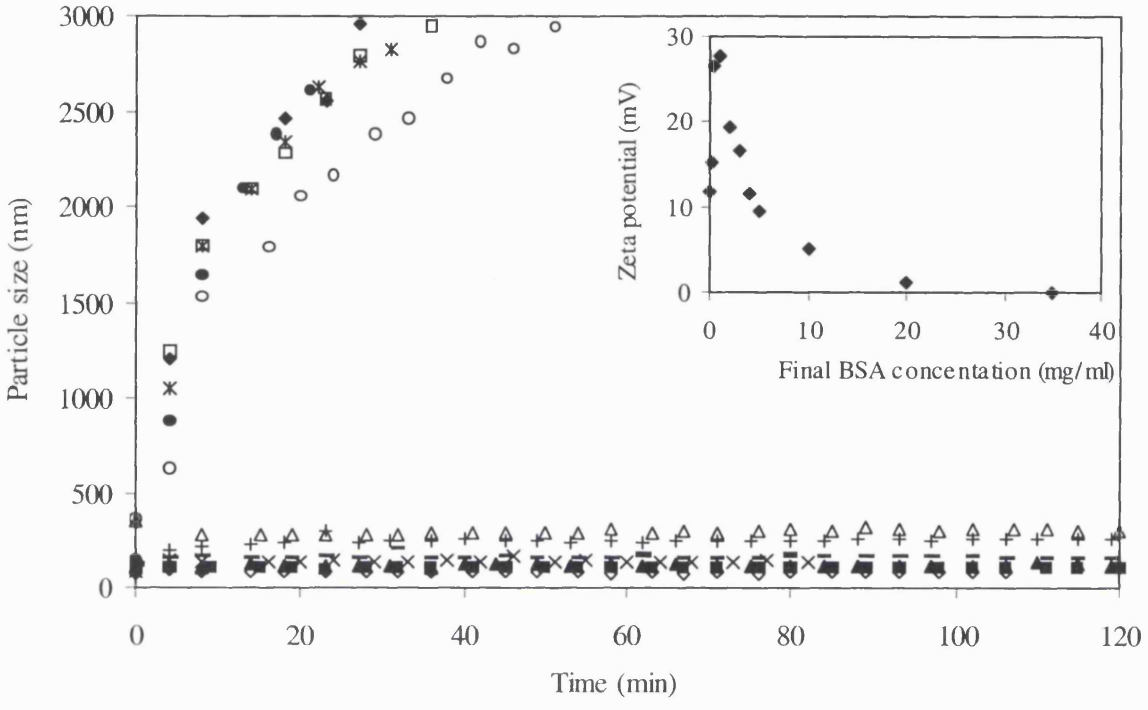

Lee et al., submitted

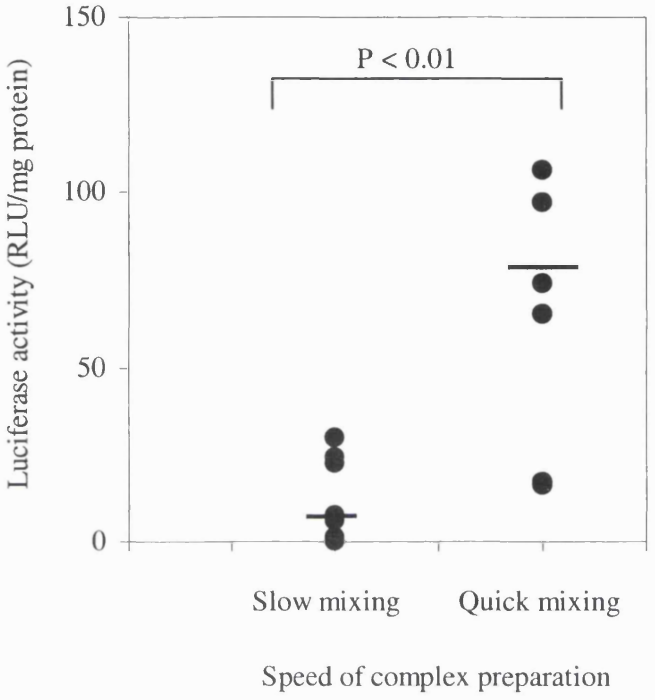
150
100
50
0
P < 0.01
Luciferase activity (RLU/mg protein)
Slow mixing
Quick mixing
Speed of complex preparation

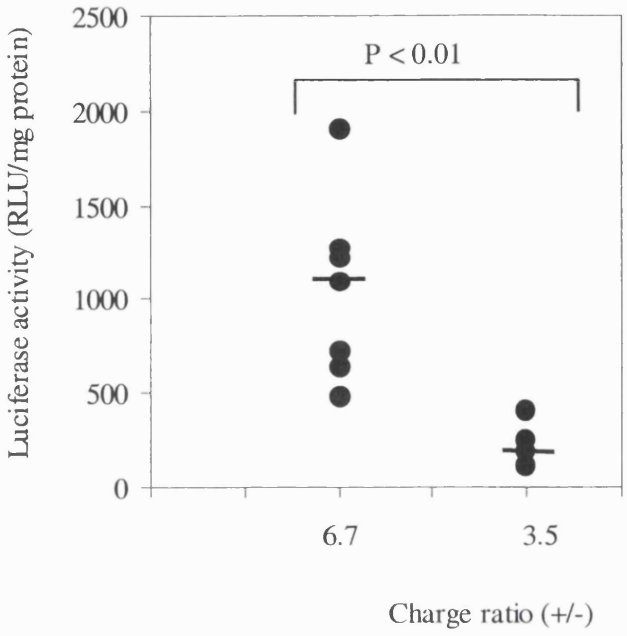
2500
2000
1500
1000
500
0
P < 0.01
Luciferase activity (RLU/mg protein)
6.7
3.5
Charge ratio (+/-)

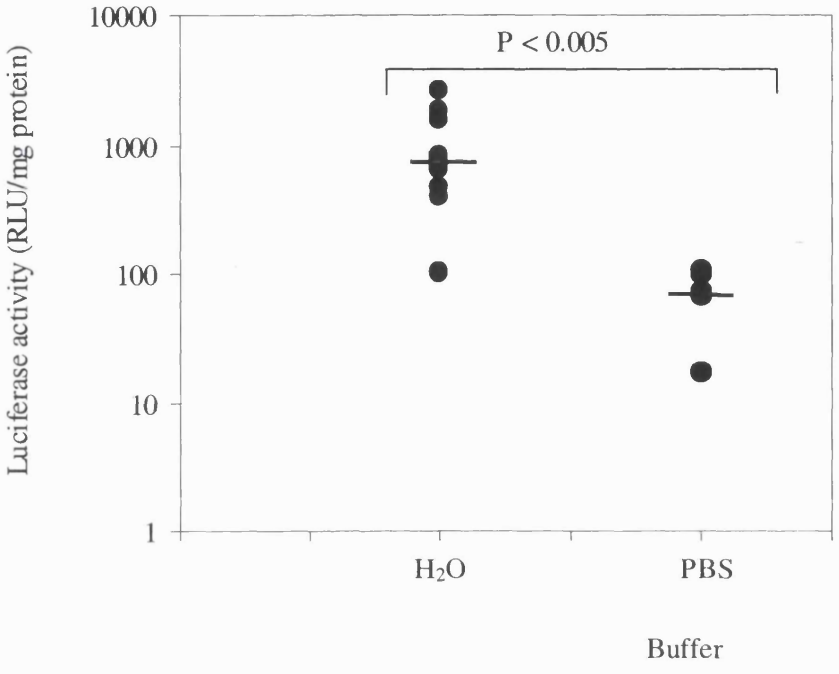
10000
1000
100
10
1
P < 0.005
Luciferase activity (RLU/mg protein)
H2O
PBS
Buffer

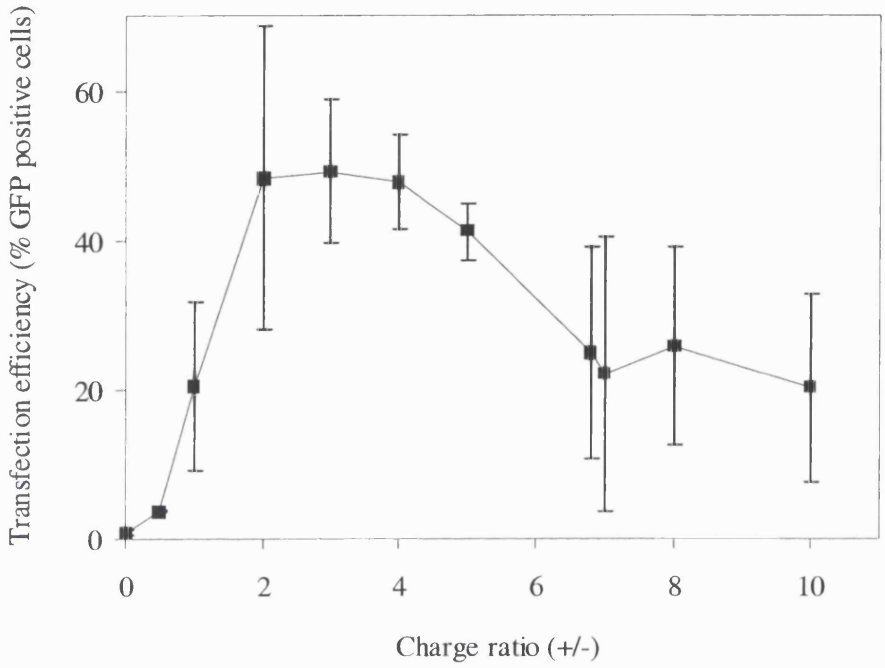
Transfection efficiency (% GFP positive cells)
60
40
20
0
0
2
4
6
8
10
Charge ratio (+/-)

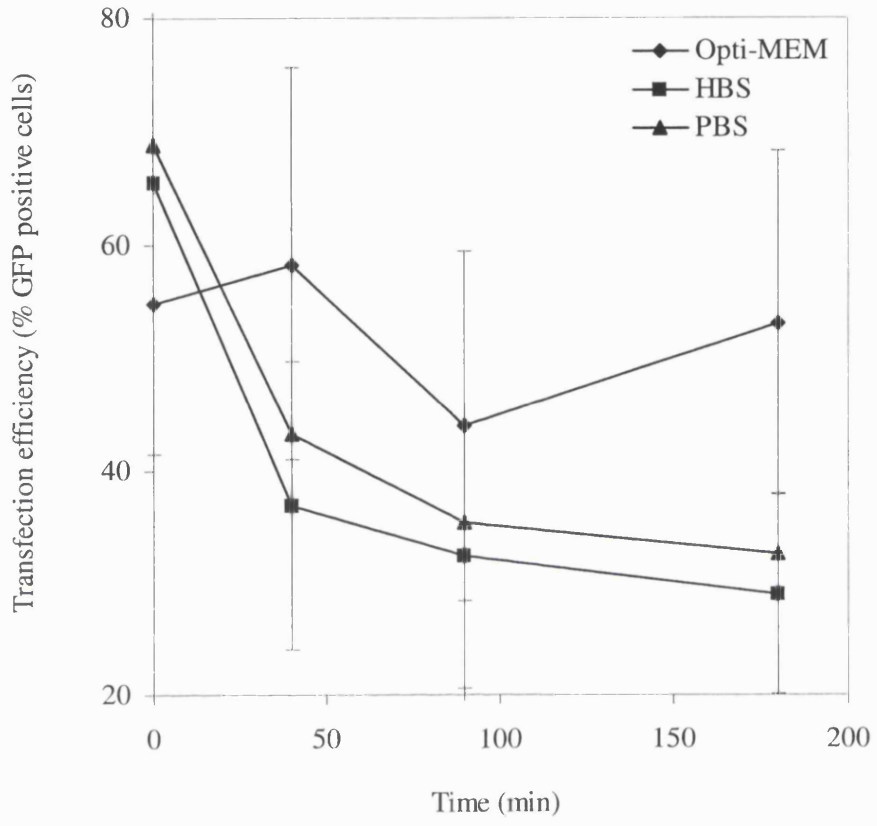
Transfection efficiency (% GFP positive cells)
80
60
40
20
0
50
100
150
200
Time (min)
Opti-MEM
HBS
PBS

FORMATION OF LID VECTOR COMPLEXES IN HYPOTONIC SOLUTION ALTERS PHYSICO-CHEMICAL PROPERTIES AND ENHANCES PULMONARY GENE EXPRESSION *IN VIVO*.

Jenkins RG[1], Meng Q-H[4], Hodges RJ[1], Lee LK[2], Laurent GJ[1], Willis D[3], Ayazi Shamlou P[2], McAnulty RJ[1*], and Hart SL[4*].

(1) Centre for Cardiopulmonary Biochemistry and Respiratory Medicine, Royal Free and University College Medical School, University College London, Rayne Institute, 5 University Street, London WC1E 6JJ, U.K.

(2) Department of Biochemical Engineering, University College London, Torrington Place, London WC1E 7JE, UK.

(3) Department of Pharmacology, Royal Free and University College Medical School, Gower Street, London UK.

(4) Molecular Immunology Unit, Institute of Child Health, University College London, 30 Guilford Street, London WC1N 1EH, U.K.

Author for Correspondence

Dr Gisli Jenkins, Centre for Cardiopulmonary Biochemistry and Respiratory Medicine, Royal Free and University College Medical School, University College London, Rayne Institute, 5 University Street, London WC1E 6JJ, U.K.

E mail g.jenkins@hotmail.com; Tel. (+44) 020-7679-6976; Fax (+44) 020-7679-6973

* These authors contributed equally to this study

ABSTRACT

The LID vector is a synthetic integrin targeted gene delivery system that has previously been shown to have high transfection efficiency in the lung. We have assessed the effect of altering methods of complex preparation on structural features of the complex, gene expression and the host response to the LID vector. We have demonstrated that making the complex hypotonic by preparing it in water affects the structure making it smaller, more stable and highly cationic. Furthermore it led to a ten-fold increase in luciferase activity compared with preparation in PBS, and luciferase activity was still evident one week following vector instillation. This enhancement may be due to altered complex structure, although hypo-osmotic effects on the lung cannot be excluded. The effects of instilling the LID vector in water led to minimal effects on pulmonary toxicity with only mild alterations in cytokine and bronchoalveolar lavage cell profiles. At optimal concentrations of DNA there was no histological evidence of pulmonary inflammation even after three administrations of the LID vector, although there was a slight reduction in gene expression. However, dose dependent lung injury limiting gene expression was observed at higher concentrations of DNA. These results demonstrate that the LID vector can generate high, and prolonged, levels of gene expression in the lung from small quantities of DNA and that careful attention to synthetic polyplex structure may be important in order to optimise efficiency of gene expression *in vivo*.

OVERVIEW SUMMARY

Current non-viral gene delivery systems, although showing promise, have low transfection efficiency and attempts to improve gene expression are hampered by dose dependent pulmonary toxicity. Improved gene expression from non-viral systems is urgently required to avoid the need for increasing dosage and associated toxicity. Assessment of the *in vitro* properties of non-viral systems does not predict success following *in vivo* transfection. This study demonstrates that attention to physical properties of non-viral systems aids optimisation of gene expression in the lung following transfection. Furthermore it demonstrates that preparation of the complex in hypotonic instillate increases both magnitude and duration of gene expression, as well as permitting repeated delivery of the vector without inducing pneumonitis. Furthermore there was evidence of only mild hypo-osmotic damage or immune responses. This study highlights the importance of assessing the structural properties of non-viral vectors and increases the considerable potential of the LID vector for pulmonary gene therapy.

INTRODUCTION

Gene therapy has the potential to lead to novel treatment strategies for diseases. Human trials have already demonstrated clinical improvement in conditions such as haemophilia (Kay *et al.*, 2000), cardiovascular disease (Yla-Herttuala and Martin, 2000), cancer (Khuri *et al.*, 2000) and severe combined immunodeficiency-X1 disease (Cavazzana-Calvo *et al.*, 2000). Many diseases affecting the lung such as asthma, lung cancer, pulmonary fibrosis and cystic fibrosis may be amenable to gene therapy. Initial clinical trials in cystic fibrosis, although promising, have highlighted the need to develop a safe and efficient vector system for pulmonary gene therapy to fulfil its potential (Alton *et al.*, 1999; Bellon *et al.*, 1997; Crystal *et al.*, 1994).

The LID vector consists of a cationic liposome (L), an integrin targeting peptide (I), with a sixteen lysine tail, and plasmid DNA (D), combined in optimal proportions to form an electrostatic complex which has previously been shown to efficiently transfect a number of cell types *in vitro* (Hart *et al.*, 1998). The LID vector efficiently transfected the lungs of rats mediated, at least in part, via the integrin-targeting component of the complex (Jenkins *et al.*, 2000). Luciferase reporter gene expression from this vector lasts for at least three days but β-galactosidase activity, with a longer half-life, was demonstrable for at least one week. A further beneficial characteristic of the vector is that it can be readministered without diminution of gene expression or significant inflammatory response. In these studies the complex was instilled into

the lungs in the physiological buffer PBS in order to minimise the damage that may occur following intratracheal instillation (Jenkins *et al.*, 2000).

Studies assessing viral vectors, and naked DNA, have demonstrated that instillation in water can lead to enhanced gene delivery due to both increased transepithelial permeability, and receptor expression, on the cell surface (Sawa *et al.*, 1996; Wang *et al.*, 1998; Wang *et al.*, 2000). Studies assessing the effect of instillate on the lung have not been performed using lipopolyplexes and would be further complicated by the observation that the physical and chemical characteristics of such complexes are altered in differing ionic environments. For example lipid fusion and aggregation occurred when lipid based vector complexes were added to physiological buffers (Ogris *et al.*, 1998) or serum (Li *et al.*, 1998), whereas in hypotonic buffers complex size was smaller and aggregation inhibited (Ogris *et al.*, 1998). However *in vitro* experiments have failed to demonstrate any relationship between physical characteristics and transfection efficiency (Ogris *et al.*, 1998). Targeted delivery of genes to the lung and liver, following intravenous administration of 10nm and 25nm complexes, with an overall negative charge ratio has been successful (Perales *et al.*, 1994; Ferkol *et al.*, 1995), but in these studies there was no formal assessment of the physico-chemical properties of these systems. Therefore, at the current time there is no consensus as to the optimal size, or charge, of non-viral complexes for *in vivo* transfection.

We have determined the effect of altering the ionic composition of the LID vector on the size and charge of the LID vector complex and levels of gene expression in the lung following intratracheal delivery. In an attempt to optimise levels of gene expression from the LID vector we have determined that the nature of the instillate alters the size and charge of the LID vector and that may be responsible for affecting its performance. Furthermore, as the toxicity of non-viral systems is related to a number of factors including the dose and route of delivery (Scheule *et al.*, 1997), the ionic nature of the instillate (Sawa *et al.*, 1996) and structural parameters of the complex (Floch *et al.*, 2000), we have assessed the pro-inflammatory profile of LID vector transfection under differing conditions. The LID vector, instilled in water, gives enhanced levels of gene expression, with minimal toxicity even after multiple administrations.

MATERIALS AND METHODS

Vector preparation

The α5β1 specific peptide (I), $[K]_{16}$-GACRRETAWACG was synthesised by Zinsser Analytic (Maidenhead, UK). Peptides were dissolved in phosphate buffered saline (PBS), or water, at a concentration of 1 mg/ml and cyclised by the formation of intramolecular disulphide bridges between cysteine residues by exposure to air overnight. Plasmid DNA was dissolved in distilled water at 1 mg/ml while Lipofectin (Valentis, Texas, USA) was provided at 1 mg/ml. The components of the LID complex: Lipofectin (L), Peptide (I) and DNA (D), were mixed in an optimized weight ratio of 0.75: 4: 1 respectively (Hart *et al.*, 1998). Lipofectin was mixed with the peptide and the resulting mixture added to the plasmid DNA. The volume of total LID complex instilled into each animal was 50μl containing between 1.6 and 32μg of plasmid DNA. For experiments instilling the LID vector in PBS and EGTA the peptides, lipofectin and DNA were prepared in a 10x concentrated stock solution of PBS and diluted to the working concentration in PBS containing EGTA at varying concentrations.

Plasmid DNA

The plasmid pAB11 contains a nuclear localising β-galactosidase reporter gene *lac Z* (Gift from J. Samulski) while pCILux consists of pCI (Promega, Southampton, UK) containing the luciferase gene both driven by the cytomegalovirus (CMV) immediate/early promoter-enhancer. Plasmid DNA was grown in *Escherichia coli* DH5α and purified, after bacterial alkaline lysis, on resin columns (Qiagen Ltd., Crawley, UK). Isopropanol-precipitated DNA pellets were washed with 70% ethanol then dissolved in water at 1 mg/ml.

Measurement of complex size

LID complexes were made as previously described, but for convenience, at a concentration of 160μg/ml (equivalent to 8μg per mouse). The particle size distributions of the complex were measured by dynamic light scattering (Van de Hulst, 1957) with a Malvern Zetasizer 3000 system (Malvern Instruments Ltd, Malvern, UK) at a scattering angle of 90°. The hydrodynamic diameter of the LID vector was calculated using the "moments" method by the autocorrelation function analysis software of the instrument. Given the power of the laser and the sensitivity of the instrument, the practical lower limit of accurate particle size is of the order of 10nm at the lower limit and 3μm at the upper limit. The size distributions were obtained from light scattering profiles reported as the intensity of light scattered by LID vector particles in each size class. For each sample, particle size distribution measurements were made five times in succession with a

counting time of approximately 180s per measurement. All measurements were made at a constant temperature of 25°C and each measurement was performed twice.

Measurement of complex zeta potential

The electrophoretic mobility of the LID vector complex was determined with the Malvern Zetasizer 3000 (Malvern Instruments Ltd, Malvern, UK). The instrument was calibrated with a –50 mV standard (DTS5050; Malvern Instruments Ltd, Malvern, UK) between measurements. For zeta potential measurements, which were conducted following dynamic light scattering measurements (2-3hrs), the LID complexes were prepared in the desired buffer (as described above) to give a final DNA concentration of 37.5μg/ml in a total volume of 4ml. Measurements were performed five times at 25°C.

Animals

Male C57Bl/6 mice at 4 - 5 weeks of age (Harlan UK), weighing 19.6±0.5g, were anaesthetised by inhaled halothane (3l/min) in oxygen (2 l/min). The trachea was exposed by ventral incision, and the transfection mixture instilled by intratracheal injection and the wound sutured. At least three animals per group were assessed for histological analysis and seven animals per group for biochemical analysis.

Biochemical assessment of luciferase activity

One or seven days following intratracheal instillation the mice were euthanised with pentobarbitonesodium (200 mg/ml; Sanofi Animal Health, Watford, UK). Following laparotomy and exsanguination the lungs were perfused via the right atrium with heparinised PBS until free of blood. The lungs were removed and blotted dry prior to snap freezing in liquid nitrogen. The lungs were weighed, then crushed under liquid nitrogen, in a pestle and mortar, prior to addition of cell lysis buffer (Roche Diagnostics, Lewes, UK) to the powdered lung (4μl/mg). The tissue was then homogenised, on ice, for 30s (Polytron PT10-35, Philip Harris, Nottingham, UK). Lung homogenates were centrifuged at 10,000 x g at 4°C for 10 min, then 20 μl of the supernatant was added to 100 μl luciferase assay buffer (Promega) and luminescence measured in a luminometer (TD-20/20; Steptech Instruments, Stevenage, UK). All results were repeated in triplicate and the mean calculated. The total protein concentration in the lysate was measured using previously described methods (Bradford, 1976) (Bio-Rad, Hemel Hempstead, UK) and using bovine serum albumin as a standard. Luciferase activity was expressed in relative light units (RLU) for each sample of lung lysate minus the background and normalised per mg of protein. It has previously

been established from luciferase standards (Roche Diagnostics, Lewes, UK) that 1 RLU is equivalent to approximately 10 femtograms of luciferase.

Bronchoalveolar lavage and analysis of bronchoalveolar lavage fluid cells and inflammatory mediators

Two days following instillation animals were euthanised as described above. Following exsanguination the trachea was cannulated and the lungs were lavaged ten times with 0.5ml aliquots of PBS. Each aliquot was instilled slowly over 15s and remained in situ for 30s prior to gentle removal of the PBS over 15s. The lavage fluid was kept on ice throughout the lavage procedure. Following bronchoalveolar lavage the samples were centrifuged at 164 x g for five minutes at 4°C (Beckman Instruments). The supernatant was removed for analysis of inflammatory mediators and stored, as 1ml aliquots, at –80°C until required. The cell pellet was resuspended in 500µl of PBS containing 100µg/ml albumin and kept on ice. An aliquot of the cellular suspension was counted. Cytocentrifuge preparations were prepared (Cytospin 3, Shandon, UK) and stained with haematoxylin and eosin and differential cell counts performed. At least 500 cells per sample were differentiated using conventional criteria for macrophage/monocytes, lymphocytes, or polymorphonuclear cells. Slides were coded and differentiated in a blinded fashion. PGE_2 levels were determined in the lavage fluid using an enzyme immunoassay according to manufacturer's protocol (Amersham, Little Chalfont, UK). TNFα, IL-1β and IFNγ were assayed in lavage fluid using an enzyme linked immunosorbent assay according to manufacturer's protocols (TNFα and IFNγ Pharmigen San Diego Ca and IL-1β R&D systems Abingdon, UK).

Histological assessment of lungs

Histological sections of lung were assessed for inflammation and β-galactosidase activity. Methods were based on those previously described (Jenkins *et al.*, 2000). Two days after intratracheal instillation the animals were euthanised with pentobarbitone sodium (200 mg/ml; Sanofi Animal Health, Watford, UK). Following laparotomy and exsanguination the lungs were perfused initially with heparinised PBS and then freshly prepared ice-cold fixative (4% paraformaldehyde and 0.2% glutaraldehyde) via the right atrium. Lungs were also fixed by intratracheal instillation of fixative at a pressure of 20cm H_2O for 15 minutes. The fixative was then removed with three PBS washes prior to instillation of X-Gal staining solution (5 m*M* $K_3Fe(CN)_6$, 5 m*M* $K_4Fe(CN)_6.3H_20$ & 0.2 m*M* $MgCl_2$ in Tris pH. 8.0) containing 1mg/ml X-gal (5-bromo-4-chloro-3-indolyl-β-D-galactopyranoside; Melford Laboratories, Ipswich, UK)

dissolved in N-N-dimethylformamide (Sigma, Poole, UK). The heart and lungs were removed *en bloc* immersed in X-gal staining solution. The lungs were incubated at 37°C for 24 hours in Tris buffer at pH 8. After further immersion in fixative overnight at 4°C, lungs were transferred to 15% sucrose in PBS prior to dehydration in alcohol. The lungs were dissected into lobes and each lobe embedded *en bloc* in paraffin wax. Sections 5μm thick, were cut and stained with 0.1% eosin for assessment of β-galactosidase activity, or haematoxylin and eosin for assessment of inflammation.

Statistical Analysis

Luciferase activity, assessed biochemically in whole lung lysates, was not normally distributed. The data is therefore shown as the median and range of values and differences between groups assessed using the Mann Whitney U test. All other data were normally distributed and therefore a student's t-test was used. A P value < 0.05 was considered significant.

RESULTS

Effect of buffer on physico-chemical properties of LID particles

In order to determine whether physico-chemical characteristics of the LID vector were affected by formation in different buffers the size and surface charge of the LID complex were determined when prepared in either PBS or deionised water (H_2O). Complexes formed in H_2O were found to be homogeneous and small with an average size of 100nm. These characteristics were stable for at least two hours. However, complexes made in PBS were much larger with an initial size of approximately 1μm and increasing to over 2μm within 20 minutes, reaching the maximal determinable size by about 40 minutes (Fig 1). Furthermore the surface charge of the complexes, as measured by zeta potential, was +50mV and +1mV when prepared in H_2O or PBS respectively.

Effect of instilling the LID vector in a hypotonic solution

Gene expression of the LID vector prepared in water and PBS was compared as hypotonic solutions influence both the physical properties of the vector complex and the host environment, either of which may affect the transfection efficiency. Complexes containing 8μg of plasmid encoding the luciferase gene (pCI-CMV-luc) were prepared either in ddH_2O (LID/H_2O) or PBS (LID/PBS), immediately prior to intratracheal instillation, and luciferase activity was measured one day later. Luciferase activity in murine lung was significantly elevated, by at least 10 fold, following LID/H_2O instillation compared with LID/PBS ($p<0.005$, Fig 2). Previous studies using

the LID vector prepared in PBS demonstrated that luciferase activity returned to control levels seven days following instillation (Jenkins *et al.*, 2000). Although, luciferase activity was significantly reduced seven days following instillation of LID/H_2O, activity was not significantly different from that one day following LID/PBS instillation and was significantly greater than non-transfected control values (Fig 2). In order to determine whether the effect was mediated via increasing transepithelial permeability, the LID vector was instilled in PBS with EGTA at concentrations from 25 to 400mM. Levels of luciferase activity were maximal using 100μM EGTA with a median RLU of 85.5RLU/mg protein (range 23 to 373). However this was not significantly greater than when instilled in PBS alone (median 65 RLU/mg protein, range 3 to 219) and significantly lower than when the LID vector was instilled in water (median 737 RLU/mg protein, range 105 to 2587, $p<0.005$).

Effect of increasing dose of luciferase cDNA within the LID vector complexed in water

Animals were transfected with the LID vector containing increasing doses of DNA in water to determine whether reporter gene activity could be further enhanced. Four doses between 1.6μg and 32μg of plasmid encoding the luciferase gene (pCI-luc) within LID/H_2O were instilled. All complexes were instilled in a total volume of 50μl per animal. Luciferase activity increased in a dose dependent manner, with an increase in luciferase activity of approximately seven-fold following a ten fold increase in plasmid dose, from 1.6μg to 16μg (Fig 3). There was no further increase following transfection with complexes containing 32μg plasmid DNA. Therefore, following LID/H_2O transfection there is a dose response of luciferase activity to increasing plasmid DNA that plateaus at approximately 16μg (320μg/ml).

Host responses to the LID/H_2O complex

a) Effect of dose and nature of plasmid within complex

Host responses to increased doses of plasmid within LID/H_2O were assessed histologically (Fig 4) and by observing weight loss. In order to assess the location of gene expression, as well as host responses to luciferase, LID/H_2O containing *lac Z* (pAB11) and pCI-luc were instilled at doses of 8μg and 32μg and assessed 48 hours later. β-galactosidase staining was not detected in histological sections (data not shown). Sections of lungs transfected with LID/H_2O containing 8μg pCI-luc, stained with haematoxylin and eosin, appeared normal without any evidence of inflammation (Fig 4a), however sections of lung transfected with 8μg of pAB11 showed small areas of inflammation evident by an increase in alveolar cellular infiltrate (Fig 4b). In contrast,

sections of lung from animals transfected with 32μg of pCI-luc had widespread areas of mild alveolar inflammation (Fig 4c & e), while animals transfected with LID/H_2O containing 32μg of pAB11 had extensive and severe inflammation throughout the lung (Fig 4d), with a predominantly monocytic infiltrate seen at high power (Fig. 4f).

Mice undergoing intratracheal injection usually lose 5% of their body weight in the first two days consequent to their surgery (unpublished observation). Weight loss following transfection with pCI-luciferase was not statistically different at any dose of cDNA used, and it was not different to mice transfected with 8μg of pAB11 (data not shown). However, mice transfected with 32μg of pAB11 lost 23.4±2% of their body weight two days following instillation, compared with only 9.1±0.2% loss of body weight following transfection with 32μg pCI-luc ($p<0.005$).

b) Effect of standard dose complex on cytological profiles and cytokines in bronchoalveolar lavage

Although there was no histological evidence of inflammation when the standard 8μg dose of plasmid DNA was instilled into the lung the inflammatory response to LID/H_2O was investigated further in order to detect mild lung damage. The LID/H_2O vector, containing pCI-luc, was instilled intratracheally and two days following instillation the lungs were lavaged for cytological assessment (table 1) and measurement of proinflammatory cytokines (table 2). Results were compared with those for animals instilled with water alone, LID/PBS or saline control. Cells from bronchoalveolar lavage (BAL) following LID/PBS instillation were almost all macrophages (see table 1) with normal morphology when compared with animals that had been instilled with saline control. There was a mild alteration in cytological profile following instillation of LID/H_2O with activated macrophages and some acute inflammatory cells being observed, however this was also seen in an animal instilled with water alone. When the cell populations were quantified, LID/PBS led to an increase in total cell number in BAL, which was due to an increase in macrophages, that was significantly greater than when LID/H_2O was instilled (see table 1). Furthermore there was significant lymphocytosis following LID/H_2O instillation compared with LID/PBS, with a similar trend observed when compared with water or saline controls (see table 1). The total cell number following instillation of water alone was similar to that following instillation with saline, but had a trend towards neutrophilia that was also observed following LID/H_2O instillation but did not reach significance (see table 1).

Assessment of inflammatory mediators in bronchoalveolar lavage fluid showed no difference in levels of prostaglandin E_2 (PGE_2), tumour necrosis factor-α (TNFα), interleukin-1β (IL-1β), or interferon-γ (IFNγ) from animals transfected with the LID vector, and the respective instillate. Levels of IL-1β and PGE_2 were low, being around the detection limits of the assay for all conditions. Levels of TNFα were measurable but there were no statistical differences between any of the treatment groups. Levels of interferon γ were low following instillation of PBS or LID/PBS but significantly increased following instillation of water or LID/H_2O, with a trend towards an increase in interferon γ following transfection compared with water alone, but this was not significant. Overall, there was no significant difference in any parameter measured between LID/H_2O and H_2O instillation alone (table 2).

c) Repeated delivery of LID/H_2O to the lung

Following adenoviral transfection of the lung, host immune responses limit transfection efficacy of the vector (Yei *et al.*, 1994; Yang *et al.*, 1995; Zabner *et al.*, 1996). Previous studies using the LID vector have demonstrated that a second instillation of the LID vector in PBS was possible without significant inflammation or diminution of transgene expression suggesting minimal immunogenicity (Jenkins *et al.*, 2000), which is supported by the above lavage data. In order to determine the immunogenic potential of LID/H_2O, the vector containing 8μg of DNA was instilled intratracheally three times at 10 day intervals and histological sections and luciferase activity was measured one day after the initial and the third instillation. Even after three instillations of LID/H_2O there was no histological evidence of pneumonitis (Data not shown). Furthermore levels of gene expression were still significantly elevated after three instillations (median 342 vs 0.5 RLU/mg control transfection $p<0.05$), although there was a 50% reduction in median luciferase activity following the third instillation compared to a single instillation (Fig 5).

DISCUSSION

Gene transfer to the lungs shows tremendous promise in the development of potential treatments for life threatening conditions such as cystic fibrosis, lung cancer and pulmonary fibrosis. Pulmonary gene transfer using non-viral systems has been hindered by low transfection efficiency. Furthermore, efforts to increase the dose of complex delivered have demonstrated dose dependent pulmonary inflammation, limiting the amount of DNA that can be administered intratracheally (Scheule *et al.*, 1997). Therefore mechanisms to improve gene expression from current non-viral systems are urgently required. Formulating the LID complex in water may alter

both the host environment of the lung and biochemical properties of the complex thus increasing levels of gene transfer and expression.

Following instillation of hypotonic solutions into the lung there may be small amounts of lung damage that may facilitate increased gene expression from non viral systems (Sawa *et al.*, 1996). Although there was no histological demonstration of lung injury following instillation of LID/H_2O there was a lymphocytosis and a trend towards granulocytosis with an increase in the interferon γ (IFNγ) with a similar trend towards granulocytosis and a lesser, but never-the-less significant, increase in IFNγ following instillation of water alone. This suggests that there was a small degree of injury following administration of hypotonic instillate that may promote enhanced transfection efficiency of the vector. However specific measures to increase transepithelial permeability with EGTA did not enhance luciferase activity suggesting that this alone is not enough to explain the increase in luciferase activity observed.

The relationship between vector structure and gene expression, for both receptor mediated and non-targeted systems such as cationic liposomes, is currently unclear (Ogris *et al.*, 1998; Freimark *et al.*, 1998). Consistent with our data, a previous study assessing the size of a PEI-transferrin DNA system on *in vitro* transfection, found that complexes made in water were smaller and more stable than those made in salt-containing buffers (Ogris *et al.*, 1998). However, in contrast to our study, where vector instillation in water led to higher levels of gene expression, Ogris *et al* demonstrated lower levels of luciferase activity *in vitro*. This probably reflects the differing environment of an *in vitro* experiment compared with the lung. If the structural properties of complexes lead to differential levels of *in vitro* and *in vivo* gene expression this would help to explain the failure to predict successful *in vivo* systems from cell culture experiments. Thus intratracheal gene transfer appears to be improved when complexes are small and do not aggregate, and this may represent a general phenomena for receptor mediated gene delivery systems *in vivo*.

The cationic nature of the LID complex is also altered when it is prepared in water and this may further affect its function. The LID vector contains poly-L-lysine as a cation and condensing agent. Despite the same molar charge ratio (cation:anion 6.7:1), the zeta potential of LID/H_2O is 50 fold greater than LID/PBS. The high positive surface charge may well increase plasmid uptake due to electrostatic association with the negative cell membrane. Whether the increased gene expression is due to an increase in transfection efficiency or improved processing of the

internalised complex is uncertain. We have previously demonstrated that pulmonary transfection efficiency following instillation of the LID vector in PBS is of the order of 25% (Jenkins *et al.*, 2000) and there is, at least, a ten-fold increase in reporter gene activity following transfection with LID/H_2O compared with LID/PBS. It is therefore unlikely that the increase in reporter gene activity can be explained entirely by increased transfection efficiency although some increase via this mechanism cannot be excluded. It is therefore likely that the enhancement seen following complex formation in water is probably due, at least in part, to enhanced efficiency of gene expression from the cells transfected.

Luciferase activity increases in a dose dependent manner with increasing dose of plasmid cDNA within the LID vector. However, a plateau effect is observed at 16μg (320μg/ml) of cDNA within the complex. Potential reasons for this effect include saturation of receptor binding or of complex solubility. However even in the absence of receptor binding the LID vector can promote cellular internalisation of DNA (Jenkins *et al.*, 2000) while there was no observed precipitation of the LID complex in H_2O at any concentration of DNA tested. There was, however, a dose dependent inflammatory response that was even more pronounced following transfection with the *lac Z* gene. This might suggest that inflammatory or immune responses are responsible for limiting gene expression following LID/H_2O transfection. Immune responses to *lac Z* have been shown to limit β-galactosidase activity following liposomal gene transfer in mice (Lukacs *et al.*, 1999). It is likely that the inflammatory responses were mediated against the plasmid, or the protein encoded, rather than other components of the LID complex, because there was no evidence of β-galactosidase activity following *lac Z* transfection at either dose.

Liposomes instilled intratracheally into the lungs of mice can cause pulmonary inflammation (Scheule *et al.*, 1997; Freimark *et al.*, 1998). Freimark and colleagues demonstrated evidence of inflammation, either alone or complexed to DNA, using lipid at doses slightly lower than those required to generate LID vector containing 32μg of cDNA (Freimark *et al.*, 1998). Therefore some of the toxicity seen at the highest dose of the LID vector may be due to the liposomal component of the complex. Furthermore, both the chloramphenicol acetyl transferase (CAT) and *lac* Z genes can stimulate specific antibody formation after a single instillation in mice (Scheule *et al.*, 1997; Dong *et al.*, 1996). These are both enzymes of enteric bacteria and rodents may well have prior exposure to these proteins, whereas luciferase is an insect derived enzyme and prior exposure is unlikely and may explain the difference in magnitude of inflammatory responses between the *lac* Z and luciferase transfected mice. Furthermore, plasmids encoding bacterial

enzymes will contain more of the immunostimulatory unmethylated CpG sequences than plasmids encoding insect derived enzymes.

Plasmid DNA, being derived primarily from bacteria, may contain unmethylated CpG sequences. These sequences are immunostimulatory and lead to the production of Th1 type cytokines IFNγ and IL-12 (Scheule and Cheng, 1998; Freimark *et al.*, 1998). Although methylation of plasmid DNA has been shown to abolish IL-12 and IFNγ production following intratracheal instillation it didn't alter the cellular infiltrate. Conversely, lipid alone can provoke cellular responses of the magnitude of lipid:DNA complexes without inducing IFNγ or IL-12 (Freimark *et al.*, 1998; Scheule *et al.*, 1997; McLachlan *et al.*, 2001). LID/H_2O vector transfection using 8μg of DNA provoked a lymphocytosis and generated significant levels of IFNγ in BALF compared with LID/PBS, although levels of IFNγ were not significantly greater than following instillation of water alone. It is possible that hypomethylated CpG sequences are responsible for the inflammation seen following LID vector transfection and these might be enhanced using bacterial plasmids. However, levels of **IFNg** were 100-fold lower than following intratracheal transfection of mice with GL67-CAT at the same time point (Scheule *et al.*, 1997) suggesting minimal immunostimulatory effects of LID/H_2O even compared with liposomal preparations. This is further supported by the absence of pneumonitis on histological sections following instillation of LID/H_2O containing 8μg of pCI-luc even after repeated dosing. Previous studies have demonstrated no diminution in gene expression following repeat intratracheal administration of the LID vector in PBS (Jenkins *et al.*, 2000) or intratracheal and intranasal administration of liposomes using HEPES as the diluent (Goddard *et al.*, 1997; Hyde *et al.*, 2001). However following repeated dosing of the vector in water there was a 50% reduction in luciferase activity. It is possible that this was to immune activation following LID vector instillation or possibly due to the effects of inhaled anaesthetics that might reduce luciferase expression (Gill *et al.*, 2001). If indeed these are immune specific effects they still represent a significant improvement compared with adenoviral transduction where a 75% reduction in luciferase activity has been observed following only a single repeated administration (Yei *et al.*, 1994).

Preparing the LID vector in water increased gene expression. This could be due to effects on the lung as there was some evidence of mild hyposmotic damage following instillation of water alone. However disruption of tight junctions with EGTA failed to enhance gene expression following LID vector transfection. It is also possible that the properties of the LID vector in water, including a high zeta potential and smaller, stable complexes favour enhanced gene

expression. Despite the highly cationic nature of the complex there was only a little evidence of pulmonary toxicity using optimal doses of the LID vector, when the luciferase gene was instilled, even after multiple instillations of the vector, although as with liposomal transfection there was dose dependent pulmonary toxicity limiting gene expression. These results further illustrate the considerable potential of the LID vector for pulmonary gene therapy, as it is able to generate high levels of luciferase activity, from very small quantities of plasmid DNA with minimal toxicity even after repeated instillation.

REFERENCES

ALTON, E.W., STERN, M., FARLEY, R., JAFFE, A., CHADWICK, S.L., PHILLIPS, J., DAVIES, J., SMITH, S.N., BROWNING, J., DAVIS, M.G., HODSON, M.E., DURHAM, S.R., LI, D., JEFFERY, P.K., SCALLAN, M., BALFOUR, R., EASTMAN, S.J., CHENG, S.H., SMITH, A.E., MEEKER, D. and GEDDES, D.M. (1999) Cationic lipid-mediated CFTR gene transfer to the lungs and nose of patients with cystic fibrosis: a double-blind placebo-controlled trial. Lancet **353**, 947-954.

BELLON, G., MICHEL-CALEMARD, L., THOUVENOT, D., JAGNEAUX, V., POITEVIN, F., MALCUS, C., ACCART, N., LAYANI, M.P., AYMARD, M., BERNON, H., BIENVENU, J., COURTNEY, M., DORING, G., GILLY, B., GILLY, R., LAMY, D., LEVREY, H., MOREL, Y., PAULIN, C., PERRAUD, F., RODILLON, L., SENE, C., SO, S., TOURAINE-MOULIN, F., SCHATZ, C., and PAVIRANI, A. (1997) Aerosol administration of a recombinant adenovirus expressing CFTR to cystic fibrosis patients: a phase I clinical trial. Hum. Gene Ther. **8**, 15-25.

BRADFORD, M.M. (1976) A rapid and sensitive method for the quantitation of microgram quantities of protein utilizing the principle of protein-dye binding. Anal. Biochem. **72**, 248-254.

CAVAZZANA-CALVO, M., HACEIN-BEY, S., DE SAINT BASILE, G., GROSS, F., YVON, E., NUSBAUM, P., SELZ, F., HUE, C., CERTAIN, S., CASANOVA, J.L., BOUSSOS, P., DEIST, F.L., and FISCHER, A. (2000) Gene therapy of human severe combined immunodeficiency (SCID)-X1 disease. Science. **288**, 627-629.

CRYSTAL, R.G., MCELVANEY, N.G., ROSENFELD, M.A., CHU, C.S., MASTRANGELI, A., HAY, J.G., BRODY, S.L., JAFFE, H.A., EISSA, N.T. and DANEL, C. (1994)

Administration of an adenovirus containing the human CFTR cDNA to the respiratory tract of individuals with cystic fibrosis. Nat. Genet. **8**, 42-51.

DONG, J.Y., WANG, D., VAN GINKEL, F.W., PASCUAL, D.W. and FRIZZELL, R.A. (1996) Systematic analysis of repeated gene delivery into animal lungs with a recombinant adenovirus vector. Hum. Gene Ther. **7**, 319-331.

FERKOL, T., PERALES, J.C., ECKMAN, E., KAETZEL, C.S., HANSON, R.W. and DAVIS, P.B. (1995) Gene transfer into the airway epithelium of animals by targeting the polymeric immunoglobulin receptor. J. Clin. Invest. **95**, 493-502.

FLOCH, V., DELEPINE, P., GUILLAUME, C., LOISEL, S., CHASSE, S., LE BOLC'H, G., GOBIN, E., LEROY, J.P. and FEREC, C. (2000) Systemic administration of cationic phosphonolipids/DNA complexes and the relationship between formulation and lung transfection efficiency. Biochim. Biophys. Acta. **1464**, 95-103.

FREIMARK, B.D., BLEZINGER, H.P., FLORACK, V.J., NORDSTROM, J.L., LONG, S.D., DESHPANDE, D.S., NOCHUMSON, S. and PETRAK, K.L. (1998) Cationic lipids enhance cytokine and cell influx levels in the lung following administration of plasmid: cationic lipid complexes. J. Immunol. **160**, 4580-4586.

GODDARD, C.A., RATCLIFF, R., ANDERSON, J.R., GLENN, E., BROWN, S., GILL, D.R., HYDE, S.C., MACVINISH, L.J., HUANG, L., HIGGINS, C.F., CUTHBERT, A.W., EVANS, M.J. and COLLEDGE, W.H. (1997) A second dose of a CFTR cDNA-liposome complex is as effective as the first dose in restoring cAMP-dependent chloride secretion to null CF mice trachea. Gene Ther. **4**, 1231-1236.

GILL, D., PRINGLE, I., DAVIES, L., and HYDE, S. (2001) The effect of dosing interval on reporter gene expression in mouse lung. Mol Ther. **3** S68.

HART, S.L., ARANCIBIA CARCAMO, C.V., WOLFERT, M.A., MAILHOS, C., O'REILLY, N.J., ALI, R.R., COUTELLE, C., GEORGE, A.J., HARBOTTLE, R.P., KNIGHT, A.M., LARKIN, D.F.,LEVINSKY, R.J., SEYMOUR, L.W., THRASHER, A.J. and KINNON, C.

(1998) Lipid-mediated enhancement of transfection by a nonviral integrin-targeting vector. Hum. Gene Ther. **9**, 575-585.

HYDE, S.C., SOUTHERN, K.W., GILEADI, U., FITZJOHN, E.M., MOFFORD, K.A., WADDELL, B.E., GOOI, H.C., GODDARD, C.A., HANNAVY, K., SMYTH, S.E., EGAN, J.J., SORGI, F.L., HUANG, L., CUTHBERT, A.W., EVANS, M.J., COLLEDGE, W.H., HIGGINS, C.F., WEBB, A.K. and GILL, D.R. (2000) Repeat administration of DNA/liposomes to the nasal epithelium of patients with cystic fibrosis. Gene Ther. **7**, 1156-1165.

JENKINS, R.G., HERRICK, S.E., MENG, Q.H., KINNON, C., LAURENT, G.J., MCANULTY, R.J. and HART, S.L. (2000) An integrin-targeted non-viral vector for pulmonary gene therapy. Gene Ther. **7**, 393-400.

KAY, M.A., MANNO, C.S., RAGNI, M.V., LARSON, P.J., COUTO, L.B., MCCLELLAND, A., GLADER, B., CHEW, A.J., TAU, S.J., HERZOG, R.W., ARRUDA, V., JOHNSON, F., SCALLAN, C., SKARSGARD, E., FLAKE, A.W., and HIGH, K.A. (2000) Evidence for gene transfer and expression of factor IX in haemophilia Bpatients treated with an AAV vector. Nat. Genet. **24**, 257-261.

KHURI, F.R., NEMUNAITIS, J., GANLY, I., ARSENEAU, J., TANNOCK, I.F., ROMEL, L., GORE, M., IRONSIDE, J., MACDOUGALL, R.H., HEISE, C., RANDLEV, B., GILLENWATER, A.M., BRUSO, P., KAYE, S.B., HONG,W.K., and KIRN, D.H. (2000) A controlled trial of intratumoral ONYX-O15, a selectively-replicating adenovirus, in combination with cisplatin and 5-fluorouracil in patients with recurrent head and neck cancer. Nat. Med. **6**, 879-885.

LI, S., RIZZO, M.A., BHATTACHARYA, S. and HUANG, L. (1998) Characterization of cationic lipid-protamine-DNA (LPD) complexes for intravenous gene delivery. Gene Ther. **5**, 930-937.

LUKACS, K.V., PORTER, C.D., PARDO, O.E., OAKLEY, R.E., STEEL, R.M., JUDD, D.V., BROWNING, J.E., GEDDES, D.M. and ALTON, E.W. (1999) In vivo transfer of bacterial marker genes results in differing levels of gene expression and tumor progression in immunocompetent and immunodeficient mice. Hum. Gene Ther. **10**, 2373-2379.

MCLACHLAN, G., STEVENSON, B.J., DAVIDSON, D.J. and PORTEOUS, D.J. (2000) Bacterial DNA is implicated in the inflammatory response to delivery of DNA/DOTAP to mouse lungs. Gene Ther. **7**, 384-392.

OGRIS, M., STEINLEIN, P., KURSA, M., MECHTLER, K., KIRCHEIS, R. and WAGNER, E. (1998) The size of DNA/transferrin-PEI complexes is an important factor for gene expression in cultured cells. Gene Ther. **5**, 1425-1433.

PERALES, J.C., FERKOL, T., BEEGEN, H., RATNOFF, O.D. and HANSON, R.W. (1994) Gene transfer in vivo: sustained expression and regulation of genes introduced into the liver by receptor-targeted uptake. Proc. Natl. Acad. Sci. U. S. A. **91**, 4086-4090.

SAWA, T., MIYAZAKI, H., PITTET, J.F., WIDDICOMBE, J.H., GROPPER, M.A., HASHIMOTO, S., CONRAD, D.J., FOLKESSON, H.G., DEBS, R.,FORSAYETH, J.R., FOX, B. and WIENER KRONISH, J.P. (1996) Intraluminal water increases expression of plasmid DNA in rat lung. Hum. Gene Ther. **7**, 933-941.

SCHEULE, R.K., ST GEORGE, J.A., BAGLEY, R.G., MARSHALL, J., KAPLAN, J.M., AKITA, G.Y., WANG, K.X., LEE, E.R., HARRIS, D.J., JIANG, C., YEW, N.S., SMITH, A.E. and CHENG, S.H. (1997) Basis of pulmonary toxicity associated with cationic lipid-mediated gene transfer to the mammalian lung. Hum. Gene Ther. **8**, 689-707.

SCHEULE, R.K. and CHENG, S.H. (1998) Airway delivery of cationic lipid: DNA complexes for cystic fibrosis. Adv. Drug Deliv. Rev. **30**, 173-184.

VAN DE HULST, H.C. (1957) Light scattering by small particles. (John Wiley & Sons, New York, NY).

WANG, G., DAVIDSON, B.L., MELCHERT, P., SLEPUSHKIN, V.A., VAN ES, H.H., BODNER, M., JOLLY, D.J. and MCCRAY, P.B., JR. (1998) Influence of cell polarity on retrovirus-mediated gene transfer to differentiated human airway epithelia. J. Virol. **72**, 9818-9826.

WANG, G., ZABNER, J., DEERING, C., LAUNSPACH, J., SHAO, J., BODNER, M., JOLLY, D.J., DAVIDSON, B.L. and MCCRAY, P.B.J. (2000) Increasing epithelial junction permeability enhances gene transfer to airway epithelia In vivo. Am. J. Respir. Cell Mol. Biol. **22**, 129-138.

YANG, Y., LI, Q., ERTL, H.C. and WILSON, J.M. (1995) Cellular and humoral immune responses to viral antigens create barriers to lung-directed gene therapy with recombinant adenoviruses. J. Virol. **69**, 2004-2015.

YLA-HERTTUALA, S. and MARTIN, J.F. (2000) Cardiovascular gene therapy. Lancet. **355**, 213-222.

YEI, S., MITTEREDER, N., TANG, K., O'SULLIVAN, C. and TRAPNELL, B.C. (1994) Adenovirus-mediated gene transfer for cystic fibrosis: quantitative evaluation of repeated in vivo vector administration to the lung. Gene Ther. **1**, 192-200.

ZABNER, J., RAMSEY, B.W., MEEKER, D.P., AITKEN, M.L., BALFOUR, R.P., GIBSON, R.L., LAUNSPACH, J., MOSCICKI, R.A.,RICHARDS, S.M., STANDAERT, T.A., WILLIAM-WARREN, J., WADSWORTH, S.C., SMITH, A.E., and WELSH, M.J. (1996) Repeat administration of an adenovirus vector encoding cystic fibrosis transmembrane conductance regulator to the nasal epithelium of patients with cystic fibrosis. J. Clin. Invest. **97**, 1504-1511.

Figure legends

Figure 1. The effect of instillate on particle size over time. The LID vector complexed in water is small (approximately 100 nm) and more stable not increasing in size over time. The LID vector complexed in PBS is larger at over 1 μm in diameter and aggregates to almost 3μm after one hour.

Figure 2. Luciferase activity in whole lung lysates, one and seven days following instillation of the LID vector in water (closed circles) or one day following instillation in PBS (open circles). Luciferase activity is significantly greater one day following instillation of the LID vector in water than in PBS. There is no statistical difference between luciferase activity seven days following transfection with LID/H_2O vector in water or one day LID/PBS. All groups were significantly greater than untransfected controls.

Figure 3. Effect of increasing the dose of luciferase plasmid DNA on luciferase activity in whole lung lysates one day following instillation of LID vector in water. Luciferase activity increases in a dose dependent manner up to 16μg of plasmid DNA but there is no increase following instillation of 32 μg plasmid DNA.

Figure 4 (not shown). Photomicrographs of lung sections stained with H & E following LID/H_2O transfection of a) 8μg luciferase cDNA illustrating normal pulmonary architecture, b) 8μg *lac Z* cDNA illustrating mild areas of inflammation, c) 32 μg of luciferase cDNA illustrating inflammation of the alveolar airspaces and d) 32 μg of *lac Z* cDNA illustrating severe inflammation throughout the lung. Original magnification x100. Panel e) shows high power view of 32μg of luciferase and f) *lac Z* transfected lung demonstrating severe mononuclear inflammatory response in *lac Z* transfected lung. Original magnification x1000.

Figure 5. Luciferase activity in whole lung lysates one day following instillation after one or three weekly administrations of the LID vector in water. Luciferase activity is significantly reduced following the third instillation of the LID vector. Both groups are significantly greater than lungs transfected with irrelevant plasmid (data not shown).

Table 1 Inflammatory cell profile in BAL following LID vector transfection in either an isotonic (PBS) or hypotonic (H_2O) instillate compared with saline control and water alone. There is no significant difference in inflammatory cell profile between LID vector transfection and control whether using an isotonic or hypotonic instillate. However there is a significant increase in lymphocyte number following LID/H_2O instillation compared with LID/PBS with a concomitant reduction in total cell number and macrophage number. All other comparisons are not significantly different. * = $p<0.05$ compared with LID/PBS and $ compared with instillate alone. Each value represents mean ±SEM for at least six animals.

	Instillate				
	Cell type	***Saline***	***LID/PBS***	***H_2O***	***LID/H_2O***
Cell Number (% of total cell count)	Total Cell count ($x10^{-5}$)	2.7±0.2	3.9±0.5	2.7±0.2	2.4±0.2*
	Macrophages ($x10^{-5}$)	2.7 ± 0.2 (99.8% ± 0.1)	3.9 ± 0.5 (99.8% ± 0.1)	2.6 ± 0.1 (98.7% ± 1)	2.3 ± 0.2* (97.7% ± 1)
	Lymphocytes ($x10^{-3}$)	0.2 ± 0.1 (0.2% ± 0.1)	0.2 ± 0.1 (0.1% ± 0.1)	0.2 ± 0.1 (0.1% ± 0.05)	2.5 ± 1.4*$ (1% ± 0.4)
	Polymorphonuclear cells ($x10^{-3}$)	0 ± 0 (0% ± 0)	0.3 ± 0.1 (0.1% ± 0.05)	4 ± 4 (1.2% ± 1)	3.3 ± 2.3 (1.3% ± 1)

Table 2 Inflammatory mediator profile in BALF following LID vector transfection in either an isotonic (PBS) or hypotonic (H_2O) instillate compared with saline control and water alone. There is no difference in inflammatory mediator profile between LID vector transfection and control whether using an isotonic or hypotonic instillate. However there is a significant increase in IFNγ following hypotonic instillation compared with respective isotonic control * = p<0.05, **=p<0.005 compared with PBS control. Each value represents the mean±SEM for at least six animals.

	Instillate			
Mediator (pg/ml)	***Saline***	***LID/PBS***	***H_2O***	***LID/H_2O***
PGE_2	40 ± 0	77.5 ± 28	41 ± 1	48 ± 5
IL-1β	22 ± 0	22 ± 0	22.4 ± 0.4	22 ± 0
TNFα	38 ± 9	40 ± 9	25 ± 6	28 ± 6
IFNγ	4.8 ± 0.1	5.1 ± 0.3	25.2 ± 7*	37.9 ± 8**

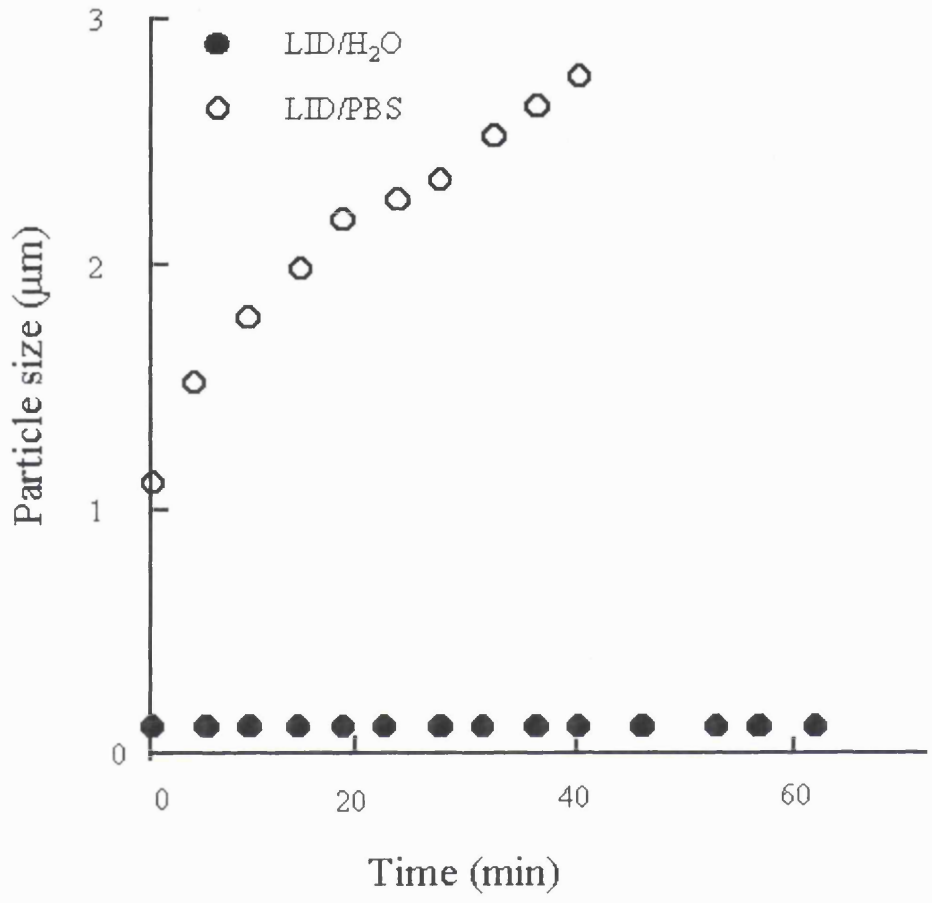
LID/H2O
LID/PBS
Particle size (µm)
3
2
1
0
0
20
40
60
Time (min)

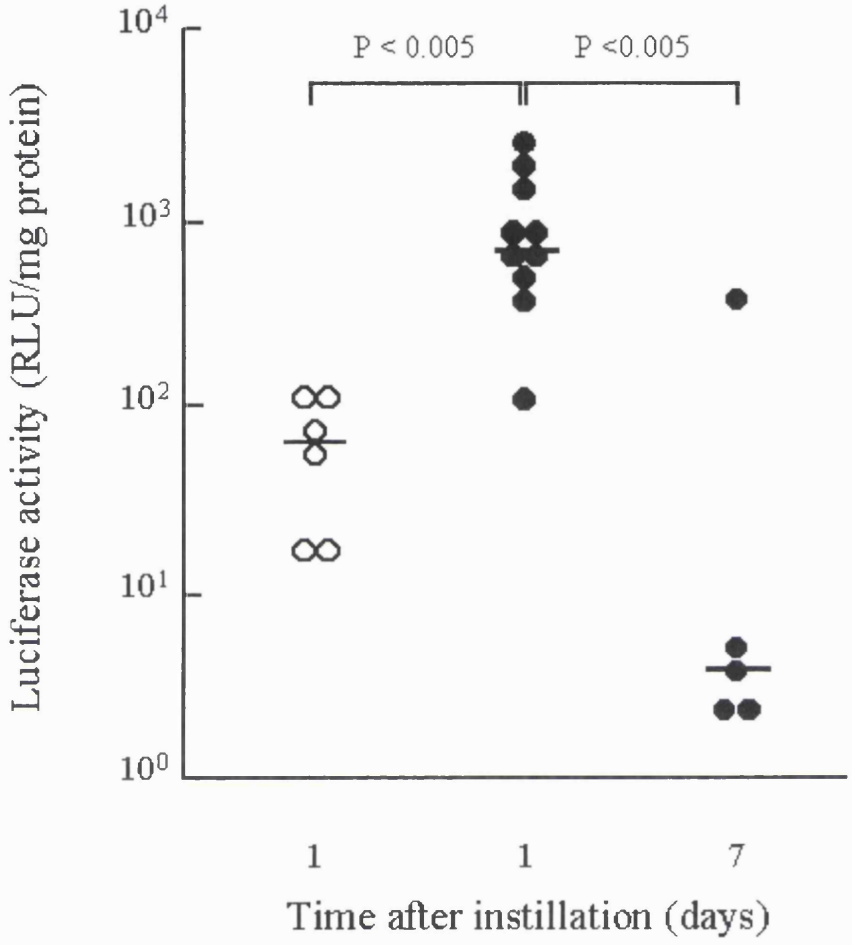
10^4
10^3
10^2
10^1
10^0
P < 0.005
P <0.005
Luciferase activity (RLU/mg protein)
1
1
7
Time after instillation (days)

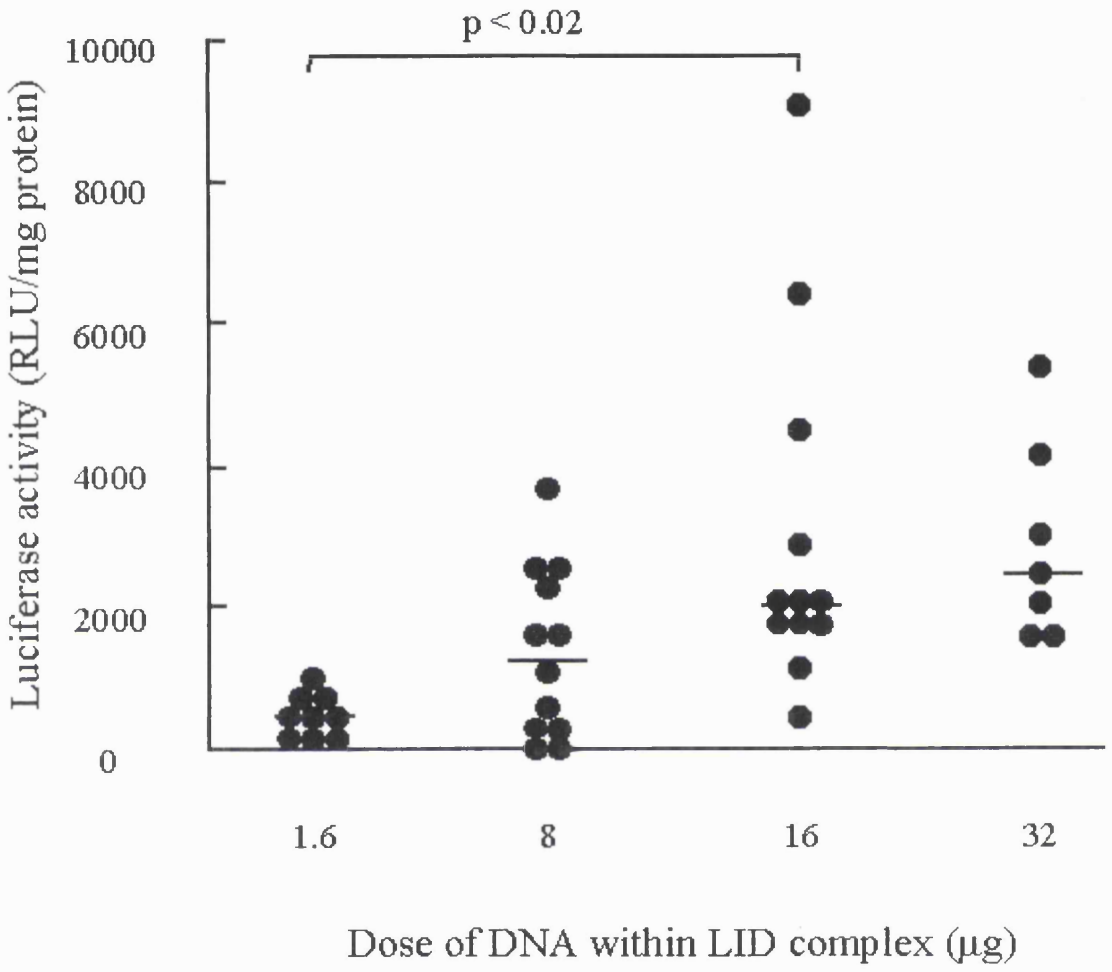
p < 0.02
10000
8000
6000
4000
2000
0
Luciferase activity (RLU/mg protein)
1.6
8
16
32
Dose of DNA within LID complex (µg)

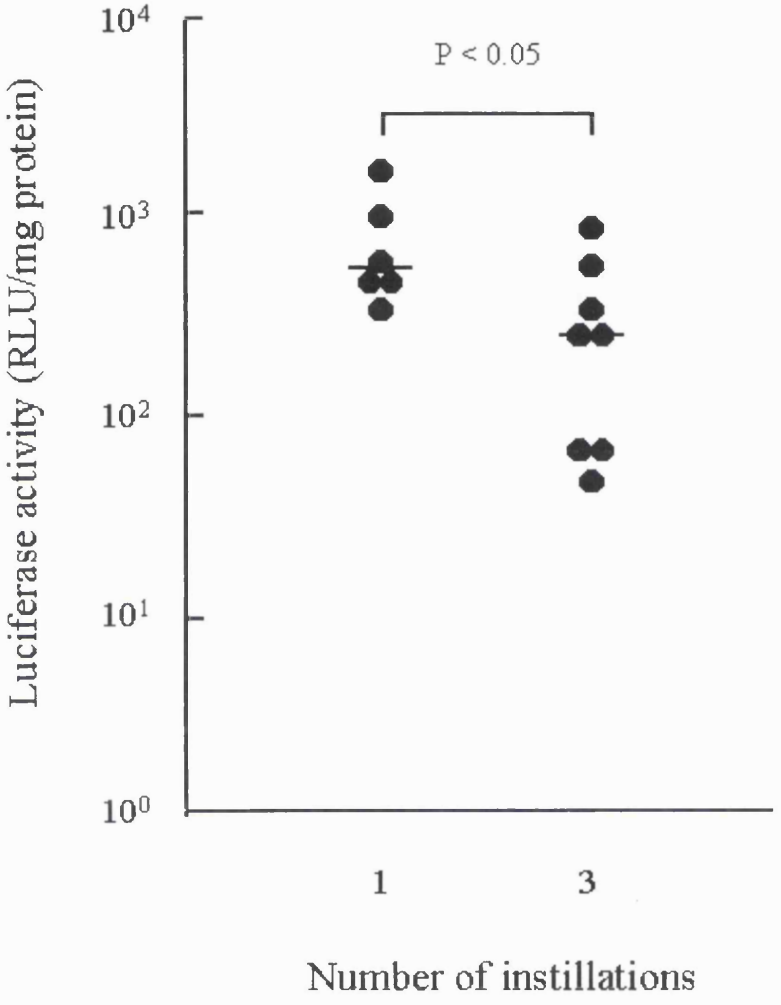
10^4
10^3
10^2
10^1
10^0
P < 0.05
Luciferase activity (RLU/mg protein)
1
3
Number of instillations

THE FRACTAL STRUCTURE OF POLYCATION-DNA COMPLEXES

(Brief Communication)

L. K. Lee, P. Ayazi Shamlou

The Advanced Centre for Biochemical Engineering, Department of Biochemical Engineering, University College London, Torrington Place, London WC1E 7JE, England

DNA vaccination and gene therapy offer a major development in the ability to treat many intractable diseases such as different cancers, AIDS and autoimmune diseases [1,2], but enormous technical challenges must be overcome before the potential of these techniques can be realised. A major challenge is the need for better delivery systems. Although viral vectors are popular, there are safety concerns regarding their use and it is difficult to produce them in large quantities with sufficient purity [3]. DNA complexes pose fewer problems than viral vectors, but suffer from unacceptably low transfection efficiencies. Considerable research has been devoted to establishing the causes of low transfection and the size of plasmid DNA complexes has been identified as an important factor. It has been demonstrated previously that colloidal aggregation of the complexes may play an important role in determining cell transfection and we recently reported that the prevailing aggregation kinetics are governed by the physicochemical properties of the system according to the DLVO theory [4]. Here we present new experimental data that show a new, and hitherto unreported, property of the structure of aggregating plasmid DNA complexes. We demonstrate that in physiological buffers these aggregates are fractal in nature and describe the dynamics of aggregation via their fractal dimension. We speculate that the spatial distribution of plasmid DNA complexes within the aggregates may provide insight into the capacity of the complexes to transfect cells.

We measured the fractal dimension of poly-L-lysine condensed plasmid DNA using static light scattering. These measurements were performed on a Malvern 4800 spectrometer equipped with a 75 mW, 488 nm, Argon ion laser. Angular scans were carried out for scattering angles, θ, between 12° and 100°, with a measurement made every 4° (23 steps) and an acquisition time of 10 seconds per angle. All experiments were carried out with a 6.9 kb plasmid, pSVβ, transformed and propagated in *E. coli*, DH5α. Poly-L-lysine of molecular weight 34,000 and the purified plasmid were mixed at a lysine/phosphate charge ratio of 2.0 and a final plasmid concentration of 12.5 μg/ml in 20 mM HEPES buffer, pH 7.2. NaCl was added to the buffer solution to give ionic strengths at 10, 50, 100, 150 and 1000 mM

Figure 1 shows the variation of the scattered intensity $I(q)$ of light as a function of the scattering angle, θ, with time as a parameter. The scattering vector, q, was calculated from $q = \frac{4\pi n \sin(\theta/2)}{\lambda}$ where n is the refractive index of the solution (1.33) and λ is the incident wavelength (488 nm). For clarity of presentation only some of the data points are shown. The conditions of our experiments always satisfied the basic requirements of the Rayleigh-Debye model but for accuracy the calculations were confined to data in the range $12° < \theta < 68°$ corresponding to $0.2 < qa < 1.0$ where the radius, a, of the scatterer within the aggregate was taken to be 50 nm. Based on the power-law dependence of the scattered intensity on the scattering vector, $I(q) \propto q^{-Df}$, we applied linear regression analysis to the data points in Figure 1. The results gave a fractal dimension, D_f, of 2.20 for buffers at physiological salt concentrations between 100 and 150mM. Theoretical considerations based on statistical physics of diffusion-limited-cluster aggregation (DLCA) and reaction-limited-cluster aggregation (RLCA) suggest that the plasmid DNA complexes aggregated in the RLCA regime, for which a theoretical mass-fractal dimension, D_f, of 2.1 ± 0.1 has been cited [5] and confirmed by computer simulations [6]. In comparison, fractal aggregates formed in the DLCA regime have a reported fractal dimension of 1.8 [5,7].

It is notable that the fractal dimension of aggregates of plasmid DNA complexes effectively remained unchanged at all times despite the fact that the aggregate size distribution shifted continuously towards larger sizes throughout the period of measurement, as shown in Figure 2. Taken together, these observations support the view that the addition of poly-L-lysine rapidly induces the condensation of plasmid DNA by charge neutralisation [8]. The decrease in the repulsive interaction force due to the electrical double layers of the complexes caused by the electrolyte in the medium results in the aggregation of the self-assembled complexes slowly over about one hour to form fairly compact structures, characteristic of aggregation in the RLCA regime. A constant fractal dimension, unaffected by experimental conditions, is evidence of little restructuring within the aggregates. To our surprise, the fractal dimension of the aggregates also remained unaffected by minor changes in salt concentration, that is, between 50 mM and 150 mM NaCl. At an electrolyte concentration of 1 M, we measured a fractal dimension of 1.44, a value that indicates these aggregates have relatively loose structures, as expected for growth in the DLCA regime.

The major biological barriers to transfection include the diffusion of DNA complexes to and their association with cell receptors, internalisation via endocytosis, escape from endosomal compartments and dissociation of the DNA from the condensing agent. Complex size is a key parameter in these interactions and here we hypothesis that complex structure may be equally important. While the relationship between the physical properties of DNA complexes and cell transfection remains to be fully established, our findings on the fractal characteristics of these complexes open up a new line of study, which may prove to be important.

ACKNOWLEDGEMENTS

We thank Stephen Ward-Smith and Mike Kaszuba for many useful and valuable discussions, and Malcolm Connah and Nicola Gummery for help with the static light scattering experiments.

REFERENCES

1. Anderson,W.F. 1998. Human gene therapy. *Nature* 392 (Suppl):25-30.
2. Crystal,R.G. 1995. Transfer of genes to humans: early lessons and obstacles to success. *Science* 270:404-410.
3. Mountain,A. 2000. Gene therapy: the first decade. *Trends in Biotechnology* 18:119-128.
4. Lee,L.K., C.N.Mount, and P.Ayazi Shamlou. 2001. Characterisation of the physical stability of colloidal polycation-DNA complexes for gene therapy and DNA vaccines. *Chemical Engineering Science* 56:3163-3172.
5. Lin,M.Y., H.M.Lindsay, D.A.Weitz, R.C.Ball, R.Klein, and P.Meakin. 1989. Universality of fractal aggregates as probed by light scattering. *Proceedings of the Royal Society of London A* 423:71-87.
6. Ball,R.C., D.A.Weitz, T.A.Witten, and F.Leyvraz. 1987. Universal kinetics in reaction-limited aggregation. *Physical Review Letters* 58:274-277.
7. Meakin,P. 1988. Fractal aggregates. *Advances in Colloid and Interface Science* 28:249-331.
8. Bloomfield,V.A. 1996. DNA condensation. *Current Opinion in Structural Biology* 6:334-341.

Figure legends

Figure 1. Light scattering curves collected at various times during the run for the poly-L-lysine-pSVβ complexes in 20 mM HEPES pH 7.2, 150 mM NaCl. The solid line is a fit using linear regression analysis and has a gradient of 2.2.

Figure 2. Particle size distributions of poly-L-lysine-plasmid DNA complexes at a charge ratio of 2.0 in 20 mM HEPES, pH 7.2, 150 mM NaCl, as a function of time after preparation. Size distributions were determined as mean of diameter on the basis of intensity of scattered light at 90°. The data shown were obtained from a single representative sample.

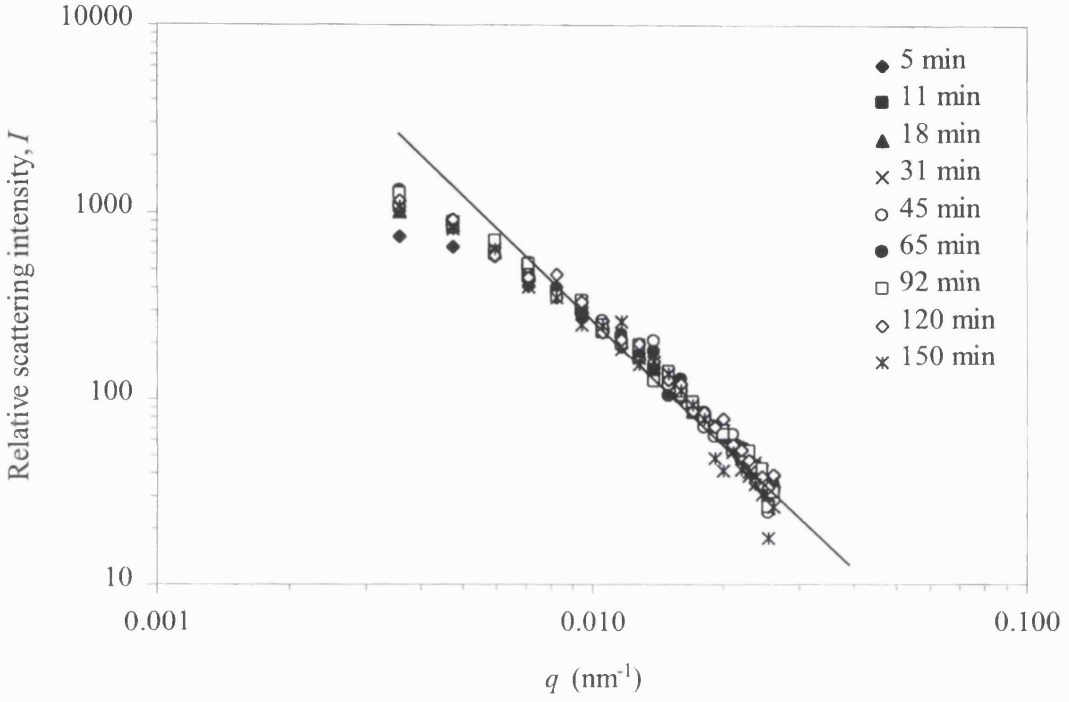
10000
1000
100
10
Relative scattering intensity, I
0.001
0.010
0.100
q (nm-1)
5 min
11 min
18 min
31 min
45 min
65 min
92 min
120 min
150 min

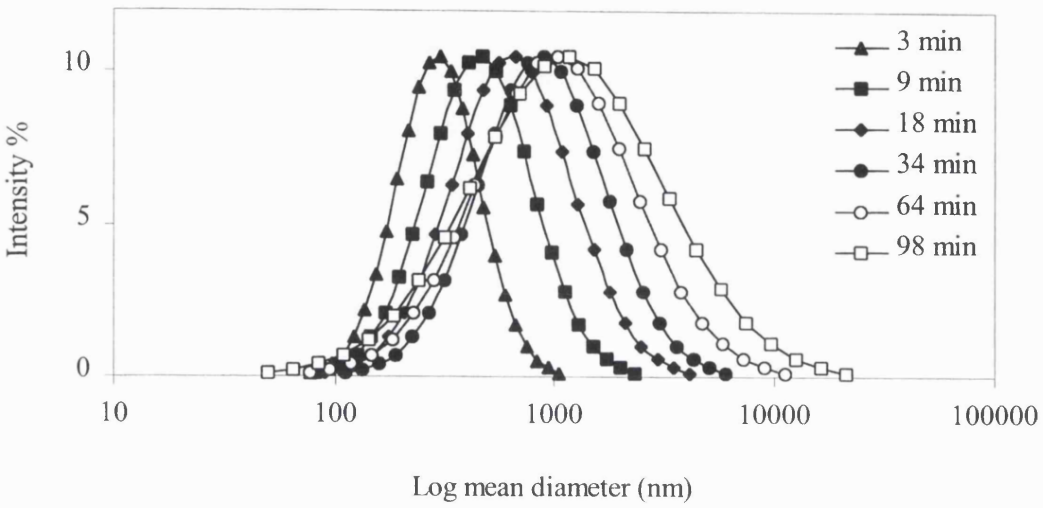
Intensity %
10
5
0
10
100
1000
10000
100000
Log mean diameter (nm)
3 min
9 min
18 min
34 min
64 min
98 min